

Exploratory analysis of future LH₂-powered aircraft ground operations at a regional airport

AE5310: Thesis Control and Operations

L.K.H. Gijzen



Delft University of Technology

Exploratory analysis of future LH₂-powered aircraft ground operations at a regional airport

by

L.K.H. Gijzen

to obtain the degree of Master of Science
at the Delft University of Technology,
to be defended publicly on Friday, 5th of April at 13h.

Student number:	4880900	
Project Duration:	April 2023 - March 2024	
Thesis committee:	Dr. O.A. Sharpanskykh	Supervisor
	Dr.ir. B.F. Lopes Dos Santos	Chair
	Dr.ir. J.A. Pascoe	Examiner
	D. van Dijk MSc	Company Supervisor (RTHA)

An electronic version of this thesis is available at <http://repository.tudelft.nl/>.

Acknowledgements

With the submission of this master thesis, my academic career at the Delft University of Technology comes to an end. Throughout the past six years, I have had the opportunity to meet inspiring people, while also being involved in extremely valuable projects, case-studies, an internship and finally this master thesis. These experiences and opportunities have shaped me into the person I have become today, for which I am super grateful.

Writing this master thesis for almost a year has been a wonderful experience, but it was not always easy. Nevertheless, with the right amount of discipline, a motivating research topic but also due to my two very supporting supervisors, I am now able to proudly present my master thesis called "Exploratory analysis of the impact of commercial LH2-powered aircraft on the ground operations". First of all, I would like to express my sincere gratitude to D. van Dijk MSc. and Dr. O.A. Sharpanskykh for your unlimited support, expertise and guidance. Your involvement has been essential in completing my master thesis, but also it has greatly contributed to my knowledge on airport operations and developed my professional skills. It was a pleasure working with you both.

A special and sincere thanks goes out to my family, (study-)friends and last but not least Lieke. Your unconditional love, support, understanding, enjoyable distractions and encouragement has formed the foundation of this achievement but also of my entire journey as a whole, which I could not have done without you. In addition, I would like to thank my colleagues at Rotterdam The Hague Airport, whom made my time at the airport really enjoyable.

To conclude, I feel disappointed that my student-ship is over, but in the meantime I am looking forward to what the future will bring me. Undoubtedly, the experience and knowledge that I have gathered during this journey will contribute to my future endeavors.

Loek Gijzen
Delft, March 2024

Contents

List of Figures	ii
List of Tables	ii
Nomenclature	ii
I Scientific Paper	1
II Literature study previously graded under AE4020	32
III Supporting Work	100
1 Background Information	101
1.1 Conventional Operations at RTHA	101
1.2 Refueling Process	102
1.2.1 Refueling Jet-A1	102
1.2.2 Refueling LH ₂	103
1.3 Aircraft Types	104
1.3.1 Conventional Aircraft	104
1.3.2 Hydrogen-Powered Aircraft	104
2 Experimental Elaboration	107
2.1 Safety Zone	107
2.1.1 State of the Art	107
2.1.2 Stand Availability	108
2.2 Turnaround Procedure	109
3 Model Inputs	113
3.1 Model Environment	113
3.2 Fuel Calculation	114
3.3 Turnaround Definition	115
3.4 Flight Schedule	116
4 Model Verification and Validation	119
4.1 Verification	119
4.2 Validation	119
5 Statistical Significance	121
5.1 Coefficient of Variance	121
5.2 Statistical Tests	121
6 Supplementary Results	123
6.1 General Results	123

- 6.2 Configuration Results 124
- 7 Implications for RTHA 126**
- 7.1 Road-map 126
- 7.2 Fuel Storage Facility 127
- 8 Pseudocode 129**
- References 130**

List of Figures

1.1	GSE arrangement during B737 turnaround. Retrieved from [16].	102
1.2	Gantt-chart of a typical turnaround procedure of a single-aisle aircraft. Information retrieved from [44].	102
1.3	Temporal refueling method for LH ₂ . Information retrieved from [11] and [14].	103
1.4	Three sustainable aircraft currently being developed by Airbus. Figure retrieved from [6].	105
2.1	Gantt-chart representing the turnaround of a LH ₂ -powered single-aisle aircraft, assuming 1500 kg LH ₂ to be refueled at a flow rate of 2.5 kg/s with no parallel turnaround processes allowed.	110
2.2	Gantt-chart representing the turnaround of a LH ₂ -powered single-aisle aircraft, assuming 1500 kg LH ₂ to be refueled at a flow rate of 5 kg/s with limited parallel turnaround processes allowed.	111
2.3	Gantt-chart representing the turnaround of a LH ₂ -powered single-aisle aircraft, assuming 1500 kg LH ₂ to be refueled at a flow rate of 10 kg/s with parallel turnaround processes allowed.	112
3.1	Environment of the agent-based model used for simulating the experiments.	113
3.2	Number of total and commercial flights per year at RTHA. Information retrieved from [8].	117
6.1	Stand occupation at RTHA for different flight schedules.	125

List of Tables

2.1	Recommended separation distances while refueling LH ₂ , all expressed in meters. Information retrieved from [20].	108
2.2	Stand availability for both conventional Jet-A1 and LH ₂ -powered aircraft, using varying safety zones.	109
3.1	Selected characteristics per aircraft type that is used within the simulation model. . . .	114
3.2	Overview of extra turnaround time component for LH ₂ -powered aircraft per experiment, required for catering and cleaning.	116
5.1	Overview of the proven statistical dependencies of each KPI versus each parameter considered within this research.	122
6.1	Overview of the most important characteristics of the three different flight schedules. .	123

Nomenclature

Abbreviations

Abbreviation	Definition
A	Arriving
CO ₂	Carbon Dioxide
D	Departing
EASA	European Union Aviation Safety Agency
EC	European Commission
GH ₂	Gaseous Hydrogen
GSE	Ground Support Equipment
IATA	International Air Transport Association
ICAO	International Civil Aviation Organization
ICCT	International Council on Clean Transportation
IEA	International Energy Agency
Jet-A1	Kerosene
KPI	Key Performance Indicator
LH ₂	Liquid Hydrogen
MAPF	Multi-Agent Path-Finding
MPP	Mission Possible Partnership
MTOW	Maximum Take-Off Weight
NASA	National Aeronautics and Space Administration
NEO	New Engine Option
OTP	On Time Performance
Pax	Passengers
QRA	Quantitative Risk Assessment
RTHA	Rotterdam The Hague Airport
SAF	Sustainable Aviation Fuel
TAT	Total Turnaround Time
TRL	Technology Readiness Level

Part I

Scientific Paper

Exploratory Analysis of Future LH₂-Powered Aircraft Ground Operations at a Regional Airport

Loek Gijzen*

Delft University of Technology, Delft, The Netherlands

Abstract

As an alternative to kerosene (Jet-A1), green hydrogen is considered a potential solution to reduce the environmental impact of the medium-range aviation industry. While the technical feasibility of liquid hydrogen (LH₂)-powered aircraft is already being researched and demonstrated, the required infrastructure, as well as its impact on the current ground operations has received little attention in literature. This research paper aims to fill this research gap with the objective of exploring the potential impact of commercial LH₂-powered aircraft on the ground operations, focusing on (the transition towards) 2050. In contribution to this main research objective, five important turnaround-related factors for ground handling LH₂ were considered to explore their respective impact on the ground operations. These five parameters include the number of LH₂ fuel trucks, LH₂ flow rate, LH₂ aircraft penetration rate, LH₂ refueling safety zone diameter and the level of restricted parallel turnaround processes during LH₂ refueling. Through varying these parameters in experiments using an agent-based simulation model, meaningful results could be obtained which are useful to consult airports and airlines on what operational and infrastructural measures need to be accommodated to ensure competitive ground operations in terms of efficiency involving LH₂-powered aircraft. The impact of the different experiments on the efficiency was expressed in terms of the turnaround time, number of aircraft delays and on-time performance of both Jet-A1 and LH₂-powered aircraft. As a case-study, the ZEROe turbofan was selected to operate at the regional airport Rotterdam The Hague Airport, featuring remote aircraft stands. The results show that the LH₂ penetration rate has the greatest influence on the efficiency of the ground operations, and increasing this rate must be carefully coordinated by the involved stakeholders in accordance with technological developments of the remaining four parameters. For a LH₂ penetration rate of up to 25%, at least 50% of the turnaround processes must be allowed to be executed during refueling, the safety zone diameter must not be greater than 30 meter and a single LH₂ fuel truck with a flow rate of at least 5 kg/s is required to ensure efficient ground operations. To accommodate LH₂ penetration rates up to 50%, there must be no restrictions on parallel turnaround processes, the safety zone diameter should be 15 meter and finally at least two LH₂ fuel trucks are required with a flow rate of at least 10 kg/s each.

1 Introduction

For the last decade, the aviation industry has been responsible for approximately 2% of the annual global carbon dioxide (CO₂) emissions, while also being the highest-emitting mode of transport in terms of CO₂ per passenger per kilometer, according to the International Energy Association (IEA) [1]. Additionally, the International Civil Aviation Organization (ICAO) expects the number of annual aerial passengers to rise at a rate of 4.3 % per annum in the next 20 years, resulting in a CO₂-emission increase in the near future if no action is undertaken [2]. This confirms the necessity of more sustainable innovations in the field of aviation, in order to contribute to the decarbonizing aims of net zero set by the IEA for 2050 [3].

As a result of these developments, various initiatives are currently ongoing in an attempt to make aviation more sustainable. Progress is being made in the field of sustainable aviation fuels, which is a bio-based CO₂-reducing fuel that is also currently the only sustainable solution for long-range flights [4]. Moreover, the short-range aviation industry is anticipating on battery-electric aircraft currently in development to replace the current CO₂-emitting aircraft within this market. Unfortunately however, there is no perspective for

these electric aircraft to also conquer the mid-range aviation market as well, as was concluded by the most recent report by the International Council on Clean Transportation (ICCT) [5]. Consequently, the mid-range commercial aviation market, accounting for 67% of the total aviation market [6], is devoted to an alternative solution in order to reduce its (non-)carbon emissions. Using green hydrogen as an energy-carrier is therefore considered a possible solution to also make this aircraft-market more sustainable, as has been acknowledged by various organizations such as Airbus [7], the European Union Aviation Safety Agency (EASA) [8] and ICAO [9].

Using hydrogen as an aircraft fuel is not new, as it has already extensively been researched in the 80's by the National Aeronautics and Space Administration (NASA) [10]. This has paved the way for numerous recent studies assessing the technological and economic feasibility of hydrogen-powered aircraft, such as the works of Hoelzen et al. [11] and Adler et al. [12], while also the supply-chain of hydrogen is reviewed within these studies. Notwithstanding this, the potential impact of hydrogen-powered aircraft on the airport ground operations has received little attention in literature, mostly due to the absence of available data, thus forming one of the largest research gaps concerning hydrogen in aviation. The main performance of the total ground operations at an airport can be expressed using four key performance indicator (KPI) groups, being the on-time performance (OTP), number of delayed aircraft, the average delay duration of these delayed aircraft and lastly the average total turnaround time (TAT), according to expert interviews and ICAO [13]. This is relevant to the airport, in order to monitor the operations and fulfill its coordinating function. Operational and infrastructural parameters which influence these KPIs and which are expected to change as a result of introducing LH₂-powered aircraft include the LH₂ flow rate during refueling, as well as the number of LH₂ fuel trucks, as was learned from expert knowledge. Moreover, the safety measures that are necessary for handling LH₂ impact the safety zone diameter and the allowed parallel sequence of the turnaround procedure, and therefore also influence the KPIs. Lastly, these KPIs are also dependent on the percentage of flights that will be replaced by LH₂-powered aircraft.

The main objective of this research is to explore the potential future impact of commercial LH₂-powered aircraft on the ground operations at a regional airport (O1). This impact will be expressed using the four KPIs groups for both Jet-A1 and LH₂-powered aircraft. In contribution to the main objective, five sub-objectives of this research focus on the specific impact of the number of LH₂ fuel trucks (O1.1), the LH₂ aircraft penetration rate (O1.2), the LH₂ safety zone diameter (O1.3), the LH₂ flow rate (O1.4) and the LH₂ turnaround procedure (O1.5) on these KPIs respectively. This impact will be analyzed using associated experiments. Finally, the outcomes will be used to answer the final objective of this research, which is to consult the aviation industry per stakeholder on the minimum requirements for each of these five parameters throughout the transition towards in hydrogen in aviation, in order to ensure efficient airport ground operations (O2).

The experiments that are mentioned above will be simulated using an agent-based simulation model. Agent-based simulations are useful to model and understand the behaviour of complex socio-technical systems, such as the ground operations at an airport. Agent-based models allow for detailed representations of static and dynamic properties of autonomous agents and their interactions. As a case-study, Rotterdam The Hague Airport (RTHA) will be used as a regional airport at which the ground operations of LH₂-powered medium-range aircraft are simulated. A discrete layout of RTHA will be incorporated in the simulation model, which consists of remote aircraft stands and thus no passenger boarding bridges. Additionally, the flight schedule of RTHA will be used in which a certain percentage of the conventional flights will be operated using the ZEROe turbofan, developed by Airbus [14]. Since this aircraft is expected to be launched in 2035, the scope of this research has been set to (the transition towards) 2050, in order to incorporate a realistic penetration of this ZEROe turbofan within the market.

This paper will be structured as follows. First, the state of the art regarding the parameters associated with the five different sub-objectives will be reviewed in section 2. Second, in section 3 the case-study at Rotterdam The Hague Airport will be further clarified. Third, the simulation model used within this research is explained in section 4. Fourth, the experiments used for the simulation will be defined and substantiated in section 5. Fifth, in section 6 the results of the research will be extensively reviewed using both contour plots and local sensitivity analyses. Sixth, the discussion, consulting the different stakeholders, is provided in section 7 and afterwards the research paper is concluded accordingly in section 8.

2 State of the Art on Hydrogen in Aviation

In this section, the state of the art regarding the five different parameters that are used for the experiments and the research objectives will be defined. First, the parameters influencing the ground operations, both for Jet-A1 and LH₂-powered aircraft, are explained in subsection 2.1. Second, the forecasted LH₂ market penetrations, defining the penetration rate of LH₂-powered aircraft, will be treated in subsection 2.2.

2.1 Ground Operations

When analyzing the ground operations at an airport, the turnaround process is a fundamental part of this. Namely, the ground operations at an airport can be divided into airside and landside processes. The airside processes yield the taking-off and landing of aircraft, as well as the aircraft taxiing towards and from the stands on the platform. The landside processes in turn refer to the passengers arriving at the airport, checking-in their luggage and passing through security. The turnaround process is the process which connects the landside and airside processes, and hence the airport and aircraft operations. Within this process, the aircraft is serviced and unloaded after its flight, and prepared for the next flight again. In order to obtain a better understanding of the conventional turnaround process, refer to Supporting Work 1.1. Furthermore, the refueling process for LH₂-powered aircraft, including the LH₂ flow rate and number of LH₂ fuel trucks, will be discussed in subsection 2.1.1. Next up, the state of the art regarding the safety zone during LH₂ refueling, being one of the five parameters, is provided in subsection 2.1.2. Thereafter, the resulting implications of LH₂-powered aircraft on the turnaround procedure will be discussed in subsection 2.1.3.

2.1.1 LH₂ Refueling Process

Whenever an aircraft needs refueling, either a fuel or hydrant truck pulls up which will deliver the amount of fuel requested by the aircraft crew. The duration of the refueling is dependent on the flow rate that the refueling vehicle can achieve, as well as the total amount of fuel required. Given that LH₂ has very unique properties, refueling this substance is expected to occur at different flow rates than the average 15 kg/s of Jet-A1. For more information regarding conventional refueling of Jet-A1, refer to Supporting Work 1.2.1. On the one hand, LH₂ is significantly lighter than Jet-A1, yielding that a lower flow rate would still result in comparable refueling times. On the other hand however, the much higher volume of LH₂ introduces new challenges, such as a larger diameter of the fuel hose and a different pumping technique for which the safety must be guaranteed at all times. For more information regarding the safe (dis-)connecting of a LH₂ fuel hose, as well as its duration, refer to Supporting Work 1.2.2. The basic mechanism to refuel LH₂ is a pressure-based cryogenic pump, which requires special couplings and safety vents to compensate for boil-off [15]. Where Jet-A1 is refueled using a dedicated fuel truck, a fuel truck specially designed to refuel LH₂ and equipped with such a cryogenic pump is required here. Nevertheless, this still has a low technology readiness level (TRL).

The state of the art is an aircraft refueling vehicle with a LH₂ flow rate of 36 kg/hour, designed to refuel a large drone [16]. In the truck industry, the achievable LH₂ flow rate is significantly higher already, with 5-8 kg/min for the LH₂-powered Daimler truck [17]. Clearly, the flow rate still needs to be increased greatly in order to refuel large commercial aircraft at a turnaround time competitive to that of conventional aircraft. There have been several researches into the field of LH₂ flow rates already. Historically, Boeing and NASA have already thoroughly researched the operations of LH₂ in aviation in the 1970's, based on which Boeing concluded a LH₂ flow rate of 15 kg/s to be possible. More recently, Mangold et al. found that an even higher flow rate of 20 kg/s is also possible if larger fuel hoses can be applied [18]. Nevertheless, due to the large diameter required to transfer these significantly higher volumes per second, manual handling is no longer possible as a result of the large size and weight, yielding that the process must be automated for these high flow rates. The recent study performed by FlyZero was significantly more conservative, as they concluded possible flow rates ranging from 1.1 - 7.2 kg/s, taking into account scenario's featuring different fill times, hose diameters and fuel amounts [19]. The latest article by Babuder et al. combined all these different flow rates into three different flow rate scenario's of 5, 10 and 20 kg/s, in order to cover the majority of the spectrum with their research and account for different developments in the next decades

[20]. These higher flow rates however can only become feasible if more powerful cryogenic pumps and new couplings are developed in the next decades. An alternative to increase the refueling productivity and minimize the average delay duration of LH₂-powered aircraft having to wait on a LH₂ fuel truck is to deploy more LH₂ fuel trucks. The resulting experiments of this state of the art, relating to the number of LH₂ fuel trucks (research objective 1.1) and the LH₂ flow rate (research objective O1.4), will be introduced in subsubsection 5.2.1 and subsubsection 5.2.4.

2.1.2 Safety Zone

When an aircraft is being refueled, this is considered a risky activity since Jet-A1 is a flammable substance. Therefore, for every aircraft being refueled at Rotterdam The Hague Airport, there may be no external critical buildings within the risk contour of 10^{-6} per year according to Dutch legislation, which is measured from the point of refueling [21]. For more information regarding this legislation, refer to Supporting Work 2.1.1. For Jet-A1, a similar safety zone with a diameter of just three meters must be acknowledged as was stated in the FlyZero project [19]. The fact that such a small safety zone is sufficient is a result of all the knowledge about the behaviour of Jet-A1 and experience with refueling this substance. When comparing the properties of Jet-A1 with those of LH₂, LH₂ can be considered significantly more dangerous and therefore 'riskier' to refuel [22]. On top of that, there is relatively little knowledge and experience with handling LH₂ at this stage, making it even riskier. From this, it can be expected that the safety zone to refuel LH₂ will be significantly larger than the three meters for Jet-A1, in order to maintain acceptable safety risks.

Since the safety standards for refueling aircraft are fully based on risk, every specific situation needs to be individually modelled and assessed by an expert to define the risk-contour, called a quantitative risk assessment (QRA). The problem with LH₂ is that this is a 'new' fuel within aviation, and obtaining such a QRA for every stand where a yet unknown amount of LH₂ can be refueled is too time-consuming for the scope of this research, while also it is subject to change rapidly as a result of all the ongoing researches and developments regarding the introduction and required refueling infrastructure of LH₂-powered aircraft. In order to still take safety into account in the research, the concept of a 'safety zone' has been introduced, based on interviews with different stakeholders, safety experts from airports and substantiated with recommended safety zones from different industries, projects such as FlyZero and authorities, in order to safely refuel LH₂ at RTHA in and towards 2050 [19]. This safety zone will be a circular area inside which no other aircraft, both conventional and LH₂-powered, is allowed to park, refuel or undergo a turnaround with passengers, and must be adhered to throughout the entire refueling process. Shortly taxiing through this safety zone is considered to be a much lower risk which would not exceed 10^{-6} per annum, and is therefore allowed. Such a safety zone can potentially have a significant impact on the airport ground operations, as adjacent stands or other infrastructure might be too close while LH₂ refueling is ongoing, influencing the airport capacity. Therefore, this research will also investigate the impact of different safety zones diameters during LH₂ refueling on the KPIs, part of research objective O1.3, as is further explained in subsubsection 5.2.3.

2.1.3 Hydrogen Turnaround

With the introduction of LH₂-powered aircraft, the existing turnaround procedure, designed for conventional aircraft, must undergo a number of adaptations to safely and efficiently accommodate these new sustainable aircraft. One of the most significant changes is the refueling process, which will be different and most likely more time-consuming than the process for Jet-A1, as was treated in subsubsection 2.1.1. Also, as was observed in subsubsection 2.1.2, the more dangerous properties of LH₂ with respect to Jet-A1 results in additional required safety measures, such as a safety zone around a LH₂-powered aircraft that is being refueled. As a result of this, the safety implications on the turnaround procedure and sequence itself must also be assessed more closely. Namely, restrictions on the ground support equipment (GSE) of the LH₂-powered aircraft could affect the turnaround sequence efficiency, hence en-longing the total turnaround time, also in combination with the more time-consuming refueling, potentially leading to additional and longer delays, disrupting the entire airport operations.

The configuration of LH₂-powered aircraft is expected to be very similar to the current conventional aircraft operating at RTHA. Therefore, the majority of the GSE can be also used also on these new aircraft,

allowing a mostly similar turnaround process as for conventional aircraft. The first difference though is the Jet-A1 fuel truck, which must be replaced with one or more LH₂ fuel trucks. Furthermore, while other turnaround processes are allowed to be executed simultaneously with refueling Jet-A1 when executed more than three meters away from the fuel hose connection, this will be more complex while refueling LH₂ as a result of the expected larger separation distances with other vehicles, tanks or cables as was reviewed by FlyZero [19]. Namely, the majority of the turnaround processes involve GSE with electrical or mechanical components that could potentially generate a flammable atmosphere which could be disastrous in combination with spilled LH₂ [19]. This might result in the restriction of all parallel turnaround processes with refueling LH₂, which was researched by Babuder et al. [20].

A more optimistic alternative would be to adapt and re-classify certain existing GSE to be used in hazardous areas such as in the vicinity of spilled LH₂, as was also introduced by FlyZero [19], allowing the partial execution of parallel turnaround processes while refueling is ongoing. The last and most optimistic alternative would be to execute all turnaround processes simultaneous with refueling, using newly designed and classified GSE which incorporate (semi-)automated subsystems, which is a combination of the proposed scenario by FlyZero [19] and Babuder et al. [20]. In this way, the turnaround procedure can be safer as the number of personnel exposed to risk is minimized. A (semi-)automated fuel hose might even be the new standard for refueling LH₂, due to the large diameter of the fuel hose at high LH₂ flow rates, which is more difficult to operate manually [18]. However, this would be a very challenging adaptation which requires years of testing before implementation is realistic [19]. In order to anticipate on different technological advancements in the years up to 2050, an experiment has been set up to analyze the effect of different turnaround procedures on the KPIs, part of research objective O1.5 and introduced in subsection 5.2.5.

2.2 Market Penetration

When setting up the flight schedule for 2050, it is fundamental to know how many of the flights are operated using the turbofan aircraft produced by Airbus. This is dependent on the European market penetration of LH₂-powered aircraft in 2050. The market penetration of this aircraft in a certain year is dependent on numerous variables, such as aircraft certification, the availability but also the profitability of both the aircraft and of operating LH₂, which ultimately drives the decision whether an airline will buy the aircraft. Since these variables remain uncertain for now, determining the penetration rate remains difficult.

There have been a number of studies aiming to forecast the market penetration of LH₂-powered turbofan aircraft in 2050, based on different expected years into service of the aircraft type but also on other factors. This includes Hoelzen et al., who projected a base 50% single-aisle market penetration, and an ambitious 87% penetration in 2050[23]. Furthermore, the European Commission also visions these optimistic penetration rates, and states that by 2050, 40% of the European fleet is powered by hydrogen in an ambitious scenario [24]. An important remark is that this 40% regards the entire fleet, so this also includes regional turboprops which are propelled by a fuel cell-powered hybrid electric propulsion system. The Mission Possible Partnership (MPP), co-written by McKinsey, is much more conservative, and expects the share of LH₂ turbofan single-aisle aircraft to be 1-6% in 2050 [25]. More specifically, an internal study performed as part of the TULIPS project estimated 20% of the flights at RTHA to be fueled by hydrogen in 2050, of which the majority is single-aisle turbofan aircraft. Another internal study performed for RTHA concluded a 5-10% penetration of single-aisle turbofan aircraft in 2050. Conclusively, these varying forecasts underline the uncertainty, and justify an experiment focusing on the impact of the penetration rate on the KPIs, referring to research objective O1.4 and further elaborated upon in subsection 5.2.2.

3 Case Description

Within this section, a description of the case study used within this research will be defined. First, the scope of the research in relation to the case study at Rotterdam The Hague Airport is introduced in subsection 3.1, including the environment, considered aircraft types as well as the flight schedule. Second, an elaborate description of the process, being ground operations at RTHA, is provided in subsection 3.2.

3.1 Case Study at Rotterdam The Hague Airport

For this research, the regional airport Rotterdam The Hague Airport has been selected as a case study. To realistically represent RTHA, the entire commercial aircraft operations at the airport will be incorporated in the simulation model, including the layout as presented in subsection 3.1.1, flight schedule and ground handling procedures, while adhering to constraints and regulations that the airport is facing. The advantage of RTHA is that the medium-range fleet currently operating at the airport can potentially be replaced entirely by the ZEROe turbofan aircraft, which is the only LH₂-powered aircraft that will be considered within this research. An evaluation of the selected conventional and LH₂-powered aircraft for this research is provided in subsection 3.1.2. As has already been announced before, the scope of this research will focus on 2050. In this way, the operations can be based on a more dominant role of hydrogen within the medium-range commercial aviation sector. In order to size the operations, infrastructure and procedures for all possible experiments, a forecasted peak-day in the summer of 2050 will be used as a flight schedule for the simulation. The reasoning behind the selection of this peak-day, together with a further explanation of the flight schedule, is provided in subsection 3.1.3.

3.1.1 Problem Environment

Within this case study, the layout of RTHA will be considered as the environment for the simulations. The airport consists of a single runway, being 2,200 meter long. Moreover, the platform is situated on the south-west end of the runway, and can be accessed from the runway at one of six runway exits, together with a taxiway parallel to the full length of the runway. This entire layout is visualized in Figure 1.

Zooming in, the platform at Rotterdam The Hague Airport consists of twelve equally-sized remote aircraft stands, capable of accommodating an ICAO Size C aircraft, arranged in a 3x3x3 configuration, as is visualized in Figure 2 [26]. At these stands, both the conventional and LH₂-powered aircraft will undergo their turnaround. The stands are labelled with a letter "A", "B", "C" or "D", referring to the row from top to bottom respectively, and with a number ranging from 1 to 3, going from left to right respectively, and are indicated by the green rectangles. The yellow lines indicate the taxiways for the aircraft, and guide each aircraft to enter the aircraft stand from the south, in order that the aircraft is parked with its nose heading north, as was learned from experience. In this way, each aircraft is able to taxi towards the runway independently which makes a push-back truck redundant, contributing to the ground operational efficiency. The yellow arrows on the right indicate the direction in which the aircraft must access and leave the platform under the runway "24" airport configuration. This is the configuration during the most dominant wind direction at RTHA [27], which is therefore also used for this research.

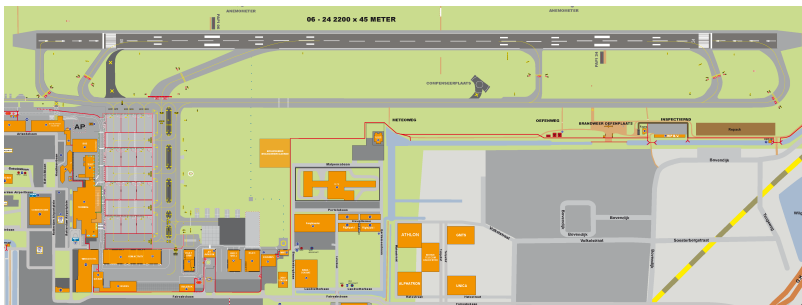


Figure 1: Entire layout at Rotterdam The Hague Airport. Retrieved from [28].

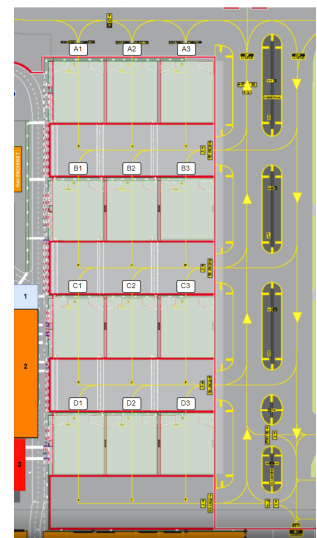


Figure 2: Platform layout at Rotterdam The Hague Airport. Retrieved from [28].

The platform as depicted in Figure 2 is accessible from a number of landside facilities, which are positioned on the bottom left-hand side of the platform. Going from top to bottom, there is the non-Schengen terminal in blue and labelled as 1, next there is the larger Schengen terminal in orange and labelled as 2, and lastly there is the arrival hall consisting of a Schengen and non-Schengen part in red, labelled as 3 [26]. The stand at which an aircraft preferably parks is dependent on a number of factors, as was learned from an interview with the 'Airport Authority', which is the authority that is responsible for the stand allocation at RTHA amongst others. Generally, a Schengen flight is parked in either the "C"-row or the "D"-row at the lowest number available, as these stands are closest to the Schengen terminal and the arrival hall. Since a flight is often (de-)boarded by passengers walking over the platform to or from the aircraft, being close to the relevant facility is rewarded by a shorter (de-)boarding time and thus a more efficient turnaround. Due to similar reasoning, non-Schengen flights rather park in the lowest possible number in the "B"-row or sometimes even the "A"-row, as this is closer to their respective terminal. Lastly, aircraft which are scheduled to undergo a longer turnaround are parked in the higher numbered stands, such that the lower numbered stands are accessible to aircraft with a shorter scheduled turnaround time.

3.1.2 Aircraft Types

When accurately representing RTHA, the aircraft types operating at the airport must also be considered. Based on the penetration rate that is selected for a given experiment, the distribution of aircraft types operating during a peak-day at RTHA in 2050 for that specific experiment can be defined. The penetration rate defines what market percentage of the entire medium-range aircraft fleet is LH₂-powered. Notwithstanding this, the remaining fleet will consist of conventional aircraft which are estimated to still be in operation in 2050. Within the simulation model, the following aircraft types and associated characteristics are gathered as shown in Table 1. The reasoning behind this selection of aircraft is elucidated in Supporting Work 1.3.1.

Table 1: Characteristics of the 3 Jet-A1 aircraft types used in the simulation. Information retrieved from [29], [30] and [31].

	Embrear 190-E2	Boeing 737 MAX 8	Airbus 320 NEO
Range [km]	5,300	6,500	6,850
Seats	97	200	180
MTOW [kg]	56,400	82,200	78,000
Cruise speed [km/h]	870	840	830

Due to the fact that these aircraft types have equal ranges and cruise speeds as the aircraft types currently in operation, it is assumed that destinations and flight times will remain unchanged with respect to the state of the art. The characteristics from Table 1 will be used as inputs in the simulation model to calculate the required amount of fuel, number of passengers and hence the boarding times, as was explained in section 3. The calculation of the amount of fuel is explained in Supporting Work 3.2. In this way, the total turnaround time can be accurately defined for each flight. The number of flights operated by a conventional aircraft in each experiment corresponds with 100% minus the selected LH₂-powered aircraft penetration rate of that specific experiment.

Oppositely, the penetration rate itself determines the percentage of flights in 2050 operated by LH₂-powered aircraft. As has been mentioned before, these flights are assumed to be operated by the ZEROe turbofan in this research. For an elaborate reasoning behind the selection of the turbofan as the LH₂-powered aircraft operating at RTHA, refer to Supporting Work 1.3.2. However, the most important performance-related characteristic of this aircraft type that is different for this turbofan when compared with conventional aircraft is the flight range, with only 3700 km [32]. Besides the range, the number of seats is identical to the number of seats of the Airbus 320 NEO, as was presented in Table 1. The cruise speed is still undetermined for the turbofan, but the European Commission assumes that the flight speed will be comparable to those of conventional turbofan aircraft [24], thus implying no further changes on the flight operations. Consequently, now only the elonged TAT will need to be taken into account when defining the flight schedule using the ZEROe turbofan, which will be elaborated upon in subsection 3.1.3.

3.1.3 Flight Schedule

The selected aircraft types as explained above, together with the selected penetration rate of the LH₂-powered aircraft, are required to ultimately arrive at the flight schedule which must be implemented in the simulation model. The flight schedule used in this research is based on the 17th of July 2023, which was the peak-day of last year in terms of commercial aircraft movements. Therefore, simulating using this busy day ensures that the outcomes are valid for every possible day throughout the year. However, the total number of movements on this day has been increased slightly, in accordance with the forecasted growth by the 'Luchthavenbesluit' in 2050, which is further explained in Supporting Work 3.4. This leads to a total number of movements of 90, yielding that a penetration rate of 5% corresponds to five movements, 25% corresponds to 23 movements and 50% corresponds to 45 movements, when rounded up. Thus, this flight schedule represents a peak-day in 2050 using runway 24, hence indicating on which side of the runway the aircraft enter and exit. By selecting a peak-day as input for this research, the maximum number of movements possible is featured, in order to ensure that the infrastructure can accommodate even the worst-case scenario. In Table 2, a sample of the flight schedules is provided, containing all relevant information for the simulation model.

Table 2: Sample of a flight schedule used as an input to the simulation model.

Total pax	A or D	Actual time	Aircraft type	Airport	Distance [km]	Schengen	Fuel type
41	D	17-7-2023 07:12	E190-E2	London City	306	Untrue	Jet-A1
140	D	17-7-2023 07:36	A320N	Alicante	1568	True	Jet-A1
186	D	17-7-2023 07:58	ZEROe	Lissabon	1801	True	LH ₂

As can be visualized in the table above, important information such as time of arrival, whether the aircraft is departing or arriving and the distance to the next destination is provided. This information serves as required input to the simulation model, so that it can realistically simulate at which time the aircraft lands, whether it prefers a Schengen or non-Schengen stand, the (un-)boarding time, and to calculate the amount of fuel required for the next flight amongst others.

3.2 Process Description

The objective of the model is to simulate the ground operations at RTHA, accommodating both conventional and LH₂-powered aircraft. With the simulation model being subject to different experiments, KPIs can be measured which can give insight into the impact of operating LH₂-powered aircraft in comparison to reference conventional traffic. The process is based on a careful examination of the ground process at RTHA, in conjunction with expert interviews, of which a description is provided below.

Based on the flight schedule, an aircraft will either arrive at one of the runway exits, or is already parked in one of the stands if it spent the night at the airport. In the former case, the aircraft is assigned a stand, based on whether it is going to a Schengen or non-Schengen destination next, as well as the stand availability. In case of a LH₂-powered aircraft, the aircraft is parked at one of the allowed stands for LH₂-powered aircraft, given the stand allocation of that specific experiment. In the rare case that there is no stand available to a specific aircraft, the aircraft is delayed. Once at the stand, the aircraft will first park there for approximately ten minutes, based on the aircraft type and number of passengers arriving. As reference, the exact duration of this step per aircraft type is presented in Supporting Work 3.3. During this step, the passengers de-board while the cargo is unloaded. Next up, in case of a conventional aircraft, one of the two available fuel trucks drives from its parking spot to the aircraft and starts refueling. The refueling time is based on the amount of fuel that the aircraft requires for its next flight. In the meantime, the aircraft is cleaned, catered and prepared for the next flight. Once the refueling is completed, the fuel truck leaves again but the aircraft remains parked for the passengers to board, together with loading the cargo. Ultimately, the aircraft taxis to the runway and is ready for departure, having successfully completed the ground operations at RTHA. For conventional aircraft at RTHA, the average turnaround time of a single aisle short-haul aircraft is 45 minutes, with a maximum of 51 minutes [33].

For LH₂-powered aircraft, the process is slightly different from when the refueling initiates. Once all passengers have exited the aircraft, the earliest available LH₂ fuel truck drives from its parking spot to the stand, in order to refuel the aircraft. In case a safety zone diameter of 30 meter or 45 meter is adhered to, surrounding stands need to be temporarily blocked. Depending on the allowable parallel turnaround procedure, processes such as servicing and catering can either still be executed while refueling, or have to be postponed until after refueling, which also in turn delays the start of boarding. Aircraft that are only arriving at the end of the day will remain parked at their stand to spend the night. These aircraft will not be refueled, as their next flight is only the next day.

4 Model Description

This section provides a detailed description of the multi-agent system model used to simulate the ground operations at a regional airport, involving Jet-A1 and LH₂-powered aircraft, which was implemented in Python. First of all, an overview of the properties of the multi-agent system model will be specified in subsection 4.1. After this, the coordination according to which a fuel truck is assigned to a refueling task, being an element of the multi-agent system model, is clarified in subsection 4.2. Lastly, the path planning of all vehicle agents simulated in the model, also part of the multi-agent system model, is explained in subsection 4.3. The validation and verification description of the model is provided additionally in Supporting Work 4.1 and Supporting Work 4.2 respectively.

4.1 Overview of the Multi-Agent System Model

The model employs a multi-agent system, which allows to simulate autonomous decision-making of agents as well as their mutual interaction within a pre-defined deterministic environment, while obeying a given set of rules and objectives [34]. This provides a framework to analyze the effects of the different parameters, influencing the environment and behaviour of the agents, on the overall system, expressed using KPIs. In this way, a process such as the ground operations at a regional airport involving different types of aircraft, flight schedules and refueling procedures can be realistically simulated. By also adding stochastic properties to the multi-agent system model such as a time variance during the (de-)boarding process, the simulation model can be made even more realistic, leading to meaningful results. A system of this kind encompasses 4 main elements, being the agents, the properties of the agents, the environment and the interaction between the agents and the environment. The structure of the multi-agent system is presented in the overview below.

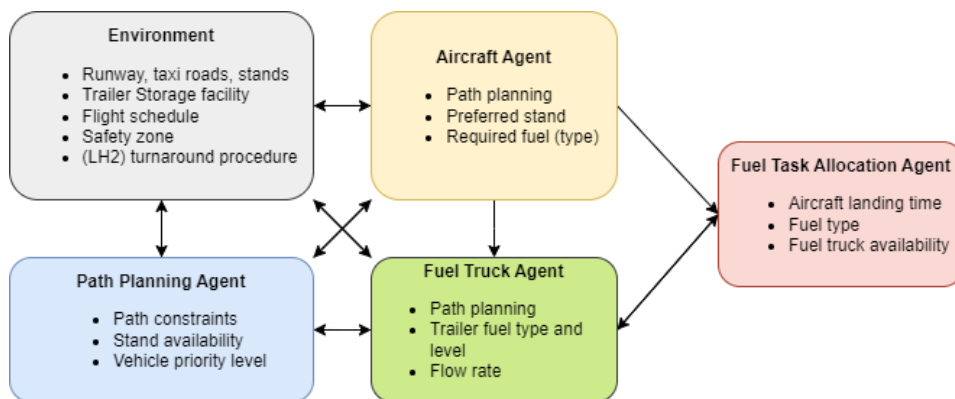


Figure 3: Overview of the agent-based components present within this multi-agent system.

As can be visualized in Figure 3, the different agents involved in the model are the aircraft agents, the fuel truck agents, the path planning agent and the task allocation agent. Complimentary to this is the environment, which defines the context in which the different agents act. For the environment, the entire airport layout of RTHA, including the runway, all taxiways, GSE roads, fuel truck parking spots and lastly the fuel trailer storage has been converted into a graph, consisting of nodes at every intersection and up-to-scale edges, in order to make the model as realistic as possible. For a visualization of the environment,

together with a number of assumptions in terms of taxiing, refer to Supporting Work 3.1. Within the individual boxes in the figure above, all tasks and properties of every specific agent are stated. Additionally, the mutual arrows represent the interactions between the different types of agents, as well as the environment. An evaluation of this learns that except for the fuel task allocation agent in red, all other agents directly interact with the environment in a double-way fashion. This is due to the fact that the two types of vehicle agents, being the aircraft and fuel truck agents, need information about the environment when defining their path goals and defining their paths, while the path planning agent needs to keep track of the stand availability and path constraints, which is all part of the environment. The fuel task allocation on the other hand does not require information about the environment, and solely receives single-way information from the aircraft agent, such as the required amount to be refueled and when the refueling is finished, which is then used to interact with the fuel truck agent in a double-way fashion to distribute this task. Moreover, the path planning agent communicates with both vehicle agents regarding their planned path and priority level. Next, the aircraft agents put forward single-way refueling requests to the fuel task allocation agent, who then converts these requests into actual tasks for the fuel truck agent. More elaboration on the fuel task allocation and path planning will follow in subsection 4.2 and subsection 4.3.

4.2 Fuel Truck Allocation

Within the simulation model, refueling the aircraft is the most complex operational process. A great number of factors need to be taken into account during this step. Prior to the simulation, the number of LH₂ fuel trucks and LH₂ flow rate must be selected. Furthermore, during the simulation, these factors include the time for which a certain aircraft needs to be refueled, the occupation of the fuel trucks carrying the required fuel type, the amount of fuel required and the stand at which the aircraft is parked amongst others. Fortunately, the number of LH₂ fuel trucks and their flow rate are model inputs and will thus be defined in advance. However, the other factors need adequate procedures and regulations in order to ensure an efficient execution of the refueling process. This is referred to as fuel truck allocation, which is a coordination aspect of the multi-agent system model, and is explained using the structure illustrated in Figure 4.

The fuel truck allocation framework as explained in the figure is valid for either two Jet-A1 or two LH₂ fuel trucks. This is because currently there are two Jet-A1 fuel trucks in operation at RTHA, and therefore the same maximum number of two LH₂ fuel trucks has been assumed to be sufficient and possible using the available layout. In case there is only one LH₂ fuel truck, this truck will need to refuel all LH₂-powered aircraft sequentially. In contrast to this, in every experiment simulated in this research, there are always two Jet-A1 fuel trucks, validating this framework for every fueling task of Jet-A1. The two Jet-A1 and one or two LH₂ trucks can operate in parallel, and are managed by two different fuel type-assigned fuel task allocation agents.

As can be visualized, every refueling task is initialized with a refueling request inputted by an aircraft agent. Next up, the fuel task allocation agent, who keeps track of the earlier fuel tasks of the fuel trucks per fuel type assigns this task to the fuel truck that is available the earliest. This decision is based on the start time of every fuel truck at their most recent fuel tasks, together with the amount of fuel that they need to refuel and their flow rate. With this information, a heuristic is calculated to predict when the fuel truck will be ready. In this way, the earliest available fuel truck can be identified and is assigned the next fuel task. In case both fuel trucks have already completed their prior tasks, the task is simply given to fuel truck 1. If the earliest available fuel truck is not refueling another aircraft, it can immediately be deployed on the incoming fuel task. Else, the aircraft is delayed as it needs to wait for the fuel truck to arrive. This delay duration is also part of the set of KPIs in this research.

Whenever the fuel truck is ready to refuel the aircraft, it first needs to assess whether its trailer still carries sufficient fuel or not. If so, the truck can drive to the aircraft, perform the refueling and return to its parking spot again. If not, the truck first needs to drive to the fuel storage facility and replace its trailer, which is a process taking up to a few minutes, dependent on which fuel type is needed. This replacing is also necessary if the LH₂ trailer arrives below 15%, since below this volume it is inefficient to cool the LH₂ at cryogenic conditions, as was researched by Hoelzen et al. [23]. As this step can be somewhat time-consuming, the fuel task allocation agent then re-evaluates if the assigned fuel truck is still the earliest

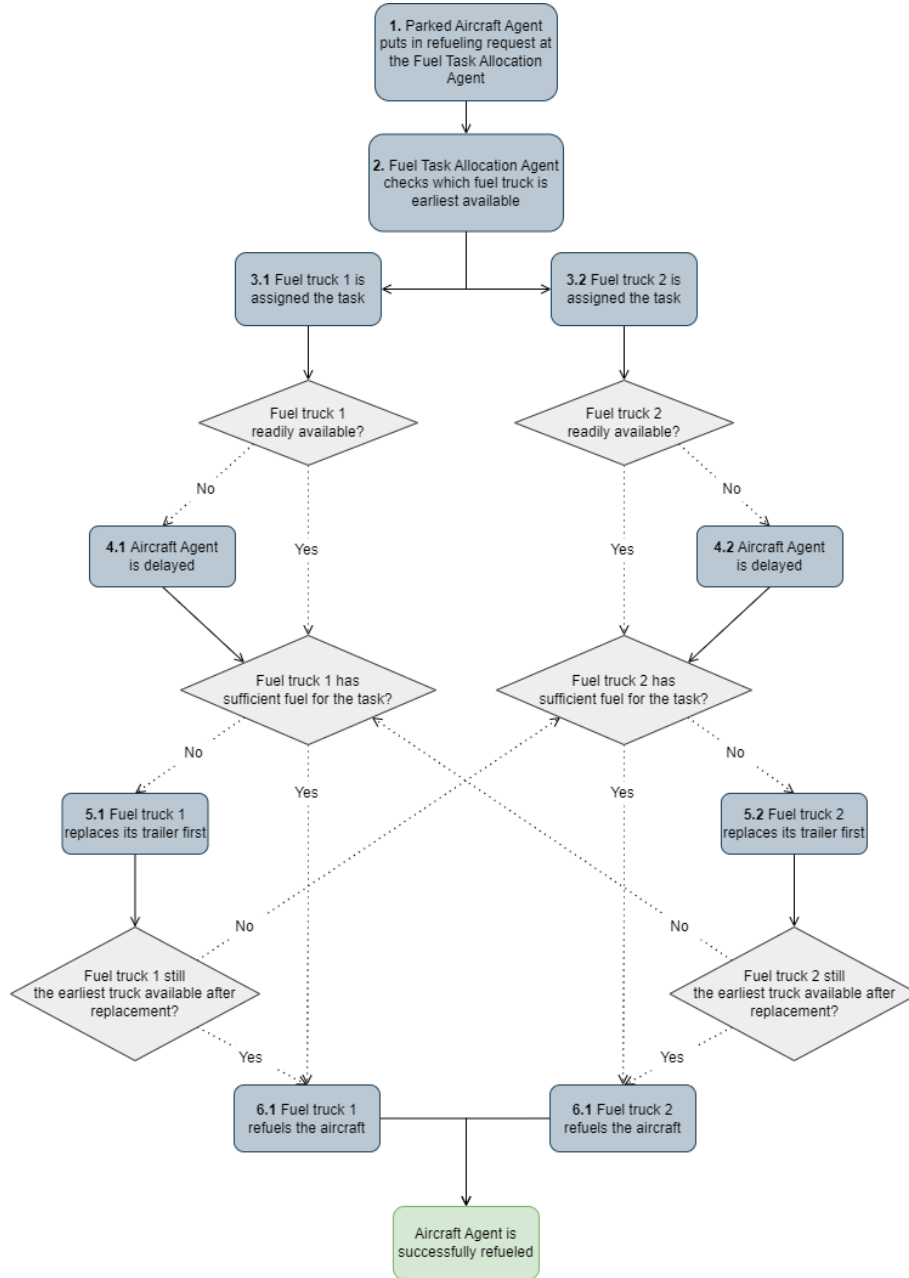


Figure 4: Fuel truck allocation framework used within the simulation model.

available truck, taking into account the additional time required for the trailer replacement. If it is still the earliest, the truck will immediately refuel the aircraft after the replacement. Nevertheless, if in the meantime the other fuel truck has completed its most recent task and is available earlier, this fuel truck takes over the fuel task in order to limit the delay of the aircraft.

4.3 Path-Planning

In order for both the aircraft and fuel truck agents to arrive at their destination safely, a reliable multi-agent path finding (MAPF) coordination approach needs to be selected for the multi-agent system model, ensuring no conflicts throughout the operations, while the paths lengths are minimized. To achieve this, the rule-based prioritized conflict resolution approach will serve as the high-level solver, combined with the A*-algorithm low-level solver. Within this coordination structure, the high-level solver determines the order in which the paths are planned, whereas the low-level solver is responsible for the actual planning of a path.

The high-level solver of the conflict resolution approach entails that every vehicle in the simulation will

be attributed a certain priority, used to determine which agent is allocated priority in case of a path-planning conflict. Namely, whenever a path is found using this approach, this path including all the timesteps is appended to the constraint table which is maintained by the path planning agent, including the priority of that vehicle agent. Thus, if a new aircraft or fuel truck agent is then planning its path and a node and timestep are corresponding with an existing path present in the constraint table which also has a higher priority, the vehicle agent will need to re-adjust its path. This can be done by either performing a waiting-action, or by taking an alternative path. In case of a conflict involving both an aircraft and fuel truck agent, the aircraft agent is always assigned priority, due to the time-pressure and more expensive delays. So, this conflict resolution approach can be characterized by a level of hierarchy. Given the context of this research, this technique was considered the most convenient and best representing the actual operations in which priority is also assigned, even though its dependence on the (random) order in which the priority is assigned might lead to sub-optimal results, as stated by Felner et al. [35].

There are many different paths that need to be planned during the simulation. For the actual planning of these paths, the low-level solver will be deployed. This includes both the paths of the aircraft agents, as well as those of the fuel truck agents. For all these instances, the start and goal node is known, but these do also require to be connected in the shortest way possible, defining the actual path. This fundamental step will be executed using the well-known A*-algorithm, of which the psuedo-code can be referred to in Supporting Work 8. The algorithm is relatively simple but extremely reliable and fast, and given that the number of vehicles to be simulated remains somewhat limited, it is highly suitable to this research [36]. In accordance with the algorithm, a suitable heuristic needs to be selected which can estimate the distance from a given node to the goal, as part of the algorithm. The nature of this heuristic influences the performance of the entire algorithm. Preferably, an admissible (underestimating) heuristic is selected since this is a guarantee to always find the shortest path. A heuristic can be made admissible by forming a relaxed version of the problem, using exact solutions to parts of the problems or by using inductive learning methods [37]. For this research, the Manhattan distance heuristic was deemed most useful as this heuristic calculates the distance between the current location (node) and goal location (node), based on a sum of the horizontal and vertical distance between these two nodes [36]. This technique is convenient given the discrete rectangular 2D graph, representing RTHA, which is used as the environment.

5 Experiments

In the following section, the experiments that will be simulated within the scope of this research will be introduced. First, the KPIs, related to the research objectives and selected to express the ground operations at an airport, are explained in subsection 5.1. Second, the actual experiments, including an overview of their relation to the associated research objectives, are provided in subsection 5.2.

5.1 Key Performance Indicators

When exploring the impact on the ground operations of different operational and infrastructural parameters using experiments, this impact can be expressed in terms of relevant KPIs, in order to be able to perform a quantitative analysis. Consequently, the following set of KPIs has been devised together with experts, which are presented together with their most relevant stakeholder(s) in Table 3.

As can be concluded from the table, during every simulated scenario, a total of seven KPIs will be measured. The KPIs can be divided into three different groups, being OTP, TAT and delays. Furthermore, the four different stakeholders are the airport, the airline, the ground handler and the passengers. In reality, the turnaround process is much more coordinated between all stakeholders, resulting in the interdependence of each stakeholder on basically all KPIs. Nevertheless, within this research, only the KPIs that directly impact a certain stakeholder are investigated. One common interest of all these stakeholders which is not mentioned above is safe ground operations of LH₂-powered aircraft. As this is a factor that is very difficult to quantify and would require a detailed safety risk assessment, it has not been incorporated as one of the KPIs. Nonetheless, by incorporating experiment 3 and 5 in this research which will be explained later in this section, the safety aspect is still accounted for.

Table 3: Overview of the key performance indicators calculated by the simulation model.

KPI	Airport	Airlines	Ground handler	Passengers
Total on-time performance (OTP)	✓	✓		✓
Average Jet-A1 A/C turnaround time (TAT)	✓	✓		
Average LH ₂ A/C turnaround time (TAT)	✓	✓		
Number of turnaround delayed Jet-A1 A/C		✓	✓	
Number of turnaround delayed LH ₂ A/C		✓	✓	
Average Jet-A1 delay duration		✓	✓	
Average LH ₂ delay duration		✓	✓	

Firstly, the OTP is defined as the percentage of flights that arrive and/or depart within 15 minutes of their scheduled arrival and/or departure time, including aircraft that exceed this time interval but have a legitimate reason such as bad weather [38]. This is important to both the airline and the passengers, as the airline uses it to present their reliability to passengers, while passengers in turn use the OTP to assess the reliability of the airline. Secondly, the average TAT is mostly relevant to the airport, as it influences their runway and stand occupation and hence airport fees generated. Additionally, for the airline, the turnaround time influences the utilization rate of their aircraft and hence also revenue [39]. Thirdly, the KPI group of delays includes both the number of turnaround delayed aircraft, as well as the average delay of these delayed aircraft per aircraft type. The number of turnaround delayed aircraft yields the aircraft that are delayed because of them having to wait for a fuel truck, either because the fuel truck needs to change its trailer or because it is over-occupied and still refueling other aircraft. An aircraft is categorized as delayed if the actual TAT is longer than the planned TAT, which is further explained in Supporting Work 3.3. The average delay duration simply means the length of this turnaround delay. This latter KPI group of delays is especially relevant to the ground handler, as this shows if there is a bottleneck in their operations, while also the airline is impacted negatively if a flight is delayed.

5.2 Experimental Overview

Within this research, a total of five different experiments will be simulated, in contribution to the research objectives which are related to the KPIs that have been introduced in subsection 5.1. Hence, it is useful to create an overview of what will actually be researched per experiment, as well as the relation between the experiments and research objectives. This is structured as follows:

- Experiment 1: Research objective O1.1 (2 number of LH₂ fuel trucks)
- Experiment 2: Research objective O1.2 (3 penetration rates)
- Experiment 3: Research objective O1.3 (3 safety zones)
- Experiment 4: Research objective O1.4 (4 LH₂ flow rates)
- Experiment 5: Research objective O1.5 (3 turnaround procedures)

In addition to the overview above, the combined outcomes of experiment 1-5 are used to fulfill research objective O1 and O2. For clarity, the five experiments can be distinguished into contextual experiments, varying the GSE, traffic and platform configuration, as well as experiments varying turnaround-related parameters. The former category includes experiment 1, 2 and 3, focusing on the number of LH₂ fuel trucks, the LH₂-powered aircraft penetration rate and the safety zone diameter respectively. The latter category refers to experiment 4 and 5 instead, in which the LH₂ flow rates and turnaround procedure sequence is alternated. Every simulation requires an input from each of the five parameters, which can be any of the scenario's within that experiment. For each combination of scenario's in the first category of contextual experiments, every scenario combination of the second category of turnaround-related experiments will be simulated using the model. An important remark is that the scenario of experiment 5 with no turnaround restrictions will not be simulated in combination with the scenario's of experiment 3 with a safety zone diameter of 30 meter and 45 meter, as it would be unrealistic to have low safety measures for the turnaround procedure itself, but high safety measures for surrounding aircraft. Another remark is that all combinations

of scenario's of the experiments are initially only simulated using one LH₂ fuel truck. Then, only the experiments in which the number of delayed LH₂-powered aircraft is more than zero will be simulated using also two LH₂ fuel truck, which is a decision that was made out of time considerations, but also to limit computational resources used. Namely, these additional simulations with two LH₂ fuel trucks potentially double the total number of experiments. In subsection 5.2.1, subsection 5.2.2, subsection 5.2.3, subsection 5.2.4 and subsection 5.2.5, each of the five experiments will be clarified in detail.

5.2.1 Experiment 1

The first research goal is to assess what the impact of a different number of LH₂ fuel trucks is on the KPIs introduced in subsection 5.1. With the introduction of LH₂-powered aircraft, RTHA also needs to facilitate refueling of LH₂. Based on the current operations at RTHA, refueling LH₂ using a fuel truck has been selected for this research. Clearly, at least one LH₂ fuel truck is required to be able to refuel the ZEROe turbofan. Nonetheless, with the uncertain impact of the penetration rate, LH₂ flow rate, safety distances and turnaround sequences on the KPIs, it might be more efficient to invest in a second LH₂ fuel truck. By analyzing the results using these two scenario's, it can be assessed whether the possible KPI improvements are worth the (financial) investment, which refers to research objective **O1.1**. In Table 4, the main characteristics of these different fuel trucks are provided.

Table 4: Characteristics of the different fuel trucks. Information retrieved from expert knowledge.

	Number at RTHA	Capacity [kg]	Trailer replacement time [min]	Taxi speed [km/h]
Jet-A1 Fuel Truck	2	34,440	2	25
LH ₂ Fuel Truck	1-2	3,500	5	25

As can be observed in the table above, especially the capacity and trailer replacement time are very different for the Jet-A1 and LH₂ trailer respectively. Due to the very low density of LH₂ with respect to Jet-A1, it is trivial that the required LH₂ in terms of weight is lower than Jet-A1. Nonetheless, the number of aircraft that can generally be refueled using one Jet-A1 trailer is still significantly higher than the number of LH₂-powered aircraft with one LH₂ trailer, as was learned from expert knowledge. This yields that the LH₂ fuel truck needs to replace its trailer more often, which is also assumed to be more time-consuming than replacing a Jet-A1 trailer, due to purging and chill-down. An important remark is that in contrast to a Jet-A1 trailer, it is assumed that a LH₂ trailer is replaced when its content is lower than 15% within this research, as below this threshold it becomes inefficient to cool the remaining LH₂ [11].

5.2.2 Experiment 2

Based on the developments, forecasts, interviews with internal experts at RTHA and the researches as explained in subsection 2.2, the following three scenario's for a penetration rate of LH₂-powered single-aisle aircraft in 2050 have been devised to establish experiment 2, in order to answer research objective **O1.2**.

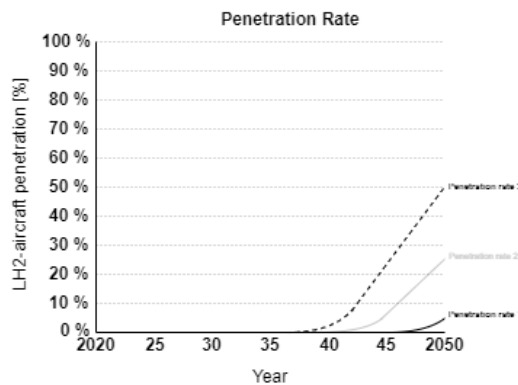
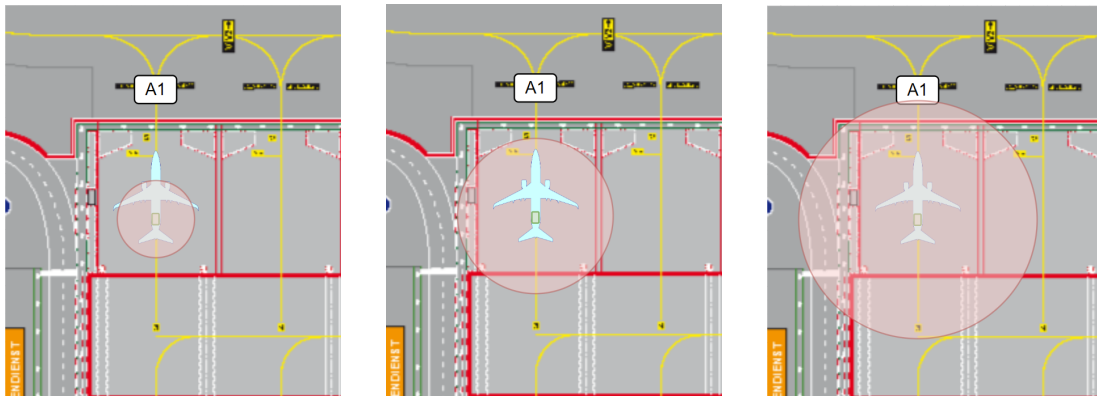


Figure 5: Forecasted single-aisle LH₂-powered aircraft penetration rates in 2050.

When considering Figure 5, the three different penetration rates for single-aisle LH₂-powered aircraft are provided for 2050. The y-axis represents the market share of these aircraft types within the single-aisle aircraft market, expressed in percentages. The actual penetration rate in 2050 is very dependent on when the turbofan actually becomes available. As can be seen in this figure, penetration rate 1 is the most conservative scenario, in which LH₂-powered single-aisle aircraft only start to be widely used in the industry from 2045. This results in a forecasted 5% market-share of LH₂-powered aircraft in 2050. The second scenario is intermediate, which predicts the LH₂-powered aircraft to be commercially available from 2040, five years later than expected, consequently having replaced 25% of all single-aisle aircraft by 2050. The final and most optimistic scenario assumes the LH₂-powered aircraft to be actually available from 2035 as planned by Airbus, leading to a forecasted 50% share within the single-aisle market by 2050.

5.2.3 Experiment 3

Following from the safety zone description in subsection 2.1.2, three different separation distances and hence safety zones have been selected whose impact on the KPIs will be considered in this research, part of research objective **O1.3**. The selected safety zones are an optimistic scenario with a diameter of 15m, an intermediate scenario with a diameter of 30m and a conservative scenario with a diameter of 45m respectively. These distances were established based on an interview with the safety expert from Schiphol Airport. The three different safety zones are depicted to scale on stand "A1" in Figure 6. These safety zones are comparable with other LH₂ safety margins used in the aviation industry as ordered by EASA [8], and together provide a good range to anticipate on the actual state of the fuel safety standards towards and including 2050. Based on an analysis of how the impact on the KPIs vary with the separation distance, the aviation industry can be consulted on an optimal safety threshold, which is part of research objective **O2**.



((a)) Safety zone radius of 15 meter. ((b)) Safety zone radius of 30 meter. ((c)) Safety zone radius of 45 meter.

Figure 6: Visual representation of the three selected safety zone diameters considered in this research.

The aircraft stands that are used in the figures at RTHA are ICAO size C aircraft stands, which are 45 meter wide and 55 meter long. In each of the three visualizations, the light blue LH₂-powered aircraft is depicted, together with the red circular fuel safety zone which is to scale. The different safety zones lead to three possible platform stand configurations with a varying number of LH₂ parking stands. As can be concluded from Figure 6(a), the fuel safety zone with a diameter of 15 meter does not exceed the aircraft stand and thus there is no interference with Jet-A1 or LH₂-powered aircraft in adjacent stands. This results in 12 available LH₂ aircraft stands, being the same maximum capacity as for conventional aircraft. In contrary to this, the fuel safety zones with a diameter of 30 and 45 meter both overlap with adjacent stands, which could potentially overlap with aircraft or GSE being parked there and result in an increased risk. Therefore, those adjacent stands must be temporarily blocked during the turnaround in which the LH₂-powered aircraft is being refueled under these safety zones, which significantly affects the stand capacity at the airport. In addition, for these two larger safety zones, the stands closest to the terminal building (being stand C1 and D1) will not be accessible for refueling LH₂-powered aircraft, out of safety and precautionary considerations. As a result, the safety zone diameter of 30 meter accommodates

six LH₂ aircraft stands, whereas the safety zone diameter of 45 meter only accommodates four LH₂ aircraft stands. This difference is because in the latter scenario, stand "A1" and stand "B1" are too close to other near buildings, which can therefore not be used by LH₂-powered aircraft. Lastly, in every of these three configurations, the conventional Jet-A1 aircraft can simply park in all remaining stands, given that these are not temporarily blocked because of LH₂ aircraft being refueled. For a more detailed explanation, including an overview of all available stands for each aircraft type per safety zone, refer to Supporting Work 2.1.2.

5.2.4 Experiment 4

Based on the sources referred to in subsection 2.1.1, discussions with experts and a forecast of the technological developments in the following decades, four different LH₂ flow rates have been selected which will be experimented within this research. The LH₂ flow rates that are considered for a regional airport using manual or (partial) automatic LH₂ fuel trucks to refuel single-aisle aircraft in and towards 2050 are:

- Conservative: 2.5 *kg/s*
- Intermediate: 5 *kg/s*
- Optimistic: 10 *kg/s*
- Reference: 15 *kg/s*

With these different values, it can be assessed what the impact of different LH₂ flow rates will be on the TAT and other KPIs of LH₂-powered aircraft as opposed to conventional aircraft, which is in line with research objective **O1.4**. In comparison, the Jet-A1 flow rate applied in the industry today which is also incorporated in the simulation model for Jet-A1 aircraft is 15 *kg/s* [40] [41]. Given that the density of LH₂ is very low and the amounts to be refueled into short-range single aisle commercial aircraft will remain limited, there is no need to consider LH₂ flow rates exceeding 15 *kg/s*. Namely, such flow rates would result in a huge reduction of the actual fuel time when compared to Jet-A1, making refueling no longer part of the critical path, while the cost would increase significantly because of the need for more powerful cryogenic pumps [11].

5.2.5 Experiment 5

In order to account for the possible turnaround sequence variations and safety developments which were introduced in subsection 2.1.3, but also to analyze the impact of different turnaround procedure sequences on the KPIs in accordance with research objective **O1.5**, the following three potential turnaround procedures of LH₂-powered aircraft in 2050 are considered. These turnaround procedure sequences can be visualized in Gantt-charts along with a detailed explanation in Supporting Work 2.2.

- **LH₂ Turnaround Procedure 1:**

The most conservative scenario assumes that no (semi-)automated or classified GSE turnaround processes are possible yet in 2050, possibly due to the extensive testing and qualification that this new GSE requires or due to legislation prohibiting its implementation. In this case, no turnaround processes shall be executed simultaneously with refueling LH₂, and parallel processes must be delayed such that these can be executed in sequence with refueling instead. This results in the most time-consuming turnaround procedure considered within this research.

- **LH₂ Turnaround Procedure 2:**

In a more optimistic scenario, some specific GSE are classified to safely operate in hazardous areas such as near or around LH₂ refueling operations. In addition, the refueling itself could be a semi-automated process in which the fuel hose is guided using a mechanical arm, allowing for a larger hose diameter and thus flow rate. (Dis-)connecting the fuel hose as well as purging and chill-down are considered to be significantly riskier than the actual refueling because of the chances of spills, and hence parallel turnaround processes are not allowed during these actions but only whilst actual refueling is ongoing, as was suggested in the FlyZero project [19]. As a result, some turnaround processes such as catering and cleaning can be executed in parallel with the actual refueling, resulting in a more time-efficient procedure than the first procedure.

- **LH₂ Turnaround Procedure 3:**

The most optimistic scenario would be no further limitations on the other turnaround processes while refueling is ongoing. This yields that all GSE are classified as safe to operate in hazardous areas, while also certain GSE processes such as the refueling itself are (partially) automated like an automated fuel arm, potentially allowing LH₂ flow rates of up to 10 and even 15 *kg/s*. This procedure leads to the shortest TAT and is also in range with conventional turnaround times at these high LH₂ flow rates.

6 Results

In this section, the results of the simulated experiments are provided. Initially, in subsection 6.1 the methods according to which the statistical significance of these results was established are presented. After that, the simulation results are categorized into three main groups. In order to analyze the outcomes of each of these groups, both contour plots and local graphical sensitivity analyses were utilized. An important remark is that for the local sensitivity analyses, the same seed was used to have a valid comparison. The first group is with regard to the turnaround time and will be discussed in subsection 6.2. The second group concerns the aircraft delays of both LH₂ and conventional Jet-A1 aircraft, which is treated in subsection 6.3. The last group considers the on-time performance of all aircraft, which will be further explained in subsection 6.4. Supplementary to the results discussed here, additional results regarding the flight schedule and platform configuration can be found in Supporting Work 6.1 and 6.2 respectively.

6.1 Statistical Significance

In order to have meaningful results, the statistical significance of the simulation model needs to be proven. Since the research applies a stochastic model, the first step in proving the statistical significance was to calculate the coefficient of variance, which is used as a threshold of when the data of a certain experiment has converged sufficiently to be subject to analysis. The second step in establishing the statistical significance was to perform statistical tests on the acquired data. This is necessary to prove that a certain experiment parameter has an influence on a given KPI, and to rule out that it is an apparent influence generated purely by chance. The statistical tests work by setting up two hypothesis, one stating that the experiment parameter **does** have an influence on the KPI, and one that the parameter **does not** have an influence.

A careful analysis of the datasets, consisting of the KPIs measured for the different experiments, led to the conclusion that this data is numerical and not normally distributed. In addition, the dataset of experiment 1 consists of two paired groups, whereas the datasets of experiment 2, 3, 4 and 5 consist of three paired groups. Consequently, on the dataset of experiment 1, the Wilcoxon signed rank test has been performed to test the hypothesis and prove the influence on the KPIs. Namely, this hypothesis test is suitable for datasets consisting of two groups, and uses a ranking technique to quantify the relationship between these groups, based on which the null hypothesis is accepted or rejected [42]. For datasets originating from experiment 2, 3, 4 and 5, the Friedman test was applied. This statistical test has a more diverse application, and is capable of quantifying the potential correlation of datasets consisting of more than two groups, which are subject to multiple parameter variations [43]. Like the Wilcoxon signed rank test, this test also incorporates a ranking technique to either accept or reject the null hypothesis. An explanation of the coefficient of variance and an overview of the statistical test results per experiment and KPI are given in Supporting Work 5.1 and 5.2.

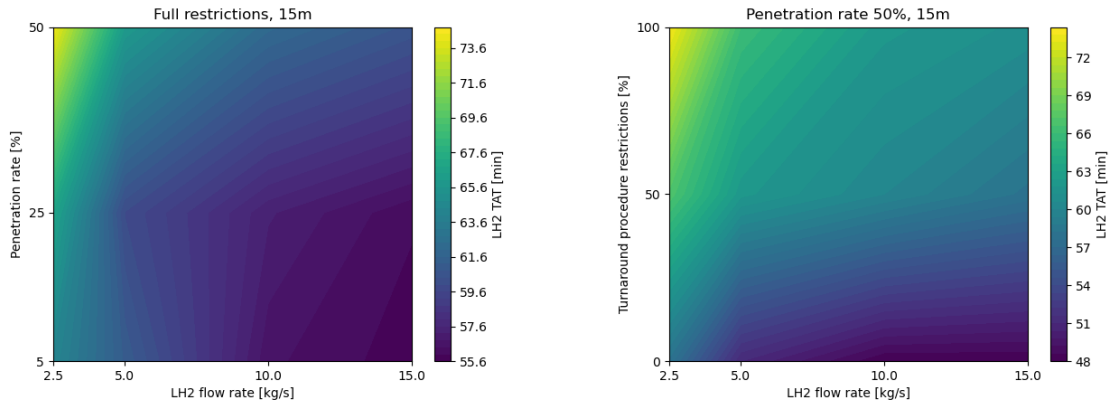
Based on the results of these statistical significance tests, it could be determined which experiments had a proven influence on which KPI. This was then used to select the strategy according to which the results could be analyzed, as part of the sensitivity analysis. Namely, for the KPIs that are dependent on multiple experiments, contour plots were applied to analyze the interdependence of variations within those experiments on the results. From this, the relative impact of the different experiments on the KPIs could be established, useful when consulting the aviation industry on the priority of each parameter as part of research objective O2. In contrast to this, on the KPIs that were proven to be dependent on only a single experiment, a local sensitivity analysis was selected as only the dependence on this specific experiment is of interest. Such an analysis yields only varying a single parameter. In the remainder of this section, the graphical sensitivity analyses of the most interesting results are presented per KPI group.

6.2 Total Turnaround Time

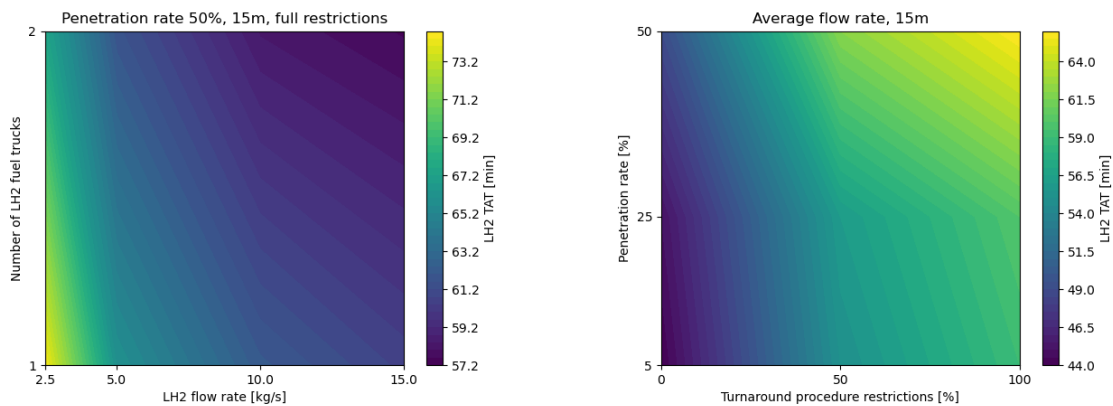
The first KPI group that will be analyzed within this research is the turnaround time. The main objective of this research is to explore the impact of LH₂-powered aircraft on the ground operations at a regional airport, especially on behalf of the airport and airlines. First, in subsection 6.2.1 the LH₂ TAT is analyzed using contour plots, due to its dependence on multiple experiments. Second, the Jet-A1 TAT, dependent on only a single experiment, is analyzed using a local sensitivity analysis in subsection 6.2.2.

6.2.1 Contour Plots of the LH₂ TAT

As the statistical tests proved the dependence of the LH₂ TAT on all five experiments, contour plots have been generated to better understand and analyze the impact of these experiments on this KPI, as well as the interdependence of the experiments. These contour plots are visualized in Figure 7. An important remark is that the safety zone diameter has not been included in this figure, as the interdependence of the LH₂ TAT on this experiment is almost identical to Figure 7(a). For illustration, the results in this section are presented using a penetration rate of 50% and one LH₂ fuel truck, as the experiment influences on the KPI become most apparent with this input. Above each plot, the inputs leading to the respective results shown in the visualization are stated. The objective within each contour plot is to achieve the lowest and thus most efficient LH₂ TAT, which corresponds with the darkest blue region within the plot.



((a)) LH₂ aircraft turnaround time with varying flow and ((b)) LH₂ aircraft turnaround time with varying flow rate and turnaround procedure.



((c)) LH₂ aircraft turnaround time with varying flow rate and number of LH₂ fuel trucks. ((d)) LH₂ aircraft turnaround time with varying levels of turnaround procedure restrictions and penetration rate.

Figure 7: Contour plots of the total turnaround time of LH₂ aircraft.

As can be concluded from Figure 7(a), the LH₂ flow rate and the penetration rate have an interdependence on each other, with the flow rate being the dominant factor. Logically, increasing the LH₂ flow rate reduces the fueling time and hence the average turnaround time. The increase from 2.5 to 15 kg/s leads to a

total LH₂ decrease of almost 30%, with the step from 2.5 to 5 kg/s being the most significant. On the contrary, increasing the penetration rate means more LH₂-powered aircraft at the airport, thus more demand for the single LH₂ fuel truck at the airport, hence introducing delays and therefore increasing the turnaround time. Namely, increasing the penetration rate from 5% to 50% increases the TAT by approximately 10%, making the process significantly less efficient, especially for penetration rates over 25%.

Next, the contour of the LH₂ flow rate and the turnaround procedure restrictions on the LH₂ TAT using one LH₂ fuel truck is depicted in Figure 7(b), with level of turnaround procedure restrictions clearly being the dominant influence. The turnaround procedure restrictions are expressed as a percentage of how many of the processes are not allowed to be executed in parallel with refueling the aircraft. Thus, the greater the percentage, the fewer processes can be executed in parallel such that these have to be executed sequentially instead, leading to a longer TAT. As becomes apparent from this plot, increasing the LH₂ flow rate from 2.5 to 15 kg/s is rewarding, with approximately 27% of LH₂ TAT decrease, with the biggest decrease going from 2.5 to 5 kg/s again. A further increase in the LH₂ flow rate to 10 kg/s already achieves the optimal LH₂ TAT in some cases. In terms of the turnaround procedure restrictions, lifting the restrictions from 100% to 50% has a small impact, compared to the 25% TAT reduction on average that can be achieved when decreasing the restrictions from 50% to 0%.

Moreover, Figure 7(c) represents the LH₂ TAT under a varying dominant LH₂ flow rate and number of LH₂ fuel trucks. As the number of LH₂ fuel trucks is increased, the demand of refueling LH₂ aircraft can be better accommodated for, hence reducing the delays and improving the LH₂ TAT. As can be concluded from this contour plot, increasing the number of LH₂ fuel trucks from one to two leads to an average LH₂ TAT reduction of up to 10% at most. Furthermore, using one fuel truck with a LH₂ flow rate of 15 kg/s results in a TAT that is also achieved with two fuel trucks at a flow rate of 6.5 kg/s each. The LH₂ TAT reduces significantly with a flow rate increase, being 22% when increased from 2.5 to 15 kg/s.

In Figure 7(d), the fourth and final LH₂ TAT contour plot is depicted. In this final figure, the contour between the level of turnaround procedure restrictions and the penetration rate is considered, using one LH₂ fuel truck with a flow rate of 8 kg/s. It is concluded that the worst TAT is achieved with the highest penetration rate, and thus refueling delays due to the high demand, together with the highest restrictions on parallel turnaround processes and therefore a more sequential and time-consuming turnaround. The main observation is that the LH₂ TAT is almost independent of the penetration rate when the turnaround procedure restrictions are lower than 50%. At a higher level of restrictions, increasing the penetration rate to 50% results in approximately a 10% longer LH₂ TAT. In terms of the turnaround procedure restrictions, going from 100% to 0% is awarded with about 30% TAT decrease.

From these analyses, the relative impact of each experiment on the LH₂ TAT can be concluded, such that the aviation industry can be consulted on which element of the ground operations must be given priority, part of research objective O2. In Figure 8, an overview of the maximum achievable impact of each scenario combined on the LH₂ TAT per parameter is provided, based on the results as presented in Figure 7.

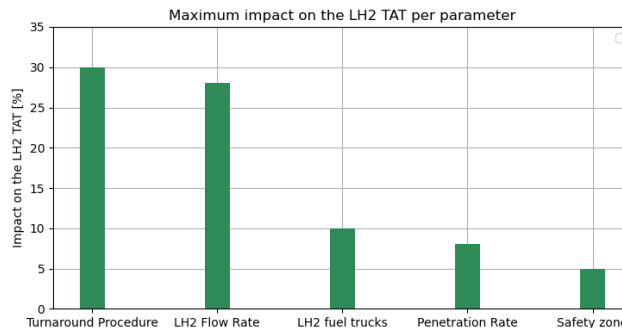


Figure 8: Maximum impact per parameter on the LH₂ TAT under the given contextual inputs.

From the figure above, it can be concluded that the experiments with the most severe impact on the LH₂ TAT are the level of turnaround procedure restrictions and the LH₂ flow rate, with about 30%. Clearly, these factors should receive the greatest attention from industry, as developments within these fields allow

for significant efficiency improvements regarding LH₂-powered aviation, which is crucial for a better and faster implementation of these aircraft types. Regarding the level of turnaround procedure restrictions, efforts should be made to reduce the level of restrictions to below 50%, which yields a LH₂ TAT reduction of 20% in many cases. In terms of the LH₂ flow rate, the minimal acceptable value of this parameter is 5 kg/s, which often results in a LH₂ TAT reduction of 10% already. A further LH₂ flow rate increase is desired, but more than 10 kg/s is not necessary, as this often results in a similar performance as 15 kg/s. The remaining parameters, being the penetration rate, number of LH₂ fuel trucks and the safety zone, individually account for a LH₂ TAT reduction of 5-10% at most. With respect to the number of LH₂ fuel trucks, the increase to two or more trucks is especially rewarding if the refueling technology has already developed to a LH₂ flow rate of at least 10 kg/s. Lastly, for the penetration rate to exceed 25% without any significant LH₂ TAT increases, the aforementioned developments of the other factors is required. In addition, the safety zone should also aim at 30 meters or lower to ensure an efficient LH₂ TAT.

6.2.2 Local Sensitivity Analysis on the Jet-A1 TAT

Another aspect of establishing the impact of LH₂ aircraft on the ground operations is assessing the impact on the TAT of conventional aircraft. In the statistical significance tests, it was established that solely the penetration rate has a proven influence on the TAT of Jet-A1 aircraft. Thus, a local sensitivity analysis is justified here. The figure depicting this relationship is provided in Figure 9.

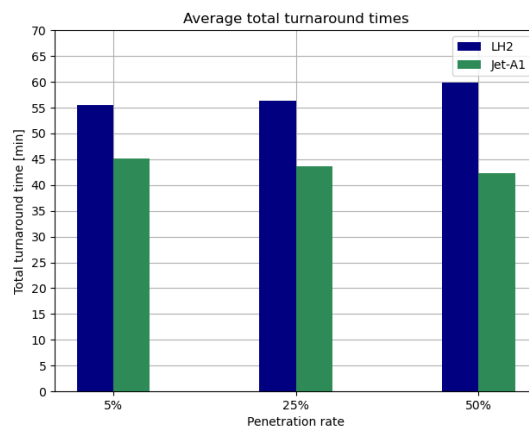


Figure 9: Average turnaround time of both LH₂-powered and Jet-A1 aircraft with increasing penetration rate.

As can be observed in the bar chart, the average LH₂ TAT is structurally higher than the Jet-A1 TAT, and thus less efficient under these conditions. The Jet-A1 TAT is reduced as the penetration rate is increased. Increasing the penetration rate from 5% to 25% reduces the Jet-A1 TAT with a little over 1 minute on average, and further increasing the penetration rate from 25% to 50% reduces the TAT with an additional 1-2 minutes. This observation can be explained by the fact that in case of a penetration rate of 5%, the two Jet-A1 fuel trucks are in fact not optimal to handle the demand without causing delays to the Jet-A1 aircraft. As the penetration rate increases, resulting in more LH₂ flights and less Jet-A1 flights, this Jet-A1 refueling demand is lowered, causing fewer delayed Jet-A1 aircraft and hence a reduced TAT. This will be further elaborated upon in subsection 6.3. In conclusion, introducing (more) LH₂-powered aircraft is beneficial to the operations of Jet-A1 aircraft in terms of the Jet-A1 TAT.

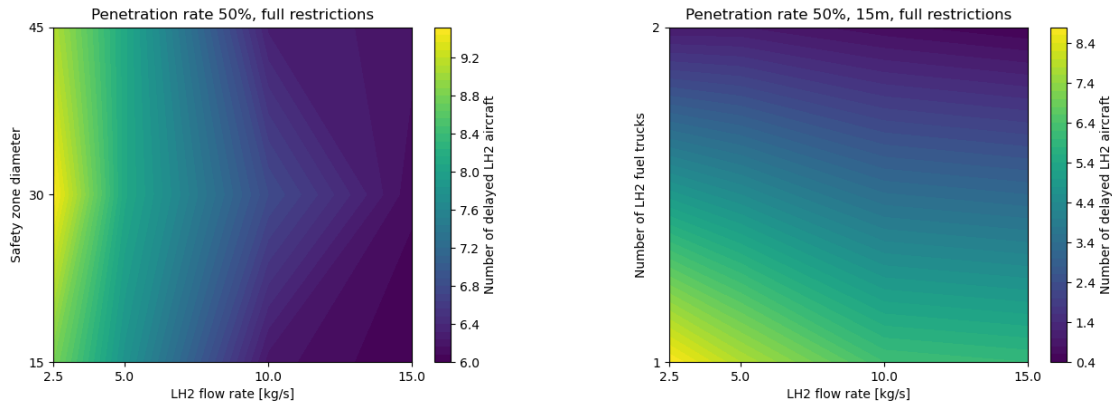
6.3 Aircraft Delays

The second KPI group that will be considered within this research are the aircraft delays. Namely, the impact of different experiments on these delays can identify important bottlenecks and provide insights in the introduction of LH₂-powered aircraft, which also explains why exploring this impact is part of the objectives of this research. For clarity, the aircraft delays are distinguished into the number of delayed aircraft due to waiting on the fuel truck, as well as the average delay duration of these aircraft. For each of

these two categories, conventional and LH₂ aircraft will be considered separately. As both categories of delay KPIs for LH₂ aircraft have a proven dependence on multiple experiments, a graphical sensitivity analysis using contour plots was applied again. This will be presented in subsection 6.3.1 and subsection 6.3.2. In terms of conventional aircraft, both type of delay KPIs are affected by a single experiment only and therefore a local graphical sensitivity analysis satisfies here, which is treated in subsection 6.3.3.

6.3.1 Contour Plots of the Number of LH₂ Delays

The different contour plots regarding the number of delayed LH₂ aircraft are visualized in Figure 10. The experiments which have a statistical proven impact on this KPI are experiment 1, 2, 3 and 4. If possible, all visual analyses regarding the LH₂ aircraft delays are done using a penetration rate of 50% since the delay effects are most apparent here, while the other penetration rates often lead to negligible LH₂ aircraft delays.



((a)) Number of delayed LH₂ aircraft with varying flow rate and safety zone diameter. **((b))** Number of delayed LH₂ aircraft with varying flow rate and number of LH₂ fuel trucks.

Figure 10: Contour plots of the number of delayed LH₂ aircraft.

Firstly, in Figure 10(a) the number of turnaround delayed LH₂ aircraft is depicted as a function of the LH₂ flow rate and safety zone diameter using one LH₂ fuel truck. As the safety zone diameter is increased, the number of delayed LH₂ aircraft tends to increase as fewer stands are available to LH₂ aircraft according to regulations. Whenever the maximum number of LH₂ aircraft is reached, incoming LH₂ aircraft will have to wait for a stand and are therefore delayed. For LH₂ flow rates especially up to 10 kg/s, the number of delayed LH₂ aircraft is almost independent of the safety zone diameter and mostly relies on the LH₂ flow rate, with an increase from 2.5 to 15 kg/s causing about 37% less aircraft delayed. The safety zone diameter on the other hand does not have many differences when ranging from 15 to 45 meter, except for a striking observation at 30 meter. Namely, for almost every flow rate, 15 and 45 meter have an equal number of delayed aircraft, while at 30 meter this number is **increased** up to 8%. The reason for 30m being the least efficient safety zone diameter can be explained by the law of diminishing returns. This law states that if you keep increasing a factor without changing any other input, at some moment a certain point is reached where an additional increase in this factor, being the safety zone diameter, results in a progressive decline of the output, being the number of delayed LH₂ aircraft in this case [44].

Next, the LH₂ flow rate in relation to the number of LH₂ fuel trucks is presented in Figure 10(b). Increasing both the flow rate but also the number of LH₂ fuel trucks makes the refueling process more efficient, therefore causing fewer aircraft having to wait to be refueled. When the LH₂ flow rate is increased but the number of LH₂ fuel trucks is kept at one, the number of delayed LH₂ aircraft is significantly reduced with a total of up to 30%, with the increase from 5 to 10 kg/s being the most rewarding, and higher flow rates causing no significant improvement. In contrary, keeping the LH₂ flow rate constant but increasing the number of LH₂ fuel trucks from one to two leads to a 83% reduction of delayed LH₂ aircraft.

In conclusion, the relationship between the number of delayed LH₂ aircraft and the four proven influential experiments becomes apparent from the contour plots above. Hence, the following overview, gathering the

combined maximum achievable impact of each of the experiments on the number of delayed LH₂ aircraft based on the results in Figure 10, has been developed.

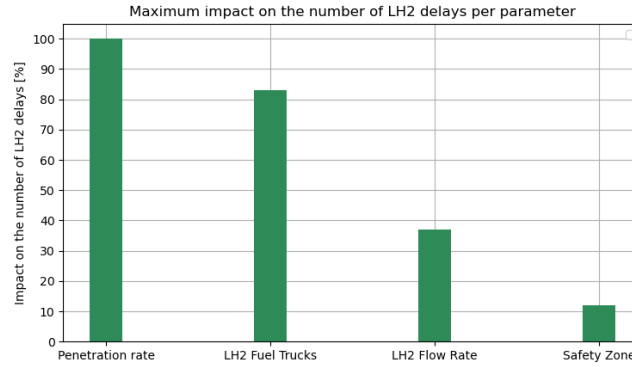


Figure 11: Maximum impact per parameter on the number of LH₂ delays under the given contextual inputs.

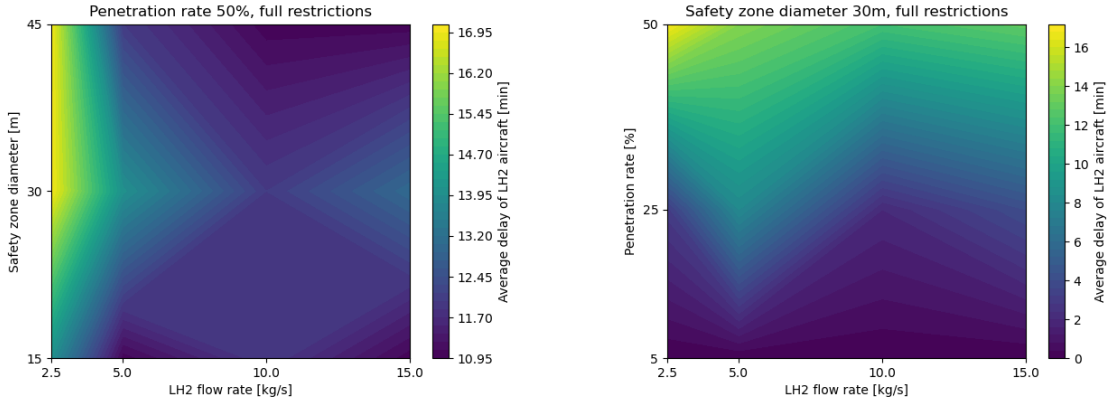
As can be seen in Figure 11, especially the penetration rate and the number of LH₂ fuel trucks are of great influence to the number of LH₂ delayed aircraft. The impact of the penetration rate on the number of delayed LH₂ aircraft is trivial and mostly linear, which is why no contour plot has been included, as this impact outweighs the impact of any other parameter. Namely, reducing the penetration rate from 50% to 25% leads to a decrease in delayed aircraft of 98%, while further decreasing the penetration rate from 25% to 5% results in an additional 2% decrease, totalling at 100%. Thus, when the penetration rate is increased to over 25%, in conjunction with the still relatively undeveloped conditions as mentioned above, exponential delays must be expected. This should be taken into account by the stakeholders when setting up the infrastructure for LH₂-powered aircraft at different stages throughout the transition. Increasing the number of LH₂ fuel trucks to two or more is one of the measures that can reduce the number of delayed LH₂ aircraft again at these high penetration rates, given its significant impact as well. Next up, the LH₂ flow rate has a much lower impact, but when combined with the previous two parameters, this can still be significant. A LH₂ flow rate of 10 kg/s is already almost optimal and a further increase to 15 kg/s is not directly necessary, especially given the associated significant investment costs. Lastly, the safety zone has a relatively low impact with at most 12%, but improvements here is still a valuable contribution.

6.3.2 Contour Plots of the Average LH₂ Delay

Next up, the following contour plot analysis concerning the average delay duration of LH₂ aircraft is illustrated in Figure 12. Likewise the previous contour plot analysis, four experiments have a proven relationship with this KPI, being experiment 1, 2, 3 and 4.

As becomes apparent in Figure 12(a), the dominant LH₂ flow rate is varied along with the safety zone diameter using one LH₂ fuel truck. Within this figure, a number of interesting phenomena occur. Firstly, at a LH₂ flow rate of 2.5 kg/s, the delay duration is the longest for the safety zones of 30 and 45 meter, since this causes the least LH₂ assigned stands and thus the longest waits. Furthermore, when the flow rate is increased to 5 kg/s, a significant reduction in delays can already be achieved of 27% in some cases, while at higher flow rates there is no significant improvement. On top of that, a flow rate of 5 kg/s in conjunction with the lowest safety zone diameter of 15 kg/s leads to an almost optimal average delay. At higher flow rates above 5 kg/s, several sub-optima can be found. Namely, for flow rates of 10 kg/s or higher, the average delay duration logically increases again when the safety zone diameter is increased from 15 to 30 meter, but decreases when further increasing the safety zone diameter from 30 to 45 meter, indicating signs of the law of diminishing returns again.

The second contour plot with respect to the LH₂ aircraft delay duration is provided in Figure 12(b), in which the LH₂ flow rate is varied along with the dominant penetration rate using one LH₂ fuel truck. The first observation is that at a penetration rate of 5%, the average delay is optimal with 0 minutes, irrespective of the flow rate. However, as the penetration rate increases, the average delay duration start



((a)) Average delay of LH₂ aircraft with varying flow rate and safety zone diameter. ((b)) Average delay of LH₂ aircraft with varying flow rate and penetration rate.

Figure 12: Contour plots of the average delay of LH₂ aircraft.

to rise, especially at a LH₂ flow rate of 5 kg/s. As the penetration rate increases further to over 25%, the average delay duration starts to increase significantly. However, the optimal LH₂ flow rate is 10 kg/s, which results in the shortest delay duration for all penetration rates. At a penetration rate of 50%, the delay duration is the greatest, with the longest delay in combination with a flow rate of 2.5 kg/s, a doubling of the delay at 25% penetration. However, a LH₂ flow rate of 10 kg/s still achieves the shortest delays.

As can be concluded from the contour plots as depicted above, the average delay duration of LH₂ aircraft is depending to a different extent on the different experiments. This is substantiated with the overview provided in Figure 13, in which the maximum combined impact of the different variations per experiment is totalled.

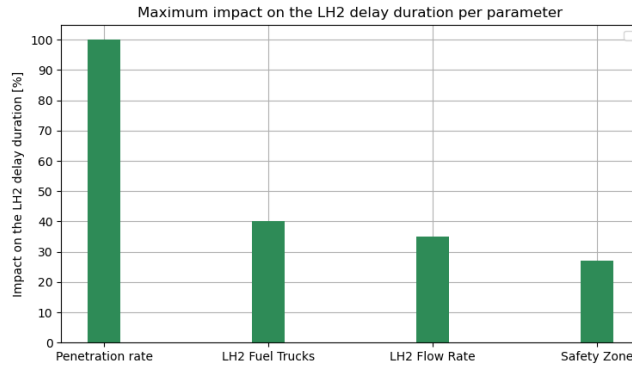
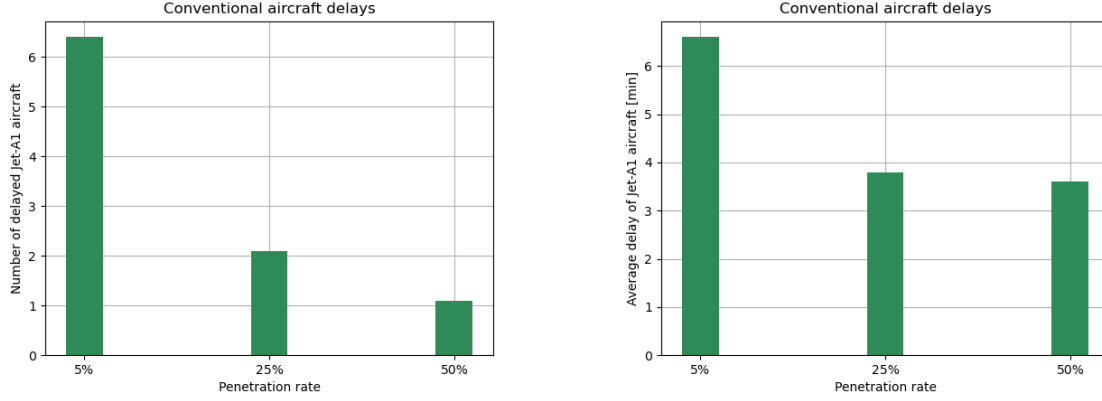


Figure 13: Maximum impact per parameter on the average LH₂ delay duration under the given contextual inputs.

As can be seen in the figure, this KPI is mostly depending on the penetration rate, in which a penetration rate of 50% introduces up to 17 minutes of average delay, in comparison to 0 minutes at 5% penetration. The intermediate scenario of 25% has average delays of around nine minutes. Thus, the other parameters should be selected and developed in such a way that this exponential delay duration at high penetration rates can be compromised, in order to be able to accommodate the efficient ground operations of LH₂-powered aircraft. The first option to do this is again by increasing the number of LH₂ fuel trucks to two or more, with a reduction in the average delay of up to 40%, making this investment very attractive. Next, the LH₂ flow rate must also be accounted for, as in some cases the difference between 2.5 and 15 kg/s is as high as 35%. In greater detail, a LH₂ flow rate of 10 kg/s is already optimal, and should thus be aimed for as a minimum, in order to minimize the delay duration. Ultimately, the safety zone diameter has the lowest impact again with a maximum duration decrease of 27% in certain cases, and 15 meter being the most desirable. A further discussion on the implications of this to the aviation industry will follow in section 7.

6.3.3 Local Sensitivity Analysis on the Jet-A1 Delays

Since only the penetration rate influences the conventional Jet-A1 aircraft delays, both in terms of the number of delayed aircraft as well as the average delay, a graphical local sensitivity analysis will be performed for these KPIs.



((a)) Number of delayed Jet-A1 aircraft with varying penetration rate. ((b)) Average delay of Jet-A1 aircraft with varying penetration rate.

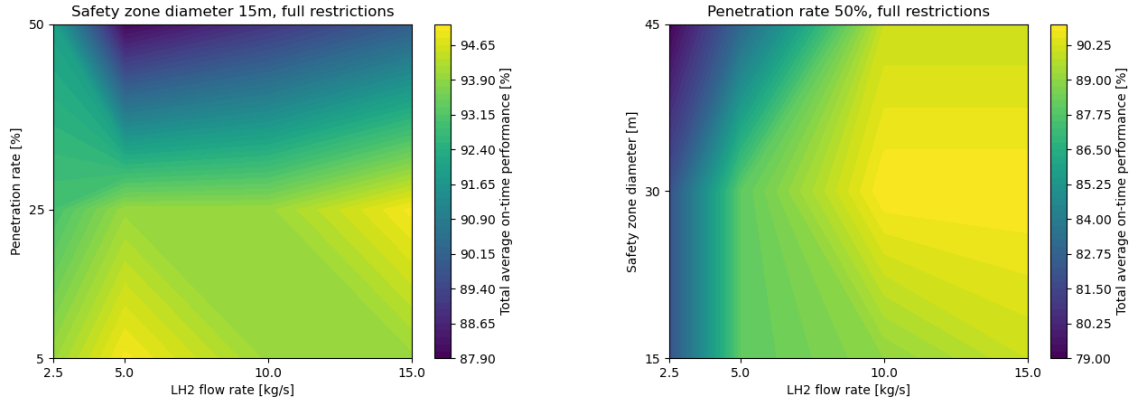
Figure 14: Local sensitivity analysis of the delays of Jet-A1 aircraft.

First of all, in Figure 14(a) the number of delayed Jet-A1 aircraft is displayed against the three different penetration rates that are considered in this research. The main observation is that as the penetration rate is increased, the number of delayed Jet-A1 aircraft is reduced significantly. Especially the increase from 5 to 25% yields almost a 70% reduction, while going from 25% penetration rate to 50% leads to another aircraft delayed less on average. The explanation for this is similar to the explanation for the reduced turnaround time in Figure 9. Namely, the greater the penetration rate, the less demand there will be for the Jet-A1 fuel trucks and the more demand for the LH₂ fuel trucks. As a result of this, the conventional Jet-A1 aircraft that are often delayed at a penetration rate of 5% will decrease with increasing penetration rates.

Secondly, the average delay duration of these conventional Jet-A1 aircraft is visualized in Figure 14(b) in relation to the penetration rate. A similar behavior can be observed as in Figure 14(a), with the average delay in minutes decreasing as the penetration rate is increased. At a penetration rate of 25%, the average delay has been reduced by almost three minutes on average with respect to a penetration rate of 5%, a reduction of more than 40%. When further increasing the penetration rate from 25 to 50%, the average delay reduction is almost negligible with only 0.2 minutes, and thus an optimum has been reached at 25% already. Thus, for this KPI the optimal penetration rate is 25%. Overall, the conventional aircraft number of delays and delay duration are impacted beneficially by the introduction of (more) LH₂-powered aircraft, as both the average duration and number of delays are decreased.

6.4 On-Time Performance

The final KPI group that is analyzed within the scope of this research is the OTP. Again, a very important KPI to the stakeholders, especially to the airlines and passengers but also to the airport and part of the research objectives. An important remark is that the OTP includes both conventional Jet-A1 and LH₂ aircraft, in contrast to the other KPI groups that were treated separately. In order to achieve the most apparent outcomes with the largest variation, a safety zone of 15m, turnaround procedure with full restrictions and a penetration rate of 50% were selected while using only one LH₂ fuel truck. Because the statistical tests proved the OTP to be dependent on experiment 2, 3 and 4 which are also interdependent on one another, contour plots were used for the graphical sensitivity analysis again, which are provided in Figure 15. Within the analysis, only the most significant and remarkable contour plots are treated.



((a)) Total average OTP with varying LH₂ flow and penetration rate. ((b)) Total average OTP with varying LH₂ flow rate and safety zone diameter.

Figure 15: Contour plots of the average OTP.

First of all, the average OTP as a function the LH₂ flow rate and penetration rate is provided in Figure 15(a). With a higher LH₂ flow rate, the turnaround of LH₂ aircraft has turned out to be faster and causing fewer and shorter delays amongst the LH₂-powered aircraft in the results discussed above, leading to an expected increase in OTP. As is concluded from the figure however, increasing the LH₂ flow rate from 5 to 15 kg/s only has a minimal impact on the OTP, with at most a 3% increase, only observed at high penetration rates. When concerning the penetration rate, which is the dominant influence in this case again, 5% penetration results in the highest possible OTP of 94% on average, 25% penetration results in an OTP decrease of at most 1%, but lastly at 50% the average OTP is significantly worsened with up to 6% compared to a penetration rate of 25%.

Secondly, in Figure 15(b) the average OTP along with the contour of the LH₂ flow rate and the safety zone diameter is depicted. Most notably, at flow rates between 2.5 and 5 kg/s, the OTP is the lowest, independent of the safety zone diameter, and responsible for an OTP increase of up to 6%. From 5 to 10 kg/s in which the OTP is increased by another 3% at most, the safety zone diameter also becomes dependent on the OTP, with 15 and 30 meter having a similar output, but when going from 30 to 45 meter the output worsens seriously with a decrease of up to 6%. Around 10 kg/s, for each safety zone diameter the OTP is relatively high and constant, causing further LH₂ flow rate increases to be negligible. At this LH₂ flow rate of 10 kg/s or higher, the OTP is optimal for a safety zone diameter of 30 meter.

In conclusion, the LH₂ flow rate has the most significant impact on the total average OTP, with over 10% in some cases. Especially the increase from 2.5 to 5 kg/s is rewarding, as this improves the OTP with up to 6%, and should thus be incorporated as a minimum requirement. Next, the penetration rate is also influential on the OTP, with up to 7%. Likewise the conclusion for the other KPI groups, it is also important in terms of the OTP to improve the other parameters, in order to be able to efficiently incorporate a penetration rate of 25% and ultimately also of 50%. This for example yields the highest possible flow rate or the lowest possible safety zone diameter. Even though the safety zone has a very limited impact on the OTP, it is still desirable to improve the safety zone diameter from 45 meter to at least 30 meter.

7 Discussion

As can be concluded from section 6, which parameter has the highest impact and should thus be focused on by a certain stakeholder throughout the transition towards LH₂-powered aviation is dependent on which KPI is of interest, part of the final research objective O2. Since the main and most influential stakeholders are the airports and airlines, these are the ones that will be considered in subsection 7.1 and subsection 7.2 respectively. For airport implications specially focusing on RTHA, refer to Supporting Work 7.1 and 7.2.

7.1 Airport Implications

The first important stakeholder that is impacted by the introduction of LH₂-powered aircraft is a regional airport. As was defined in Table 3, the KPIs that are mainly of interest to the airport is the OTP and the TAT, both of Jet-A1 and LH₂-powered aircraft. Namely, this influences the airport reliability, capacity, duration of the turnaround and hence the stand occupation, impacting the airport revenue and daily operations amongst others. The objective of the airport is to ensure a short TAT and high OTP, such that all aircraft are handled efficiently throughout the day, hence satisfying the airlines. Namely, (more) loyal airlines results in more flights operating, generating more revenue from passenger expenses at the airport, together with a greater revenue from airport fees charged to the airlines.

The statistical significance tests turned out that all five experiments have a proven effect on the LH₂ TAT, only experiment 2 has a proven effect on the Jet-A1 TAT and experiment 2, 3 and 4 have a proven effect on the OTP. As was established in subsection 6.2.1, the parameters influencing the LH₂ TAT most significantly were the level of turnaround procedure restrictions, together with the LH₂ flow rate. Furthermore, the penetration rate turned out to be the only influential factor on the Jet-A1 TAT in subsection 6.2.2. Lastly, the penetration rate and the LH₂ flow rate were the experiments with a severe impact on the OTP, according to subsection 6.4. The remaining parameters, being the number of LH₂ fuel trucks and the safety zone diameter, had a severely lower impact on each of these three KPIs. From this, it can be concluded that airports should prioritize research and be involved in developments especially regarding these three most influential parameters experiments.

First, potentially accommodating (semi-)autonomous or safety certified turnaround processes can be done by accommodating tests on airside to prove certain techniques or to obtain the required legislation, but also by initializing projects involving relevant companies involved in autonomizing (turnaround) processes and in the (safe) handling of hydrogen. A 50% parallel execution of certain turnaround processes such as semi-automated refueling, but also automated cleaning or catering, would yield significant LH₂ turnaround times and hence capacity improvements. Second, the airport can push the aircraft refueling industry to achieve a LH₂ flow rate of at least 5 kg/s during the transition, and at least 10 kg/s by 2050. This can be done by giving contracts to ground handlers or fuel suppliers that are working on such developments, in order to support these partners, but also by negotiating service level agreements with the ground handlers, demanding a certain minimum LH₂ flow rate by a given year. Autonomous refueling would be useful for this, allowing high LH₂ flow rates to be achieved more easily. Third, the airport can control its own penetration rate by allocating slots and communicating with airlines which aircraft types are deployed, in order to control the penetration rate to 25% at most under the initial conditions to limit the LH₂ TAT and OTP from degrading exponentially. Only when successes are achieved in the other fields, the penetration rate can be coordinated to increase further. In contribution to this, being able to increase the LH₂ aircraft penetration rate also reduces the Jet-A1 TAT. As a result of all these developments, both the Jet-A1 and LH₂ TAT can be potentially reduced while the OTP is potentially increased, contributing to the airport objective of accommodating fast and reliable turnarounds. This overall strategy would make LH₂-powered aviation easier to adopt for regional airports which allows for a better and faster transition.

7.2 Airline Implications

The second main stakeholder that is impacted by the introduction of LH₂-powered aircraft is the airline. In Table 3 it was established that all three KPI groups, being the TAT, the OTP and the aircraft delays, are relevant to this stakeholder. Namely, these parameters represent the entire operations of the airline, and hence the impact of introducing LH₂ aircraft on these KPIs must be analyzed. The TAT is important to an airline as this determines the utilization rate of the aircraft in the fleet, with a higher utilization rate leading to more possible flights in the same period of time, resulting in a greater revenue. Moreover, the OTP indicates the reliability of the airline, which passengers take into account when deciding which airline to fly with. In other words, the OTP also impacts the revenue. The OTP is also related to the turnaround delays of its aircraft, which is the last KPI. Namely, both the number of delays and average delay duration are extremely important to an airline, as delays can result in cancelled flights, expensive compensations,

(noise) fines for late arrivals and much more [39]. Eurocontrol has calculated that for every minute of ground delay, a cost of 0.30 euro per pax per flight is introduced to the airline. With an aircraft having an average of 180 passengers on board and being deployed on four flights per day, one minute of delay during each turnaround can cost an airline 80,000 euro per year for just one aircraft. Thus, minimizing the turnaround time, the number of delays but also the average delay is of utmost importance to the airline.

As was already discussed in subsection 7.1, the LH₂ TAT was proven to be mainly dependent on the level of restrictions on parallel turnaround processes and the LH₂ flow rate. Moreover, the Jet-A1 TAT is only influenced by the penetration rate. Furthermore, subsection 6.4 implied that mainly the LH₂ flow and penetration rate are relevant to the OTP. Continuing, the parameter influence on the KPIs related to aircraft delays was explained in subsection 6.3. This included the number of delayed LH₂ and Jet-A1 aircraft and the average delay duration, for which both the penetration rate together with the number of LH₂ fuel trucks are especially relevant. Lastly, the impact of the safety zone is minimal for all KPIs.

Out of the four influential experiments as reviewed above, the parameter that dominates the impact for almost all relevant KPIs is the penetration rate. Fortunately for the airline, this is a parameter that can be influenced themselves. Namely, it depends on how many LH₂ aircraft are purchased and operated by an airline, which dictates the penetration rate. The two other experiments which significantly influence the KPIs relevant to the airline are the LH₂ flow rate and number of LH₂ fuel trucks. These parameters must not be considered separately, but collectively instead, as more LH₂ fuel trucks is not necessarily always better. For example, two fuel trucks with a LH₂ flow rate of 5 kg/s would be less efficient than one fuel truck with a LH₂ flow rate of 15 kg/s in many cases. As these factors are mainly dependent on the GSE operated by the ground handler, the airline but also the ground handler would benefit from a closer relationship, such that objectives, intentions and technology updates can be communicated in an open and constructing fashion. In this way, the airlines can scale up the share of LH₂ aircraft within their fleet in accordance with the infrastructure provided by the ground handler, and in this way also better coordinate their penetration rate. In addition to this, the ground handler can also better coordinate when to upgrade the number of LH₂ fuel trucks to two or more, as well as when to use better cryogenic pumps to accommodate higher LH₂ flow rates. This will ultimately contribute to a faster transition and more efficient implementation of LH₂-powered aviation.

8 Conclusion and Future Work

This exploratory research has shown how the three most important KPI groups of airport ground operations are potentially impacted by the introduction of commercial LH₂-powered aircraft at a regional airport. By using different experiments to alternate five parameters, being the penetration rate, turnaround procedure, safety zone diameter, LH₂ flow rate and number of LH₂ fuel trucks, the associated variations with respect to the KPIs could be analyzed to find the parameter inputs leading to the most optimal impact during different stages of the transition period, using graphical sensitivity analyses. As a result of this, the following thresholds as gathered in Table 5 were concluded which can be taken into account by the stakeholders to ensure efficient ground operations involving LH₂ penetration rates up to 25%, as well as up to 50%.

Table 5: Overview of the minimum requirements of the different parameters to ensure efficient ground operations with a LH₂ penetration rate of 25% and 50% respectively.

	Penetration rate <=25%	Penetration rate <=50%
Level of turnaround restrictions	<=50%	0%
Safety zone diameter	<=30m	<=15m
Number of LH ₂ fuel trucks	=>1	>=2
LH ₂ flow rate	>=5 kg/s	>=10 kg/s

The first parameter is the level of turnaround restrictions, which potentially causes up to a 30% shorter LH₂ TAT when decreased from 100% to 0% restrictions. In terms of the safety zone diameter, a reduction from 45 to 15 meter would provide an almost 18% shorter LH₂ turnaround delay duration in minutes. However, for the majority of the KPIs, the impact of the safety zone diameter remains minimal. Next up, it was concluded that increasing the LH₂ flow rate from 2.5 to 15 kg/s accounts for a combined LH₂ TAT reduction of 28%. Whenever the penetration rate exceeds 25%, it is also worth the investment of a second LH₂ fuel truck in many cases, potentially reducing the average LH₂ turnaround delay in minutes by up to 40%. Ultimately, the most important parameter, being the penetration rate, must be carefully coordinated by both airlines and airports. Only in accordance with required developments of the other four parameters, efficient Jet-A1 and LH₂ ground operations with a penetration rate towards 50% or even higher could be possible towards 2050, in contribution to the decarbonization goals of the aviation industry in 2050.

This study serves as a framework for future studies on this topic. With the optimal range of each parameter being defined, it is recommended to execute additional experiments with (continuous but) smaller ranges of the penetration rate, LH₂ flow rate, more LH₂ fuel trucks and to introduce additional turnaround procedure variants to find better optima for different stages throughout the transition towards LH₂-powered aviation. By using better path-finding techniques like safe interval path planning but also by incorporating additional turnaround procedures, the simulation model can also be further enhanced. This can be substantiated with flight schedules based on more peak-days, featuring a better spread of the flights throughout the day, in order to account for a more diverse and hence more realistic operations while the infrastructure is utilized more efficiently. Ultimately, it is highly recommended to further investigate and improve the TRL of the different parameters, necessary to eventually operate commercial LH₂-powered aircraft.

References

- [1] International Energy Association. Aviation. 2022. URL <https://www.iea.org/energy-system/transport/aviation>.
- [2] International Civil Aviation Organization. Future of aviation. 2017. URL <https://www.icao.int/Meetings/FutureOfAviation/Pages/default.aspx>.
- [3] International Energy Association. Net zero emissions. 2020. URL <https://www.iea.org/reports/net-zero-by-2050>.
- [4] International Air Transport Association. Developing sustainable aviation fuel (saf). 2022. URL <https://www.iata.org/en/programs/environment/sustainable-aviation-fuels/>.
- [5] J. Mukhopadhyaya and B. Graver. Performance analysis of regional electric aircraft. Technical Report 1, ICCT, 2022.
- [6] T. Casinader. Avolon Forecasts Global Passenger Fleet To Almost Double By 2042, 6 2023. URL <https://simpleflying.com/avolon-global-fleet-size-double-2042/>.
- [7] Airbus. Hydrogen, 2022. URL <https://www.airbus.com/en/innovation/low-carbon-aviation/hydrogen#:~:text=If%20generated%20from%20renewable%20energy,by%2Dproduct%20of%20CO2%20emissions>.
- [8] European Union Aviation Safety Agency. Hydrogen and its potential in aviation, 2023. URL <https://www.easa.europa.eu/en/light/topics/hydrogen-and-its-potential-aviation>.
- [9] G. Llewellyn and V. Miftakhov. Hydrogen power - boldly going to the heart of climate-neutral aviation. Technical Report 1, ICAO, 2022.
- [10] NASA. Lh2 airport requirements study. Technical Report Amendment 26, NASA, 1976.
- [11] J. Hoelzen et al. H2-powered aviation at airports – design and economics of lh2 refueling systems. *Energy Conversion and Management: X*, 14, 5 2022. doi: 10.1016/j.ecmx.2022.100206.

- [12] J. Adler and J. Martins. Hydrogen-powered aircraft: Fundamental concepts, key technologies, and environmental impacts. *Progress in Aerospace Sciences*, 141, 8 2023. doi: 10.1016/j.paerosci.2023.100922.
- [13] International Civil Aviation Organization. Kpi overview. Technical Report 1, ICAO, 2016.
- [14] Airbus. Zeroe - towards the world's first hydrogen-powered commercial aircraft, 1 2023. URL <https://www.airbus.com/en/innovation/zero-emission-journey/hydrogen/zeroe>".
- [15] Z. Abdin et al. *Chapter 3.1 - Current state and challenges for hydrogen storage technologies*. Towards Hydrogen Infrastructure, second edition, 2024.
- [16] H2fly to apply lessons learned from liquid-hydrogen flights, 2023. URL <https://aviationweek.com/aerospace/advanced-air-mobility/h2fly-apply-lessons-learned-liquid-hydrogen-flights>.
- [17] Daimler Truck. Safe, fast and simple: Daimler truck and linde set new standard for liquid hydrogen refueling technology. Technical report, Daimler, 2024.
- [18] J. Mangold et al. Refueling of lh2 aircraft—assessment of turnaround procedures and aircraft design implication. 3 2022.
- [19] Boeing. Hydrogen infrastructure and operations. Technical report, FLYZERO, 2022.
- [20] D. Babuder et al. Impact of lh2 aircraft propulsion on commercial airline operations. 10 2023.
- [21] RIVM. Afstanden en gebieden. Technical Report 1, Rijksinstituut voor Volksgezondheid en Milieu, 2023.
- [22] V. Mantzaroudis et al. Computational analysis of liquid hydrogen storage tanks for aircraft applications. 2023.
- [23] J. Hoelzen et al. H2-powered aviation at airports – design and economics of lh2 refueling systems. 5 2022.
- [24] European Commission. Quiet and green: Why hydrogen planes could be the future of aviation, 7 2020. URL <https://projects.research-and-innovation.ec.europa.eu/en/horizon-magazine/quiet-and-green-why-hydrogen-planes-could-be-future-aviation#:~:text=For%20a%2045%2Dseater%20aircraft,747%2C%20according%20to%20Dr%20Kallo>.
- [25] P. Martin. Future global demand for hydrogen fuel in aviation could require more than half of all power produced in EU today, 5 2023. URL <https://www.hydrogeninsight.com/transport/future-global-demand-for-hydrogen-fuel-in-aviation>.
- [26] Rotterdam The Hague Airport. Capacity declaration rotterdam the hague airport summer 2021. Technical Report 1, RTHA, 2021.
- [27] Windfinder. Jaarlijkse wind- en weerstatistieken voor vliegveld zestienhoven, 2023.
- [28] Rotterdam The Hague Airport. Zakboek - safety & security. Technical Report 1, RTHA, 2023.
- [29] Airlines Inform. Embraer 190-2, 1 2016. URL <https://www.airlines-inform.com/commercial-aircraft/embraer-e190-e2.html>.
- [30] Airlines Inform. Boeing 737 MAX 8, 1 2016. URL <https://www.airlines-inform.com/commercial-aircraft/boeing-737-max-8.html>.
- [31] Airlines Inform. Airbus A320neo, 1 2014. URL <https://www.airlines-inform.com/commercial-aircraft/airbus-a320neo.html>.
- [32] Airbus. ZEROe, 1 2023. URL <https://www.airbus.com/en/innovation/low-carbon-aviation/hydrogen/zeroe>.
- [33] M. Schmidt. A review of aircraft turnaround operations and simulations. 7 2017.
- [34] A. Sharpanskykh. Ae4422-20 agent-based modelling and simulation in air transport, 9 2021.
- [35] A. Felner et al. Search-based optimal solvers for the multi-agent pathfinding problem: Summary and challenges. *International Symposium on Combinatorial Search*, 10(1), 2017.

- [36] Geeks for Geeks. A* search algorithm, 2023.
- [37] Engati. Admissible heuristic. <https://www.engati.com/glossary/admissible-heuristic>.
- [38] OAG. What is on-time performance (otp)?, 12 2023. URL <https://www.oag.com/on-time-performance-airlinesairports#:~:text=In%20aviation%2C%20an%20airline%20departure,minutes%20of%20the%20scheduled%20time>.
- [39] A. Cook et al. Evaluating the true cost to airlines of one minute of airborne or ground delay. Technical report, Eurocontrol, 2004.
- [40] FINAVIA. How is an aircraft refueled? Here are the facts, 11 2016. URL <https://www.finavia.fi/en/newsroom/2016/how-aircraft-refueled-here-are-facts#:~:text=The%20aircraft's%20fuel%2Dtanks%20are%20located%20on%20each%20wing&text=Once%20parked%2C%20trucks%20park%20under%20the%20wing%20of%20the%20aircraft.&text=æThe%20driver%20of%20the%20fuel,begins%20refueling%2C%20Bergman%20narrates>.
- [41] R. James. How Long to Refuel an Airplane? – 15 Most Common Planes, 1 2021. URL <https://pilotteacher.com/how-long-to-refuel-an-airplane-15-most-common-planes/>.
- [42] F. Wilcoxon. Individual comparisons by ranking methods. *Biometrics Bulletin*, 1(6), 1945.
- [43] M. Friedman. The use of ranks to avoid the assumption of normality implicit in the analysis of variance. *Journal of the American Statistical Association*, 32(200), 1937.
- [44] K. Montevigen. Diminishing returns. Technical report, Britannica Money, 2007.

Part II

Literature study **previously graded under AE4020**

Contents

List of Figures	iii
List of Tables	iv
Nomenclature	v
1 Introduction	1
2 Hydrogen in Aviation	3
2.1 Energy-Transition.	3
2.2 History.	5
2.3 Properties.	6
2.4 Hydrogen-Powered Aircraft	7
2.5 Different Hydrogen-Applications in Transport.	9
3 Ground Handling of Hydrogen-Powered Aircraft	11
3.1 Conventional Turnaround	11
3.2 Hydrogen Aircraft Turnaround	14
3.3 Turnaround Performance	26
3.4 Cost of Hydrogen.	29
4 Hydrogen Turnaround Simulation & Optimization Approach	30
4.1 Modelling Applications in Aviation	30
4.2 Multi-Agent Path Finding	32
4.3 Conflict Resolution Approaches	36
5 Research Proposal	44
5.1 Research Objective & Research Questions	44
5.2 Case-Study at Rotterdam The Hague Airport.	45
5.3 Research Methodology.	49
5.4 Research Planning	55
References	63

List of Figures

2.1	Global CO ₂ -emission in Gt of each transport mode, forecasted until 2070. Retrieved from [8].	3
2.2	Representation of the annual growth of aviation in terms of passengers from 2004-2022. Retrieved from [12].	4
2.3	Timeline of the main hydrogen applications in aviation. Retrieved from [19].	5
2.4	Main safety properties of LH ₂ versus Jet A-1. Retrieved from [27].	7
2.5	Schematic overview of the power-train of a hydrogen aircraft. Retrieved from [29].	7
3.1	Typical turnaround procedure of a B737. Information retrieved from [60][61][62][63][64][65].	13
3.2	GSE arrangement during B737 turnaround. Retrieved from [66].	13
3.3	Graphical representation of the spark-free zones during the dispensing of hydrogen. Figure retrieved from [27].	18
3.4	Visual representation of hydrogen dispensing operations at the apron. Figure retrieved from [80].	19
3.5	Visual representation of a scalable car-inspired hydrogen dispensing facility. Figures retrieved from [83].	20
3.6	Visual representation of a bunker-inspired dispensing facility. Figure retrieved from [84].	21
3.7	Flexible storage facility consisting of lined-up cryogenic trucks. Figure retrieved from [88].	24
3.8	The largest commercially available LH ₂ fuel tank today. Figure retrieved from [89].	24
3.9	Schematic representation of a large drone-oriented hydrogen refueling station at RTHA.	25
3.10	Visual representation of a conceptual mobile hydrogen dispensing truck, which is expected to be utilized in the later of the transition phase. Figure retrieved from [32].	26
3.11	Typical turnaround procedure of a LH ₂ narrowbody aircraft, in the early stages of the transition phase.	27
3.12	Typical turnaround procedure of a LH ₂ narrowbody aircraft, in the later stages of the transition phase.	27
4.1	Graphical representation of a 3-agent MAPF problem. Retrieved from [110].	33
4.2	Example of 9 different simple 2D-grids which can be used as the environment in a simulation. Figure retrieved from [111].	34
4.3	Visual representation of a vertex conflict. Figure retrieved from [107].	35
4.4	Visual representation of a swapping conflict. Figure retrieved from [107].	36
4.5	Schematic overview of the most relevant conflict-resolution approaches for MAPF. Information retrieved from [109].	36
4.6	Schematic visualization of the ICTS approach. Figure retrieved from [114].	38
4.7	An example of an agent travelling in an environment with two dynamic obstacles, using SIPP as the conflict-resolution approach. Figure retrieved from [115].	40
4.8	Schematic visualization of path-finding in a 2D-grid using the A* algorithm. Figure retrieved from [116].	42
5.1	Layout of Rotterdam The Hague Airport. Retrieved from [71].	46
5.2	Visual representation of the (temporary) fuel storage facility at RTHA.	48
5.3	Visualization of the supply-chain of LH ₂ to RTHA. Figure retrieved from [27].	48
5.4	Potential locations for different hydrogen facilities at RTHA. Figure retrieved from [122].	50
5.5	Graphical representation of initial ABS-simulation environment, based on the layout of RTHA.	52
5.6	Visual representation of an aircraft agent.	54

List of Tables

2.1	Most important properties of LH2 versus Jet-A1. Retrieved from [24].	6
2.2	Overview of ongoing projects to develop hydrogen-powered aircraft. Information retrieved from [32, 34, 35, 36, 37, 38, 25, 39, 40, 33].	8
3.1	Overview of the turnaround processes which are affected by the introduction of hydrogen. .	15
3.2	Table representing the liquid hydrogen Supply Chains for different airport sizes at different transition stages. Information retrieved form [27].	16
3.3	Spark-free zones for dispensing different types of fuel in different years throughout the transition phase. Information retrieved from [27] and [78].	17
3.4	Trade-off table representing the main (dis-)advantages of each hydrogen dispensing facility.	22
3.5	Different single hose refueling configurations with the accompanying refueling times. Information retrieved from [27].	22
3.6	Estimated kerosene and hydrogen TAT for different aircraft sizes and levels of turnaround process autonomy. Information retrieved from [27].	27
4.1	Trade-off table representing the main (dis-)advantages of each simulation technique.	32
4.2	Trade-off table representing the main (dis-)advantages of each MAPF solving approach. . . .	41
5.1	Forecasted traffic distribution with the associated noise penalty at RTHA in 2021. Information retrieved from [119].	45
5.2	Overview of the required GSE per aircraft, including stalling location and priority. Information retrieved from [101] and [121].	47
5.3	Project planning for master thesis.	57

Nomenclature

List of Abbreviations

ABS	Agent-Based Simulation	MILP	Mixed-Integer Linear Programming
AHM	Airport Handling Manual	ML	Machine Learning
AI	Artificial Intelligence	MP	Methane Prolysis
ANWB	Algemene Nederlandsche Wielrijders Bond	MTOW	Maximum Take-Off Weight
CBS	Conflict-Based Search	NASA	National Aeronautics and Space Administration
CCS	Carbon Capture and Storage	OPS	Operations
COVID-19	Corona Virus Disease 2019	PAX	Passenger
DES	Discrete Event Simulation	PEMEL	Polymer Electrolyte Membrane water Electrolysis
DOC	Direct Operating Cost	PRD	Pressure Relief Device
EU	European Union	REG	Regulation
FUE	Fuel	RTHA	Rotterdam The Hague Airport
GPU	Ground Power Unit	SAF	Sustainable Aviation Fuel
GSE	Ground Support Equipment	SIPP	Safe Interval Path Planning
IATA	International Air Transport Association	SMR	Steam Methane Reforming
ICAO	International Civil Aviation Organization	TAT	Total Turnaround Time
ICTS	Increasing Cost Tree Search	TRL	Technology Readiness Level
ID	Identity	TUR	Turnaround
IGOM	IATA Ground Operations Manual	USA	United States America
KPI	Key Performance Indicator	WAT	Water
LH2	Liquid Hydrogen		
MAHEPA	Modular Approach to Hybrid Electric Propulsion Architecture		
MAPF	Multi-Agent Path Finding		

List of Symbols

$1D$	1-Dimensional
$2D$	2-Dimensional
$3D$	3-Dimensional

Introduction

One of the biggest challenges for aviation that has been afflicting the industry for years now is its significant environmental impact. This environmental impact not only limits itself to CO₂ emissions, but also non-CO₂ emissions such as noise, NO_x, soot and contrails which arguably have an even worse contribution to the greenhouse effect [1]. In 2021, the aviation sector alone was responsible for over 2% of the global CO₂ emissions while also being one of the fastest growing travel-industries [2]. Namely, the number of aerial-passengers has been increasing steadily over the past decades and is expected to continue to increase at a rate of 4.3% per annum for the next 20 years [3]. The COVID crisis only temporarily delayed this growth, as the number of passengers is rapidly catching up again to pre-COVID values, yielding that there is no sign of an emission reduction anytime soon. With the announcement of the European Commission to achieve net zero CO₂ emissions by 2050 in order to limit the global temperature rise to 1.5 °C, action needs to be undertaken now [4].

Consequently, efforts have already been made by researchers in an attempt to reduce the impact of aviation on the climate. The main achievements include using more efficient or electric aircraft, replacing kerosene with sustainable aviation fuels [SAF] and aircraft being propelled using hydrogen. Aircraft using electric batteries is very positive as there is no emission at all, given that the electricity used to charge these batteries is green. The main disadvantage of this application however is the low energy-density of batteries, yielding a lot of additional weight, making it currently unsuitable for aviation. Furthermore, the second solution is using SAF to propel aircraft. The idea behind this concept is that instead of kerosene, an alternative fuel is used which has similar properties as kerosene but is partially generated from household or natural waste such as oil. The downsides however are that it is very expensive to produce, while also the emissions are still significant. Ultimately, the final innovation is thus aircraft being propelled using hydrogen. This fuel has the advantage of being very light, which is very useful in aviation, while having water as its only emission. The downsides however are the large volume of hydrogen, together with the novelty of the fuel in aviation which raises concerns about safety as well as its operational and economical feasibility. Nevertheless, many experts have declared hydrogen the most promising solution to reduce the emissions of global aviation.

Hydrogen as an alternative fuel for aviation has already been significantly researched in the late 70's and 80's of past decade, but was soon disregarded due to more promising rising techniques like electric flying and SAF. Also, at this time the severity of human impact on the environment was not publicly known yet. Only recently, hydrogen has been receiving more attention again mostly because of politics pushing to reduce the impact of aviation on the environment through strict regulations. This has led to a great number of researches especially into the technology behind aircraft being propelled through hydrogen, the supply-chain of hydrogen towards the airport as well as the required hydrogen-related infrastructure. Notwithstanding this, a significant research gap still exists in terms of operation, which will form the basis of this study. Namely, this study will include an overarching literature study which combines all the researched elements into one clear overview, and after that it will be put into practice through research using the case-study.

Based on all these developments, the following research objective for this master thesis, part of the curriculum of the master sustainable air transportation at the faculty of aerospace engineering of the Delft university of technology, has been established; To design and evaluate a simulation-based model to

optimize the ground operation of hydrogen-powered aircraft, focusing on the early stages of the transition period towards hydrogen-powered aviation between 2025-2035. As a case-study, Rotterdam The Hague Airport will be used who is partnering up with ZeroAvia and Shell to accommodate the first commercial hydrogen-powered aerial route starting in 2025. Through executing different simulation scenarios, varying in traffic distributions, aircraft types, refueling locations and procedures at RTHA, a comparative analysis can be performed. In this way, operational procedures, fundamental knowledge and valuable experience can already be established at an early stage which is useful in the further transition of aviation towards hydrogen. The simulations will be performed using an advanced AI model in which all ground movements of both conventional and hydrogen-powered aircraft are simulated as accurately as possible at RTHA. Using relevant KPI's to measure the performance of each scenario, the optimal airport layout and procedures can be selected, while also the impact of introducing hydrogen-powered aircraft on the overall airport capacity can be assessed, in order to identify potential bottlenecks in advance.

The first step of this master thesis is to perform a literature study. This literature study will consider and identify all relevant available studies and material, in order to understand the current developments of hydrogen and set the basis for the rest of this master thesis. Additionally, the research objective will flow naturally from the findings, limitations and recommendations of this existing literature. On top of this, the review is used to set the boundaries of the research which limits the scope, contributing to the overall quality of the results. First of all, the history of hydrogen in aviation together its properties, production techniques and current market-trends will be discussed in Chapter 2. Secondly, the turnaround procedure of both conventional and hydrogen-powered aircraft, together with the required infrastructure and potential refueling concepts will be reviewed in Chapter 3. Next up, in Chapter 4 the different available simulation and optimization techniques will be presented and explained together with a trade-off to select the most applicable approach for this research. Lastly, the research objective and questions, as well as the case-study at Rotterdam The Hague Airport, research methodology and project planning, defining the framework of this research, are all provided in Chapter 5.

Hydrogen in Aviation

This chapter starts with explaining the need for an energy-transition through the substitution of kerosene with alternative fuels such as hydrogen in aviation in Section 2.1. In order to gain a better understanding of hydrogen, its history in aviation and properties are discussed in Section 2.2 and Section 2.3 respectively. Thereafter, the working principle behind hydrogen-powered aircraft, including the current market-trends, are provided in Section 2.4, whereafter other hydrogen applications in transportation are briefly explored in Section 2.5. Together, this will serve as an introduction into the field of hydrogen-powered aircraft while it also sets the basis for the rest of this literature study.

2.1. Energy-Transition

Over the past few decades, humanity has become more and more aware of the ongoing climate change. The main effects such as temperature rise, a rising sea-level, health effects, more unpredictable weather but also natural disasters like floods are experienced in different parts of the world at increasing rates. With the EU setting up initiatives and providing associated funding, like net-zero CO₂ to be achieved in 2050 to limit the global temperature rise to 1.5 °C, its really all hands on deck in an attempt to reduce the emissions as fast as possible by reducing every possible emission-source [5]. One of the dominant contributors towards the global CO₂-emissions is the transportation sector. In 2019, the transportation sector alone was responsible for more than 8 Gt of CO₂ emitted, which is 21.6% of all CO₂ emitted by humanity in that year [6] [7]. The aviation industry was responsible for a total of 1.04 Gt of CO₂ in 2019, thus accounting for 13% of all transportation emissions and almost 3% of the global emission. In the following figure, the environmental footprint of aviation is presented in relation to the other transportation modes available and all impacts are forecasted until the year 2070. It must be noted that the dotted lines represent vehicles abruptly stopping using fossil fuels such as trains in 2050, thus explaining reducing trends of emitted CO₂ afterwards for that specific transportation mode.

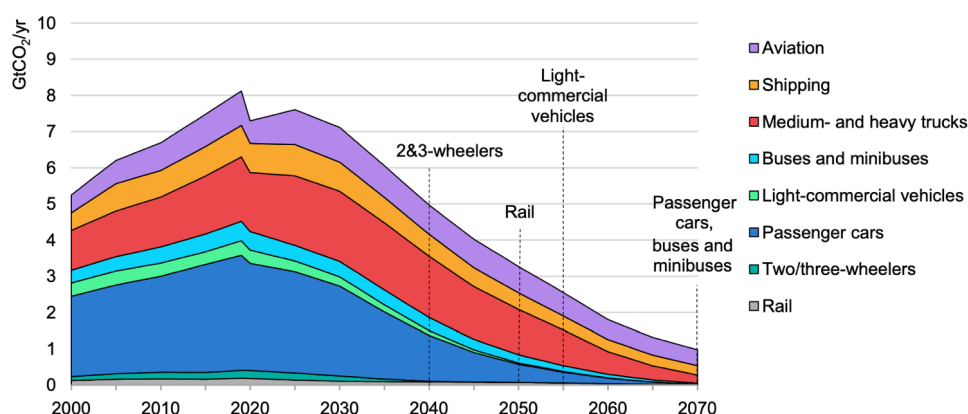


Figure 2.1: Global CO₂-emission in Gt of each transport mode, forecasted until 2070. Retrieved from [8].

As can be observed in Figure 2.1, the top three of most emitting transportation modes are passenger

cars, trucks and aircraft respectively. Even though there was a slight recession in emissions during COVID-19 around the year 2020, emission growth rates are quickly catching up again, underlining the necessity to undertake action as fast as possible in order to achieve the reductions forecasted in this figure. One important thing to note is that each transportation mode is expected to significantly reduce its emissions between now and 2070, with aviation being the only exception. Namely, whereas virtually every transportation industry has already made achievements in reducing its environmental footprint, like the introduction of electric cars, better and greener public transport facilities but also electric trains and busses, aviation keeps on lagging behind a bit [9]. This does not mean that no effort is made at all within the aviation industry to minimize its emissions, as there have been various green improvements in the past already. These improvements not only limit themselves to operational measures like optimized flight trajectories and higher load factors, but also technical innovations like a larger by-pass in the engines, lighter materials such as composites and better aerodynamics which together have improved the fuel efficiency of aircraft by approximately 2-3 % annually [10] [11]. Nevertheless, as a result of the market-competition between airlines, the rise of low-cost carriers and the consequent decrease in ticket prices, flying is accessible to more people than ever. As a result, the number of people flying every year is increasing at a greater rate than the rate at which the (fuel) efficiency is reduced, leading to a net increase in CO₂-emission compared to a reduction in all other sectors. This growth in aerial passengers can be visualized in the following graph.

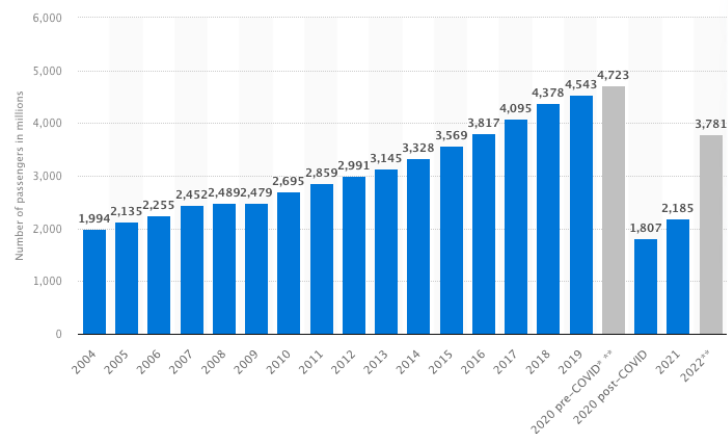


Figure 2.2: Representation of the annual growth of aviation in terms of passengers from 2004-2022. Retrieved from [12].

As becomes apparent in Figure 2.2, the number of aerial passengers worldwide has been increasing steadily over the past two decades. On average, the number of passengers increased with 5.5% per annum before COVID, yielding a likewise growth in number of flights. Taking into account the 2-3 % increase in aircraft efficiency as explained above and the fact that number of flights is directly proportional to the amount of CO₂ emitted, leaves a net increase in emissions of approximately 3%. Additionally, this only considers the CO₂ effects of aviation, while the non-CO₂ effects such as NO_x, contrails and soot which arguably have an even worse contribution to the greenhouse effect [1]. From this information, it can be concluded that the annual efficiency-improvement of aircraft is not sufficient to decrease its emissions, and thus greater measures need to be undertaken.

Recently, a lot of research has been devoted to identifying greater measures as such. The first potential solution is the use of Sustainable Aviation Fuels [SAF] to propel aircraft, in an attempt to reduce the carbon emissions. SAF refers to the usage of a combination of synthetic fuels together with bio or waste, to propel aircraft. Even though SAF emits approximately as much CO₂ as kerosene does, the mixture can result in up to 80% less CO₂ entering the atmosphere [13]. This is due to the fact that for example during the growth of this bio, CO₂ is extracted from the atmosphere in turn, resulting in a net lower environmental impact. The advantage of SAF is that it already has a very high technology readiness level, and its use has already been demonstrated by KLM who add 1% of SAF to the fuel system at Schiphol for every departing flight [14]. The main challenge however is that SAF is very cost-ineffective due to its high production cost, making it an unsuitable solution for the long-term, while also its environmental footprint reductions remain limited as opposed to different solutions [13].

Another potential solution to resolve the emissions coming from aviation is the use of battery-electric aircraft. The great advantage of this application originates from the fact that there are no emissions at all during operation of any kind, due to its electric characteristics. A compromise however is that this electricity must be generated completely green as well, in order to still contribute towards the emission reduction. Otherwise, it is simply a replacement of the problem as CO₂ is emitted nonetheless. Most importantly however, another concern of battery-electric aircraft is its low energy-density. With the current available batteries, the battery-mass required to be carried on board to supply sufficient electric energy is simply too high. In aviation, lightweight is extremely important to allow for efficient operation. Therefore, as long as there are no major improvements in the current battery-technology, battery-electric flying will be unsuitable to tackle the issue as concluded by J. Hoelzen et al. [15].

The final potential solution to make aviation more sustainable is the introduction of hydrogen as a fuel. Given that the hydrogen is produced in a green fashion, water is the only product emitted in-flight. Consequently, there is no CO₂-emission at all, as the emission only contributes to non-CO₂ effects such as contrail formation. However, due to the novelty of hydrogen as a fuel there still exists a knowledge gap in this field. Notwithstanding this, hydrogen is a very promising technique to propel aircraft because of its very high energy-density. The main challenge however is the infrastructure to operate hydrogen, as well as the operational procedures for both safe and efficient turnarounds of hydrogen-powered aircraft. Nonetheless, using hydrogen as a fuel shows the best potential in terms of scalability for long-term application [15].

2.2. History

Even though it is often considered as a very innovative substance, hydrogen has been around for a long time already. It was originally discovered in 1766 by the English physicist Henry Cavendish [16]. Nevertheless, it had already been widely used before that but it was simply not recognized as hydrogen yet. Back in these days, hydrogen was obtained in gaseous form and soon after its discovery, its production process of electrolysis was defined as well. Electrolysis is the operation in which gaseous hydrogen is formed through the application of an electric current to water, also forming gaseous O₂ as a by-product [17]. A few decades later, the reverse process of electrolysis was founded, yielding the birth of the fuel cell. The practice of the fuel cell is that whenever gaseous hydrogen and oxygen are mixed, an electric current together with water is formed via a chemical process [18]. This electric current can then be used for a wide variety of purposes and applications, while the hydrogen can be used as an ideal energy-carrier.

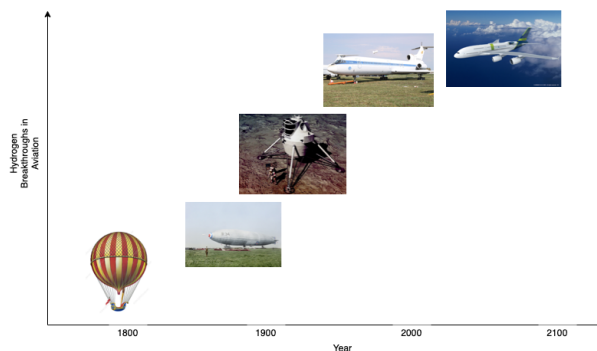


Figure 2.3: Timeline of the main hydrogen applications in aviation. Retrieved from [19].

The figure above presents the major breakthroughs of hydrogen-applications in the aviation industry. As can be seen in Figure 2.3, in the late 1800's the first efforts to utilize hydrogen in modes of aerial transportation were made. This was done through balloons being filled with hydrogen, providing sufficient lift-force to lift the basket underneath. These vehicles were very dependent on the wind though, since there was no other source of (horizontal) propulsion. In the period after this, the hydrogen-applications mostly limited themselves to the replacement of internal combustion engines with hydrogen fuel cells, being applied in road vehicles. Nonetheless, about a century later came the next major aerial application of hydrogen with the introduction of the zeppelin. Likewise the balloons as discussed before, these balloon-fashioned vehicles were also filled with gaseous hydrogen, which would keep the vehicle afloat, due to the extremely high abundance of hydrogen [19]. The zeppelin also had its own propulsion source, which was done using

a number of fossil fuel-run engines on the back. Due to the high flammability of hydrogen, which was sadly demonstrated at the Hindenburg disaster, the zeppelin was soon divested by society unfortunately. This, in combination with the fact that the best resembling gas, namely helium, was very expensive to obtain, meant the end of the commercial zeppelin-era [20].

In the 1950's came the reappearance of hydrogen in the aeronautical industry, with its application in propulsion systems of various space programs [19]. With the oil crisis of 1970 and the associated rise of oil prices at the time came the need for alternative fuels [21]. Therefore, scientists also considered the use of hydrogen in other transportation sectors such as aviation more thoroughly. Numerous researches were performed in the late 1900's which looked into hydrogen-propelled aircraft, due to its seemingly beneficiary properties. There were even test flights which explored the usage of hydrogen in real-life aircraft. An example of this is the Tupolev Tu-154 aircraft, which performed a successful test flight with one of its three engines being driven solely by liquid hydrogen [19]. Nevertheless, with kerosene being very effective to propel aircraft, its lower cost and high safety, but also due to the absence of environmental concerns at this time, further experiments with hydrogen aircraft were eventually called to a hold.

Only recently, hydrogen has regained attention from scientists with the rising efforts of humanity to reduce emissions and in this way limit the severity of climate change. With aviation being a main contributor to the global emissions and the limited results of other promising innovative solutions such as electric flying so far, hydrogen-powered propulsion is considered to be one of the most promising solutions. This is being accelerated by restrictions and targets implied by both national as well as international governmental organizations, with aims to achieve net zero CO₂ emissions in 2050 [22].

2.3. Properties

Even though it is globally observed that hydrogen will not solve climate change completely, its potential is very promising and when implemented in hybrid-form with other novel innovations, it can be a big step towards the right direction. Hydrogen is especially attractive as an aircraft-fuel due to its very low density which is extremely useful in a weight-optimization industry such as aviation, but also due to the fact that no greenhouse gasses are emitted during flight [23]. In the following table, the main properties of hydrogen and conventional kerosene are presented and compared.

Table 2.1: Most important properties of LH2 versus Jet-A1. Retrieved from [24].

Property	LH2	Jet-A1
Energy content per unit mass (MJ/kg)	120	42.8
Energy content per unit volume (MJ/L)	8.49	31.2
Density (kg/m^3)	71	811
Specific heat capacity (J/gK)	9.69	1.98

As can be concluded from Table 2.1, considering the density and energy content per unit mass, Liquid Hydrogen [LH2] is highly favourable over Jet-A1 (kerosene). The former is about 11 times as high for kerosene with a density of $71kg/m^3$ versus $811kg/m^3$ for LH2, while the energy content per unit mass is roughly 3 times as much for LH2 with respect to kerosene with $120MJ/kg$ compared to $42.8MJ/kg$ respectively. Notwithstanding this, it would be wrong to simply conclude LH2 to be the better option over kerosene based on these observations. Namely, as can also be seen in the table above, the energy content per unit volume is almost 4 times higher for kerosene when compared to LH2. Obviously, saving weight has always been one of the main objectives in aviation, since a weight reduction implies less fuel necessary, therefore smaller fuel tanks needed and thus a lower structural weight, initializing the famous snow-ball effect in aircraft design. Nevertheless, volume is another limiting factor inside aircraft and should therefore be considered thoroughly as well. 1 kilogram of gaseous hydrogen may hold up to 3 times as much energy as kerosene, but would require roughly 3000 times the volume as the same amount of energy being provided by kerosene. An alternative is to store the gaseous hydrogen in highly pressurized tanks of 700 bars, but in this scenario one still needs 6 times as much volume for hydrogen than for kerosene though, making it unsuitable as an aviation fuel [25]. Another solution however could be to liquefy the gaseous hydrogen, and in this way reducing the required volume even further. Hydrogen has a boiling

temperature of $-253\text{ }^{\circ}\text{C}$, yielding that lowering the temperature to below this boiling point results in LH2 [26]. At this point, the volume needed by this 1 kilogram of LH2 only needs about 4 times the volume required by kerosene, corresponding to the values as shown in Table 2.1 of 8.49MJ/L and 31.2MJ/L respectively, which is acceptable. This cryogenic state of hydrogen raises a number of concerns however, mainly regarding its safety and technical feasibility.

	Jet A-1 (kerosene)	Cryogenic hydrogen, LH ₂	Implications
Boiling Point ($^{\circ}\text{C}$)	167-266	-253	Frostbite, hydrogen boil-off, material embrittlement
Flammability Limits (%)	0.6-4.7	4-75	High likelihood of hydrogen fire, but higher concentration required to start it
Min. ignition energy (mJ)	0.25	0.02	High likelihood of hydrogen fire with weak sparks
Burning velocity (cm/s)	18	265-325	A hydrogen fire would burn out faster than a kerosene one
Buoyancy	-	14x lighter than air, rises at 20 m/s	Gaseous hydrogen disperses quickly
Self Ignition Temp ($^{\circ}\text{C}$)	210	585	Harder to ignite with pure heat
Fire heat radiative fraction	30-40%	10-20%	Hydrogen fires could be less destructive, as they radiate less heat, but present challenges due to invisible flame

Figure 2.4: Main safety properties of LH2 versus Jet A-1. Retrieved from [27].

These concerns become apparent through thorough consideration of Figure 2.4, in which the leaking characteristics of Jet-A1 and LH2 are summarized. The fact that LH2 needs to be stored in cryogenic conditions introduces a great challenge towards the aviation industry and pushes aircraft design to new limits. It is of great importance to keep this hydrogen temperature under the limit of $-253\text{ }^{\circ}\text{C}$, since a rise in temperature would boil the hydrogen, causing a significant pressure increase which could damage the fuel tank or even possibly lead to an explosion. Furthermore, as can be observed in Figure 2.4, the minimum ignition of LH2 is only 0.02mJ , more than 12 times less than conventional Jet-A1. This means that in case of a leakage, a spark containing just 8% of the energy that a spark needs to set Jet-A1 on fire, would be sufficient to light LH2. This also explains the high flammability limits of cryogenic hydrogen as opposed to kerosene. One top of that, hydrogen as a much higher burning velocity than kerosene, meaning that a hydrogen fire would propagate much faster which potentially introduces additional safety risks [28]. Nevertheless, a great advantage of LH2 in comparison with kerosene is that hydrogen has a very high buoyancy, yielding that it disperses very rapidly in case of a leak.

2.4. Hydrogen-Powered Aircraft

With hydrogen being a very promising fuel to reduce the climate impact of aviation, its technical feasibility must be evaluated first before operational aspects can be considered. There have been different studies already to evaluate the techniques that can be used to propel aircraft using hydrogen. A significant study was executed by M. Marksel et al. on behalf of the MAHEPA project, who defined the working principle behind a hydrogen-powered aircraft [29]. A schematic description of the power train for a hydrogen-powered aircraft is provided in Figure 2.5.

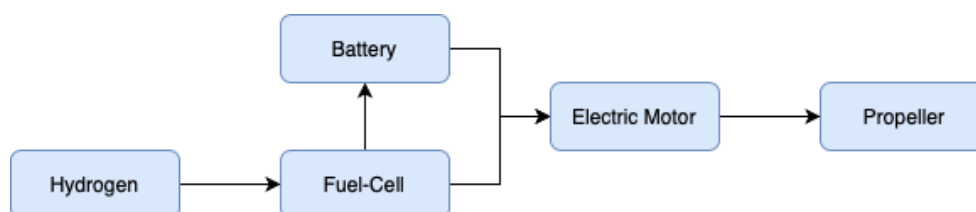


Figure 2.5: Schematic overview of the power-train of a hydrogen aircraft. Retrieved from [29].

As can be visualized in the the overview above, the sole fuel used by the aircraft propulsion system is hydrogen. The hydrogen can both be stored in gaseous-or liquid form, based on the aircraft configuration. Depending on its state, the hydrogen can then either be supplied directly into the fuel-cell, or must first be boiled, since the input of the fuel-cell typically must be gaseous. The former structure has the advantage of being more light-weight, as it discards the necessity of an on-board boiling facility, but requires larger fuel tanks to contain the more volumetric-demanding gaseous hydrogen. The latter structure has the advantage of requiring a lower tank volume to carry the liquid hydrogen, but the cryogenic properties introduce more complex subsystems while also a boiling facility should be carried on-board.

The fuel-cell converts hydrogen and air into electric-energy and water vapour through a reverse electrolysis, as gaseous hydrogen and oxygen react to form water, which is examined in great detail by S. Mekhilef et al. [30]. Once this electric current is generated, part of the electricity goes directly towards an electric motor, while the rest is stored in a battery which is integrated in the propulsion system for redundancy purposes [29]. In case of a low-throttle setting by the pilot, part of the electricity is stored in the battery, such that whenever the fuel-cell can not supply sufficient power to the electric motor during a high-throttle setting, the battery can provide additional power. The electric motor ultimately drives the propeller, by which the aircraft is actually propelled in the end. Besides being completely carbon-free, hydrogen aircraft also contribute to the environment through their very low noise which potentially allows for a reconsideration of the number of airport movements, considering the noise restrictions near populated areas [31].

2.4.1. Market-Trends

A number of initiatives have already taken-off regarding the actual development of hydrogen-powered aircraft. Due to the novelty of the application, there still exists a wide variety in terms of aircraft types, stage of development but also the state of hydrogen used inside the aircraft, underlining the lack of standardization. Therefore, the following table provides a clear overview of all ongoing projects in the field of developing hydrogen-powered aircraft.

Table 2.2: Overview of ongoing projects to develop hydrogen-powered aircraft. Information retrieved from [32, 34, 35, 36, 37, 38, 25, 39, 40, 33].

Organization	Aircraft Type	Seats	Range [km]	H2 State	Fuel Cell [kW]	Retrofit (Y/N)	Year Into Service	Origin
ZeroAvia	Dornier-228	9-19	480	Gas	600	Yes	2025	UK&US
H2-Fly	Dornier-238	40	2000	Liquid	TBD	Yes	2025	DE
Universal Hydrogen	ATR72 & DHC-8	40-80	TBD	Liquid	1600	Yes	2025	US
ZeroAvia	DHC-8	40-80	1100	Liquid	2000	Yes	2027	UK&US
Conscious Aerospace	DHC-8	40-80	TBD	Liquid	2100	Yes	2028	NL
Airbus	ZEROe	<100	>1600	Liquid	TBD	No	2035	FR

As can be seen in Table 2.2, the first commercially available hydrogen-powered aircraft are expected to go into service in the year 2025. Because of the novelty of hydrogen in aviation, the coming years are mainly focusing on the exploration and transition towards hydrogen before full commitment to hydrogen as a fuel is shown. This is reflected in the aircraft types that will be used by the different initiatives. Rather than designing an entirely new aircraft type, development will first mainly be limited to retrofitting existing aircraft types as can be seen in the table above. At the end of this transition phase once working principles have been established and procedures are ought to be more standardized, Airbus is planning on becoming the first company to actually launch a completely new design in 2035. In the meantime, the retrofitted aircraft will increase in size and number of seats, while also the fuel cells are getting increasingly powerful.

ZeroAvia has proven the suitability of gaseous hydrogen to propel aircraft with their first flight partially powered by a hybrid hydrogen-electric powertrain [32]. The aircraft that was used for this flight test was a Dornier-228, with a capacity of up to 19 passengers. Instead of designing an entire new aircraft, ZeroAvia chose to retrofit an old conventional Dornier-228 with a pair of electric motor-driven propellers, while fitting

a high-pressure hydrogen tank (700 bar) in the back of the fuselage. The aircraft has a range of 250 Nm, which could replace short regional flights in the near future. By using already existing aircraft for the transition towards hydrogen flying, the time to market is reduced significantly while also fundamental knowledge regarding operation, ground handling, on-and off-site infrastructure can already be obtained to accelerate the learning curve. Through scalability, increasingly larger aircraft, such as the DHC-8 in 2027, can then be introduced until eventually entirely new designs can replace conventional commercial aircraft.

H2-FLy, Universal Hydrogen and Conscious Aerospace have resembling ambitions, but instead of concentrating their focus on the more readily available gaseous hydrogen, they are all planning on utilizing the more volumetric-compact liquid state of hydrogen. Due to the more complex storage, handling and production of liquid hydrogen, the year of service that these companies foresee is somewhat delayed with a few years though. Nevertheless, through advancements in fuel cell capacity during these years, they can introduce these LH2 power plants on larger aircraft already such as DHC-8-like sized aircraft.

Another example of hydrogen-powered aircraft put into practice comes from Airbus, who are aiming to launch the world's first newly designed hydrogen-powered commercial aircraft in 2035. They are currently working on 3 different concepts; a turbofan, turboprop and blended-wing body aircraft. The turboprop working principle will be similar to Figure 2.5 and the other initiatives which are presented in the table above, whereas the turbofan aircraft has two potential types of propulsion. Either the hydrogen is combusted in a gas turbine, or a hybrid-electric architecture is selected in which the hydrogen gas turbine is combined with fuel cells delivering electricity [39]. Currently, tests on engines and other hydrogen-related subsystems are planned to be performed on the A380 MSN1 test-bed aircraft of the aircraft manufacturer, on which a fifth engine can be mounted to gather in-flight performance data [41].

In the long-term future however, hydrogen-powered aircraft are likely to adopt transformations in terms of configuration with respect to the (retrofitted) conventional aircraft of today. Namely, conventional aircraft usually carry around 25% of its MTOW in fuel. Nevertheless, as was clarified in Section 2.3 hydrogen is very light, yielding only a very slight difference between the weight of the aircraft with and without the fuel [42]. Consequently, the use of hydrogen allows for a much lower structural weight of the aircraft, resulting in a smaller wing area amongst others as found by D. Verstrete, which could result in an alternative vehicle approach during the turnaround or different operational procedures [43]. Another ongoing consideration is the elongation of the existing fuselage, in order to provide sufficient volumetric storage for the hydrogen while limiting the sacrifice in number of seats [37]. This could in turn also influence the gate location and ground operational strategies. While designing a concept of operations for the turnaround hydrogen-powered aircraft, the potential adjustment of aircraft configurations should be accounted for via the use of modular simulation and optimization methods.

In order to account for the different aircraft that are expected to be launched throughout the transition phase towards hydrogen propulsion, 3 different aircraft types will be included in this research. This includes a D-228 in the early stages, followed by a DHC-8 and ultimately a B-737-like aircraft such as the ZEROe.

2.5. Different Hydrogen-Applications in Transport

Hydrogen has already been widely used in other transportation industries, which for example have a lower safety benchmark or use the hydrogen for different applications. While matters such as ground handling of hydrogen-powered aircraft are still extremely novel, for other industries these infrastructures and operational procedures are already significantly more mature which sets a useful basis for the aviation sector. Some other transportation sectors which are also still in the exploratory phase and can benefit from advancements elsewhere are hydrogen-powered boats and drones, which can all collaborate in order to achieve the joint goal of being CO₂-neutral in 2050.

The oldest significant application of hydrogen is the propulsion of space applications. For different Apollo missions in space, liquid hydrogen was used as rocket fuel to propel numerous booster-and thruster applications due to its high energy and light weight [44]. A large difference between space and aircraft applications is that in the former case, a cryogenic hydrogen tank is designed to withstand a very small number of flight cycles, whereas in aviation such a tank would need to be designed and certified to last for tens of thousands of flight cycles, yielding both a refuel and thermal cycle [25]. Even though the design is fundamentally different in both cases, there also exist similarities, especially in the operational aspect. For example, the refueling of cryogenic fuel tanks, storage, supply or safety regulations for ground handling

personnel are extremely relevant and pose a good first order insight for hydrogen-propelled aircraft such as the retrofitted Dorniers, DHC-8 and eventually ZEROe. Several studies have also been executed by NASA to assist in the extension of hydrogen-applications from space-vehicles towards aircraft, such as the required airport infrastructure to support hydrogen aircraft and the storage of hydrogen in aircraft [45] [46].

The first commercial application of hydrogen in transportation came a few decades later, with the introduction of hydrogen-powered cars. Today, there already exist over 56,000 hydrogen-powered cars which can be refueled at over 800 sites world-wide, mainly situated in Korea and the USA [47]. This further-developed refueling infrastructure and distribution system is also what is of most interest to the aviation industry. In general, hydrogen-powered cars make use of gaseous hydrogen which is refueled into the tank of hydrogen cars at a pressure of 700 bars [48]. Elements of the operational procedure behind this, such as fuel storage, fuel hose connection mechanism and safety measures are extremely relevant and thus can assist in setting the standards for aircraft-applications like the hydrogen-powered D-228 of ZeroAvia, which is also fueled with gaseous hydrogen.

Ground Handling of Hydrogen-Powered Aircraft

This chapter will first clarify the operational procedure behind a conventional turnaround in Section 3.1, including all relevant processes and regulations, in order to later introduce the turnaround of a hydrogen-powered aircraft, in Section 3.2. This latter section includes all affected procedures, applying safety regulations, different dispensing concepts and required infrastructure for operating hydrogen during a turnaround. Thereafter, the effect of hydrogen on the turnaround performance, as well as on the performance of the airport as a whole is treated in Section 3.3. Ultimately, in Section 3.4 the implications of hydrogen on the cost such as the fuel cost and airport fees will be shortly discussed.

3.1. Conventional Turnaround

The turnaround process is a very elaborate and critical process whose execution is fundamental for efficient aircraft operation. An aircraft turnaround literally yields *'the physical process of preparing an aircraft in the period it lands until it takes off again for a new flight'* [49]. It embodies every single process that needs to be executed from the moment that the aircraft comes to a halt at the gate, until the moment the brakes are released again. In general, there are two different types of commercial turnaround procedures, intended for short-haul and long-haul flights respectively. The duration of these two turnarounds varies in terms of the aircraft type, number of passengers on board and the amount of cargo and most importantly the flight distance [50]. Due to the scope of this research and the traffic typically operating at small international airports, forming the most appealing airports for the initial phase of the transition towards hydrogen, only the short-haul turnaround procedure and its associated processes and regulations will be considered.

3.1.1. Processes

For a short-haul turnaround, the focus is mostly on minimizing the turnaround time rather than on other factors such as level of service or cleanness. Short-haul turnarounds are often operated by low-cost carriers, whose objective is to save cost, due to the already very thin profit margins in this market. Consequently, it is of utmost importance to incorporate efficiency wherever possible. This is visible in efforts of airlines to bypass redundant turnaround processes, such as Ryanair equipping some of its aircraft with internal stairs to save time, and thus ultimately also saves cost. Another example is airlines who refill the fuel tanks of their aircraft at airports with a lower fee cost, such that the aircraft will not have to (fully) refuel at the destination airports which potentially issues a higher fuel cost, also saving time again [27]. By reducing the turnaround time [TAT], more flights can be executed within a certain period by the same aircraft, enhancing the aircraft utilization and generating more revenue. The following list enlists the typical processes that are at least carried out during a conventional turnaround of a reference Boeing 737 at a small international airport such as Rotterdam The Hague Airport [51][52][53].

- **(Dis-)connect GPU**
- **Positioning stairs**
- **Passenger (de-)boarding**
- **(Off-)loading cargo**

- **(Dis-)connect refueling equipment**
- **Refueling the aircraft**
- **Safety checks & aircraft inspection**
- **Servicing the aircraft**
- **Removing stairs**

The processes which are included in the list above are listed in chronological order. However, this order is subject to change depending on the airline, airport, availability of ground services or other factors. The turnaround is initiated with the aircraft having safely parked on the apron. Once the engines are turned off and the blockades are placed at the wheels, the aircraft is connected to the ground power unit [GPU] to provide power to all systems on board. Subsequently, the stairs are installed first on the left side of the aircraft, such that the cabin crew can open the cabin doors. In the meantime, the suitcase belt is installed on the right-hand side of the aircraft while the baggage cart can park behind it. Immediately after, the unloading of both cargo and suitcases as bulk rather than using pallets begins, due to the limited number of items.

After the first passengers have disembarked the aircraft and everything is secure, the refueling truck pulls up to the aircraft in order to refuel the fuel tanks once the refueling equipment has been connected. In some instances, the passengers are transported to the terminal by busses, because of jet blast, weather, Schengen or other reasons. Depending on the urgency of a quick turnaround, the refueling configuration can be adjusted such that 2 instead of 1 refueling truck refuel the aircraft simultaneously in order to save time. Preferably, the least number of people possible are on board during refueling operations from a safety perspective. Otherwise, additional safety measures will have to be taken such as pre-installed evacuation routes, loose seat-belts and everybody on board being made aware of the ongoing operations [54]. In the mean time, the cabin crew can quickly clean the aircraft while also the safety checks and external inspection can be executed, which are integral of the preparation for the next flight, and the galleys are serviced and resupplied.

Whenever all cargo has been offloaded, the cargo and suitcases for the next flight can already be loaded into the aircraft. Sometimes, the aircraft will also quickly be serviced during a short-haul turnaround. This yields removing the wastewater from the aircraft by means of the wastewater vehicle, while another vehicle refills the water tanks with fresh water. Through the use of large tanks on board the aircraft, this process does not necessarily need to be executed after every single flight. Finally, when the refueling procedure is finished, the aircraft has been serviced and the cabin inspection is finished, the new passengers can board the aircraft. Adopting innovative boarding strategies such as back-to-front or zone boarding as investigated by Nyquist et al. [55] and Jaehn et al. [56], can help to reduce the boarding process by up to 25%. Furthermore, a more sophisticated and recent boarding strategy was developed by Milne et al. in which the assigned seats of each passenger were based on the amount of luggage that the passenger in question carries along [57]. By distributing the passengers carrying large amounts of luggage over the aircraft, the chances of congestion are reduced which potentially decrease the boarding time by up to 28%. After the cockpit crew finalizes the preparation of all flight-systems, the turnaround is completed.

3.1.2. Procedure

The processes as described in Section 3.1.1 are executed all together in well-defined procedures. These procedures vary per aircraft type, since this also determines the specific processes to be performed, as well as their respective order [58]. At many other airports in Europe, an external company like Aviapartner is responsible for most of the ground handling services executed during a turnaround procedure [59]. Whereas some processes have to be executed sequentially, others can be executed simultaneously in order to save time. A convenient representation of the turnaround procedure of a short-haul turnaround at a small international airport can be given through the use of a Gantt-chart. Typically, a short-haul turnaround lasts anywhere between 25-60 minutes, but this is highly dependent on the airline [51].

In Figure 3.1, a Gantt-chart representing the short-haul turnaround of a B737, having 170 passengers on board, is provided. As can be observed in the figure on the left, each individual turnaround process is represented by a bar whose length is proportional to its duration. Furthermore, each set of coloured bars represents a sequence of processes which have to be executed sequentially. Notwithstanding this, the different colors yields different sequential sets of processes which can be executed simultaneously.

It is easily noticeable that the set of blue turnaround processes has the overall longest duration, with 35 minutes. This set of processes is therefore referred to as the critical path. The critical path implies the tasks which define the entire duration of the turnaround. In other words, the only way to shorten the turnaround procedure is to incorporate temporal improvements in the processes included in the critical path. For example, if the refueling configuration is switched to 2 refueling trucks instead of 1 in the example above, the refueling time will decrease but the TAT will remain 35 minutes. Notwithstanding this, implementing one of the more efficient boarding strategies as reviewed by Schmidt would in turn potentially decrease the TAT [50].

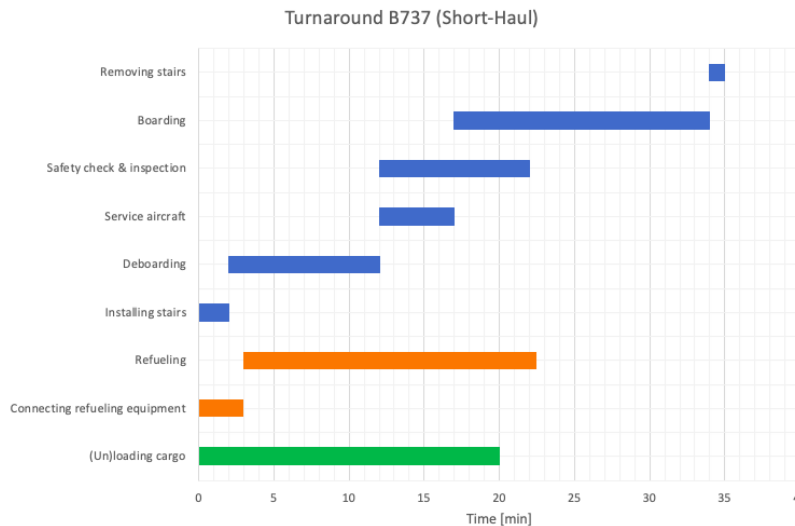


Figure 3.1: Typical turnaround procedure of a B737. Information retrieved from [60][61][62][63][64][65].

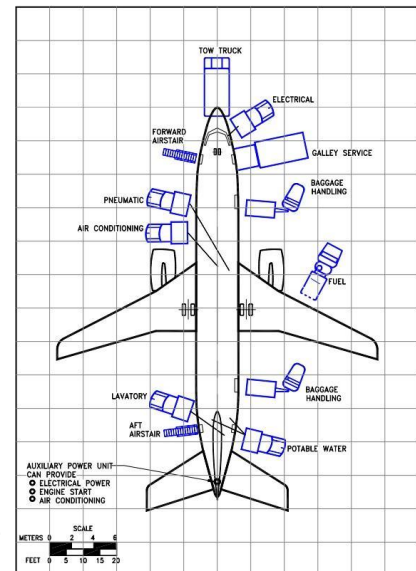


Figure 3.2: GSE arrangement during B737 turnaround. Retrieved from [66].

The turnaround procedure as described above is to a great extent influenced by the accessibility of the aircraft with respect to ground support equipment [GSE]. Whenever certain vehicles interfere with each other, this could potentially lead to the necessity of sequential instead of simultaneous operation, possibly being part of the critical path and thus extending the TAT. The way GSE approaches the aircraft highly depends on the aircraft type, as the location of different subsystems such as hatches, tanks and doors also varies per aircraft type. In Figure 3.2, the typical GSE arrangement during the turnaround of a B737 is graphically described. It must be noted that a number of GSE included in the figure are redundant at RTHA and therefore will not be included in the turnaround procedure. These vehicles are the tow truck, air conditioning and pneumatic vehicle, which can all be left out of consideration.

During the turnaround, all passenger-related vehicles approach the aircraft from the left-hand side, as can also be observed in Figure 3.2. This is done for safety reasons but also to avoid interference with the ground crew, who usually handle the aircraft on the right [67]. Because of this simultaneous approach, the first processes as described in the Gantt-chart can be executed simultaneously. Namely, once the aircraft has parked and forward and aft stairs are installed on the left side, on the opposite side of the aircraft the baggage handling can be initiated at the front and aft as well. In the meantime, the refueling process can start on the right-hand side while unloading baggage is ongoing, since the fuel tanks are situated inside the wing, and thus the middle of the aircraft, with sufficient safety margin towards the other ongoing processes. Furthermore, the GPU and servicing of the aircraft can all be executed without individual interference, as this is both situated at different locations around the cockpit. Lastly, the lavatory waste and fresh water can both be deposited and filled at the empennage of the aircraft. These final two vehicles do interfere with each other, but can easily be executed sequentially since neither of them are part of the critical path.

3.1.3. Regulations

Aviation is arguably the safest transportation mode in existence in terms of injuries and fatalities. This can be explained by the strict regulations that are incorporated in the industry, in order to maximize the safety and minimize accidents. Since the turnaround process is such a critical and time-sensitive performance, all ingredients are present to make mistakes by ground personnel. In order to avoid this, it is of utmost importance to implement and maintain rules that allow safe and efficient operation. Most of these operational regulations are imposed and specified by the International Air Transport Association [IATA] AHM, the European Commission Regulations [EU] and the IATA Ground Operations Manual [IGOM] [50] which together serve as a framework for legal operation. In the following list, the most important regulations which impact the execution of the turnaround procedure, and thus the associated simulation, are gathered:

- **REG-TUR-1.1:** Every airline should have a pre-determined ground time which is designed to meet operational requirements, but does not compromise safety (AHM 021) [50].
- **REG-TUR-1.2:** Whenever passengers are (still) on board and ground operations are ongoing, the crew must always be present (EU-OPS 1.311).
- **REG-TUR-1.3:** For every 50 passenger seats on board, one crew member should be present in order to ensure safe operation (EU-OPS 1.990).
- **REG-WAT-2.1:** Due to hygienic standards, the supply of fresh water is to be completed before waste water depositing may initialize (AHM 440, 441) [68].
- **REG-FUE-3.1:** Kerosene (Jet-A1) refueling is allowed while passengers are on board, boarding or disembarking, given the necessary precautions are taken (EU-OPS 1.305).
- **REG-FUE-3.2:** The aircraft must be refueled while parked at the apron [69].
- **REG-FUE-3.3:** The refueling truck must be parked in such a way so it can directly leave in case of an emergency [70].
- **REG-FUE-3.4:** While refueling the aircraft including (dis-)connecting the fuel hose, a circular safety zone with a radius of at least 3 meters should be maintained [27].
- **REG-FUE-3.5:** While refueling the aircraft including (dis-)connecting the fuel hose, the GPU may not be turned on nor installed [71].
- **REG-CHE-4.1:** Flight crew must execute pre-flight external check (visual inspection) before every flight [72].
- **REG-TXI-5.1:** The aircraft linear taxi speed shall not exceed 30 knots (16 km/h), while the aircraft turn taxi speed shall not be higher than 10 knots (5 km/h) [ICAO].

The regulations that have been presented above are mostly self-explanatory. Nevertheless, a few remarks have to be made for clarity purposes regarding some of the regulations. First of all, in an attempt to reduce the pressure on the ground personnel involved in the turnaround, **REG-TUR-1.1** has been introduced to limit the workload and maintain the safety at all times. Furthermore, **REG-WAT-2.1** should be extended with the practice to keep the clean water hoses a certain distance away from the waste storage or other service equipment when operated in parallel with waste servicing [68]. Next up, the precautions which are referred to in **REG-FUE-3.1** in order to allow refueling with passengers on board imply that every door should be manned by at least one crew member, while the air-stairs have been installed to accommodate for fast evacuation. Simultaneously, the passengers on board should have unfastened seat-belts and be made aware of the ongoing refueling [54]. Moreover, **REG-FUE-3.3** is also used by other GSE in practice as not only is it beneficial in case of an emergency, reverse parking also enhances the focus and thus reduces the chances of a collision. Lastly, as specified in **REG-FUE-3.4**, while refueling operations are ongoing there can be no execution of other operations, due to the risk of generating a spark, inside a circle with a radius of 3 meters from the refueling operation. Since these regulations define the turnaround procedure, it is extremely relevant for the simulation of this research as well because it constrains the model that will ultimately be selected, in the form of rules. Examples of this are the aircraft maximum taxi speed and the refueling safety zone that must be adhered to.

3.2. Hydrogen Aircraft Turnaround

The turnaround of a hydrogen-powered aircraft will be fundamentally different from the turnaround for conventional aircraft which was described in Section 3.1. This is mainly caused by the different properties

of hydrogen, when compared with conventional Jet-A1. These differences have a significant effect on the operations, required infrastructure and even the performance of the airport. Namely, alternative safety measures should be taken, while also new procedures have to be designed. Recently, research has been mainly focusing on the supply-chain of hydrogen to the airport, together with addressing the concerns about the associated cost. Examples of this are Amos who evaluated the different scenarios to transport and store hydrogen at the airport [73], and Hoelzen who considered the impact of hydrogen-infrastructure on the DOC [74]. Even though the logistic and economic aspect are definitely important to consider, these works are slightly outdated and lack practical examples, which prove the actual operation using realistic concepts. Attempts to cover the entire concept of operation of hydrogen-powered aircraft, including operational procedures, determining and designing required infrastructure and introducing safety measures, have been made by FlyZero [27] and by the MAHEPA project [29]. The main limitation of these two researches however is that the focus is too generic, while also the transition-phase is disregarded to immediately focus on a dominant hydrogen-powered aviation industry instead. This clarifies the existence of the current research gap, and the necessity of a practical case-study, designing a practical concept of operations for the transition towards commercial hydrogen-powered aircraft at a small international airport.

3.2.1. Affected Turnaround Processes

In order to be able to set up a concept of operations for hydrogen-powered aviation, it is important to know what aspects of the turnaround procedure are expected to undergo changes and should thus gain additional attention. Namely, some turnaround processes are affected because of the introduction of hydrogen in comparison with conventional aircraft, whereas others are not. In Table 3.1, every turnaround process is listed together with an indication whether or not the process in question is affected, in order to obtain a structured overview for the remainder of this section.

Table 3.1: Overview of the turnaround processes which are affected by the introduction of hydrogen.

Turnaround Process	Hydrogen Turnaround
(Dis-)connect GPU	-
Positioning stairs	-
Passenger deboarding	-
(Off-)loading cargo	x
(Dis-)connecting refueling equipment	x
Refueling the aircraft	x
Safety checks & aircraft inspection	x
Servicing the aircraft	x
Passenger boarding	-
Removing stairs	-

As can be concluded from the table above, a significant number of turnaround processes are (negatively) affected by the introduction of hydrogen into the turnaround procedure, as they either can not be executed simultaneously, or have become more time-consuming. The fact that connecting refueling equipment and refueling the aircraft will be affected is straightforward, considering that a new fuel with different properties and handling regulations is used. However, all other processes which are normally executed simultaneous with the refueling are affected as well, as they have to be executed at a different moment during the turnaround. For example unloading and loading cargo, which was previously done subsequently, but is now split up into unloading before refueling and loading after refueling. Also, servicing the aircraft was previously executed simultaneous with refueling, but is now shifted to after refueling has been completed, thus further delaying the turnaround. Other processes which are executed at the start or end of the turnaround, such as connecting the GPU, installing the stairs and passenger boarding, remain unaffected. Also, a few additional turnaround processes will be added because of the alternative refueling procedure. However, these have not been included in this list yet but will be introduced later in this chapter instead.

3.2.2. Supply-Chain

In order to accommodate the turnaround of hydrogen-powered aircraft, the airport obviously needs to be able to facilitate hydrogen. There exist several different possibilities for an airport to obtain hydrogen, which mostly depends on the airport size and the moment in the transition phase, defining the supply-chain. Since almost every aircraft that was introduced in Table 2.2 is propelled by liquid hydrogen, this research will only limit itself to a liquid state of the hydrogen. Consequently, the required volume is also smaller than when it would have been transported in gaseous state, which is very beneficial during logistic operations, also from a cost perspective [29]. In general, there exist three main variations of a liquid hydrogen supply-chain for airports which are summarized in the following list [27]:

- **Supply-Chain 1:**
Off-site hydrogen production and liquefaction, transportation to the airport using cryogenic tankers.
- **Supply-Chain 2:**
Off-site hydrogen production, pipeline transportation to the airport and on-site liquefaction.
- **Supply-Chain 3:**
On-site hydrogen production and liquefaction.

As can be seen in the list above, the airport can either produce the hydrogen on-site, bypassing the need for transportation of hydrogen towards the airport, or having the hydrogen produced off-site and transported towards the airport afterwards. Whichever option is most suitable for an airport depends on the required amount of LH₂, but also on factors such as the geographic location and available infrastructure. This is dependent by the airport size, but also the stage of the transition phase that the airport is currently in. In the following table, the typical liquid hydrogen supply-chain per airport size category is provided. As a specification for the rest of this literature study, a small international airport is considered.

Table 3.2: Table representing the liquid hydrogen Supply Chains for different airport sizes at different transition stages. Information retrieved from [27].

Airport Category	2035	2050
Regional Airport	Supply-Chain 1	Supply-Chain 1
International Airport	Supply-Chain 1	Supply-Chain 2
Intercontinental Airport	Supply-Chain 1/2	Supply-Chain 2

As can be seen in Table 3.2, for regional airports with low required quantities and short travel distances, the off-site production and liquefaction, followed by truck-delivery, as specified in Supply-Chain 1, is the most efficient solution. Namely, this avoids the high capital cost of a pipeline system, as was studied by Amos [73]. Even though this study is relatively old, the general observed trends are still representative for today. On top of that, this observation was also confirmed by a more recent study performed by MAHEPA, who concluded cryogenic truck-delivery of LH₂ is the most feasible solution for regional and small international airports with limited demand [29]. Yang even extended the study through developing a model which also considers aspects such as geographic site, market characteristics and local transportation emissions and energy usage, also to find that truck-delivery is the ideal solution for most regional and small international airports as long as the demand of LH₂ remains limited and the off-site production facility is relatively near [75]. This is also the case for RTHA, which can simply be supplied with hydrogen from the Rotterdam harbour. This saves huge investment costs in terms of infrastructure, while also requiring relatively little free space at the airport.

In contrast to this, international and intercontinental airports facing a high LH₂ demand are more likely to opt for the pipeline transportation system of Supply-Chain 2. As further stages of the transition phase are reached towards 2050, the demand is expected to increase and thus more airports will consider building a pipeline system as is also visible in the table above. A model to design a cryogenic liquid-hydrogen pipeline system for an airport ground distribution system has been designed by Jones [76], while also the economic aspect was analyzed. The findings proved that a pipeline system is very expensive to construct, but has a very low operating cost, and is thus especially beneficial for a high demand of hydrogen. Supply-Chain 3 is considered infeasible until 2050, because of the high energy requirements for on-site production and liquefaction together with the large surface area required for these facilities, limiting further growth of the airport.

3.2.3. Dispensing

The most critical part of a hydrogen turnaround, with respect to a conventional turnaround, is dispensing the aircraft. Consequently, this step of the procedure is subject to the most severe changes, caused by a number of factors. Given the alternative properties of hydrogen, a new refueling procedure will have to be developed. This refueling procedure will be mainly driven by the safety measures which should be taken in order to safely handle hydrogen. A number of studies have already been performed on different refueling techniques for LH2, allowing for both safe and efficient operation. This subsection will analyze the safety measures that must be adhered to while refueling, and provide an overview of the most promising subsequent refueling concepts, including the equipment that is required for this.

Safety

One of the most important aspect that should be accounted for during fuel dispensing are the safety aspects. Aviation has been proven to be the safest mode of transportation, with the odds of being in a fatal crash while flying being more than 2200 times smaller than dying in a car crash, as was discovered in a research executed by Harvard University [77]. This is a result of the strict regulations which apply in the industry, including appropriate safety measures, safety factors and redundant subsystems amongst others. A considerable aspect of this is with regard to the refueling processes, which can be considered the turnaround process with the highest safety risk. With the introduction of hydrogen, the safety aspect during dispensing becomes an even larger concern. This is due to the high flammability of hydrogen, together with the low minimum ignition energy and high burning velocity, as was presented in Figure 2.4. Another critical aspect is the fact that LH2 needs to be stored at temperatures below 20K, while also hydrogen as a fuel is very new in aviation. These safety concerns are worsened by the drive for efficiency, in order to keep aviation a profitable business. Hoelzen et al. concluded that a large number of studies have exclusively focused on the safety aspect already, but the operational efficiency aspect is often disregarded which causes the absence of a concrete concept to operate hydrogen aircraft at airports [74].

While refueling conventional Jet-A1, a circular area with a radius of 3 meters around should be kept clear of any spark-free objects which could potentially burn (leakages of) the fuel, as was specified in **REG-FUE-3.4**. This safety zone is referred to as the so-called spark-free zone, and has been established based on very elaborate research, testing and experience with Jet-A1 over the past decades. The spark-free zone implies that this area should be kept free from any unnecessary equipment or objects which could potentially cause sparks, including GSE, with the exception of the dispensing truck and personnel performing the fuelling [29]. Since kerosene has been used as a fuel in aviation for several decades now, this safety-zone is highly optimized to ensure efficient but safe operation, allowing many other turnaround processes to be executed simultaneously. The main issue with hydrogen however, is that it is completely novel for the aviation industry. As a result, not much is known about the usage and risks of hydrogen as a fuel in practice, besides the fact that with the right mixture of hydrogen and oxygen, hazardous explosions may occur.

After reviewing the regulatory and obligatory standards of handling hydrogen and other comparable explosive substances in different applications, such as those of NASA who are experienced in handling hydrogen in propulsion systems, a spark-free zone radius ranging between 20-60 meters has been established for current operation in the aviation sector by FlyZero, Schiphol and Mangold [27] [78] [79]. In Table 3.3, the hydrogen dispensing spark-free zones for different years throughout the transition phase, together with the kerosene spark-free zones as reference, are provided.

Table 3.3: Spark-free zones for dispensing different types of fuel in different years throughout the transition phase. Information retrieved from [27] and [78].

Fuel	2020	2035	2050
Jet-A1	3m	3m	3m
LH2	30-60m	20m (connecting) & 8m (refueling)	<8m

As can be seen in the table above, the spark-free zone of Jet-A1 has already been optimized and will remain unchanged with a radius of 3 meters. Nonetheless, the spark-free zone radius while dispensing hydrogen is expected to undergo a decreasing trend. Currently, the radius has been established between

30-60 meters as has been discussed above already, due to the novelty of the fuel and the current stage in the transition phase. However, FlyZero suggested that in 2035 when more knowledge and experience is hopefully available, this radius can be reduced to 20 meters. Additionally, even though 20 meters might be required while (dis-)connecting the dispensing hose, once the hose is actually secured the fuel safety zone could potentially be reduced up to 8-10 meters because the risk of spillage and hazards is smaller. All these values are still preliminary however, and first have to be extensively tested and validated in practice. Towards 2050, the radius is expected to decrease even further as a result of the learning curve. These safety zones will also need to be maintained for the storage facility, with the actual distance also slightly depending on the amount of hydrogen being stored.

From these observations, it can be concluded that a larger spark-free zone will have to be maintained for dispensing purposes of hydrogen in comparison with kerosene. Assuming a progressive safety margin radius of just 20 meters during (dis-)connection and 8 meters during refueling, a graphical representation of the safety zone for hydrogen dispensing during a turnaround is provided in the following figure.

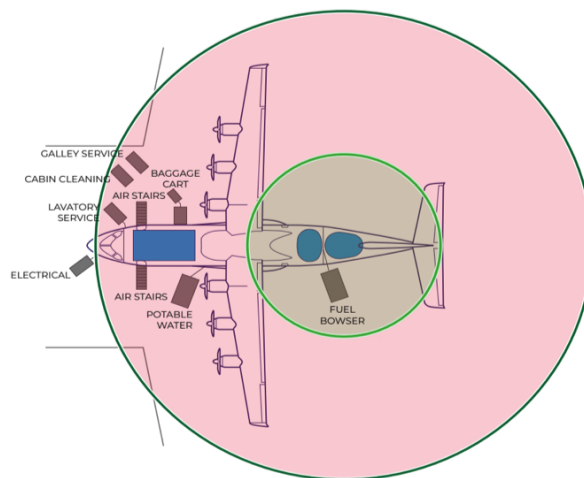


Figure 3.3: Graphical representation of the spark-free zones during the dispensing of hydrogen. Figure retrieved from [27].

As becomes apparent in Figure 3.3, the spark-free zone required during (dis-)connecting the refueling hose, represented by the red circle, covers the entire aircraft. This is problematic for the turnaround procedure in the years up to 2035, as it implies that no other turnaround process can be ongoing at this time, especially considering that in these years mostly small aircraft will be converted to hydrogen-powered. Consequently, the dispensing process should be executed separately and sequentially from all other processes which significantly extends the turnaround time. When the hydrogen-powered aircraft get larger in later stages of the transition, the front part of the aircraft might become available for simultaneous operation again.

Moreover, the green circle surrounding the aft part of the aircraft represents the potential spark-free zone during the actual refueling, which could potentially be achievable around the year 2035. The reason for the refueling being situated at the aft of the aircraft, is because the cryogenic fuel tank will be located there. Due to the high volume of hydrogen, the wings do not provide sufficient volume to store all the fuel anymore [32]. Therefore, the most appealing alternative aircraft configuration is to store the hydrogen inside the fuselage behind the aft pressure bulkhead. This new refueling position causes the refueling truck to potentially interfere with other GSE which were originally positioned at this aft part of the aircraft, such as the stairs, baggage belt, baggage cart but also catering services. In fact, while refueling is ongoing, access to the aft part of the aircraft is completely restricted for any GSE as can be concluded from the green circle. Consequently, the way and order in which all GSE approach the aircraft should be re-evaluated and re-scheduled to determine a new optimized critical path for the turnaround of hydrogen-powered aircraft. Nevertheless, this configuration does at least allow certain turnaround processes to be executed simultaneously with refueling, unlike the scenario up to 2035, which makes the TAT-increase less significant.

Besides extending the spark-free zone, there are additional measures which can be implemented to assist in mitigating hazards while refueling. Namely, it has been specified that while refueling vehicles with a capacity of 49,7 L of hydrogen or more, a well-established refueling-protocol must be recognized [78]. Moreover, a hydrogen explosion can be avoided by making use of a pressure relief device [PRD] which releases the hydrogen away from the fuel tank in case of an emergency [80]. Furthermore, through using robust and simple-to-use dispensing equipment, cryogenic glasses, high-visible clothing and other protective equipment, the breach of safety on the ground personnel can be reduced. Also, by using adequate ventilation, but also through monitoring the conditions inside hydrogen tanks via monitors, sensors and UV-detectors, the chances of leaks or boil-off can be minimized which highly contributes to the safety as was found by FlyZero [27].

Ultimately, Benson performed a study on the safety of LH₂-handling at airports, in which the flammability of LH₂ clouds and pools during leakages were modelled. It was found that the wind is of considerable effect in the spatial distribution of hydrogen and during explosions, which can contribute to intensifying hazards, and should thus be accounted for in the design of the refueling facility [81]. A suggestion would be to surround the dispensing facility or pick a sheltered site. Finally, the last safety aspect that should be taken into account while dispensing hydrogen is the weight and balance of the aircraft. Because the hydrogen tanks are situated in the aft of the aircraft, the center of gravity of the aircraft shifts further backwards while refueling. This has significant implications on the weight and balance of the aircraft, and dictates the order in which certain turnaround processes can be executed, such as loading passengers and cargo, in order to avoid the aircraft from tipping over and causing incidents [27].

Dispensing Concepts

After evaluating the safety implications on the turnaround processes which have been described above, several dispensing concepts including the required facilities were developed which potentially fulfill all requirements of dispensing a hydrogen-powered aircraft both safely and efficiently. Since hydrogen-powered cars are ahead of aviation in the development-curve, the refueling stations in this industry are already more mature and well-developed. This is proven by Genovese, who considered different car refueling station configurations, including infrastructure and delivery, in an attempt to achieve optimization and standardization in this field, also providing a good benchmark for the aviation industry [82]. In the following list, the 4 most promising dispensing concepts for hydrogen-powered aircraft at a small international airport are introduced.

- **Concept 1:**

The first fuel dispensing concept for hydrogen-powered aircraft is perhaps the most ambitious one, as it mostly resembles the current kerosene dispensing operation, and was proposed by H₂-aero [80]. Basically, a refueling truck will pull up to the aircraft parked at its stand on the apron and refuel liquid hydrogen into its tanks, adhering to the spark-free zones which were announced previously. In Figure 3.4, a visual representation of this concept is presented.



Figure 3.4: Visual representation of hydrogen dispensing operations at the apron. Figure retrieved from [80].

The main advantage of this concept is that the impact on current operations is low, since no significant additional infrastructure is required, while also allowing a relatively fast and efficient turnaround procedure, given that the spark-free zone has been improved. Furthermore, standardization of conventional turnarounds can be maintained to a certain extent which minimizes the required effort in adopting this new turnaround, as no additional movement is required. This is however at the cost of a higher safety risk due to the lack of a safety barrier and the proximity to other infrastructure and aircraft, possibly temporarily blocking nearby stands of being used by (conventional) aircraft while also causing the need for extensive certification. One of the alternatives that has been looked into by FlyZero is the (partial) automation of certain turnaround processes such as an automated fuel dispensing arm and automatic baggage loading using a robotic arm [27]. This not only improves the efficiency as it allows certain turnaround processes to be executed simultaneously while hydrogen refueling is ongoing, but also provides a significant contribution to the safety of ground personnel since mistakes are minimized in this way. This is a very complex solution however, since many processes will have to be automated while also the GSE will have to be reclassified to operate in hazardous areas.

- **Concept 2:**

The second concept has been proposed by the National Aeronautical Charting Office [NACO] in collaboration with Rotterdam The Hague Airport, and is inspired on the refueling facilities used by cars. Namely, it comprises of a side-path at the taxiway, leading to a refueling station where the aircraft can be refueled locally. This concept can be visualized by looking at the figure provided in Figure 3.5.

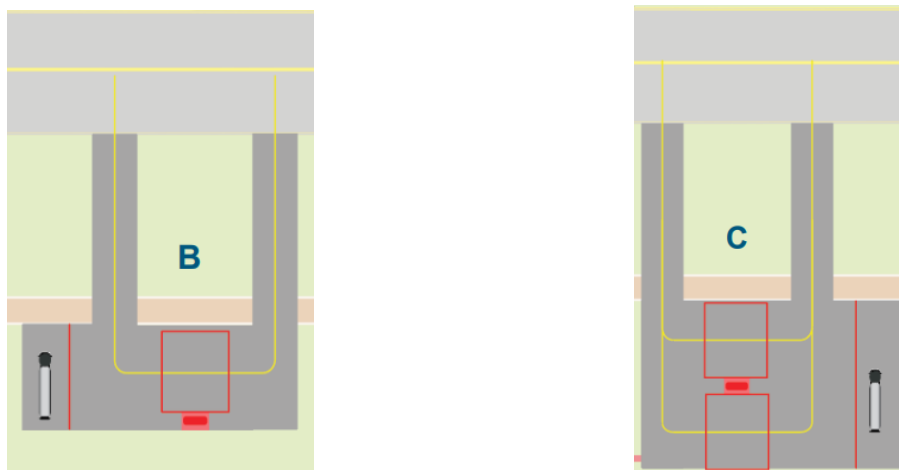


Figure 3.5: Visual representation of a scalable car-inspired hydrogen dispensing facility. Figures retrieved from [83].

As can be noticed in the figure, the refueling station can be positioned anywhere along the taxiway, depending on the airport layout, and is designed in such a way that the aircraft does not need a push-back truck to enter or exit the facility. The yellow lines are used to guide the aircraft inside the facility, and in order to refuel it must park inside the square outlined by the red lines, to acknowledge the safety distances. The solid red square attached to this outlined square is the actual refueling pump. Similar to a car refueling station, the aircraft will park next to this refueling pump which is connected to a small reservoir, supplied with LH₂ through the refueling trucks parked next to the facility behind the red line for safety (For the record, the light pink bar just above the red outlined square has no special significance). The main advantage of this concept is the possibility to position the refueling facility remotely in such a way that a possible explosion would not harm anything surrounding the facility, and in this way enhance the safety, while also it can easily be scaled up to two refueling spots as can be seen in the figure on the right.

The main disadvantages are however that it requires new infrastructure to be build, while also the efficiency of the turnaround process is highly reduced. Namely, as no passengers are allowed to be

on board during refueling, the aircraft must first taxi to the apron to deboard, subsequently taxi to the refueling facility to refuel and afterwards taxi to the apron again to board, introducing an additional movement. This impact can potentially be reduced somewhat because hydrogen is so light, yielding that if sufficient volume can be carried along the aircraft would perhaps not have to be refueled after every flight. This process is known as tankering, and could be especially useful in the transition phase as not every airport is expected to be capable of providing hydrogen dispensing facilities [27]. Nonetheless, this dispensing concept calls the need for an optimization of the position of this refueling facility in order to minimize the impact on the TAT. RTHA is already realizing this dispensing concept for the refueling of large hydrogen-powered drones at the airport, which poses the first step towards achieving commercial hydrogen-powered aviation. This specific application is using gaseous hydrogen instead of liquid hydrogen though.

- **Concept 3:**

Thirdly, Airbus has invented a conceptual bunker-inspired dispensing facility to accommodate the safe refueling of hydrogen into aircraft [84]. As can be seen in Figure 3.6, the circular construction is a physical representation of the spark-free zone, with the surrounding walls providing a safety and noise barrier for the environment in case of hazards during refueling. As a result of these walls, the spark-free zone can be reduced which is convenient for the surrounding infrastructure.



Figure 3.6: Visual representation of a bunker-inspired dispensing facility. Figure retrieved from [84].

The representation shown above might be slightly infeasible for the transition phase as it is mainly focusing on large aircraft, instead of small-to medium range aircraft which are most likely to be used at this point, and requires considerable space and investment costs. Moreover, since the refueling is again not executed at the apron, likewise concept 2, an additional ground movement is introduced in the turnaround, contributing to the TAT. Nevertheless, the concept also shows good potential, especially during the introduction of hydrogen into aviation. In the beginning of operation when uncertainties still exist, this concept provides a very redundant and safe solution to obtain more knowledge about the safety while handling hydrogen. Another benefit is that the surrounding walls not only protect the surroundings from the hydrogen inside, but this also works oppositely. As Benson concluded that wind can worsen hazards due to its impact on spatial distribution, this facility is ideal as it provides shelter from some external meteorological influences [81].

- **Concept 4:**

The fourth and final concept is still very preliminary, but potentially accommodates a very efficient turnaround. The concept was proposed by Godula et al., and is known as a cartridge-system [42]. This implies that instead of refueling the aircraft after a flight, the fuel tank will simply be swapped with a pre-fueled one like a battery instead. This concept is very efficient as the safety zones only need to be adhered to for a very short amount of time, allowing most of the other turnaround processes to be executed normally. When considering the fact that the refueling of hydrogen is expected to be part of the critical path, this concept could in theory be much faster, while also reducing number of ground personnel required. The disadvantage however is that this concept is very novel, and also the robustness and integrity of the aircraft and its propulsion system are discounted, which could pose a big safety risk. In addition, it is uncertain whether this can be executed on the apron or an additional movement towards a remote location is necessary for the tank-swap.

Whichever of these four different concepts introduced above is the most optimal one not only depends on the airport itself, but is also influenced by the different characteristics of these concepts, as well as the stage in the transition phase. In the following table, the main characteristics, resulting advantages and disadvantages and other relevant aspects of each concept are considered, relative to a conventional turnaround, which eventually leads to the most optimal dispensing facility for the transition towards and ultimately adoption of hydrogen-powered aviation.

Table 3.4: Trade-off table representing the main (dis-)advantages of each hydrogen dispensing facility.

Dispensing Facility	Safety	TAT	Cost	TRL	Scalability
Concept 1	-	+	+	-	++
Concept 2	++	--	-	+	+
Concept 3	++	--	--	+	--
Concept 4	--	++	-	--	+/-

As can be concluded from Table 3.4, all four concepts excel in different aspects. Concept 1 is very similar to a kerosene turnaround, which also explains its positive effect on the turnaround time and cost. The main additional advantage of this concept is its lack of required infrastructure, making it very scalable which is beneficial during the later phase of the transition phase, and applicable for both small and wide-body aircraft. The only concern is the slightly reduced safety and TRL, and it requires a new spatial ordering of the apron to place the aircraft in such a way that safety distances are respected. Furthermore, concept 2 and 3 are very 'safe' proposals which are technologically feasible on relatively short notice, but this comes at the cost of a significantly en-longed TAT because of the additional movement while also the infrastructure investment costs are significant. The advantage of concept 2 over concept 3 is its scalability, due to the opportunity of extending the concept to a double refueling station to accommodate a growth in demand, and being slightly less expensive. However, the required additional movement and dispensing facility of concept 2 can only accommodate small to medium-sized aircraft, while concept 3 also accommodates larger aircraft. Finally, concept 4 is estimated to have a very efficient TAT but has a hugely reduced safety and integrity, is expensive and also not technically feasible in the near future. Which (combination of) concept(s) is be the best option for RTHA will be evaluated later in this thesis, based on expert knowledge and a more in-depth analysis of the requirements and possibilities at the airport.

Dispensing Equipment

With the expected increase in TAT, action needs to be undertaken in order to make all other processes as efficient as possible to limit the overall impact on the TAT. One of these aspects is the dispensing technique itself through which the LH2 can be transferred into the fuel tank of the aircraft. This has already been done by Hettinger amongst others more than 20 years ago already [85], but today more powerful pumps and equipment are available. The main factor which influences the refueling time is the refueling rate, referring to the amount of hydrogen that flow in a specific time. Since liquid hydrogen has a much higher density than kerosene, more volume needs to be transported in a comparable time, which yields either using more hoses, using hoses with a larger diameter or a combination of these two solutions [27]. In the following table, the different refueling times for different single hose dispensing configurations are provided. The main interest for the transition phase is on the regional and narrow-body aircraft, and the refueling times are verified by MAHEPA [29].

Table 3.5: Different single hose refueling configurations with the accompanying refueling times. Information retrieved from [27].

Concept	LH2 quantity [kg]	Fill Time (2.5 m/s)		Fill Time (5 m/s)		Fill Time (7 m/s)	
		4" Line	6" Line	4" Line	6" Line	4" Line	6" Line
Midsized	11698	175 min	78 min	87 min	39 min	62 min	28 min
Narrowbody	2718	41 min	18 min	20 min	9 min	15 min	6 min
Regional	1300	19 min	9 min	10 min	4 min	7 min	3 min

As can be concluded from Table 3.5, the refueling rate can be doubled approximately as the hose diameter is increased from 4" (10.16 cm) to 6" (15.24 cm). As reference, for Jet-A1 refueling a hose diameter of 3" (7.62 cm) is used. A similar doubling of the hydrogen refueling rate can be achieved by using a more powerful pump, as can also be seen in the table above in the different "Fill Times". The refueling pressure should be at least over 700 kPa in order to achieve acceptable fueling times, and the fueling speeds achieved by the pump are either 2.5, 5 or 7 m/s [27]. Typically, the **complete** (starting with absolutely empty tanks) refueling of a small-to medium-sized hydrogen-powered aircraft will last anywhere between 5-20 minutes. It must be noted that these values are rather taken more conservative in order to be as accurate as possible at this early stage and not overestimate the performance. This provides useful input to the early-stage quantification of a hydrogen TAT, which will be treated in Section 3.3.

One important thing that also should be accounted for though is that the weight and force of the hose increases significantly with an increasing diameter and pumping speed, and at some point becomes too heavy to be manually handled by the fuel dispensing personnel. This sets the limit of a maximum hose diameter, guaranteeing that the refueling connector should not exceed 10 kg to remain manually manageable [29]. This obviously changes again if autonomous refueling is considered, potentially allowing the achievement of even higher refueling rates. However, considering the TRL and the fact that this master thesis focuses on the transition phase, it can be assumed that the initial hydrogen-powered aircraft will be manually refueled. This also raises the need for ground personnel to be specially trained for handling hydrogen, including all safety procedures and regulations, while also the fire fighters should be trained for hydrogen-caused hazards.

3.2.4. Additional Infrastructure

Accommodating a hydrogen turnaround at an airport requires a considerable amount of infrastructure being specially designed and optimized to allow efficient but most importantly safe operation. This infrastructure not only limits itself to the conceptual dispensing facilities as were proposed in Section 3.2.3, but also includes storage facilities.

Storage

Hydrogen-storage is arguably one of the most space-demanding subsystem of the entire infrastructure, and should thus not be underestimated. There are different ways of storing hydrogen, varying in state of the hydrogen, shape of the tank and more. Several studies have been performed on the pressing topic of determining the ideal process to store hydrogen throughout the entire aviation industry. Hydrogen can be stored as a gas inside underground caverns, as a compressed supercritical fluid, as a liquid in a cryogenic tank or trailer, in material-based H₂ storage systems, as a slush hydrogen (solid state) and in cryogenic tanks as cold-compressed or cryo-compressed hydrogen [29]. As was already announced before, the most probable state of hydrogen during the transition phase will be liquid, and thus storing hydrogen as a liquid in a cryogenic tank is the most straightforward solution. However, more specifics on the storage facility highly varies with airport size.

In contrast to kerosene, LH₂ will need to be stored insulated because of its cryogenic state, yielding keeping it at temperatures below the boil-off temperature of 25 K. Liquid hydrogen is often stored in spherical or cylindrical tanks, because those shapes have the highest volume over surface area, minimizing the heat transfer with the environment as was discovered by Timmerhaus et al. [86]. Spherical tanks are the most efficient, but as cylindrical tanks are way cheaper to produce, this shape is standard in most other industries. Burying the tank underground makes it easier to control the conditions of the hydrogen, but given the current transition phase and the difficult related maintenance, this is infeasible at this point [87]. Because hydrogen has such a low density, the required storage volume is 3 times more than for conventional kerosene. As long as the hydrogen demand at an airport remains relatively low, the refueling tank can be placed horizontally. Nonetheless, for larger quantities the fuel tank will be turned vertically due to structural reasons. Given this wide variety of possible ways of storage, the following list discusses the most convenient storage options of hydrogen per airport category and transition-phase stage:

- **Option 1:**

A flexible storage facility would be to leave the LH₂ in the delivered cryogenic fuel trailers such that it can be picked up by on-site dispensing trucks, as is currently done with conventional Jet-A1 at RTHA, which was learned from expert knowledge. Due to the low investment costs and easy scalability of this solution, this is the most potential storage facility for regional and small international airports

but also international and intercontinental airports at early stages of the transition phase. Namely, the only required infrastructure would be special parking places for these trailers. Special attention should be given to maintaining the cryogenic conditions inside the trailer while it is stored though. In Figure 3.7, an impression of such a temporary hydrogen storage facility, consisting of lined-up cryogenic trucks, is provided.



Figure 3.7: Flexible storage facility consisting of lined-up cryogenic trucks. Figure retrieved from [88].

- **Option 2:**

For larger hydrogen demands at international and intercontinental airports, or at further stages in the transition phase, permanent hydrogen storage facilities are expected to be more efficient. Namely, as the hydrogen demand increases, so does the number of daily truck deliveries, which at some points becomes too high which leads to congestion and is thus infeasible. Consequently, a hydrogen tank will be installed which can either still be refueled using trucks, or is connected to a pipeline system. The main concern of liquid hydrogen storage tanks however are heat leaks, which are a function of the size, shape, and thermal insulation of the fuel tank used. Nonetheless, compressed hydrogen is still the preferred option for storing and distributing hydrogen due to quick refueling and mature infrastructure in the automotive industry already [42]. FlyZero has recently introduced large insulated hydrogen tanks, produced from different materials such as metals, composites or a hybrid of these two material-groups [27]. However, due to the novelty of these techniques, the testing of such tanks is still ongoing, including thermal and load cycling, in an attempt to obtain the required certification. This will eventually point out which material is most suitable, and could start a market trend. In the following figure, a conceptual storage facility is shown to give an impression of what the fuel tank(s) required for the latter stages of the transition-phase at a international or intercontinental airport with a considerable hydrogen demand could look like.



Figure 3.8: The largest commercially available LH2 fuel tank today. Figure retrieved from [89].

In Figure 3.8, a concept of the fuel tanks carrying the hydrogen is presented. Nevertheless, the infrastructure required at the storage facility not only limits itself to the fuel tanks. Due to environmental concerns, there needs to be a suitable underground to protect the environment from spills in case of leaks. Moreover, in case the airport is supplied with LH2 using cryogenic trucks, a (un-)loading station needs to be provided on site at the storage facility. Finally, in order to facilitate this (un-)loading

procedure, special pumps are required which typically have a flow capacity of almost 20 liters per second, taking about 30 min to unload an entire truck [90].

Another crucial aspect of the storage facility is its location. Usually, such sites are positioned at remote airport areas because space near the terminals is often required for other purposes which benefit the airports revenue by being in the proximity of the terminal [27]. However, one of the constraints is that the storage facility site should be easily accessible by the external refueling trucks to reload the LH2 trailers if it is not supplied using a pipeline system. Ideally, the storage facility will be positioned in the vicinity the refueling station(s) which was introduced in Section 3.2.3, or as close to the gates as possible. As the ideal location highly depends on the airport layout, it varies per scenario where this location will be. One of the objectives of this research is therefore to determine the most efficient location for the storage site at a small international airport like RTHA, both allowing efficient taxi-routes of the aircraft and being accessible by the tanker truck, while also adhering to the remote location constraint because of safety reasons and taking into account other existing infrastructure.

Dispensing Facility

Depending on the selected dispensing concept in Section 3.2.3, a dispensing facility will need to be constructed as well. In the following list, the different possible dispensing facilities for the transition-phase will be elaborated upon.

- **Option 1:**

In case of refueling concepts 2 and 3 in Section 3.2.3, a special refueling facility will be required. Namely, the hydrogen will actually be provided to the aircraft through a fuel dispensing station. The dispensing facility that was introduced with fuel dispensing concepts 2 and 3 is based on a car refueling station, in which the aircraft comes to the fuel, instead of the other way around. There actually already exist smaller hydrogen filling stations for the supply of ground service vehicles at some airports, which have a resembling layout [91]. The schematic representation of this aircraft-dispensing concept is provided in Figure 3.9 though, together with its main subsystems.

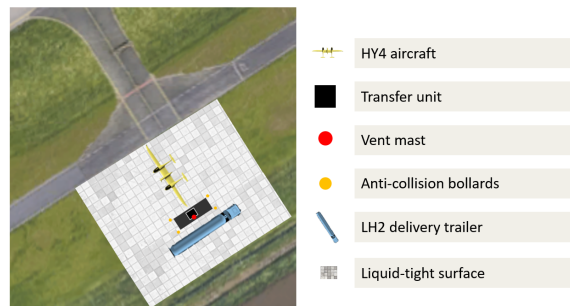


Figure 3.9: Schematic representation of a large drone-oriented hydrogen refueling station at RTHA.

As can be seen in the figure above, the fuel dispensing facility is relatively simple. The main element is the transfer unit, represented in black, through which the LH2 will actually be pumped into the aircraft. Next up, the aircraft can simply park next to the transfer unit, with the anti-collision bollards installed to avoid the aircraft damaging the fuel tank. By means of the ventilation mast serving as a PRD, that the transfer unit is equipped with, the LH2 conditions can be controlled. Ultimately, it can be visualized that the entire site is covered by a liquid-tight surface to avoid spillages leaking into the ground that could potentially harm the environment.

- **Option 2:**

In case it is selected to refuel the aircraft at the gate such as in concept 1 in Section 3.2.3, a dispensing facility like option 1 will not be necessary anymore. Namely, instead of the aircraft having to travel towards a site to be refueled, the aircraft will simply be refueled on the apron using a mobile dispensing truck carrying a trailer filled with LH2. This configuration is much more convenient and scalable for the larger aircraft that are expected at this stage, while also the large number of refueling stations needed would occupy too much space and is very expensive. It must however be studied first whether the existing gates of an airport can be used to refuel hydrogen-powered aircraft, or new

gates with larger subsequent distances will have to be constructed. The mobile refueling trucks will be produced and delivered by Shell, which has been learned from expert knowledge. In Figure 3.10, a concept of such a mobile dispensing truck for refueling hydrogen is provided, which will most likely be equipped with a hydrogen trailer similar to the one shown in Figure 3.7.



Figure 3.10: Visual representation of a conceptual mobile hydrogen dispensing truck, which is expected to be utilized in the later of the transition phase. Figure retrieved from [32].

In case a dispensing facility will be required, as with option 1, the location of this facility is still undetermined. Similarly to the storage facility, this location is highly dependent on the specific airport layout. While determining this location, a few factors have to be taken into account, such as the vicinity to other infrastructure, while still the location should allow efficient operation through minimizing the travel distance for the hydrogen-powered aircraft and the impact on conventional aircraft. Thus, another objective of this research is to establish the most efficient location for the dispensing facility or site as well. In case of refueling on the apron as with option 2, the objective changes to determining the ideal layout and/or location of these special hydrogen-oriented gates on the apron. This can either be a reallocation of existing gates, or the development of a new set of gates somewhere on the airport.

3.3. Turnaround Performance

The turnaround performance at RTHA, which is normally expressed using key performance indicators [KPI], could be considerably affected by the introduction of hydrogen-powered aircraft. This not only limits itself to the performance of hydrogen-powered aircraft turnarounds themselves, but also affects all other (conventional) traffic at the airport. The main effects on these two stakeholders will be considered in this section.

3.3.1. Hydrogen Turnaround Time

The most convenient KPI which is used to assess the turnaround performance is the turnaround time [TAT], yielding the time that is needed to completely prepare the aircraft for a new flight after its landing. For conventional aircraft, the turnaround procedure is highly standardized and determined because of which a well-defined quantification for the TAT can be provided. In the left column of Table 3.6 table, the average turnaround times for different aircraft size categories are provided. As can be concluded, the regional and narrowbody aircraft have fairly low and comparable TAT's, in comparison to the midsize aircraft. This is because the latter category includes larger aircraft, on which more processes have to be executed during the turnaround which are also more time-consuming due to the size.

With the introduction of hydrogen in the turnaround procedure, a number of processes during the turnaround change as was discussed in Section 3.2. The biggest of these changes is the fuel dispensing process, which is subject to a number of strict regulations like the safety zone. This limits other turnaround processes from being executed simultaneously, but also requires an additional movement to and from the refueling facility, en-longing the hydrogen TAT and also rescheduling the other turnaround processes. Depending on whether (semi-)autonomous execution of (some) turnaround processes becomes available, this increase in the TAT can be (partially) reduced again. This leaves a total of 3 potential autonomy scenarios per aircraft category, whose respective expected TAT's are represented in the 3 most right columns of Table 3.6.

Table 3.6: Estimated kerosene and hydrogen TAT for different aircraft sizes and levels of turnaround process autonomy. Information retrieved from [27].

Aircraft Type	TAT [min]			
	Kerosene		Hydrogen	
	No Autonomy	No Autonomy	Semi-Autonomy	Full Autonomy
Midsized	60-90	130	100	60
Narrowbody	25-30	46	35	27
Regional	20-25	42	32	23

The table above shows that for each aircraft category, the hydrogen TAT is highly influenced by the level of autonomy, possibly allowing the simultaneous execution of (some) turnaround processes. For each of the three aircraft categories, the semi- and full autonomous scenario show a similar TAT with respect to the upper and lower limit of the conventional TAT's in the left column respectively, and thus do not show very alternating performance. This is because either some or all processes can be executed simultaneously while refueling is ongoing. Nevertheless, the scenario in which no autonomy can be achieved shows a significantly longer TAT of up to 50% more when compared to the conventional TAT's, as during refueling no other process can be executed simultaneously. This is something that must be accounted for when simulation the ground operation of hydrogen-powered aircraft, especially in the initial stages of the transition phase. However, these values are expected to change (decrease) soon as the hydrogen-aircraft utilization rate is increased, while also the turnaround time decreases exponentially with shorter trip times as was accounted for by Boeing [92]. Lastly, it must be noted that these values are averages and that TAT is a highly variable process which is reluctant to change depending on many external factors. These different TAT scenario's can be complimented with the following two Gantt charts, which are created for the initial phase (2020-2035) of the transition towards hydrogen-powered aviation considering a remote refueling station in Figure 3.11, as well as the later phase (2035-2050) of the transition considering refueling on the apron in Figure 3.12. The information about the duration of all turnaround processes has been obtained from [60][61][62][63][64][65][79].

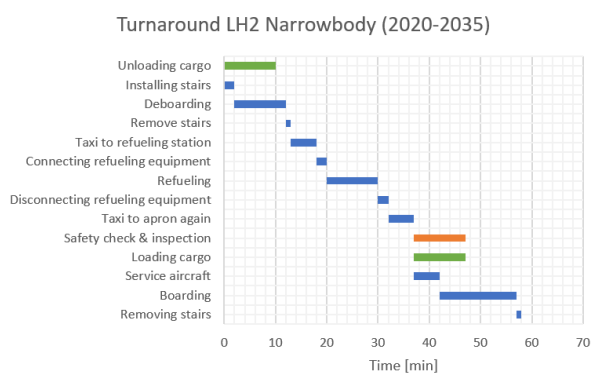


Figure 3.11: Typical turnaround procedure of a LH2 narrowbody aircraft, in the early stages of the transition phase.

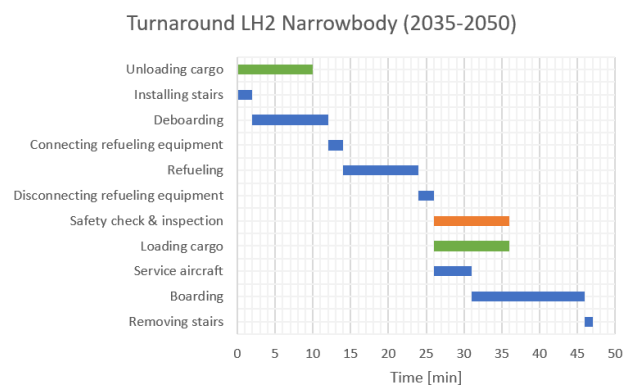


Figure 3.12: Typical turnaround procedure of a LH2 narrowbody aircraft, in the later stages of the transition phase.

First of all, the Gantt Chart on the left represents the individual turnaround processes of a LH2 narrowbody aircraft between 2020 and 2035. As was announced in Table 3.3, the safety zones which have to be adhered to while refueling will most likely cover the entire (small) aircraft, which prevents other processes from being executed simultaneously. In addition, in Section 3.2.3 it was concluded that during the initial stage of the transition phase towards hydrogen-powered aviation, a remote refueling facility will most likely be operated at small international airports, due to safety considerations. The consequence of this concept are two additional movements to and from the refueling facility, which is positioned somewhere along the

runway. This therefore causes some new processes to be included in the turnaround procedure, as well as a few changes in the process-order with respect to a conventional turnaround as was presented in Figure 3.1.

As can be seen in Figure 3.11, the entire duration of the turnaround procedure approaches 60 minutes, being considerably more than the values presented in Table 3.6. This is mainly due to these additional movements which have been estimated to last 5 minutes both, together with the fact that the entire refueling operation should take place sequentially. These 5 minutes includes the taxiing to the facility, together with the disembarking of all crew on board. As a result of this procedure, refueling is now part of the critical path, which is indicated by all the blue process-bars in the figure. The new critical path of the turnaround procedure now consists of installing the stairs, deboarding the passengers, removing the stairs again, taxiing to the refueling facility to refuel, taxiing back to the apron for servicing the aircraft and passenger boarding, and finally removing the stairs again. The additional processes of (un-)loading cargo and the safety check & inspection can be executed simultaneously with other processes like (de-)boarding or servicing the aircraft, as long as no refueling is ongoing. While the aircraft is being refueled, no personnel and passengers are allowed in or near the aircraft.

Secondly, in Figure 3.12 the turnaround procedure of a LH2 narrowbody aircraft in a further stage of the transition-phase is discussed, relevant for the period between 2035-2050. As becomes apparent, the main difference with Figure 3.11 is the absence of the taxi movements from and to the refueling facility, reducing the TAT to 46 minutes, which is corresponding to the values provided in Table 3.6. All other processes are exactly the same as in the earlier stages of the transition phase, so the refueling procedure can still not be executed simultaneously with other processes. This underlines the assumption that no autonomy of turnaround processes is available at this point. Nevertheless, as time progresses autonomy can potentially be incorporated in operation, causing the TAT to reduce accordingly. The turnaround times that have been used in Table 3.6 and the two Gantt charts are based on a single fuel hose with a diameter of 15.24 cm for the regional aircraft, and two fuel hoses with the same diameter for the narrowbody and midsize aircraft, together with a fill velocity of 5 m/s, thus generating conservative and accurate estimates [27]. This allows the hydrogen refueling times to approach those of conventional kerosene, at the cost of using an additional refueling hose though.

During the remainder of this thesis, the hydrogen TAT's as discussed above will be iteratively improved to ultimately obtain meaningful results in the simulation. Namely, one of the research objectives is to establish the detailed TAT of a regional hydrogen aircraft, such as the D-228, a hydrogen-powered narrowbody aircraft, comparable to the DHC-8, and finally a midsize aircraft like the ZEROe. In later stages of the research, the more autonomous scenarios and thus shorter turnarounds can also be considered more in depth, to account for all transition stages. Ultimately, these TAT results will serve as an input during the simulation of different scenarios which will be used to optimize the locations of the refueling facility, storage facility and assess the impact on the airport performance, which will be further discussed in Chapter 4.

3.3.2. Parallel Operation

Since the main focus of this research is on the transition phase towards hydrogen-powered aviation, conventional aircraft will be operating in parallel with hydrogen-powered aircraft at the airport. As was specified in Section 3.3.1, the TAT of hydrogen-powered aircraft will be longer than the TAT of conventional aircraft. This has a number of consequences for the other aircraft operating at the airport, as well as on the airport performance as a whole. Longer turnarounds yields a longer occupancy of gates, while also the taxi-ways are blocked for additional fuel dispensing movements, affecting the runway capacity and potentially also disrupting conventional traffic due to convergence. This could ultimately even have consequences on the total airport capacity, which is a very important KPI for the airport. No studies on gate limits and other potential changes in ground handling due to LH2-powered aircraft are found as stated by Hoelzen, and thus a research gap exists in this field as well [74]. This therefore serves as another objective of this research, in order to simplify the further transition towards hydrogen as a fuel in aviation.

By making use of applicable simulation and optimization techniques, the longer turnaround and additional movements of hydrogen-powered aircraft can be accounted for to foresee the main consequences of both aircraft types operating in parallel. This can provide insights into matters that the industry is currently unaware of, while solutions can be derived at an early stage to achieve a better integration of hydrogen and conventional aircraft in the end. Examples of this are assigning certain gates specially for hydrogen-powered aircraft, identifying the need for additional dispensing facilities or optimizing the location of this

hydrogen refueling facility. Also optimal decisions in priority of either conventional or hydrogen-powered aircraft in the case of a conflict during taxiing can already be derived. Through the use of graphical simulation techniques like agent-based modelling, meaningful results can be obtained to consult the airport.

3.4. Cost of Hydrogen

One of the biggest concerns in the adoption of hydrogen in aviation besides safety and technical feasibility is the operational cost, which is a direct element of the operation of hydrogen-powered aircraft. This cost consists of the fuel cost, which is partially defined by the transportation and storage cost of the fuel as well. Besides that, the airport revenue is to a certain extent also defined by the incoming airport fees, which are also subject to change for hydrogen-powered aircraft. This section will serve as a qualitative literature review of these cost factors to provide preliminary insights and find the main effects of hydrogen on these costs.

3.4.1. Fuel Cost

The fuel cost is one of the largest contributors to the operational cost in aviation, and this is no different for hydrogen. Today, the most convenient and economically available liquid hydrogen is unfortunately still produced as grey hydrogen, while also the expensive process of liquefaction should be accounted for in the cost. Assuming that the energy efficiency of the propulsion system of a hydrogen-powered aircraft is similar to conventional aircraft, a retrofitted D-228 would need approximately 200 kg of LH2 for 500 km range flight, resulting in production, liquefaction, off-site storage, truck-delivery and on-site storage cost of around 2500 euro. Similarly, a retrofitted DHC-8 would need approximately 700 kg of LH2 for the same flight, leading to a total cost of around 8500 euro [29]. This total cost includes all investments in infrastructure, retail margins, transportation and labour cost amongst others, coming down to approximately 10 euro/kg of LH2 today, as opposed to 0.64 euro/kg for kerosene excluding delivery, according to IATA [93]. In other words, LH2 is currently roughly 15 times more expensive than kerosene, and thus governmental financial aid is required to make it economically viable to operate LH2 in the near future. This cost also includes the investment of infrastructure such as well-insulated storage vessels to prevent boil-off, a docking station for the (un-)loading of hydrogen delivery and the transportation cost [29]. As the transition towards hydrogen in aviation progresses, the total cost is expected to decrease significantly however. Reasons for this are a larger economy of scale, technological improvements, a lower energy cost and the learning curve, as was identified by TULIPS [94], which will make hydrogen even more appealing.

3.4.2. Airport Fees

One of the main sources of income for an airport to be a profitable business, besides the car-parking fees and the sales of passengers in the terminal, are the aircraft fees. This yields that the operating airline of a landing or departing aircraft should pay the airport a certain fee for the services provided by the airport, such as facilitating the runway, occupying a gate and all (passenger) services that are associated with a turnaround. For commercial aviation, these fees are well-defined and depend on factors such as the MTOW of the aircraft, the number of passengers on board, the time of arrival, the parking time and the noise category of the aircraft. As reference, an airline operating a kerosene-driven DHC-8 with 70 passengers on board, landing and departing between 08:00-18:00, would have to pay Rotterdam The Hague Airport 2142 euro [95]. This is excluding all ground services provided to the aircraft during the turnaround, as this is outsourced to the ground-handler Aviapartner at RTHA and many other airports.

With the introduction of hydrogen-powered aircraft, the typical airport fees are subject to change with respect to the kerosene variants. There exists a research gap in this field, as no studies on potential changes in ground handling and landing fees due to LH2 aircraft have been researched yet according to Hoelzen [74]. The airport fees as discussed above are mainly driven by the aircraft weight, as well as the number of passengers on board. However, with the market trends of hydrogen-powered aircraft potentially becoming lighter due to a lighter structure required to support the low-weight hydrogen, the airport fees paid by these aircraft will most likely become lower in the end. Also, since the fuel tank is located inside the fuselage at the cost of a certain number of seats, the passenger fee will possibly also decrease slightly. This is an important thing to take into account for airports, and it is advised to research this topic more thoroughly and possibly incorporate an alternative determination of the airport fees on the long-term, as otherwise the costs will increase while the income will decrease. Else, governmental aid is also required in this field in order for this operation to be economically viable for airports.

4

Hydrogen Turnaround Simulation & Optimization Approach

This chapter will address the simulation and optimization aspect of a hydrogen turnaround, which is fundamental for the actual research which is to be performed. Firstly, Section 4.1 will give an overview of the most-used modelling techniques in aviation, including practical examples. Next up, the formal definition of a multi-agent path finding problem including all important model elements will consequently be provided in Section 4.2. Finally, in Section 4.3 a detailed insight into and analysis of the most relevant conflict resolution techniques, including their applications and (dis-)advantages, will be provided, as well as the optimal algorithm and different available heuristics.

4.1. Modelling Applications in Aviation

Simulation and optimization techniques have been and are still widely used in the aviation industry today. The initial thought often goes towards simulators used by pilots, in order to gain experience and obtain certification for flying specific aircraft types. Nonetheless, the applicability of simulation and optimization techniques goes far beyond this as it can be applied as a tool to resolve a wide variety of issues inside the industry. Namely, it provides the opportunity to evaluate the performance of a proposed solution or procedure without having to build it first and thus saving huge amounts of investment costs. In this way, the most suitable solution, based on KPI's, can be immediately adopted to allow efficient operation.

Generally, in the initial design phase, simulation is predominantly useful to assess the viability of different solutions as there is nothing of a similar kind in existence yet. Thus, simulation provides the best alternative to be able to compare the performance of a solution with something else, minimizing the risk of eventually adopting a poor solution, as was gained from expert knowledge. In a later stage when a certain process has already been adopted, optimization comes into play. Namely, optimization provides a tool to assess the current performance and seek improvements to gain more efficiency, save costs or else depending on the specific application.

As such, the initial focus of this literature study will be on selecting an appropriate simulation technique for the proposed research. In order to achieve this, the main simulation techniques together with relevant practical examples will be provided in the following list. These practical examples mostly address simulating operations such as different aspects of the turnaround process like taxiing and passenger (de-)boarding, ensuring safety through conflict detection of GSE and optimizing the airport layout.

- **Simulink & Matlab:**

Matlab and Simulink provide platforms which are relatively straightforward to adopt by engineers. Its main usage is providing building blocks for simulating air operational purposes, such as simulating aircraft behaviour which can be used both during aircraft design as well as as an actual simulator for pilots to obtain experience [50]. This makes the model very flexible and widely applicable. Additionally, it is also suitable for other purposes on the ground, as long as the complexity remains somewhat limited. For example, Voulgarellis established the number of required GSE given an expected flight schedule, using Matlab [96].

- **System Dynamics:**

This simulation technique is very relevant for systems in which the state variables change continuously

over time, such as the level inside a fuel tank [97]. This can be for fuel tanks of aircraft in-flight, but also fuel tanks of storage facilities on the ground. The application of this technique is thus very specific and detailed, but this limits its applicability and the scope on which it can be applied. Nonetheless, this makes the technique very robust and time efficient.

- **Markov Chains:**

This simulation technique is especially strong to account for unpredictability, which is very useful for processes which are reluctant to broad variations. One of such processes is the turnaround process, in which the performance is highly dependent on a lot of factors which thus incorporates unpredictability, but there are many more. Examples of this are Yildiz et al., who accounted for the unpredictability during boarding processes using Monte Carlo/Markov Chains in an attempt to find bottlenecks [98]. Also, the work of Wu and Caves is a good example for the use of Markov chains together with Monte Carlo simulation for investigating turnaround performance [99].

- **Agent-Based Simulation:**

ABS is a relatively novel simulation technique, in which different entities are simulated as autonomous and independent agents who make their own decisions within a system based on their allocated cognitive characteristics and constraints [97]. These agents can be representing passengers, aircraft or GSE for example. This type of Artificial Intelligence [AI] is highly suitable to represent the interaction of different stakeholders in dynamic uncertain systems, which can be used for collision detection, task allocation or path planning amongst others. This technique is relatively difficult to implement and can be very time-consuming, but the achievable results are detailed and can be extremely meaningful.

Examples of this application are the work of Ip et al., who performed GSE allocation based on existing datasets, using ABS, in order to achieve the shortest TAT and in this way minimize cost and delays [100]. Moreover, Chen extended the GSE allocation with collision detection of aircraft during ground movements [101]. An example in which the agents represent passengers was done by van Langehem, who simulated the passenger egress and ingress using agent-based modelling, analyzing different boarding patterns based on the the passenger seat allocations [102]. Additionally, rather than deciding the most optimal boarding strategy based on the seat allocation, J. Audenaert et al. introduced a different manner of simulating the boarding strategy based on individual passenger's characteristics [103].

- **Discrete-Event Simulation:**

DES on the other hand is especially suitable for analyzing systems in which the stakeholders follow a recognizable sequence of processes. In contrast to ABS, the state variables change discretely at varying time steps depending on the duration of the process, rather than continuously over time [101]. Consequently, this technique is characterized as being dynamic, stochastic, asynchronous and provides relatively fast results, making DES ideal to simulate the turnaround procedure. It can be tedious to implement, but produces relatively fast results while also forming a robust model.

Some practical examples using this technique include the work of Chung and Adeleye, as they use DES to identify the bottlenecks in turnaround processes [104]. In addition, the research from Norin et al. use an optimization algorithm for finding a sub optimal scheduling and then they create a discrete event system approach for testing the solution for the turnaround as well[105]. Another example was Mota et al., who utilized DES to assess the performance of different apron layouts at Lelystad Airport in order to conclude the most efficient airport configuration leading to the quickest turnarounds [97]. These examples are all relatively broad, but DES can also be useful for including very detailed operations such as de-icing as was done by Norin et al. [105].

Based on these descriptions, a trade-off table can be generated to assess the performance of every technique in different fields. These fields include how applicable the technique is for the specific simulation at hand, the complexity of developing a model using the respective technique, how flexible it is to incorporate changes, its time efficiency when running the simulation and finally the robustness of the eventual model [101]. This leads to the following classification, as provided in Table 4.1, in which the scores range from - - to + +.

Table 4.1: Trade-off table representing the main (dis-)advantages of each simulation technique.

Simulation Techniques	Applicability	Complexity	Flexibility	Time Efficiency	Robustness
Simulink & Matlab	-	++	+	+	+
System Dynamics	--	+/-	-	+	+
Markov Chains	+/-	+	+	+	+/-
ABS	++	-	++	+/-	+
DES	+	+/-	+	+	+

Nevertheless, simulation and optimization not only limits itself to operational procedures as described in the overview above, but can also be highly valuable in designing infrastructure at different stages of airport design. Namely, the applicability of simulation in the early stages of airport design was proven by Zak et al., who investigated the ideal runway direction and taxiway system in order to maximize the airport capacity using simulation [106]. Moreover, the work of Mujica put focus in terminal buildings and the development of the initial airside models for small airports [97]. In addition, simulation can also be used to assist in the adoption of operational procedures to accommodate novel aircraft configurations, such as hydrogen-powered aircraft or a blended wing-body [50]. This illustrates the potential of simulation and optimization in this research to generate the most optimal airport design as well as operational frameworks.

As can be seen in Table 4.1, the different techniques are very different in terms of the selected field. First of all, Simulink & Matlab score very well in most of the fields except for one of the most important fields, applicability to the problem. Furthermore, system dynamics is again arguably good in most fields except for the applicability. Next up, Markov Chains performs decent in every field but still slightly lacks applicability to this research, as well as robustness. This leaves only two possible candidates for the simulation technique, which are ABS and DES, which both perform fairly similar and have a good applicability to the problem. Namely, both techniques allow the different stakeholders in the simulation to be represented independently, while also both frameworks are capable of providing a graphical simulation for a complex problem of this kind. Additionally, both techniques allow the simulation to be built from the bottom up, making it easy to extend the model at a later point through modularity once more information becomes available. Through analyzing the practical examples for which ABS and DES have been used respectively, it becomes apparent that ABS has been used amongst others for conflict detection and path planning which highly resembles the simulation to be performed in this research. ABS is especially useful when analyzing independent behaviour, the interrelation of individual processes on one another, as well as its mutual intercourse [97].

On the other hand, with DES the focus is rather on combining a set of processes as is done in a turnaround procedure, but can be used for the assessment of different airport configurations as well. Nevertheless, the main strength of DES is that its application is relatively simple and broad which leads to fast results [97]. However, since this research puts the focus on small international airports and the number of different scenarios to be considered remains limited, the quality of the results could be a higher at the cost of more time-consuming results. This proves the suitability of agent-based simulation as a simulation framework in this context, and justifies the decision to select this technique. Namely, through path-planning of the ground movements of both conventional as well as hydrogen-powered aircraft, including the additional ground movement for refueling, the effect on the TAT of both aircraft types can be evaluated in order to assess the implications on the airport capacity and infrastructure.

4.2. Multi-Agent Path Finding

Considering the objective of the research to optimize the ground handling of hydrogen-powered aircraft, the modelling goal is to set up a simulation for this procedure. As was declared in Section 4.1, agent-based modeling has been selected as the most suitable technique for this simulation as it had the most relevant

examples which addressed the turnaround operation and spatial arrangement. Its primary usage will be for path-planning to resolve conflicts during aircraft taxiing and simulate the ground movements of conventional aircraft, as well as hydrogen-powered aircraft including the additional movement towards the refueling station or the special hydrogen gates, to assess the impact on the airport performance.

A typical MAPF-problem consists of a set of agents, an environment, a source and goal vertex for each agent and an objective function for the entire system [107], which will all be evaluated in this section. Furthermore, there exist different ways in which agent-based modelling can be applied to resolve these conflicts, which will be discussed in this section as well. Also, the different types of conflict, assumptions and limitations and solving algorithms will be treated. This information was obtained from Felner et al. and Stern et al. [108, 109] who both published clear overviews of ABS definitions and applications, as well as the Agent-Based Modelling course taught by Sharpanskykh [107].

4.2.1. Problem Definition

The MAPF problem is defined by an undirected graph $G = (V, E)$, together with a set of k agents a_1, a_2, \dots, a_k . Regarding the graph, this set of nodes is used to define the environment of the simulation consisting of vertices, V , together with edges, E . In terms of the agents, every one of these agents a_i is assigned a pre-determined starting location $s_i \in V$ and goal location $g_i \in V$ [108]. This means that the agent must both initialize and finish its actions on a vertex. The time is discretized such that at t_0 , agent a_i is positioned at node s_i . As time progresses, with each time-step the agent is allowed to only perform 1 action, either staying at its current node or move towards an adjacent node. Ultimately, the agent will arrive at its goal, g_i , having successfully traversed its path P , thus defining a single-agent plan [109]. The goal is to ultimately find a solution for the entire system, yielding a set of k paths for each agent i which all successfully complete their tasks conflict-free, while adhering to certain rules, as well as an objective function. From this, the incentive is then to establish an emergence; a pattern, structure or something else which had not been taken into account before [107]. An example of this is provided in Figure 4.1.

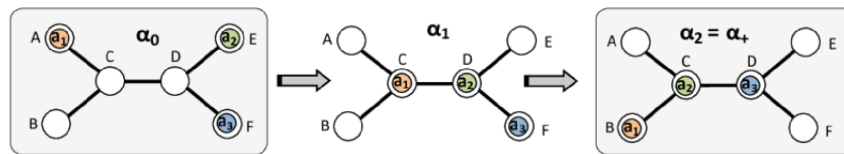


Figure 4.1: Graphical representation of a 3-agent MAPF problem. Retrieved from [110].

As can be seen in the example above, the three different agents either move to an adjacent node or remain positioned at the same node with respect to their initial states, as the time progresses towards the next time-step. Ultimately, the agents move towards their goal destination node and have consequently accomplished their task.

Environment

One of the fundamental elements of a MAPF-problem is the environment. This sets the boundaries of the simulation, and defines the limits of the research. It comprises of non-agent objects, which the agents can observe, act upon, interfere with and potentially change [107]. The environment can either be static or dynamic, depending on the specific application, with the former remaining indifferent with respect to the initial state, while the latter has a final state which can differ from the initial state due to actions from the agents or because of other reasons. Furthermore, the environment can be deterministic or non-deterministic, yielding that actions of agents have a guaranteed single outcome or this outcome will be uncertain, respectively. Finally, an environment is also characterized by its associated accessibility. Whenever an environment is accessible, the agent has full access to all aspects of the environment, including complete and up-to-date information about its state and other characteristics, as opposed to an inaccessible environment [107].

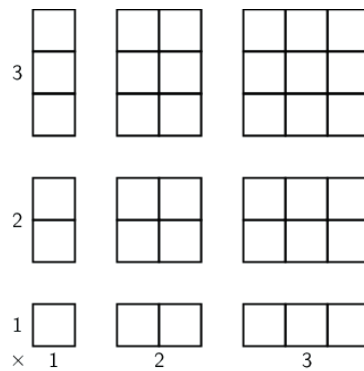


Figure 4.2: Example of 9 different simple 2D-grids which can be used as the environment in a simulation. Figure retrieved from [111].

In Figure 4.2, some graphical examples of 2D grids, defining the potential environment of a MAPF-problem, are provided. As can be seen in the figure, the dimensions of an environment are very flexible which is useful in resembling and setting the context for the specific simulation. Furthermore, the environment consists of cells which the agents can use to move themselves through the environment towards their goal-cell. Each cell can accommodate at most 1 agent per timestep, while the available directions of movement are left, right, up and down, as long as this takes place within the perimeters of the environment. Whenever from a given cell it is possible to move up and/or down AND to move left and/or right, or stay at the given node, the cell is referred to as an edge, as is the case for all cells in (2,2), (3,2), (2,3) and (3,3) in Figure 4.2. Otherwise when it is either possible to only move left and/or right, OR up and/or down, or stay at the current node, the cell in question is considered a vertice. This is the case for the environments (2,1), (3,1), (1,2) and (1,3) in Figure 4.2.

Agents

The agents embody the most important aspect of the simulation. They are autonomous entities who cooperate together or compete and make decisions based on their characteristics, observations of states and phenomena, therefore determining the way in which they physically react in order to reach their goal in a timely manner [107]. These decisions or responses can be immediate, or delayed, while also these are possibly fixed or vary depending on other factors. The set of observations that a specific agent perceives is denoted as follows; $O = \{o_1, o_2, \dots\}$, while the subsequent actions of this agent are denoted as $A = \{a_1, a_2, \dots\}$. The actions are affected by the observations of the agent, but also depend on its internal states $I = \{i_1, i_2, \dots\}$. The associated internal structure relating the observations and internal states to the action can be defined as follows for example; $O \times \dots \times I \rightarrow A \times \dots \times A$. The actions following an internal state can vary from the actions following an observation AND an internal state [107].

These characteristics thus define the behavioral and cognitive qualities of the agents, which in turn influences the way of communication with other agents, its decisions or the way the agent moves through the environment. The set of communication acts that an agent has, with either the environment or other agents, is defined by $C = \{c_1, c_2, \dots\}$. The quality of this communication varies from communication via the environment, direct communication and even coordination in order to cooperate or compete [107]. In greater detail, the communication can be sequential, parallel or mixed, also depending on the different properties. The personality of the agent can be very goal-oriented, or helpful towards other agents, as well as proactive or cognitive. Also, the personality (or internal state) of the agent can differ in problem solving, planning, learning of decision making capabilities. These internal states can even develop during the simulation itself. Agents can be used to represent a wide variety of physical entities, like persons, vehicles, animals and much more. Also, the number of agents can range from one to millions, depending on the specific intention of the simulation.

Objective

In the world of MAPF, there are two main types of objective functions in order to quantify the performance of an executed simulation and to be able to compare this performance with another simulation. In the following list, these two objective functions are listed which can be easily implemented as packages in a computer programming solver language such as Python [109].

- **Makespan:** The number of timesteps required for all agents to reach their goal.
- **Sum of costs:** The sum of timesteps required by each agent to reach their goal.

In the short list above, the two main objectives during MAPF are provided. Firstly, the former objective, 'Makespan', yields the number of timesteps that is necessary for all agents to finish their tasks, and thus represents the time-efficiency of the solution. As time is a very important KPI, this objective needs to be minimized to obtain the best solution. Secondly, 'Sum of costs', yields individually adding the total number of timesteps that is required by each agent. Likewise, this objective is preferably minimized to have the most optimal and efficient solution. There exist variations of these objectives which have been used in prior work, such as disregarding the the timesteps in which an aircraft waits for example, but the two objectives which have been discussed above are the most-used [109].

The first objective is especially useful for compilation-based issues in which the entire system needs to be solved as a whole, whereas the second objective is more relevant for individually search-based assessing the performance of all agents. Considering the incentives of the different stakeholders involved in aviation, the most suitable objective function can be determined. For example, for airlines the 'Sum of Costs' objective is most appealing as in this way their aircraft have the best performance. As opposed to this, the airport would prefer the 'Makespan' objective since this stakeholder has a greater focus on solving the problem of all arriving aircraft as a whole.

Rules

During the simulation, the agents must adhere to a given set of strict rules which are implemented to ensure safe operation and resemble the process which is being simulated as much as possible [108]. The first and also most important rule is that no conflict of any kind may occur during operation. In the following paragraph, the different types of conflict will be clarified. Furthermore, the agents must be spawned at their starting node and exit at the goal node. Moreover, in addition to moving it could also be possible for the agents to wait a (number of) timestep(s), depending on the application. This set of rules can be extended based on the specific problem at hand, in order to make the model as realistic as possible and in this way obtain the most meaningful results as possible.

Conflict types

One of the requirements of a MAPF-solver to be classified as 'valid' is to for paths which are completely conflict-free. This yields that none of the individual agents' paths physically interferes with another path during operation [109]. There exist several definitions for different types of conflicts, of which the two most relevant ones are presented below. Once a conflict has been detected, the fashion in which it will be resolved depends on the conflict resolution approach that is selected for the specific application which will be discussed later in this section.

- **Vertex Conflict:**

A vertex conflict refers to the situation in which two different agents are planning to occupy the same vertex at the same timestep. A visual representation of this situation is provided in Figure 4.3, in which agent 1 moves from X to Y, while agent 2 moves from Z to Y simultaneously.



Figure 4.3: Visual representation of a vertex conflict. Figure retrieved from [107].

- **Swapping Conflict:**

A swapping conflict yields that two different agents plan to swap locations at a timestep, which is physically impossible without having a collision. This type of conflict is depicted in Figure 4.4, where agent 1 moves from X to Y while agent 2 is moving oppositely from Y to X.

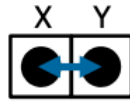


Figure 4.4: Visual representation of a swapping conflict. Figure retrieved from [107].

Limitations

Since MAPF is a simulation and thus a discretization of reality, the model contains a number of limitations. These limitations must be taken into account while analyzing the outcome, while also the validity of all limitation must be considered.

The first limitation of using MAPF is that time is discretized. This leaves the problem of how large the timesteps must be to adequately represent continuous operation, while also allowing fast computations. Another limitation is that the speed of different aircraft can not be varied per aircraft subsequently. In other words, at each time-step the aircraft agent can either move forward at a constant speed or stand still. Thirdly, the environment is discrete which leaves the runway, taxiways and apron unchanged after operation, while also curvilinear corners in reality are represented by 90 degrees corners in the simulation. Lastly, each agent is represented by a discrete point-mass which can not accelerate but only move at a constant speed.

4.3. Conflict Resolution Approaches

The coordination of the different agents within the system influences the way in which conflicts will be resolved, and thus has a significant effect on the results. It can either be centralized or decentralized, distributed or hierarchical, depending on the process which the simulation is designed for to represent, and varies per selected conflict-resolution approach. A framework of all relevant conflict-resolution approaches and solvers is provided in the following figure, which will all be further elaborated upon later.

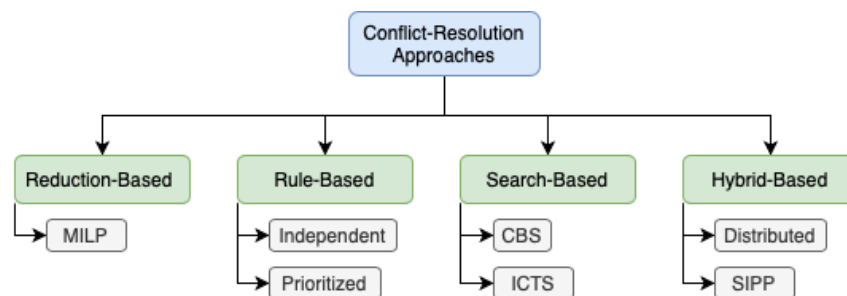


Figure 4.5: Schematic overview of the most relevant conflict-resolution approaches for MAPF. Information retrieved from [109].

In the figure above, the most relevant MAPF conflict-resolution techniques are structurally presented in order to obtain a clear overview of the possible solutions. As becomes apparent in Figure 4.5, the conflict-resolution approaches can be split into reduction-based, rule-based, search-based and hybrid-based MAPF solvers. Regarding the first category of reduction-based solvers, MILP is the main conflict resolution technique in terms of MAPF problems. Next up, in terms of the rule-based approaches, there is independent and prioritized. In these two approaches, there is no conflict search at all but the paths of all agents are completely planned according to rules. Furthermore, there is the category of search-based approaches. In here are CBS and ICTS, which are both two-level-based approaches as well, yielding that the search consists of two different stages. Lastly, there is the hybrid-based approaches, meaning that the approach consists of both rule-based and search-based elements, which is the case for distributed and SIPP. In the following subsections, the different approaches presented in Figure 4.5 will be discussed in greater detail, including their common practices, characteristics and main (dis-)advantages.

4.3.1. Reduction-Based Approach

One of the ways to solve a multi-agent path finding problem is through a reduction-based approach. This incorporates that the problem is reduced or relaxed to a simpler version of the problem, which can then be solved more easily by using a more efficient technique. The principle is very effective, as the problem is still solved optimally, however in a much faster and simpler manner now, making the need for complex approaches redundant. In the following list, the main reduction-based approach that will be considered in this study is explained.

- **MILP:**

Mixed Integer Linear Programming [MILP] is a very efficient algorithm to resolve conflicts in MAPF, as has been proven by Tang et al. [112] and Lihua [113]. MILP is a mathematical programming method, which expands conventional continuous linear programming with the possibility to select binary or integer decision variables and constraints, in order to relax the problem. The mix between these type of constraints can be very useful to represent a wide range different types of phenomena of processes, both continuous and discrete. MILP provides a set of constraints and an objective function, in order to find the optimal solution to the problem. It has been proven to be especially suitable for trajectory planning and terrain obstacle avoidance in a 3D discrete or dynamic airspace environment [112].

This main practice or 3D terrain avoidance yields that a triangular grid represents the environment, including irregularity such as elevations, which together forms a network mutually exchanging information. From the lengths of these vertices, the distance to any obstacle can be determined and its presence including a safety margin must be acknowledged by the agents, as specified by one of the MILP constraints. Based on a pre-defined radius, the agents detect conflicts with the environment throughout their actions, and adjust their flight direction accordingly in case of a detected obstacle, while following the terrain as close and thus as efficient as possible [112]. This approach of thus resembles the radar-based distributed approach to a great extent, as will be discussed later. Given this information, the structure of this approach is also distributed but centralized, since the agents make their own decision, but based on a shared objective. This technique can provide very good results, but is relatively complex to develop and implement, is very computationally expensive while also having a high computation time and a limited applicability.

4.3.2. Rule-Based Approaches

The second category of conflict-resolution approaches is rule-based. Within this approach, the standard is to not search for conflicts during the simulation, but to resolve conflicts based on pre-defined rules instead. In this way, results can be obtained relatively fast, sometimes at the cost of some optimality however. In the following list, the two main practices of this approach will be discussed.

- **Independent:**

The simplest example of a rule-based MAPF solver is the independent approach. In this technique, a single agent is spawned at its origination node and travels to the goal node in the most efficient way possible while avoiding all obstacles [107]. However, since there is only one agent at this point, no attention needs to be given to avoiding or resolving collisions. Nonetheless, this can serve as the foundation of the model which can then be later extended with other functions and features such as more agents which therefore allows the modular extension of the model. This approach can be defined as centralized and hierarchical, as the agent is ordered to follow a pre-defined path while adhering to a set of rules, thus having no authority to make independent decisions.

- **Prioritized:**

Moreover, a relevant sub-optimal rule-based MAPF solver available is the prioritized approach. This approach entails that the expected number of agents are each given a pre-defined order of importance or priority, which can be dependent on different factors. Once this priority has been established, the paths of the agents are planned, starting with the agent with the highest priority, and so on. Whenever a suitable path has been found for an agent, successfully connecting its start and goal node in a conflict-free fashion, the path, consisting of a set of locations and associated timesteps, will be added in a list. This list then serves as a constraint list for all following agents, which implies that they have to find a path beforehand which does not interfere with any of the agents with a higher priority, and in this way the entire system will be solved [107, 108].

Disregarding the fact that this approach does provide a result, it is not always optimal since it is dependent on the (random) order in which the priority has been assigned. However, as this approach resembles processes which are also characterized by a first-come first-serve principle, this could also be a very useful application. Furthermore, the technique is also suitable for simulating certain traffic situations with applying rules, like for example vehicles coming from the right at an intersection, which are then given priority. This technique is characterized as centralized hierarchical, implying that the 'orders' are given by an overarching central planning agent who has authority over the agents who are actually operating in the environment.

4.3.3. Search-Based Approaches

Another category of MAPF conflict-resolution approaches is in a search-based fashion. Instead of solving conflicts based on a given set of rules or simplifying the problem first, this approach is characterized by searching for conflicts during the simulation itself. Whenever a conflict is identified, it is solved simply by searching for different solutions and choosing the most optimal one. In the following list, two examples embodying this technique are provided. These examples are both characterized by a two-layer search as well.

- **CBS:**

The first optimal search-based MAPF conflict resolution technique is Conflict-Based Search [CBS]. This technique is more advanced than the independent approach as discussed above. The principle is that whenever a new aircraft is spawned, it is evaluated whether this 'new' path collides with any of the agents who are already travelling. If not, there is no problem and the new agent can simply execute its planned actions. Nevertheless, whenever the path of this new agent does interfere with the path of an existing agent, both paths have to be re-evaluated. This can either yield that the new agent or the already travelling agent has to re-direct, depending on what is more efficient [107]. The actual conflict resolution action can either consist of a waiting action, or an actual redirection. Depending on how time-efficient the model needs to be, it can be decided to only limit the scope of evaluated agents to the ones who were affected first because of the new agent. When also analyzing the affected agents because of the path(s) that have already been redirected, the modelling can become extremely time-intensive.

CBS is not very fast, but can find high-quality results. Furthermore, the approach is a modular one which allows it to easily adjust, improve or extend the algorithm based on the application. Examples of this are the way the conflict is resolved or for how many steps the rescheduled paths should be considered during the conflict resolution, as was shown by Stern et al. [108]. The structure is highly centralized and hierarchical, in which all authority is assigned to the overarching planning agent and the other agents simply execute their tasks.

- **ICTS:**

The second search-based MAPF conflict resolution approach that will be considered in this research is the Increasing Cost Tree Search [ICTS]. It is fundamentally different from some of the approaches explained earlier, as it is based on the principle that the solution to the entire solution consists of the individual paths of each agent. This therefore underlines a centralized hierarchical structure. There exist two stages of ICTS, being the high-level and low-level stage [108]. A schematic overview of this technique helps in the understanding, and is provided in Figure 4.6.

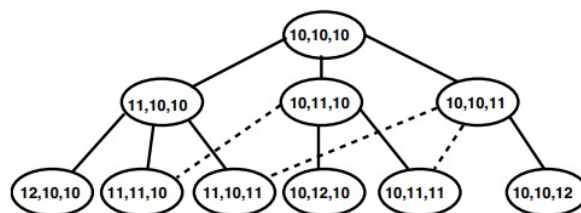


Figure 4.6: Schematic visualization of the ICTS approach. Figure retrieved from [114].

As can be visualized in the example above, the algorithm starts with high-level search in which a root including the optimal path lengths for the 3 agents **without** taking into account the paths of the

other agents is set up, (10, 10, 10). Subsequently, a child is generated in which the path length of one of the agents is increased with 1, as can be seen in the node below the root, (11, 10, 10). This process is continued until a valid conflict-free solution can be found. Subsequently, this solution can be iteratively found by means of the low-level search, which consists of a single-agent path planning algorithm, generating paths for each agents with a total length equal to the value defined in the considered node. When a solution-free optimum is found, the loop is finalized, and if not, a new set of nodes is generated in the high-level search as was specified by Sharon et al. [114]. Conclusively, the authority completely lies with the planning agents who defines and plans the paths to be travelled by the operating agents.

4.3.4. Hybrid-Based Approaches

The final approach that will be considered in this study is referred to as hybrid-based. In fact, this means a combination of the rule-based and search-based approach which have been discussed in Section 4.3.2 and Section 4.3.3 respectively. In practice, this yields that the approach will first perform a search-based approach, but whenever a conflict is found the strategy switches to rule-based, achieving the best of both worlds and thus being a very effective technique. The two most relevant examples using this approach are discussed below.

- **Distributed:**

The first hybrid-based and therefore more sophisticated conflict resolution technique is distributed. In this method, the coordination structure is distributed, instead of centralized, as was the case with the two methods discussed previously, and the agents are characterized by more cognitive properties. In fact, the agents have more authority in resolving conflicts, instead of a central planning agent taking care of this. Namely, each operating agent is equipped with a radar which is activated at each timestep. The goal of this radar is to detect any potential conflicts in the next coming timesteps, thus explaining the search-based aspect of this approach. If no conflict is foreseen, there is no problem and the agent can simply continue its path as planned.

Nevertheless, in the case that a conflict is detected, the conflicting objectives will be resolved according to a negotiation game-theoretic approach. Namely, an auction is set up in which the two conflicting agent will bid on being allocated priority, and in this way the conflict can be resolved in a fair manner. The agents start their route with a pre-determined budget, and in the case of a potential conflict they bid an amount which represents how valuable priority is to them [107]. The winning agent can then continue its path undisturbed, while the other agent is either re-scheduled or has to perform a waiting action. The additional time required in order to resolve the conflict by the losing agent also influences the amount of budget that will eventually be subtracted.

An auctioneer agent is involved in this procedure, in order supervise the pre-established rules of the auction, to collect the bids, determine the winner and define the updated budgets of both agents. In case both agents offer the same bid, additional rules can be set up such as departing agents having priority over arriving agents, or the oldest agent having priority over younger agents. The auction-part of this technique therefore represents the rule-based aspect of the approach, thus making it a hybrid-based approach overall. This technique also embodies hierarchy to some extent, as the auctioneer agent has more authority than the bidding agents. Through varying how far the selected range of the radar is, but also by adjusting the height of the initial budget of each agent, determining how many auctions they can theoretically win, this method can be made more time-intensive or more efficient instead.

- **SIPP:**

The second considered hybrid-based approach used for the conflict resolution of MAPF problems is Safe Interval Path Planning [SIPP]. This is a very smart technique, which is especially useful for path planning with dynamic obstacles, such as other agents. In fact, whereas many approaches such as the distributed technique above discretize a dynamic obstacle at every time-step in order to treat it as a set of static problems, this approach is fundamentally different, which results in a better optimality. Namely, it makes use of so-called safe time intervals in which the agent can move from one node to the other, aiming to reach its goal, which it searches for. As this number of safe time intervals to move is much smaller than the number of safe timesteps to move, the problem becomes much easier to solve by limiting the number of dimensions. Whenever there is a safe time interval, the agent will move immediately. However, whenever there is no safe time interval, the agent will remain in its

current node and has to perform a waiting action, defining the rule-based aspect of this approach as well. In Figure 4.7, an example using SIPP is provided to better understand its actual implementation.

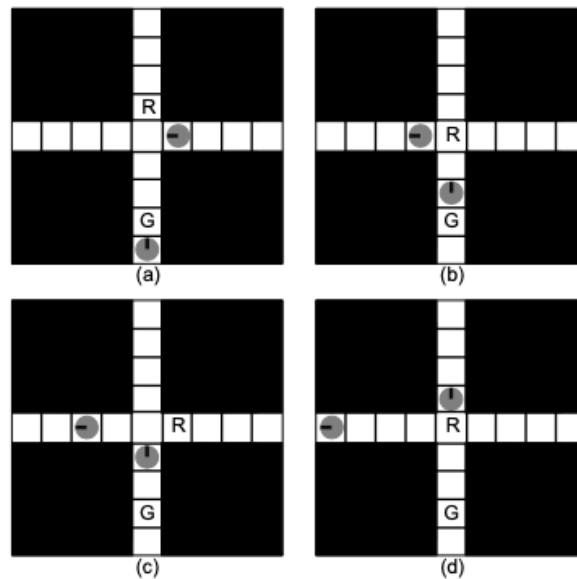


Figure 4.7: An example of an agent travelling in an environment with two dynamic obstacles, using SIPP as the conflict-resolution approach. Figure retrieved from [115].

Considering the figure above, the location of the agent is being represented by cell "R", and its goal destination is shown as "G", with the grey circles being dynamic obstacles that the agent can not conflict with. The dynamic obstacle positioned in the cell below G is moving upwards, while the other agent is moving towards the left, both at a speed of 1 cell per timestep, being the same speed at which the agent can move. Because the upper dynamic obstacle will have moved to the center cell after one timestep as can be concluded from (a), there is no safe time interval after one timestep yet, as this interval only starts after two timesteps [115]. However, as the other dynamic obstacle is moving upwards, the end of the safe time interval is at 3 seconds once the simulation has started, setting the first safe time interval at $[2, 3]$. Because this is insufficient for the agent to reach its goal, it must use this safe time interval instead to get out of the way of the vertical agent, which is shown in (b) and (c). Only after both dynamic obstacles have passed and the agent has waited in the meantime, another safe time interval opens at 5 seconds again which extends to infinity $[5, \infty]$, providing sufficient time for the agent to reach its goal.

By reducing the number of variables from timesteps to intervals, this technique is more efficient than other techniques which leads to faster results, while also the optimal results are better, since the agent always immediately moves once the safe time interval opens. This feature can be changed however using pre-defined rules, to for example always make the agent move the second possibility of the safe time interval instead, if this suits better to the problem. Also, because of its effectiveness on dynamic obstacles, the application is also significantly enhanced [115]. The coordination structure of this technique is still centralized and hierarchical as the movement options are evaluated and ordered by a central planning agent, but the agent itself has better developed cognitive qualities as it is able to observe and communicate the behaviour and position of the dynamic obstacles.

4.3.5. Trade-Off

Now that these different MAPF solving techniques have been clarified, it is time to compare them to find the most optimal one. In order to achieve this, a total of 6 categories has been established. These are the computation time, the quality of the results, but also how complex it is to develop the solver, its applicability in simulating ground movements at an airport, the scalability and the robustness of the model. This leads to the trade-off table as presented in Table 4.2, in which the scores range from -- to ++.

Table 4.2: Trade-off table representing the main (dis-)advantages of each MAPF solving approach.

MAPF Solver	Computation Time	Quality of Results	Development Complexity	Applicability	Scalability	Robustness
Prioritized	++	-	+	++	++	+
Independent	++	+/-	++	--	--	-
CBS	+/-	+	-	++	+	+/-
Distributed	+/-	+	-	+	+	+
MILP	--	++	--	-	+	+
ICTS	-	+	-	+	+/-	+/-
SIPP	++	++	-	++	+/-	+/-

As becomes apparent in the table above, each technique excels in different aspects. Prioritized has a very low computation time, is extremely scalable and applicable to this specific research and is also not very hard to develop, with a very good scalability and robustness too. The only downside is that the quality of the results remains somewhat limited. Next up, the independent approach is also very efficient time-wise while also easy to develop, but its robustness is low because of its reliance on a simple input. Moreover, the scalability is low while also the quality of the results and the applicability to the specific research are marginal, since it can only simulate a single aircraft. Furthermore, CBS and distributed are very similar, with their discussable computation time which is flexible and depends on factors such as the range of the radar and the number of agents considered in the conflict-resolving. Furthermore, their quality of results is already much better than prioritized and independent, while also they are having a very good applicability. This leads to a medium to good robustness, while also being easily scalable. However, this comes at the cost of some development complexity again due to the sophisticated algorithms.

Moreover, MILP and ICTS are quite similar to CBS and distributed and possibly even have a better quality of results. Nevertheless, their applicability is slightly worse, as MILP is mainly intended for 3D obstacle avoiding, as well as a very long computation time which is undesirable. Lastly, SIPP performs extremely good in terms of computation time and quality of the results. Furthermore, it is not too complex to develop while also being applicable to the problem. The only downsides are the scalability and robustness, which are both somewhat uncertain.

This analysis concludes that different conflict-resolution techniques can be useful for different applications. The most potential techniques to this research however are prioritized, CBS, distributed and SIPP. Prioritized allows to obtain fast results and is very scalable and applicable, but at the cost of a lower quality of the results. Moreover, CBS and distributed result in better quality results and are also very applicable and scalable, at the cost of a longer computation time and more complexity however. Lastly, SIPP is extremely fast and provides high-quality results, but is slightly less scalable and more complex again. Whichever conflict-resolution technique will be the most optimal for the research thus depends on the phase of the modelling, and the associated interest in different model characteristics. Early on, prioritized could be interesting because of its fast results, but later on, SIPP might be better because of the results having a higher-quality. Additionally, the optimal technique also depends on which scenarios will ultimately be selected for the research, as well as the applicability on the final airport layout and problem that will be utilized, and thus the necessity of scalability as well.

4.3.6. Path Planning Algorithm

The MAPF conflict resolution approaches that were introduced in Section 4.3 mainly address the coordination of the resolution of conflicts. Notwithstanding this, for low-level searches or single-agent shortest path planning, these approaches rely on efficient path planning algorithms to actually determine these paths. There exist many different algorithms to determine the shortest path like the Dijkstra, the Bellman-Ford or the Branch and Bound algorithm. However, there also exist more complicated algorithms in which the algorithm has 'knowledge' which helps in reaching the goal through a shortest path quicker. Namely, the algorithm is then able to remember the shortest path to each node, such that whenever an alternative path with a higher cost to a previously visited node comes up, this can completely be disregarded, being very efficient. This subsection will discuss the most applicable algorithm for this problem, which is A*.

A*-algorithm

The algorithm A* is one of the most famous and widest-used path-finding algorithms available. Its practice can be explained fairly easily, which will be done using the following example.

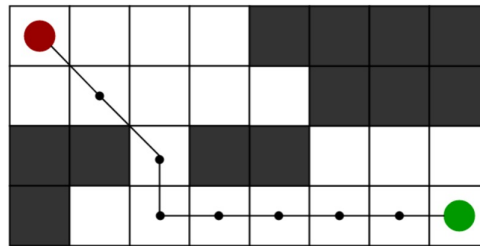


Figure 4.8: Schematic visualization of path-finding in a 2D-grid using the A* algorithm. Figure retrieved from [116].

In Figure 4.8, the red circle represents the source cell, whereas the green circle represents the goal cell. Furthermore, the black line with the dots refers to the traversed path. It must be noted that in the actual research, it will only be possible to make 90-degree corners, in contrast to the 45-degree corner as is shown above in the first two steps from the start cell. The goal is to reach the goal cell, starting from the source cell, while avoiding all obstacles (black cells), as fast as possible.

The working principle behind the algorithm is that after each timestep, the model determines its next step based on achieving the lowest possible f , and processes that specific cell. The variable f is equal to the sum of factors g and h , which have the following significance:

- g : The total cost of moving to a certain cell on the grid, starting from the source cell. This is a sum of the entire path, including all individual steps, to reach this particular cell, and is exactly known [116].
- h : The estimated total cost to move from a specific cell on the grid to the goal node [116]. This cost is highly uncertain, and can not take into account any obstacles yet. However, it is important to be as accurate as possible in terms of this estimation, which is also known as the heuristic, and can be calculated in lots of ways. Together, this forms the following equation:

$$f = g + h \quad (4.1)$$

The equation above represents the subsequent equation representing the cost for a certain path with the current knowledge. Next up, the A*-algorithm search is provided [116]:

A*-algorithm Pseudo Code

1. Generate and initialize the open list (unexplored), and put all nodes in this list.
2. Generate and initialize the closed list (visited), and put the starting node on the open list.
3. While the open list is not empty:
 - i) Find the node closest to the starting point on the open list, call it "q".
 - ii) Remove q from the open list.
 - iii) Establish q's successors.
 - iv) For each successor:
 - (a) If successor is the goal node, the algorithm ends.
 Else, compute both g and h for successor:
 - $\text{successor.g} = \text{q.g} + \text{distance between successor and q}$
 - $\text{successor.h} = \text{distance from goal to successor}$ (Can be calculated using a heuristics)
 - $\text{successor.f} = \text{successor.g} + \text{successor.h}$
 - (b) If a node with the same position as the successor node is in the OPEN list with a lower f than the successor, skip this successor.
 Elif a node with the same position as the successor is in the CLOSED list with a lower f than the successor, skip this successor.
 Else, add the successor node to the open list.
- "End for loop"
- v) Push q onto the closed list
- "End (while loop)"

Heuristics

Now that the algorithm has been elaborately explained, it is time to look at suitable heuristics to support this algorithm. The overall performance of the entire algorithm is actually defined by this heuristic, which is nothing more than an estimate of what the remaining path cost towards the goal will be. Preferably, the heuristic is admissible (underestimating) since this gives a guarantee to always find the shortest path. There are different techniques in existence to make a heuristic admissible, like forming a relaxed version of the problem, utilizing exact solutions to parts of the problem or by using inductive learning methods [117]. Regarding the environment, a 2D grid as was shown in Figure 4.8 will be considered. In the following list, a few examples of the most popular heuristics are provided [116]:

- **Manhattan Distance:** The sum of the absolute differences in horizontal and vertical locations of the current and goal nodes.
- **Diagonal Distance:** The maximum of the absolute differences in horizontal and vertical locations of the current and goal nodes.
- **Euclidean Distance:** The distance between the current and goal node, determined using the Pythagoras distance formula.

5

Research Proposal

In this final chapter, the research proposal for this master thesis is provided. First of all, in Section 5.1 the research objective and associated research questions, forming the framework behind this thesis, will be presented. Secondly, Section 5.2 will introduce the context of this research, Rotterdam The Hague Airport, including all its relevant characteristics. Next up, the research methodology will be discussed in Section 5.3, consisting of the simulation and optimization practices, together with the model, selected solution technique and hypothesis. Lastly, this chapter will be concluded with the forecasted planning for this master thesis in Section 5.4.

5.1. Research Objective & Research Questions

Based on the literature study as provided in this document, the following research objective can be formulated:

"To design and evaluate a simulation-based model to optimize the ground operation of hydrogen-powered aircraft, focusing on the early stages of the transition period towards hydrogen-powered aviation between 2025-2035, using Rotterdam The Hague Airport as a case-study"

This research objective will be answered through the following supporting set of research questions:

1. What does the turnaround of a hydrogen-powered aircraft look like?
 - (a) Which turnaround processes are impacted by the introduction of hydrogen as a fuel?
 - (b) Which additional safety measures must be taken to safely operate hydrogen at an airport?
 - (c) Which hydrogen-powered aircraft types will be operating at small international airports?
 - (d) How long will the TAT of a hydrogen-powered aircraft last?
 - (e) How does the TAT vary (decrease) throughout the transition-phase?
 - (f) How can the turnaround of a hydrogen-powered aircraft be modelled?
2. What is the optimal spatial arrangement of hydrogen-related infrastructure at RTHA?
 - (a) What additional infrastructure is required at RTHA at what point in the transition phase?
 - (b) What existing infrastructure can be used to also accommodate hydrogen-powered aircraft?
 - (c) How many additional ground personnel is necessary?
 - (d) Which and how many GSE are necessary for hydrogen-powered aircraft?
 - (e) What are the potential and optimal locations to build new hydrogen-related infrastructure at RTHA?
 - (f) Does the hydrogen-related infrastructure interfere with existing infrastructure?
 - (g) How many hydrogen refueling locations are required to accommodate the most optimal turnarounds at RTHA?
3. How can the paths of conventional and hydrogen-powered aircraft agents be planned at the airport?
 - (a) What type of agents can be used or are necessary?

- (b) What environment must be considered for this path planning?
 - (c) How will agent conflicts be resolved?
 - (d) What is the objective while performing path planning?
 - (e) What assumptions and limitations have to be made?
 - (f) How are the priorities of the agents determined?
4. How can the multi-agent model be implemented?
 - (a) What input data is required?
 - (b) How can this data be acquired?
 - (c) How can the model be tested?
 - (d) How can the model be verified and validated?
 - (e) How can the statistical significance of the model be established?
 5. How can the optimal ground operation of hydrogen-powered aircraft at RTHA be evaluated?
 - (a) What are suitable KPI's to express the airport performance?
 - (b) Which scenarios of traffic distribution (hydrogen/conventional) traffic should be considered?
 - (c) What is the effect of the different airport configurations on the airport performance?
 - (d) How does the forecasted traffic (distribution) vary throughout the transition phase?
 - (e) What are the associated noise and (non-) CO2 emissions at RTHA?

5.2. Case-Study at Rotterdam The Hague Airport

This master thesis will utilize Rotterdam The Hague Airport as a case-study. RTHA is currently the third-largest airport in the Netherlands, behind Schiphol and Eindhoven airport, with about 2500 employees, 29 destinations and over 2 million annual passengers in 2019 [118]. This underlines the importance to sketch the context at the airport, which includes the daily operation, infrastructure, including airport layout and personnel, and the available ground support equipment. In this way, the inputs, restrictions and rules to the simulation can be defined in greater detail which eventually forms the basis of the research.

5.2.1. Airport Operation

The main operation of the airport consists of commercial short-haul flights, together with private flights, a flight school and the life-liner helicopter operated by the ANWB. Furthermore, since the airport is part of the Schiphol group, it is also used as a test-bed for numerous innovations at a relatively small scale, thus minimizing the risk and investment. In contrast to many airports, RTHA's capacity is currently not limited by its number of movements, but by a noise quota instead [119]. The forecasted amount of emitted commercial noise depends on the expected distribution of traffic, which is defined by the number of aircraft from a specific type visiting the airport, who have been given a slot. It must be noted that aircraft which do not comply with noise limitations can not be assigned new slots. In the table below, the assumed traffic at the airport over a period of 24 hours is shown, together with the amount of noise emitted.

Table 5.1: Forecasted traffic distribution with the associated noise penalty at RTHA in 2021. Information retrieved from [119].

Aircraft size	Percentage of flights	Average penalty L_{den}
Propeller aircraft 19-34 seats	<0,1%	-
Propeller aircraft >35 seats	1,3 %	1,64
Jet aircraft <120 seats	19,1 %	1,58
Jet aircraft >120 seats	79,6 %	1,63
Total	100,0 %	

As can be seen in Table 5.1, the big majority of operation at RTHA consists of large jet aircraft, with almost 80%. The runner up is the small jet aircraft, which mainly consists of private jets. This distribution of traffic

could potentially influence the allocation of slots by the slot coordinator, whenever the noise capacity is expected to be exceeded. Even though the airport has no limitation on the number of annual movements, the slot coordinator still has a specified number of commercial slots to assign. In the summer season (March–October) of 2021 (COVID), there were 11,995 slots available. The total number of movements at RTHA in this complete year however, was a lot higher with 46,000 [119]. These flights are allowed to perform movements at the airport between 7 am and 11 pm in general, with a maximum turnaround duration of 120 minutes. However, exceptions can be made for early slots, night-delays or else, in mutual consultation with the airport. These delayed aircraft can land at the airport up to 2 hours later, at an increased airport fee though, and these night-delays can not exceed 3% of the slots allocated to an operator [119]. The opening times of the airport are defined by the first outgoing and last incoming flight of the day.

Furthermore, the airport terminal has a normal capacity of up to 900 passengers, but depending on the time of day this flexible capacity can actually range from 600–1200 [119]. Typically, passengers spend up to 1 hour before departure in the terminal of the airport, defining the average airport passenger capacity of 900 passengers per hour. These passengers can be distributed over 10 gates in total, which can be flexibly split between Schengen and non-Schengen, with the exception of high risk flights to the USA and Israel. In terms of arriving passengers, the airport has a higher maximum capacity of 8 arriving aircraft with a total of 1150 passengers, every 35 minutes [119].

5.2.2. Infrastructure

Besides suitable GSE as will be discussed in Section 5.2.3, adequate infrastructure is another fundamental element to accommodate the turnaround of aircraft. It highly varies per airport, so this review of available infrastructure will be limited to RTHA. The infrastructure is mainly defined by the airport layout at which the simulated operation will be performed. The airport layout consists of both the airside and landside, which together defines the entire airport. The former yields the area where the aircraft operate, including the runway, taxiways, apron and terminal, while the latter refers to the airport area which is accessible to the public. For this research, only the airside is important and therefore the landside will be left mostly out of consideration. In the following figure, the layout of RTHA is presented.

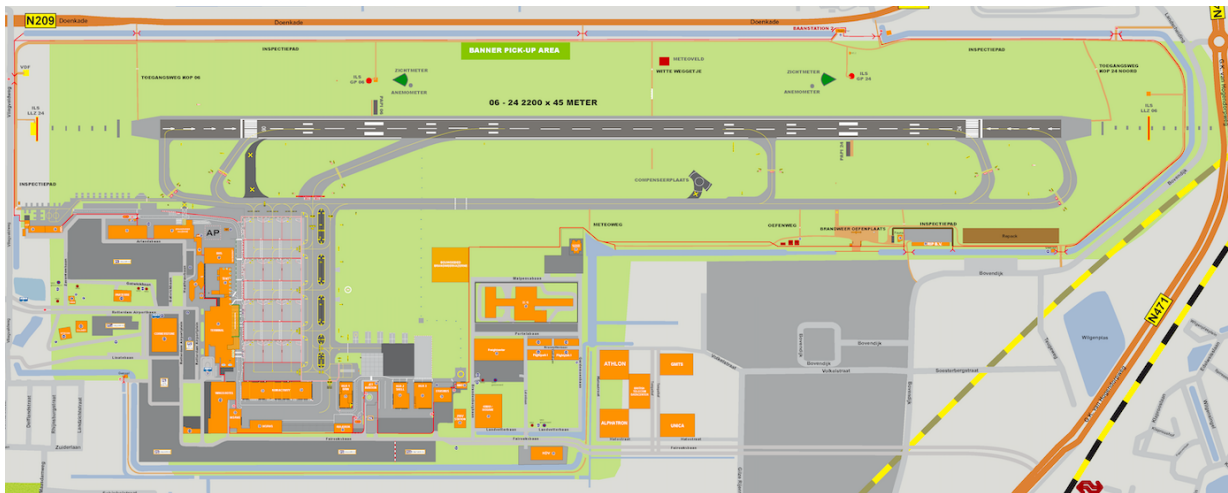


Figure 5.1: Layout of Rotterdam The Hague Airport. Retrieved from [71].

As can be observed in Figure 5.1, RTHA has a single runway configuration, with 06/24 as its only runway, being 2200 meters long and 45 meters wide. The orientation can be explained from the fact that at the airport, the south-west is the dominant wind-origin direction [120]. Parallel to the runway is a taxiway, which is connected to 06/24 via 7 taxiways in total. These taxiways are placed at different points along the runway to allow different aircraft types who have different landing distances to exit the runway as fast as possible and clear the runway for other aircraft. Furthermore, at the south-east side of the runway there is a rapid exit taxiway which is at a slight offset angle with respect to the runway, leading directly to the apron.

The commercial part of the apron consists of 12 identical ICAO size C aircraft stands, arranged in a 3-3-3-3

configuration, which can accommodate aircraft with a maximum wingspan of 36 meters [119]. This allows the highly-used B737 and A320 aircraft to be the largest aircraft types to be commercially handled at RTHA. Incidentally and under special permission, aircraft of ICAO size D or E can land at the airport and park at 2 the two first stands with respect to the runway. This allows for example a B777, B787 or B747 to divert to RTHA during extraordinary weather or other kinds of emergency circumstances, as the airport is the official diversion airport for Schiphol Airport. In this case, the aircraft can land at RTHA and must leave completely empty afterwards again because of the short runway. Additionally, Rotterdam The Hague Airport also has its own fire department who are standby 24/7 for (medical) emergencies.

5.2.3. Ground Handling Equipment

Throughout the turnaround procedure, a wide variety of vehicles, also referred to as GSE, are involved to execute the different processes. In order to relate to the case-study at RTHA, all GSE assets of the airport that are utilized in the turnaround of a conventional B737 are listed in the table below. Furthermore, the priority of each vehicle for the case of a path collision, together with the storage location of each vehicle and the number of vehicles required, are provided. The information in this table has been obtained from expert knowledge.

Table 5.2: Overview of the required GSE per aircraft, including stalling location and priority. Information retrieved from [101] and [121].

Ground Support Equipment	Required	Location	Priority
GPU	1	Positioned at gate	2
Stairs	2	Positioned at gate	1
Refueling Truck	1	Central, shared usage	4
Baggage Carts	3	Central, shared usage	6
Baggage Belt	1	Positioned at gate	5
Servicing Waste Water	1	Central, shared usage	9
Potable Water	1	Central, shared usage	8
Galley Service	1	Central, shared usage	7
Busses	2-4	Central, shared usage	3

As can be seen in Table 5.2, the different GSE-vehicles that are necessary to turnaround a B737 are listed, together with the number of vehicles required of each individual GSE. Whereas of most GSE, either only 1 or 2 vehicles is sufficient, the number of baggage carts and busses is significantly higher. This is because of the large number of luggage and passengers that have to be transported towards the aircraft respectively. This can be done using either different busses and baggage carts, or re-deploying the same vehicles every time. As specified by the airport however, the baggage cart can carry at most 6 trailers at once [119]. As a result of strategic, financial and demand incentives, the GPU, airbridge and baggage belt are stalled and provided independently at every gate, whereas all other GSE is stored centrally next to the terminal building and are shared by all aircraft, which in turn impacts the TAT and airport capacity. Furthermore, each GSE-vehicle has its own assigned priority. This priority is based on the duration of the process executed by the specific GSE, so that the vehicles which execute the most time-consuming turnaround process, such as refueling and deboarding, can access the aircraft as fast as possible.

5.2.4. Kerosene Storage Facility at RTHA

Due to the limited demand of Jet-A1 at RTHA, the storage facility is relatively small. In fact, the airport is supplied with pre-filled refueling trailers of Shell which are delivered by trucks via the public road. Once at the airport, the truck drops off the full trailer at the storage facility and immediately picks up an empty trailer again. This configuration saves investment costs, maintenance and also time and thus is the most efficient solution for the current operation. In the figure below, a visual representation of this storage facility is provided.



Figure 5.2: Visual representation of the (temporary) fuel storage facility at RTHA.

As can be seen in Figure 5.2, the fuel trailers are lined up next to each other. In total, there are 6 stands positioned next to each other. The facility is equipped with a liquid-tight ground surface which collects spillages in a large container while also protecting the environment from harm. The number of deliveries per day varies highly with the expected traffic, and can range from a few to up to 10 deliveries. As a rule of thumb, it is assumed that one of these trailers as depicted in the figure above can refuel approximately 3 narrow-body aircraft, as was learned from expert knowledge. Whenever the trailer is empty, the refueling truck which can also be seen in the picture above drops off the empty trailer for it to be picked up after the next delivery, while it picks up a pre-filled trailer again to continue its operation. This process is very efficient and only takes a few minutes at most. The facility is located at the western part of the airport, easily accessible to these delivery trucks via a gate which is only approximately 30 meters away.

5.2.5. Off-site Hydrogen Supply-Chain

For a small airport like Rotterdam The Hague Airport, a pipeline system for hydrogen delivery is not realistic at this stage. Given that the small supply of hydrogen will most likely originate from the Rotterdam Harbour, which is only about 30 km away, the transportation cost and emissions will be relatively small. As pipelines are more permanent, at this point this is simply not feasible considering the current transition phase. In addition, current delivery of Jet-A1 at the airport is also done using truck-delivery. This results in a defined hydrogen supply-chain for RTHA, of which a graphical depiction is presented in the figure below.

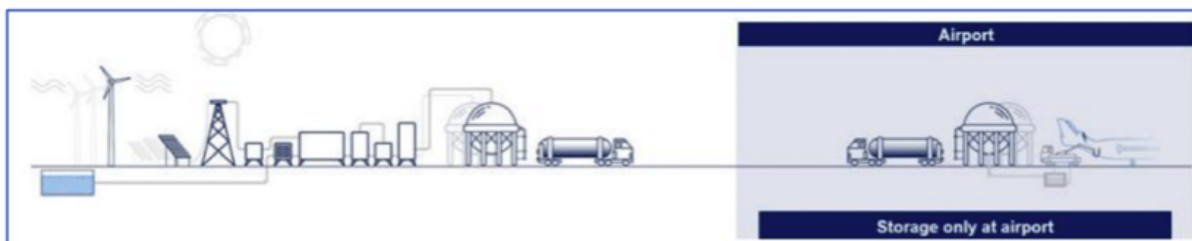


Figure 5.3: Visualization of the supply-chain of LH2 to RTHA. Figure retrieved from [27].

With the supply-chain provided in Figure 5.3, the least space is required at the airport itself while also the cost is kept as low as possible. Namely, as can be seen on the left, all electricity generation, electrolysis and liquefaction practices will take place off-site, where the LH2 will also be initially stored. By means of a cryogenic truck, the LH2 will then be transported from the off-site facility towards the airport, where it will be stored subsequently. More details on the on-site storage facility will follow in Section 5.2.6. In 2030, it is estimated that during peaks there will be at most 5-6 commercial hydrogen-powered flights per day at RTHA, performed by a retrofitted DHC-8 or similar as was forecasted by TULIPS [94]. Assuming that one such aircraft needs approximately 700 kg of LH2, this sets the maximum daily required supply of LH2 at RTHA at 4500 kg including a safety margin [29]. As a typical cryogenic truck can carry 2200-3500 kg of

LH2 at once, this results in just 1-2 daily LH2 tanker deliveries. Nevertheless, this delivery rate is expected to increase to up to 5 daily deliveries by 2050, also requiring a larger on-site storage facility [118] [29].

5.2.6. Hydrogen Storage Facility at RTHA

Considering the forecasted traffic at RTHA in 2030 of TULIPS in Section 5.2.5, the demanded space for the storage facility can be roughly established. In order to accommodate these 5-6 hydrogen-powered flights per day including a safety margin, using DHC-8's, would thus require about 4500 kg of LH2, equal to 63450 L. This leads to a total space requirement of approximately 270 m^2 for the storage facility [27]. As reference, Rotterdam The Hague Airport is planning on installing its first LH2 tank which holds 1500 L (135 kg), making the required cylindrical storage facility of 2030 almost 50 times as large [118]. However, storing the hydrogen in a similar fashion as is currently done with Jet-A1, namely by keeping it inside the tanks, is also one of the possibilities. The exact storage facility will be defined at a later stage in this thesis.

5.3. Research Methodology

The research methodology is fundamental to this master thesis, as it establishes and contributes to the academic value of the research. First of all, the scope of the research will be defined in Section 5.3.1, as well as the the simulations and optimization specific to the case-study at RTHA. Secondly, the selected conflict resolution methodology will be shortly discussed in Section 5.3.2. Third and finally, in Section 5.3.3 all relevant aspects of the model used for these simulation and optimization practices are briefly discussed, together with a hypothesis.

5.3.1. Research Scope

As has been announced in Section 5.1, the objective and thus the main scope of this research is to design and evaluate a simulation-based model to optimize the ground operation of hydrogen-powered aircraft, focusing on the early stages of the transition period towards hydrogen-powered aviation between 2025-2035, using Rotterdam The Hague Airport as a case-study. Since ground operation is a very broad and vague concept, it is important to set the scope of the research at an early stage, in terms of the assumptions made, what will exactly be simulated and optimized and which techniques will be used for this. Namely, having a well-defined scope generally improves the quality of the executed research, avoiding the focus to become too broad.

In short, the scope of this research has been set on the ground operations of hydrogen-powered aircraft at an airport. This yields all taxi movements to and from the runway towards the apron, together with the turnaround procedure itself. Due to the case-study at RTHA, the entire research will focus on this specific airport, which can also serve as a reference for other airports as well. In order to simulate and optimize the aircraft operation at this airport, an agent-based model will be used. This model will face different flight schedules, varying in aircraft types and thus the associated turnaround times, as well as the selected fuel of the different aircraft, being either kerosene or hydrogen. These turnaround times will be based on a pre-executed study which considers different fuel dispensing concepts with their associated duration, order of turnaround processes and safety margins, as has been discussed in Section 3.2.3. Furthermore, the flight schedule including the distribution of hydrogen and conventional traffic will be based on the results the TULIPS traffic forecast [94]. Next up, RTHA and the different aircraft will be discretized to establish the environment and agents, defining the basis of the simulation. After that, the most suitable conflict resolution technique will be selected out of the considered alternatives in Section 4.3 such that the different flight schedules can be simulated.

Simulation and Optimization at RTHA

As hydrogen-powered aviation is a very novel concept, there are no reference concepts of operations in existence yet, besides those of conventional aircraft. This underlines the necessity of simulation, pioneering both the operational procedures as well as the spatial arrangement of the required infrastructure at RTHA, in order to obtain the first hands-on performance data.

Before the simulation can begin with the objective to accommodate hydrogen-powered aircraft at a small international airport such as RTHA in a safe and efficient manner, while minimizing the interference with regular airport operation, a few steps need to be taken. In Chapter 3, a number of possible options regarding the operational aspect of ground handling hydrogen-powered aircraft have already been identified. This includes different supply chains, storage facilities and several refueling concepts. In terms of the supply-

chain, the decision is straightforward and has already been made in Section 5.2.5. Nevertheless, it is still uncertain whether the hydrogen can be best stored inside a special fuel tank at the airport, or can be better kept inside the cryogenic trailers that it is delivered in. Furthermore, in case refueling concept 1 is deemed the most suitable for the airport, new gates will most likely have to be built in which the mutual distances are sufficient to respect the significant safety zones of refueling hydrogen. This leaves the question not only at where these gates can and should be built, but also how many of them. Additionally, in case of refueling concept 2, special refueling stations will have to be developed. The same questions are valid for this concept, namely; what is their most optimal location and how many of them are necessary. What option should be chosen highly varies per airport. The next step is therefore to determine which of these options suit best for RTHA. This decision will be made using available information, together with interviewing experts.

Regarding the best location at RTHA for every type of infrastructure, different possible locations for this, proposed originally by Rotterdam The Hague Airport, are provided in Figure 5.4. This will be useful in selecting the best possible location for all the infrastructure with the help of experts, such that it can later define the context of the simulation.

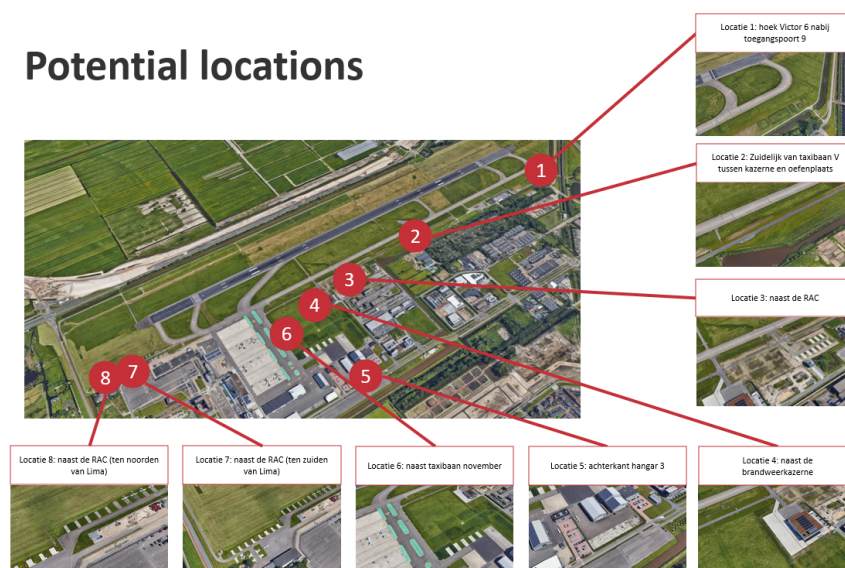


Figure 5.4: Potential locations for different hydrogen facilities at RTHA. Figure retrieved from [122].

As becomes clear in the figure above, there are a total of 8 potential locations for the different facilities, all positioned along either the taxiway or apron. These locations vary in proximity to the apron and remoteness to other infrastructure, and all have a different potential effect on the operational efficiency of the airport. In the following list, the requirements which have been taken into account while identifying these potential locations are provided:

- Easily accessible for refueling trucks
- Out of jet blast of departing aircraft
- Space is not reserved for other purposes in the future
- Clear zone, free of obstacles
- Close to fire department

For every type of infrastructure, there is at least one potential location out of these 8 locations. For example, in case refueling is done at the apron and a new set of gates is required, designed in such a way that the required increased safety distance for refueling hydrogen are respected, this could only be realized at the large field of location 4. Nevertheless, for some options there are more possibilities. Namely, in case a refueling station is selected, this could be developed at position 1, 2, 3 and 6 as well. After expert interviews, preferably 1 suitable location will be selected for every type of infrastructure. In case it is still

uncertain which location is the best, a limited number of different locations can also be incorporated in the scenarios for the simulation, in order to find out the optimal location based on a comparison of the KPI's.

Once the spatial allocation of the infrastructure has been completed, the simulations can finally initialize in order to quantify the effects of the introduction of hydrogen-powered aircraft on the airport capacity and local airport emissions. In order to quantify the operational performance of a certain airport configuration of this kind, simulation of different scenarios is required. These scenarios vary in stage of the transition phase, and thus in the fraction of hydrogen-over kerosene-powered aircraft, the range and size of the kerosene-powered aircraft, possibly the locations of the hydrogen refueling gates and the locations of the hydrogen dispensing and storage facilities, in order to ultimately establish the most optimal ground operation. The selected simulation technique, being ABS, will consequently be extended using probability distributions to account for the variability in certain processes like the time of arrival of aircraft, the exact duration of the turnaround procedure and the dominant wind direction, and as such contribute to the quality of the model by making it as realistic as possible. For this, the well-defined but slightly outdated statistical density functions of Schultz can be used as a basis [123, 124], in order to further extend these with more relevant and up-to-date specs regarding hydrogen turnarounds at Rotterdam The Hague Airport.

Scenarios

In order to be able to find the optimized solution to the different research questions, different scenarios will have to be simulated. This paragraph will therefore provide an overview of the different scenarios that will be used in the simulation, focusing on the initial stage of the transition-phase between 2025-2035:

- The location/number of hydrogen refueling stations/gates
- The forecasted number of flights at RTHA
- The fraction of hydrogen-powered over conventional flights at RTHA
- The hydrogen-powered aircraft types operating at RTHA, all having different TAT's

The gates specially intended for the turnaround of hydrogen-powered aircraft not only influence the taxi movements of conventional and hydrogen-powered aircraft, but also potentially limits gates in the vicinity to be utilized by other aircraft due to the spark-free zones. In consultation with Aviapartner, it will be determined how many gates should be developed, as well as the location of these gates intended for special operation. Besides variations in the airport configuration, the (hydrogen-powered) traffic demand at the airport is still uncertain and will consequently introduce additional sets of scenarios. It must be noted that RTHA is currently operating at its maximum capacity, due to the noise quota which restricts the airport from further growth. However, there are numerous signs that the airport capacity might increase in the near future. Causes for this are that the noise efficiency of new conventional aircraft will become better, thus relaxing the noise emission of the airport and allowing more aircraft to operate at the airport. Furthermore, with more (quieter) hydrogen-powered aircraft operating at the airport, the growth potential becomes even more. Lastly, changes in (inter)national noise regulations might also cause the possibility for RTHA to grow further and serve a larger demand.

By varying all these inputs to the simulation, extremely useful insights can be obtained. Namely, the most optimal airport configuration, as well as the effect on the airport capacity and noise emissions, provide insights into important infrastructure and operation developments which can be identified and standardized at an early stage through the simulations and optimization, assisting in the ultimate implementation of hydrogen in aviation.

Assumptions

In the following list, the most relevant assumptions of the research, being a result of the discretization and selected simulation technique, have been gathered to provide an understandable overview of the scope, including what will and what will not be considered. This then completes the scope of the research.

- Only commercial aviation is considered at RTHA (no private, helicopters or flight school flights)
- Aircraft are represented as single-point masses
- Aircraft can only stand still or travel at a fixed speed
- Aircraft can only make 90, 180 or 270 degrees turns
- The entire turnaround procedure is simulated as one single event with a pre-determined TAT
- GSE movements are left out of consideration within the simulation

5.3.2. Conflict Resolution Methodology

The selected conflict resolution methodology defines the coordination of the agents within the environment, and has a significant impact on the simulation results. As was concluded from the trade-off performed in Section 4.3, the 4 most suitable and potential MAPF conflict resolution approaches for simulation were prioritized, CBS, distributed and SIPP. In the initial phase of the research when getting fast results is more important than the quality of the results, prioritized is the most likely candidate. This technique yields that every aircraft will receive a planned path based on its priority. The priority will be assigned according to a first-come first-serve principle, which is very similar to current operation at airports. This rule-based conflict resolution technique allows very fast results, at the cost of sub-optimal results however.

Once this prioritized technique has been successfully implemented, a more sophisticated technique can be selected for simulating more complex traffic demands for which high-quality results are of greater importance, at a later stage in the research. This technique can either be CBS, distributed or SIPP. In case of CBS, every time a new aircraft lands, all existing paths will be re-planned based on specific rules. These rules are that hydrogen-powered aircraft will get priority over kerosene-powered aircraft, in order to reduce their already longer TAT. Furthermore, landing aircraft will receive priority over departing aircraft. Instead of CBS, distributed or SIPP can also be used as a more sophisticated approach. These are both slightly more complex techniques, in which the aircraft agents are more advanced. The former makes use of an auction-principle, while the latter converts safe timesteps to move into safe time intervals.

In all four approaches, the A*-algorithm is applied to determine the initial shortest path from the start to goal node for each agent. This algorithm has been introduced in Section 4.3.6. In order for this algorithm to work, a suitable admissible heuristic must be selected, which provides an 'estimate' of the remaining distance to a certain node. Out of the three introduced heuristics that have been introduced, the Manhattan Distance will be used in this simulation given its applicability and usefulness with respect to the environment in Figure 5.5.

5.3.3. Modelling Technique

In order to perform the agent-based simulations and optimization at Rotterdam The Hague as clarified above, an adequate model is required. This agent-based model is characterized by the environment, agents, constraints, inputs and outputs, which will all be explained in this subsection.

Environment

In Figure 5.5, a preliminary graphical representation of the environment of this research is presented. This setup can later be improved and generated in NetworkX, in order to make it available for the actual simulation. Variations in the locations of certain facilities can be easily implemented as well to simulate the different scenarios.



Figure 5.5: Graphical representation of initial ABS-simulation environment, based on the layout of RTHA.

In the figure above, the set of nodes defining the playground of the agents is defined. On top, the black horizontal bar represents runway 06/24 of RTHA, with the red vertices representing the arrival or departure nodes of the aircraft agents. Which of these two nodes will be selected by the incoming or outgoing agent depends on the probability density function representing the alternating wind direction at the airport. Moreover, all orange nodes represent the vertices on which the agents can move only in 1 directions, or in other words, the taxiways which the aircraft can use to move around the airport. Besides the orange

nodes, there are also black nodes which represent the edges. On these edges, the agent has two or more potential directions to travel in on top of the option of remaining on the current node.

Furthermore, the 12 purple nodes, spatially distributed in the vicinity of the airport terminal on the bottom left, represent the gates at which the aircraft can undergo its turnaround. On the right of these gates, there are two vertical paths which can be used to travel between the runway and the gates, as an agent is not allowed to travel over an empty gate. Finally, in the square configuration just right of these two vertical paths, the blue node represents the hydrogen refueling facility. This facility can be positioned anywhere along the taxiways or the two vertical paths next to the apron. The environment for this research as discussed above is static, as its states do not change over time, while also being completely accessible and deterministic, with the outcome of actions being completely guaranteed and all information available. For each gate, there exists a defined taxi route to and from the runway.

Agents

The most important element of the model are the actual agents and their associated behavioural properties, which are both fundamental in simulating hydrogen-powered as well as conventional independent aircraft. In fact, there can be different types of agents involved in the simulation, which changes with the selected conflict resolution approach.

In case of the prioritized conflict resolution approach, there are two types of agents involved in the simulation, which are listed below:

- **Aircraft agents:**

Represent a single aircraft, and have the task of travelling from the start node towards the goal node, while adhering to all applying rules. They act extremely goal-oriented, and have no advanced cognitive properties besides knowing which direction to go at which node. At last, their only communication is following orders given by the airport agent, thus having no autonomy.

- **Airport agent:**

Represents the entire airport, but has no physical appearance. It has the task to plan the paths for all aircraft agents, and communicate this to them via a one-way communication structure. The airport agent is therefore responsible for the entire coordination within the system, and has full autonomy. The cognitive properties of this agent are very limited though, since it can only re-plan the path of the new aircraft agent if a conflict occurs.

Secondly, in case of CBS the involved agents are identical to the prioritized approach. Nevertheless, even though the aircraft agents also have similar characteristics as in the prioritized case, the airport agent is more advanced in CBS. Namely, the airport agent has better cognitive capabilities, such that in case a conflict is detected, it can establish the alternative routes for both agents and determine which solution would have the smallest consequence on the total travel time of both agents, which is in mutual interest. This makes the coordination structure of this technique very cooperative. Also, the communication skill has improved since now every time a new aircraft is spawned, all existing paths are checked for conflicts and existing agents potentially have to re-direct, instead of always the new aircraft agent. In addition to this, in case of SIPP, the involved agents are also exactly the same as in prioritized. However, this time the aircraft agents have better capabilities, as they are able to observe the dynamic obstacles and communicate these observations to the airport agent.

Finally, in case of distributed, an additional agent is added to the system on top of the aircraft and airport agent:

- **Auction agent:**

This agent is also not physically present in the model, and is individual just like the airport agent. The agent is responsible for leading the auction in case two aircraft agents have gotten into a conflict. It has more authority than the aircraft agents, as it collects the bids of both agents, determines who will ultimately get priority and also subtracts the bid from the budget of the winning agent. The aircraft are the only agents that the auction agent can communicate with.

In addition to this new agent, the roles of the aircraft and airport agent have also slightly changed. In terms of the aircraft agents, they have received much more autonomy and cognitive properties since they can now autonomously (in collaboration with the other aircraft agent and the auction agent) resolve conflicts, removing this responsibility from the airport agent. Also the aircraft agent is much more active now, since it

is constantly looking forward to detect potential collisions, using its radar. On top, also communication-wise there has been an enhancement, since the aircraft agent is now communicating its planned paths with other agents in order to detect collisions, while it is also communicating with the auction agent in case of a collision. Lastly, its cognitive property is now also able to assess how valuable priority is in a certain case, and express this in the height of the bid. Thus, the aircraft agent has more observations now which in turn influences the internal states and in this way its actions.

The airport agent is still responsible for the safe arrival of all aircraft agents at their goal nodes, but the responsibility of resolving conflicts has been re-distributed. Finally, the coordination structure of this technique has shifted towards competitive, since the aircraft agents want to win the auction only in their own interest. When at later stages of the research, ICTS will also be used as a solution methodology, additional agents will be involved in the model.

In Figure 5.6, the physical entity of an agent representing an aircraft is provided. Its colors can be varied to indicate the type of propulsion of the aircraft for example, which could be kerosene or hydrogen.



Figure 5.6: Visual representation of an aircraft agent.

In the environment as was presented in Figure 5.5, the aircraft agents will be deployed to represent a given flight schedule. Accordingly, the number of agents depends on this flight schedule which is inputted in order to be resolved by the simulation.

Inputs

In order for the model to be able to execute the simulation, a number of inputs are required. This includes the flight schedule, defining which and how many aircraft will arrive at what time. Furthermore, the dominant wind direction must be known to spawn the aircraft at the correct side of the runway. Also, it must be known in advance which airport configuration will be used for the simulation and how long the simulation can run. In addition to all this, per arriving a number of other inputs are also required, which are summarized in the following list:

- ID
- Departing or arriving
- Fuel Type
- Aircraft type
- TAT
- Assigned gate

All these inputs are 1D, namely an exact value representing a mean, characteristic or state of the aircraft [107]. Once this has all been inputted into the model, the simulation can initialize.

Outputs

Once the model has finished, the outputs form the remainder of the simulation. These outputs are also referred to as key performance indicators, as they express the performance of a certain simulated configuration or procedure. The KPI's must be identified wisely beforehand, as this is what the ultimate conclusions will be based upon. For this master thesis, the following initial set of KPI's has been determined and will thus be used to compare the different traffic distributions and airport configurations to ultimately find the optimal locations for the hydrogen-related facilities:

- **Airport Performance:**
 - Average TAT
 - Number of movements per day

- Number of aircraft per day
- Number of delayed aircraft per day
- Length of each delay
- Local noise and (non-)CO2 emissions
- **Model Performance:**
 - Model computation time

As can be seen in the list above, the KPI's can be categorized into 2 different categories. The first category addresses the performance of the airport, ultimately influencing parameters like the airport capacity and the on-time-performance which are both very important drivers for the airport but also other stakeholders like airlines, who use this in selecting new airports while extending their flight network. Also, the effect on the local noise, CO2- and non-CO2 emissions is of importance here. The second category yields the computation time of the model, which can be used to determine the efficiency of the different conflict resolution approaches, which is useful in selecting which approach to use for which simulation(s).

Through simulating the different scenarios which were discussed in Section 5.3.1, the associated changes in KPI's can be evaluated to find the optimal option for RTHA and see what change in scenarios affects which the KPI's the most. Due to the variability in the results, it is important to run every simulation a certain number of times to establish statistical significance. While evaluating these KPI's, it is important to not only look for the scenario with the 'best' KPI's such as the shortest TAT, but also consider the stability of the solutions. Namely, this is often related to the predictability of a given scenario, which is something that is also very useful in aviation.

Hypothesis

The main hypothesis of this master thesis is that the impact of hydrogen-powered aircraft on the airport performance will be significant. Especially in the early stages of the transition in which the safety zones while refueling are still considerable, the TAT of hydrogen-powered aircraft is expected to be almost 50% more than that of the same conventional aircraft, while also the additional movements might cause congestion. This combined creates the expectation that the airport performance will be worsified, with a lower capacity and more delays for all traffic. However, through testing different locations this impact can most likely be limited using the optimal airport configuration. Regarding the emissions, these will be lowered as a result of the hydrogen-powered aircraft. Due to the special circumstances at RTHA, which is limited by a noise quota, these more silent aircraft are expected to eventually result in a growth-potential for the airport as well. As the transition phase progresses and possibly smaller safety zones can be adopted, technological improvements will cause this turnaround to resemble conventional turnaround operation in the end which will improve the airport capacity again, while the emissions are estimated to still steadily decrease further due to more hydrogen-powered and less conventional traffic.

5.4. Research Planning

In this section, the research planning will be provided. This serves as a guide for the research in an attempt to allocate a representative amount of time to each step of the project, allowing a thorough and structured execution while also avoiding delays. First of all, the different building blocks, forming the planning of developing the model, will be discussed in chronological order in Section 5.4.1. After this, in Section 5.4.2 the general time planning for the entire research is presented.

5.4.1. Model Construction Plan

The model represents the main framework of this master thesis, and its generation will thus demand significant time and effort. One of the reasons why ABS has been selected as the simulation technique is because of its modularity, allowing a model to be constructed through building blocks. These building blocks can be developed independently, to only incorporate it into the main model at a later point.

Firstly, a detailed study has to be performed, selecting the most suitable hydrogen-related infrastructure out of each set of options, as well as the best location for every type of infrastructure at RTHA. This will be done through interviews, using expert knowledge and from available information. Once this has been done, building the simulation model can be initialized. This involves setting up the environment of RTHA in NetworkX, as well as writing the code in Python to simulate a single independent aircraft. Once this works,

the model can be extended with more aircraft that are added in a prioritized or other conflict-resolution fashion. Simultaneous with this development, the individual building blocks shall be verified and validated, as well as the model as a whole. Next up after the mid-term meeting, the different traffic scenarios can be defined in greater detail, including the traffic forecasts from TULIPS amongst others [94], establishing the TAT per considered aircraft type, and the variation of these aircraft types. After that, the scenarios are ready to be tested and simulated. The results should afterwards be gathered into a overview, such that they can be easily analyzed. Once the prioritized simulations have been completed, the conflict resolution approach can be adjusted to create CBS, distributed or SIPP if necessary. Likewise, once this updated model has been verified and validated and all scenarios are simulated, the same can be done for the updated results. Finally after this has all been finished, the actual results can be analyzed and plotted in graphs, in order to draw conclusions from them.

5.4.2. Time Planning

In order to finish the master thesis in time and to avoid getting stuck at a certain step in the process, a time planning has been made. The main objective of this planning is to serve as a guide throughout the entire project. In short, the planning includes establishing and spatially arranging the hydrogen-related infrastructure at RTHA, building the simulation model including verification and validation, defining the different scenarios that will be used in the simulation, obtaining the inputs for the simulation such as quantifying the different TAT's, performing the actual simulations, analyzing and optimizing the results and lastly drawing conclusions from these results. In Table 5.3, a more elaborated version of the time planning is provided with the associated number of weeks in the right-hand column.

Table 5.3: Project planning for master thesis.

High-level tasks	Low-level tasks	Duration
Background knowledge	Study research and methodology	2
Familiarization	Analyze existing ABS tools	1
Stakeholder interviews	Establish hydrogen-related infrastructure at RTHA	1
Basic model conceptualization	Generate model environment	1
	Set up the model for an independent agent	1
	Code the prioritized conflict resolution approach	1
Basic model implementation	Perform visualization of the multi-agent system	0,5
	Implement the model	0,5
Full model conceptualization	Implement the CBS conflict resolution approach	2
	Implement distributed or SIPP	2
Full model implementation	Implement final model	0,5
	Modify final model and optimize the visualization	0,5
Mid-term	Prepare mid-term presentation	1
Define model inputs	Set up test scenarios	0,5
	Determine TAT's for all relevant aircraft types	0,5
Test the model	Set up test scenarios	0,5
	Test the model using these test scenarios	0,5
	Verify the model	1
	Validate the model using reference data	1
Perform simulations	Finalize the different scenarios	1
	Simulate the different scenarios	2
Find statistical significance	Perform sensitivity analysis on the results	1
Analysis of results	Create visualizations of the results	0,5
	Draw conclusions from the results	0,5
	Answer the research objective and questions	0,5
Finalize thesis	Write the final paper	4
	Prepare green light meeting	1,5
	Prepare for the defense	2

References

- [1] Transport & Environment. *Non-CO2 effects of aviation*. 2022. URL: <https://www.transportenviro%20nment.org/challenges/planes/airplane-pollution/non-co2-effects>.
- [2] IEA. *Aviation - Analysis*. Sept. 2022. URL: <https://www.iea.org/reports/aviation>.
- [3] ICAO. *Future of Aviation*. 2018. URL: <https://www.icao.int/Meetings/FutureOfAviation/Pages/default.aspx>.
- [4] IEA. *Net Zero by 2050*. May 2021. URL: <https://www.iea.org/reports/net-zero-by-2050>.
- [5] EU. *Langetermijnstrategie voor 2050*. Feb. 2018. URL: https://climate.ec.europa.eu/eu-action/climate-strategies-targets/2050-long-term-strategy_nl.
- [6] IEA. *Transport - Improving the sustainability of passenger and freight transport*. 2021. URL: <https://www.iea.org/topics/transport>.
- [7] Our World In Data. *CO2 emissions*. 2021. URL: <https://ourworldindata.org/co2-emissions>.
- [8] Our World In Data. *Cars, planes, trains: where do CO2 emissions from transport come from?* Oct. 2020. URL: <https://ourworldindata.org/co2-emissions-from-transport>.
- [9] Office of Energy Efficiency Renewable Energy. *Sustainable Transportation*. 2017. URL: <https://www.energy.gov/eere/sustainable-transportation>.
- [10] R. et al. Babikian. "The historical fuel efficiency characteristics of regional aircraft from technological, operational, and cost perspectives". In: *Air Transport Management* 8.6 (2002), pp. 389–400.
- [11] AIRBUS. *A350 - Less Weight. Less Fuel. More Sustainable*. Jan. 2018. URL: <https://aircraft.airbus.com/en/aircraft/a350/a350-less-weight-less-fuel-more-sustainable>.
- [12] Statista. *Number of scheduled passengers boarded by the global airline industry from 2004 to 2022*. June 2022. URL: <https://www.statista.com/statistics/564717/airline-industry-passenger-traffic-globally/>.
- [13] E. et al. Cabrera. "Use of Sustainable Fuels in Aviation—A Review". In: *Energy and Environment* (2022).
- [14] KLM. *Sustainable aviation fuel*. 2023. URL: <https://www.klm.com/information/sustainabi%20lity/sustainable-aviation-fuel>.
- [15] J. et al. Hoelzen. "Hydrogen-powered aviation and its reliance on green hydrogen infrastructure – Review and research gaps". In: *International Journal of Hydrogen Energy* 47.5 (2022), pp. 3108–3130.
- [16] A. Blaszczyk-Boxe. *Facts About Hydrogen*. Jan. 2015. URL: <https://www.livescience.com/28466-hydrogen.html>.
- [17] Office of Energy Efficiency & Renewable Energy. *Hydrogen Production: Electrolysis*. 2023. URL: <https://www.energy.gov/eere/fuelcells/hydrogen-production-electrolysis>.
- [18] Office of Energy Efficiency & Renewable Energy. *Fuel Cells*. 2023. URL: <https://www.energy.gov/eere/fuelcells/fuel-cells>.
- [19] J. Jonas. *THE HISTORY OF HYDROGEN*. Jan. 2009. URL: <https://www.altenergymag.com/article/2009/04/the-history-of-hydrogen/555/>.
- [20] J. Szalay. *Hindenburg Crash: The End of Airship Travel*. May 2017. URL: <https://www.livescience.com/58959-hindenburg-crash.html>.

- [21] Energy Education. *Oil crisis of the 1970s*. 2009. URL: https://energyeducation.ca/encyclopedia/Oil_crisis_of_the_1970s.
- [22] IATA. *Our Commitment to Fly Net Zero by 2050*. 2021. URL: <https://www.iata.org/en/programs/environment/flynetzero/>.
- [23] Gencer, E. *Hydrogen*. Tech. rep. MIT, 2021.
- [24] V.K. et al. Mantzaroudis. "Computational Analysis of Liquid Hydrogen Storage Tanks for Aircraft Applications". In: (2023).
- [25] Airbus. *How to store liquid hydrogen for zero-emission flight*. Dec. 2021. URL: <https://www.airbus.com/en/newsroom/news/2021-12-how-to-store-liquid-hydrogen-for-zero-emission-flight>.
- [26] Nuclear Power. *Hydrogen – Melting Point – Boiling Point*. Nov. 2021. URL: <https://www.nuclear-power.com/hydrogen-melting-point-boiling-point/>.
- [27] Postma-Kurlanc, A. et al. *Hydrogen Infrastructure and Operations*. Tech. rep. Aerospace Technology Institute, 2022.
- [28] R. et al. Cracknell. "Laminar burning velocity as a fuel characteristic: Impact on vehicle performance". In: *Internal Combustion Engines: Performance, Fuel Economy and Emissions* (2013).
- [29] Marksel, M. et al. *Modular Approach to Hybrid Electric Propulsion Architecture*. Tech. rep. D10.1. European Commission, 2019.
- [30] S. Mekhilef et al. "Comparative study of different fuel cell technologies". In: *Renewable and Sustainable Energy Reviews* 16.1 (2012), pp. 981–989. DOI: <https://doi.org/10.1016/j.rser.2011.09.020>.
- [31] Engie. *Hydrogen-Powered Aircraft: Challenges Of Taking H2 Into The Sky*. Oct. 2020. URL: <https://innovation.engie.com/en/news/news/green-mobility/hydrogen-powered-aircraft-challenges/22584#:~:text=SILENT%5C%20FLIGHTS%5C%20A%5C%20hydrogen%5C%20engine,combustion%5C%20engine%5C%20of%5C%20a%5C%20car..>
- [32] ZeroAvia. *ZeroAvia Makes Aviation History, Flying World's Largest Aircraft Powered with a Hydrogen-Electric Engine*. Jan. 2023. URL: <https://www.zeroavia.com/do228-first-flight>.
- [33] The Guardian. *Dutch group targets hydrogen-fuelled commercial flight in 2028*. Nov. 2022. URL: https://www.theguardian.com/environment/2022/jun/13/dutch-group-targets-hydrogen-fuelled-commercial-flight-in-2028?CMP=Share_iOSApp_Other.
- [34] G. - Composites World Gardiner. *Will the Airbus-CFM H2 flight demonstrator use metal or composite tanks?* Aug. 2022. URL: <https://www.compositesworld.com/articles/will-the-airbus-cfm-h2-flight-demonstrator-use-metal-or-composite-tanks>.
- [35] H2-Fly. *Company*. 2022. URL: <https://www.h2fly.de/company>.
- [36] AERO Friedrichshafen. *H2FLY sets hydrogen-electric flight world record*. Apr. 2023. URL: <https://www.aero-expo.com/h2fly-sets-hydrogen-electric-flight-world-record>.
- [37] Universal Hydrogen. *Product*. Jan. 2023. URL: <https://hydrogen.aero/product/>.
- [38] M. Harris. *Universal Hydrogen takes to the air with the largest hydrogen fuel cell ever to fly*. Mar. 2023. URL: <https://techcrunch.com>.
- [39] Airbus. *ZEROe - Towards the world's first hydrogen-powered commercial aircraft*. Jan. 2023. URL: <https://www.airbus.com/en/innovation/zero-emission-journey/hydrogen/zeroe>.
- [40] Conscious Aerospace. *Technology*. Jan. 2023. URL: <https://www.consciousaerospace.com>.
- [41] Airbus. *Airbus reveals hydrogen-powered zero-emission engine*. Nov. 2022. URL: <https://www.airbus.com/en/newsroom/press-releases/2022-11-airbus-reveals-hydrogen-powered-zero-emission-engine>.

- [42] A. Godula-Jopek et al. "4 - Hydrogen-fueled aeroplanes". In: *Compendium of Hydrogen Energy*. Ed. by Michael Ball et al. Woodhead Publishing Series in Energy. Oxford: Woodhead Publishing, 2016, pp. 67–85. DOI: <https://doi.org/10.1016/B978-1-78242-364-5.00004-X>.
- [43] Dries Verstraete. "Long range transport aircraft using hydrogen fuel". In: *International Journal of Hydrogen Energy* 38.34 (2013), pp. 14824–14831. DOI: <https://doi.org/10.1016/j.ijhydene.2013.09.021>.
- [44] NASA John Uri. *55 Years Ago: Apollo AS-203 Mission Tests Liquid Hydrogen Behavior*. June 2021. URL: <https://www.nasa.gov/feature/55-years-ago-apollo-as-203-mission-tests-liquid-hydrogen-behavior>.
- [45] NASA. *LH2 airport requirements study*. Tech. rep. Amendment 26. NASA, 1976.
- [46] NASA. *Hydrogen Storage for Aircraft Applications Overview*. Tech. rep. NASA, 2002.
- [47] Cision. *Over 56 thousand Hydrogen Passenger Vehicles Sold So Far*. Feb. 2023. URL: <https://www.prnewswire.com/news-releases/over-56-thousand-hydrogen-passenger-vehicles-sold-so-far-301743054.html>.
- [48] H2. *Filling up with H2 Hydrogen mobility starts now*. Mar. 2023. URL: <https://h2.live/en/>.
- [49] DCS aero. *Aircraft Turnaround Management*. 2023. URL: <https://dcs.aero/product-category/type/software/turn-around-management/>.
- [50] Michael Schmidt. "A review of aircraft turnaround operations and simulations". In: *Progress in Aerospace Sciences* 92 (2017), pp. 25–38. DOI: <https://doi.org/10.1016/j.paerosci.2017.05.002>.
- [51] Iain Coutts. *Turnaround: Here's What Happens When An Aircraft Is On The Ground*. June 2022. URL: <https://simpleflying.com/aircraft-turnaround-process/>.
- [52] Alec Wignall. *How it works: the aircraft turnaround*. Nov. 2022. URL: <https://www.aerotime.aero/articles/32767-how-it-works-the-aircraft-turnaround>.
- [53] Justin Hayward. *What Happens To An Aircraft During Its Turnaround?* July 2021. URL: <https://simpleflying.com/aircraft-turn-around/>.
- [54] SKYbrary. *Refuelling with Passengers on Board*. 2023. URL: <https://www.skybrary.aero/articles/refuelling-passengers-board>.
- [55] David C. Nyquist et al. "A study of the airline boarding problem". In: *Journal of Air Transport Management* 14.4 (2008), pp. 197–204. DOI: <https://doi.org/10.1016/j.jairtraman.2008.04.004>.
- [56] Florian Jaehn et al. "Airplane boarding". In: *European Journal of Operational Research* 244.2 (2015), pp. 339–359. DOI: <https://doi.org/10.1016/j.ejor.2014.12.008>.
- [57] R. John Milne et al. "A new method for boarding passengers onto an airplane". In: *Journal of Air Transport Management* 34 (2014), pp. 93–100. DOI: <https://doi.org/10.1016/j.jairtraman.2013.08.006>.
- [58] Aviation File. *What is Turnaround Time ?* 2023.
- [59] Aviapartner. *About Us*. 2023.
- [60] Tom Boon. *The Boeing 777X Could Be Turned Around In Just 30 Minutes*. Sept. 2020. URL: <https://simpleflying.com/boeing-777x-30-minute-turn-around/>.
- [61] Airbus. *What is the average time taken to load and unload the luggage?* Aug. 2015. URL: <https://aviation.stackexchange.com/questions/17564/what-is-the-average-time-taken-to-load-and-unload-the-luggage>.
- [62] Modernairlines. *Boeing 737 Max, a new generation of this highly successful City Jet*. 2018. URL: <https://modernairliners.com/boeing-737/boeing-737-max/>.

- [63] Matt Ryan. *Is Boeing 737-800 the Same as 737 MAX?* 2022. URL: <https://knavigation.net/are-737-800-and-max-the-same/>.
- [64] Quora. *How long does it usually take to unload the passengers from an airplane such as a Boeing 737?* 2022. URL: <https://www.quora.com/How-long-does-it-usually-take-to-unload-the-passengers-from-an-airplane-such-as-a-Boeing-737>.
- [65] Ted Reed. *KLM: We Can Board A Boeing 737-800 In 17 Minutes*. Nov. 2013. URL: <https://www.forbes.com/sites/tedreed/2013/11/16/klm-we-can-board-a-boeing-737-800-in-17-minutes/?sh=680ea1bb36ea>.
- [66] Laurine Dehée et al. "Cranfield Aerospace Composite Repair - Group Project Thesis". PhD thesis. May 2017. DOI: 10.13140/RG.2.2.27923.89123.
- [67] Jake Hardiman. *Why Do Passengers Almost Always Board From The Left?* <https://simpleflying.com/why-do-passengers-almost-always-board-from-the-left>.
- [68] International Air Transport Association (IATA). *Airport Handling Manual (AHM) –34th Edition*. IATA. Jan. 2013.
- [69] Open Flight School. *The Airfield: Structure, Traffic Rules and Procedures*. 2023. URL: <https://www.openflightschool.de/mod/book/view.php?id=262&chapterid=315>.
- [70] Mike Arnot. *How aircraft get refueled: A look behind the scenes*. Dec. 2019. URL: <https://thepointsguy.com/news/how-aircraft-get-refueled/>.
- [71] Rotterdam The Hague Airport. *Zakboek - Safety & Security*. Tech. rep. 1. RTHA, 2023.
- [72] SKYbrary. *Flight Crew Pre Flight External Check*. 2023. URL: <https://www.skybrary.aero/articles/flight-crew-pre-flight-external-checkd>.
- [73] Wade A. Amos. "Costs of Storing and Transporting Hydrogen". In: *National Renewable Energy Laboratory* 1.1 (1998).
- [74] J. Hoelzen et al. "Hydrogen-powered aviation and its reliance on green hydrogen infrastructure – Review and research gaps". In: *International Journal of Hydrogen Energy* 47.5 (2022). Hydrogen Energy and Fuel Cells, pp. 3108–3130. DOI: <https://doi.org/10.1016/j.ijhydene.2021.10.239>.
- [75] Christopher Yang et al. "Determining the lowest-cost hydrogen delivery mode". In: *International Journal of Hydrogen Energy* 32.2 (2007), pp. 268–286. DOI: <https://doi.org/10.1016/j.ijhydene.2006.05.009>.
- [76] L. Jones et al. "Model of a cryogenic liquid-hydrogen pipeline for an airport ground distribution system". In: *International Journal of Hydrogen Energy* 8.8 (1983), pp. 623–630. DOI: [https://doi.org/10.1016/0360-3199\(83\)90231-8](https://doi.org/10.1016/0360-3199(83)90231-8).
- [77] Bailey, J., Hardiman, J. and Pickett, R. *How Flying Today Is Safer Than At Any Time In The Past*. 2023.
- [78] Schiphol. "Basiseisen - Brandveilige toepassing van installaties voor de opslag, aflevering en het transport van waterstof". In: (Apr. 2023).
- [79] J. Mangold. "Economical assessment of hydrogen short-range aircraft with the focus on the turnaround procedure". master thesis. University of Stuttgart, Apr. 2021.
- [80] H2-aero. *Multimodal Hydrogen Airport Hub*. Tech. rep. 1. H2-aero, 2022.
- [81] Claire Benson et al. "Combined Hazard Analyses to Explore the Impact of Liquid Hydrogen Fuel on the Civil Aviation Industry". In: (Sept. 2020). DOI: 10.1115/GT2020-14977.
- [82] M. Genovese et al. "Hydrogen refueling station: Overview of the technological status and research enhancement". In: *Journal of Energy Storage* 61 (2023), p. 106758. DOI: <https://doi.org/10.1016/j.est.2023.106758>.

- [83] NACO and Royal HaskoningDHV. *Rotterdam The Hague Airport (RTHA) - Design and Safety Analysis of the proposed Hydrogen fuel storage and dispensing facility RTHA*. Tech. rep. 2. RTHA, 2023.
- [84] Airbus. *Airbus and ArianeGroup to pioneer liquid hydrogen technology*. Nov. 2022. URL: <https://www.airbus.com/en/newsroom/press-releases/2022-11-airbus-and-arianegroup-to-pioneer-liquid-hydrogen-technology>.
- [85] W. Hettinger et al. "Refueling equipment for liquid hydrogen vehicles". In: *International Journal of Hydrogen Energy* 23.10 (1998), pp. 943–947. DOI: [https://doi.org/10.1016/S0360-3199\(97\)00137-7](https://doi.org/10.1016/S0360-3199(97)00137-7).
- [86] K. Timmerhaus. *Cryogenic Process Engineering*. University of Colorado - Aeronautics Group, 1989.
- [87] U. Bünger et al. "7 - Large-scale underground storage of hydrogen for the grid integration of renewable energy and other applications". In: *Woodhead Publishing Series in Energy* (2016). Ed. by Michael Ball et al., pp. 133–163. DOI: <https://doi.org/10.1016/B978-1-78242-364-5.00007-5>.
- [88] Chart Industries. *Cryogenic Transport Trailers*. <https://www.chartindustries.com/Products/Cryogenic-Transport-Trailers>.
- [89] ET Infra. *INOXCVA flags off India's largest liquid hydrogen tank*. 2022.
- [90] F. Saad. "Transitioning to sustainable aviation: A techno-economic analysis of hydrogen fuel potential at Rotterdam The Hague Airport". master thesis. TU Delft, July 2022.
- [91] L. Jones et al. "Strategic analyses/safety issues/existing and emerging". In: *Proceedings of the WHEC. 18th World Hydrogen Energy Conference 2010* (2010). DOI: <https://doi.org/978-3-89336-655-2>.
- [92] Boeing. *Economic Impact of Airplane Turn-Times*. Tech. rep. 1. Boeing, 2007.
- [93] IATA. *Jet Fuel Price Monitor*. <https://www.iata.org/en/publications/economics/fuel-monitor/>.
- [94] Royal Netherlands Aerospace Centre. *D2.1 - Feasibility study Airports delivering energy supply for future aircraft*. Tech. rep. 1. NLR, 2023.
- [95] Rotterdam The Hague Airport. *Airport Charges Regulation Summary*. RTHA. Apr. 2022.
- [96] P.G. Voulgarellis et al. "A MATLAB Based Simulation Language for Aircraft Ground Handling Operations at Hub Airports (SLAGOM)". In: *Proceedings of the 2005 IEEE International Symposium on, Mediterrean Conference on Control and Automation Intelligent Control, 2005*. 2005, pp. 334–339. DOI: [10.1109/.2005.1467037](https://doi.org/10.1109/.2005.1467037).
- [97] Miguel Mujica Mota et al. "Simulation-based turnaround evaluation for Lelystad Airport". In: *Journal of Air Transport Management* 64 (2017). Selected papers from the 19th ATRS World Conference, Singapore, 2015, pp. 21–32. DOI: <https://doi.org/10.1016/j.jairtraman.2017.06.021>.
- [98] Yildiz B. Förster P. Feuerle T. Hecker P. Bugow S. Helber S. "A generic approach to analyze the impact of a future aircraft design on the boarding process". In: *Energies* 11.2 (2018), p. 303.
- [99] Cheng Lung Wu et al. "Modelling and simulation of aircraft turnaround operations at airports". In: *Transportation Planning and Technology* 27.1 (2004), pp. 25–46. DOI: [10.1080/0308106042000184445](https://doi.org/10.1080/0308106042000184445).
- [100] W. IP et al. "A novel power divider design with enhanced harmonic suppression and simple layout". In: *2010 IEEE MTT-S International Microwave Symposium*. 2010, pp. 1–1. DOI: [10.1109/MWSYM.2010.5515224](https://doi.org/10.1109/MWSYM.2010.5515224).
- [101] S. Chen. "Multi-agent Planning and Coordination for Automated Aircraft Ground Handling". master thesis. TU Delft, Aug. 2022.
- [102] H. et al. van Landeghem. "Reducing passenger boarding time in airplanes: A simulation based approach". In: *European Journal of Operational Research* 142.2 (2002), pp. 294–308.
- [103] J. Audenaert. "Multi-Agent Based Simulation for Boarding". master thesis. KU Leuven, Jan. 2009.

- [104] S. Adeleye et al. "A Simulation Based Approach for Contingency Planning for Aircraft Turnaround Operation System Activities in Airline Hubs". In: *Journal of Air Transportation* 11.2 (2013).
- [105] Anna Norin et al. "Airport logistics – A case study of the turn-around process". In: *Journal of Air Transport Management* 20 (2012). Notes, pp. 31–34. DOI: <https://doi.org/10.1016/j.jairtraman.2011.10.008>.
- [106] J. Zak P. Golda K. Cur T. Zawisza. "Assessment of airside aerodrome infrastructure by Saw method with weights from Shannon's interval entropy". In: *Archives of Transport* 60.4 (2021).
- [107] A. Sharpanskykh. *AE4422-20 Agent-based Modelling and Simulation in Air Transport*. Sept. 2021.
- [108] A. et al. Felner. "Search-Based Optimal Solvers for the Multi-Agent Pathfinding Problem: Summary and Challenges". In: *International Symposium on Combinatorial Search* 10.1 (2017).
- [109] A. Felner R. Stern N. Sturtevant. "Multi-Agent Pathfinding: Definitions, Variants, and Benchmarks". In: *International Symposium on Combinatorial Search* 12.1 (2019).
- [110] Pavel Surynek. "On the Tour Towards DPLL (MAPF) and Beyond". In: 1.1 (2019).
- [111] Koen van der Blom et al. "Configuring Advanced Evolutionary Algorithms for Multicriteria Building Spatial Design Optimisation". In: (June 2017). DOI: [10.1109/CEC.2017.7969520](https://doi.org/10.1109/CEC.2017.7969520).
- [112] L.W. Tang et al. "The Implementation of Trajectory Planning in Real DEM Maps based on MILP". In: *IFAC Proceedings Volumes* 46.20 (2013). 3rd IFAC Conference on Intelligent Control and Automation Science ICONS 2013, pp. 86–90. DOI: <https://doi.org/10.3182/20130902-3-CN-3020.00190>.
- [113] Lihua Zhu et al. "A 3D collision avoidance strategy for UAV with physical constraints". In: *Measurement* 77 (2016), pp. 40–49. DOI: <https://doi.org/10.1016/j.measurement.2015.09.006>.
- [114] Guni Sharon et al. "The increasing cost tree search for optimal multi-agent pathfinding". In: *Artificial Intelligence* 195 (2013), pp. 470–495. DOI: <https://doi.org/10.1016/j.artint.2012.11.006>.
- [115] Mike Phillips et al. "SIPP: Safe interval path planning for dynamic environments". In: *Proceedings - IEEE International Conference on Robotics and Automation* (June 2011), pp. 5628–5635. DOI: [10.1109/ICRA.2011.5980306](https://doi.org/10.1109/ICRA.2011.5980306).
- [116] Geeks for Geeks. *A* Search Algorithm*. 2023.
- [117] Engati. *Admissible Heuristic*. <https://www.engati.com/glossary/admissible-heuristic>.
- [118] Rotterdam The Hague Airport. *Feiten en Cijfers*. Tech. rep. 1. RTHA, 2023.
- [119] Rotterdam The Hague Airport. *Capacity declaration Rotterdam The Hague Airport summer 2021*. Tech. rep. 1. RTHA, 2021.
- [120] Windfinder. *Jaarlijkse wind- en weerstatistieken voor Vliegveld Zestienhoven*. 2023.
- [121] F. Mora-camino D. A. Tabares. "Aircraft Ground Handling: Analysis for Automation". In: *17th AIAA Aviation Technology, Integration, and Operations Conference* (2017).
- [122] Rotterdam The Hague Airport. *Verkenning locatie LH2-opslag*. Tech. rep. 1. RTHA, (2023).
- [123] Hartmut Fricke et al. "Delay Impacts onto Turnaround Performance - Optimal Time Buffering for Minimizing Delay Propagation". In: June 2009.
- [124] Michael Schultz et al. "Improving Aircraft Turnaround Reliability". In: June 2008.

Part III

Supporting Work

1

Background Information

Within this chapter, the background information regarding the process simulated by the simulation model used in this research will be further clarified. First, the conventional operation at RTHA, on which the entire simulation is based, will be explained in section 1.1. Second, the refueling process of both Jet-A1 and LH₂ will be described in section 1.2. Third, in section 1.3 the reasoning behind the selection of aircraft types used in the simulation will be clarified.

1.1. Conventional Operations at RTHA

The conventional operations at Rotterdam The Hague Airport include the entire ground handling of aircraft, with the turnaround as the most significant and relevant part of this. A conventional turnaround procedure at a regional airport is initiated with the aircraft parking at its assigned stand and the chocks being placed. This moment is also known as the on-block time, the start of the turnaround. The next step is that all necessary ground support equipment (GSE) pulls up and positions themselves in order to be able to access the required door, hatch or tank connection of the aircraft. Since the turnaround is such a standardized procedure, most of the different GSE can access the aircraft and execute their respective turnaround process simultaneously. In this way, the turnaround can be executed as efficiently as possible which increases the aircraft utilization rate, hence generating more revenue to both the airline and the airport.

The first turnaround process is to plug in the ground power unit (GPU), in order to provide power to all on-board systems such as air-conditioning but also flight systems while the engines are turned off [23]. In the mean time, the passenger stairs are placed at the forward door and if necessary also at the aft door on the left side, while on the right side the baggage and cargo belts are installed. Once in place, the unloading of both passengers and cargo can commence. Simultaneously, the potable water can be replenished. In general, when the last passenger has disembarked, refueling the aircraft is initiated, as stated in EU-OPS 1.305 [25]. This is such that in case anything goes wrong, the chances of injuries or worse are minimized as only the trained fundamental personnel is exposed.

While refueling is ongoing under the right wing, the cabin crew can check the cabin which is simultaneously cleaned, and the forward and aft catering trolleys are subsequently replaced. These are processes that are preferably executed without any passengers on board as a contribution to passenger comfort [49]. At the same time, the cockpit crew can prepare the flight systems for the next flight and perform a visual inspection of the aircraft. Whenever the refueling is completed, the new passengers are allowed to embark the aircraft, while new cargo and baggage is loaded into the cargo compartments. Once all passengers have found their seats and all cargo is loaded into the aircraft, the hatches and doors may be closed and all GSE removed. Next, the chocks may be removed and with that, the off-block time is set and the turnaround is completed, such that the aircraft is ready for departure again. In Figure 1.1, the top view layout of the aircraft and the GSE is provided to create a better understanding of the turnaround procedure. The pneumatic, air conditioning and tow vehicle are redundant at RTHA.

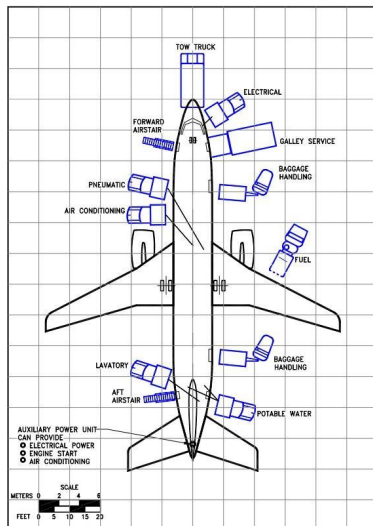


Figure 1.1: GSE arrangement during B737 turnaround. Retrieved from [16].

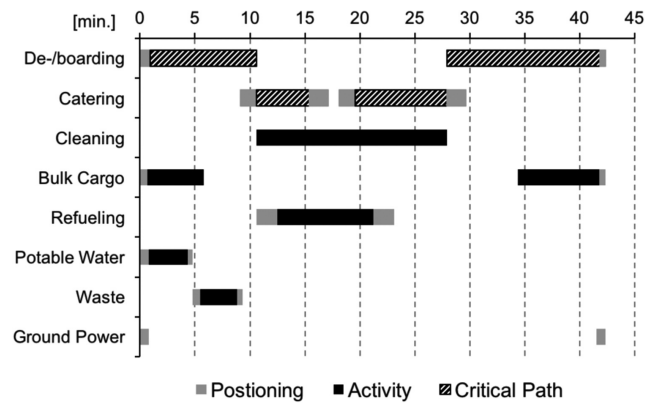


Figure 1.2: Gantt-chart of a typical turnaround procedure of a single-aisle aircraft. Information retrieved from [44].

In Figure 1.2, a Gantt-chart representing the turnaround processes as described above is provided. Every bar represents a certain turnaround process with its length being proportional to the duration. As can be concluded from this Gantt-chart, the total turnaround time in this example is equal to 43 minutes for a single-aisle aircraft. For most of the processes in the Gantt-chart, a few minutes before and after the actual process are allocated to correctly positioning the vehicle. Furthermore, some turnaround processes can be executed simultaneously, while other processes have to be executed sequentially. As can be also seen in the figure, the combination of catering and (de-)boarding processes all belong to the critical path. The critical path is the most time-consuming sequence in the entire turnaround process, which defines the overall duration. In other words, a time-reduction in one of the processes that are not part of the critical path, such as loading bulk cargo, would not necessarily lead to a shorter turnaround time. In reality, the average turnaround time of a single aisle short-haul aircraft at RTHA is 45 minutes, with a maximum of 51 minutes [44]. This variance can be explained by the stochastic nature of the procedure, due to its dependence on so many variables. This includes the aircraft type, number of passengers on board as well as their behaviour due to their demographic nature, such as slower boarding when there are many elderly passengers and the amount of fuel to be refueled among others.

1.2. Refueling Process

With the introduction of LH₂-powered aircraft, it is important to better investigate the refueling procedure of Jet-A1, such that it can be assessed what alternations need to be made to also accommodate refueling of LH₂ with its different properties. Therefore, the refueling process of Jet-A1 will first be explained in subsection 1.2.1. After that, the resulting defined refueling process of LH₂ is introduced in subsection 1.2.2.

1.2.1. Refueling Jet-A1

The characteristic of the refueling process that is considered most important in this research is its duration. Namely, in some cases refueling can be part of the critical path, thus defining the overall TAT. The parameter which defines the refueling duration is referred to as the fuel flow rate. The flow rate is a fixed variable which is dependent on the airport refueling infrastructure, such as whether a hydrant or fuel truck is operated. At regional airports such as Rotterdam The Hague Airport, a hydrant system including underground pipelines is simply not profitable and thus fuel trucks are the most cost-efficient

solution [13]. Currently, RTHA operates a total of two Jet-A1 fuel trucks as was learned from a study of the airport operations. An important remark here is that Shell has one additional Jet-A1 fuel truck, which is interchangeable with Eindhoven Airport, which is where this truck is currently stationed. A fuel truck for kerosene has an average flow rate of 1150 L/min , which translates to approximately 15 kg/s [26] [35]. The total refueling process then becomes equal to the amount of fuel required, divided by the flow rate, plus two minutes of connecting the fuel hose and another two minutes of disconnecting the fuel hose at the end, totalling at four minutes of additional time. According to ICAO, commercial aircraft are obliged to carry at least 5% of their trip fuel for unforeseen circumstances such as a diversion or loitering [40], which slightly reduces the refueling time as most aircraft arrive with some reserves left. Ultimately, the entire refueling process including (dis-)connecting the fuel hose lasts around 15-20 minutes on average for conventional single-aisle aircraft [26][44].

1.2.2. Refueling LH₂

The LH₂ flow rate is still very uncertain, but its impact and optimal value will be investigated in this research. However, not only the flow rate itself, but also the (dis-)connecting of the refueling equipment will need to be re-considered when using LH₂ instead of Jet-A1. The overall objective during the refueling procedure is to ensure explosion avoidance as stated by Mangold et al. [14]. Currently, there is no standardized procedure for refueling LH₂ in existence yet. However, additional safety measures are required to ensure the safety of the fuel handler for low LH₂ flow rates and to enhance explosion protection, as this will most likely be executed manually in the early stages. One of these safety measures is carefully connecting and disconnecting the fuel hose, in order to avoid spillage and thus potential feed for explosions, as introduced by Mangold et al. [14]. An additional measure is purging, which is necessary before and after the refueling to ensure that no unknown gasses remain inside the hose, which could potentially cause an explosion when being exposed to LH₂ [18]. Lastly, as LH₂ will be stored at a temperature of $-253 \text{ }^\circ\text{C}$, there will be enormous temperature gradients between the LH₂ and the hose. In order to avoid failure of the hose due to these stresses but also to ensure a vapor-free steady liquid mass flow, a certain chill-down time must be introduced as was suggested by Barron et al. [19]. During this chill-down time, a reduced flow rate is established to gradually introduce the temperature gradient, cool down the hose and also get rid off all remaining vapors inside the hose. In [11] and [14], the temporal duration of all these additional processes has been investigated, leading to the following overall refueling method as depicted in Figure 1.3 that will be adhered to within this research.

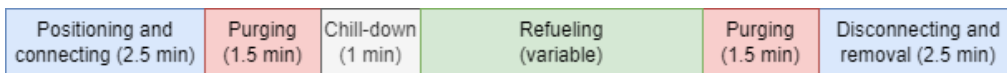


Figure 1.3: Temporal refueling method for LH₂. Information retrieved from [11] and [14].

As can be concluded from the figure above, the positioning and connecting, but also the disconnecting of the fuel hose is assumed to last two and a half minute each. This is slightly longer than the two minutes which are taken to position and connect the fuel hose while refueling Jet-A1, due to the extra caution to avoid spillage [44]. Next up, before and after every refueling activity, purging of the fuel hose should take place, lasting one and a half minute individually. Furthermore, before the actual refueling can start, a chill-down time of one minute must be adhered to. Ultimately, the duration of the actual refueling of LH₂ is variable as this is dependent on the achievable flow rate, as well as the total amount of LH₂ required. Nonetheless, the entire refueling method excluding the refueling already lasts nine minutes using this approach, as opposed to only four minutes for Jet-A1. This, in combination with the still relatively low achievable flow rates of LH₂, potentially results in considerably elonged turnaround times in comparison to Jet-A1 at this stage, as well as in the coming years.

1.3. Aircraft Types

Another important aspect when researching the impact on the ground operations of introducing LH₂-powered aircraft is which aircraft types to incorporate in the simulation model. Given that the research focuses on 2050 in which conventional aircraft are expected to still be operating as well, subsection 1.3.1 will focus on the reasoning behind the selection of these aircraft types. After that, an explanation of the characteristics, development and expected introduction year of the LH₂-powered aircraft used in the model is provided in subsection 1.3.2.

1.3.1. Conventional Aircraft

Currently, the flight operations at Rotterdam The Hague Airport are dominated by Transavia, who operate over 70% of the flights. These flights are either operated by the Boeing 737-700 or Boeing 737-800, likewise most other airlines permanently flying at the airport such as TUI and Pegasus. The only exception is British Airways, which operates an Embraer 190 four times per day. Transavia already started renewing its fleet with the Airbus 320 NEO and Airbus 321 NEO, which are planned to have replaced the existing fleet entirely by 2035, with the first aircraft stationed at RTHA from 2027, as was learned from expert knowledge. Due to the terminal capacity and runway length at RTHA, only the Airbus 320 NEO can be stationed at the airport as the Airbus 321 NEO is too large. Furthermore, TUI has published that they are currently replacing their current Boeing 737-800's with the more efficient and 'quieter' Boeing 737 MAX 8 [28]. Lastly, all other aircraft currently flying at the airport are assumed to have been replaced by its modern variant in 2050. The most significant assumption in this aspect is that British Airways will have replaced their Embraer 190 with the more efficient Embraer 190-E2.

1.3.2. Hydrogen-Powered Aircraft

As of today, the main developments concerning hydrogen-powered aircraft concern retro-fitted aircraft, being technologically less complex to develop while also having a shorter time-to-market, which is beneficial for a faster transition towards hydrogen in aviation. The main aircraft that are used for this transformation are the propeller-driven ATR72 and DHC-8, developed by ZeroAvia [51], H2-Fly [29], Universal Hydrogen [30] and Conscious Aerospace [2] among others. These 80-seater retro-fitted aircraft are expected to finish development between 2025-2030, with the first aircraft using gaseous hydrogen (GH₂), while the later aircraft will be utilizing the less volumetric-demanding LH₂. This can be explained by the fact that storing hydrogen in a cryogenic state introduces major technical challenges such as fuel tank cooling techniques and evaporation prevention mechanisms. Hence, first utilizing GH₂ is more realistic and can pave the path for future LH₂-powered aircraft.

Disregarding of which state the hydrogen is stored in, the occupied volume by the fuel is still significantly larger than the current volume necessary to store Jet-A1. As a result of this, the current fuel tanks inside the wings are not sufficient and thus an additional fuel storage tank is required. Several aircraft developers have concluded that the optimal location of this additional fuel tank would be in the aft fuselage, such as Airbus [5]. This would result in the compromise of a number of seats inside the cabin, and thus a slight reduction in passenger capacity. This, in combination with the already significantly lower seat capacity of the ATR72 or DHC-8 and also short range yields that these retro-fitted aircraft have both insufficient range and capacity to potentially replace the current fleet of B737's and A320's operating at RTHA without any significant alternations in destinations and flight frequency. Nonetheless, these aircraft can be very useful experiments in the transition to hydrogen however, by gaining experience, knowledge and tackling the first bottlenecks.

Taking these developments into account, the Airbus ZEROe turbofan is the only hydrogen-powered aircraft announced so far that is capable of potentially replacing commercial medium-range flights. Namely, the ZEROe turbofan is estimated to be able to carry up to 200 passengers as was stated by



Figure 1.4: Three sustainable aircraft currently being developed by Airbus. Figure retrieved from [6].

Airbus, while also it is propelled using a turbofan [6]. Therefore, this aircraft will be directly burning LH_2 , so no fuel cell is involved in the propulsion system [5]. Unfortunately however, the expected maximum range that Airbus expects this aircraft to cover is only 3700 km, which is approximately half of the maximum range of conventional aircraft [38]. Nevertheless, out of the 50 destinations that currently are being flown to from RTHA, every destination is within this range and thus it is assumed that each route can also be flown to using the ZEROe aircraft [10]. Consequently, the ZEROe turbofan will be selected in this research as the only LH_2 -powered aircraft operating at RTHA.

As Airbus is developing the ZEROe from scratch which is specially designed to be propelled using hydrogen, a few configuration modifications can be expected with respect to the A320 or B737 currently operating at RTHA. The first one is that the LH_2 -powered aircraft is expected to have a slightly longer fuselage, in order to fit the fuel tanks while limiting the number of compromised seats as a result of this [6]. Also, Adler et al. found that the wings need more structural support since the fuel is no longer stored here, which was previously used to counteract the flexing of the wings in-flight, hence requiring additional empty weight as well [1]. As a result, more powerful engine are required to still have a comparable cruise speed and performance as the Airbus 320 NEO. Therefore, the engine that will be used on the ZEROe aircraft is the new General Electric Passport TM Turbofan [4]. This will also be helpful when later defining the amount of LH_2 consumed by the aircraft, which can be derived from the conventional fuel consumption. Conclusively, given that these modifications are relatively small, this validates that the Airbus ZEROe not only resembles the current B737 and A320 in terms of aircraft characteristics, but also in terms of physical dimensions and configuration, hence being a suitable replacement in the operations.

The ZEROe turbofan was originally planned to be launched in 2035, according to Airbus [6]. However, as has been observed recently with the Boeing 777X, incorporating unconventional subsystems in the design such as the moveable wing-tip design, certification delays of up to a few years already can be faced [46]. With this in mind, it is more likely to expect the also unconventional LH_2 -powered turbofan to be certified a few years later than 2035. This is confirmed during the recent press conference by Airbus, in which it was announced that not all three LH_2 -powered aircraft, but only the regional turboprop will be released in 2035, implying that the other two designs including the turbofan will follow a few years later [3]. One advantage however is that this turboprop, but also the retro-fitted LH_2 -powered aircraft which were introduced above, allow to already enter the learning-curve of classifying LH_2 -powered aircraft. This is beneficial for when the turbofan will undergo its aircraft type classification, since bottlenecks in this process will have already been (partially) overcome by these turboprops.

Furthermore, when ordering a new aircraft which is already in production, this aircraft will be actually delivered a few years later as a result of high demand [37]. This, in combination with the fact that

the production line must also be set up first before the aircraft can actually be delivered to airlines at a considerable rate, raises uncertainty as to when the turbofan can actually be delivered. Hoelzen et al. forecasted a base and ambitious scenario, taking three and five years respectively, in order to get the production line to full capacity [12]. In the meantime, airlines also need to train their cockpit, ground and maintenance crew to directly operate these new aircraft types as well, while airports have to accommodate refueling hydrogen, train their fire department and other crew, which all takes time. From all this, it has been assumed that the first turbofan aircraft will be put into service after 2040. As a result of this, the scope of this research has been set to focus on 2050, giving the turbofan sufficient time to have steadily conquered a noteworthy market share. The exact market share in 2050 is still uncertain however, explaining the need for the different simulation experiments on the penetration rate that will be researched in this paper.

2

Experimental Elaboration

In this chapter, some of the experiments which have been used within this research demand a further elaboration for clarity reasons. First, in section 2.1 the underlying legislation behind the safety zones used within the experiment 3 is introduced, as well as an overview of the impact of the safety zones on the stand availability. Second, the turnaround procedures used in experiment 5 are visualized using Gantt-charts in section 2.2.

2.1. Safety Zone

The safety zone is a complex topic within aviation that must be carefully considered when assessing new operational processes such as the ground operations involving LH₂-powered aircraft. On one hand it ensures the safety of both passengers and personnel, but on the other hand it can pose a bottleneck for efficient operations. Hence, it is important to evaluate what the exact influence on the operations is of a certain safety zone. In order to achieve this, the state of the art regarding safety zones will first be introduced in subsection 2.1.1. Afterwards, the effects of these safety zones on the stand availability will be reasoned in subsection 2.1.2.

2.1.1. State of the Art

While executing a risky activity such as refueling a flammable substance, so-called risk-contours must be respected, according to Dutch legislation concerning external safety, inside which no critical buildings such as schools, hospitals or large offices among others may be situated [41]. This measure is a protocol introduced by the RIVM and is in place to ensure the protection of the surroundings. An important remark is that it only concerns buildings outside of the facility at which the activity is executed. It is stated that the risk-contour outlines the region outside which the chance of one death due to the risky activity equals 10^{-6} or smaller per annum [41]. The dimensions of a risk-contour are very specific to whatever activity is executed and the flammable substance used for this, and takes into account as much as possible, such as materials of buildings and even the dominant wind direction to predict the most likely direction of an explosion for example. The shape usually varies from circular to oval. In addition, several risky activities being executed in each others' vicinity in turn affect the risk-contours, as the individual contours must be replaced with one overlapping risk-contour [41].

Refueling LH₂ is also categorized as a risky activity and must also adhere to relevant risk-contours. However, since refueling LH₂ is novel, there are no defined risk-contours in place yet for refueling aircraft. Fortunately though, FlyZero has gathered the state of the art regarding separation distances while refueling LH₂, consisting of recommendations and distances from comparable industries, in the following overview.

Table 2.1: Recommended separation distances while refueling LH₂, all expressed in meters. Information retrieved from [20].

Description	BCGA	BSi	EIGA	NFPA	NASA
Place of public assembly	-	-	20	23	22.9
Public establishments	-	-	60	-	-
Compressor, ventilator and air conditioning intakes	15	15	20	23	22.9
Other LH ₂ tanker	-	-	3	-	-
Electricity cable and pylons	1.5	10	10	-	-

As can be concluded from Table 2.1, NASA, the NFPA and EIGA recommend a separation distance of approximately 23 meter from the point of refueling towards a place of public assembly. On top of this, EIGA even prescribes a separation of 60 meter towards public establishments. Both a place of public assembly and public establishments can refer to the terminal building and should thus be considered. The significant increase with respect to the three meter fuel safety zone distance of Jet-A1 expresses the more dangerous properties of LH₂, together with the lack of experience in handling this substance in combination with aircraft in terms of risk [20]. This raises the concern on whether additional safety measures would be necessary in order to ensure the safety of all other surrounding ground operations at the airport while refueling LH₂ is ongoing. Namely, while the risk-contours mentioned above only address buildings, it might also be necessary to assess the risk and ensure the safety of nearby vehicles, personnel and passengers during refueling. This topic is still uncertain, as is visible in the highly varying recommended safety separations for different objects. Also, different experts disagree on whether an aircraft should be treated as a vehicle, a building or require a separate class.

Within this research, it has been assumed that additional risk-contours must be in place to account for this increased risk towards other aircraft and thus passengers and personnel. Based on an interview with different experts including the safety expert of Schiphol, three different safety zones have been devised that will be alternated using different experiments, in order to assess the variations of the outputs as these distances are increased. The safety zone diameters that will be considered are an optimistic, intermediate and conservative variant, being 15 meter, 30 meter and 45 meter respectively. When refueling is ongoing, it is not allowed for other aircraft to be parked inside this safety zone.

2.1.2. Stand Availability

As a result of the three different safety zones that have been introduced above, different stand availability combinations are in place during the operations. Namely, due to the aircraft stand size at RTHA, the intermediate and conservative scenario overlap with adjacent aircraft stands, causing these adjacent stands to be temporarily blocked from other aircraft while refueling is ongoing. On top of this, certain aircraft stands are per definition not accessible to LH₂-powered aircraft, as these stands are located near buildings that would violate the safety distances from Table 2.1. Therefore, the resulting possible aircraft stand configurations at RTHA that will be considered in this research are provided in Table 2.2.

As can be concluded from this table, the three different safety zones during refueling as explained before result in different possible stand availability's for Jet-A1 and LH₂-aircraft during the simulation, which will in turn affect the ground operations at the airport. Initially, a safety zone with a diameter of 15 meter does not put any constraints on the stand allocation, as the safety zone does not exceed the stand dimensions, yielding there is no interference with adjacent stands. Therefore, if available, both Jet-A1 and LH₂-powered aircraft can park in every stand, leading to a capacity of 12 aircraft of either category.

Table 2.2: Stand availability for both conventional Jet-A1 and LH₂-powered aircraft, using varying safety zones.

Stand	Safety zone = 15 meter		Safety zone = 30 meter		Safety zone = 45 meter	
	Jet-A1 Aircraft	LH ₂ Aircraft	Jet-A1 Aircraft	LH ₂ Aircraft	Jet-A1 Aircraft	LH ₂ Aircraft
A1	✓	✓	✓	✓	✓	×
A2	✓	✓	✓*	×	✓*	×
A3	✓	✓	✓	✓	✓	✓
B1	✓	✓	✓	✓	✓	×
B2	✓	✓	✓*	×	✓*	×
B3	✓	✓	✓	✓	✓	✓
C1	✓	✓	✓	×	✓	×
C2	✓	✓	✓*	×	✓*	×
C3	✓	✓	✓	✓	✓	✓
D1	✓	✓	✓	×	✓	×
D2	✓	✓	✓*	×	✓*	×
D3	✓	✓	✓	✓	✓	✓
Total	12	12	12*	6	12*	4

Next, when the diameter of the fuel safety zone is increased to 30 meter, a number of implications are introduced. As was explained earlier, the fuel safety zones with a diameter of 30 and 45 meter interfere with adjacent stands, which must therefore be temporarily blocked. Due to the configuration of the platform at RTHA in which the 12 aircraft stands are positioned in a 3x3x3 configuration, it would be sub-optimal to park the LH₂-powered aircraft in the middle of three stands, as then both adjacent stands in the same row would need to be blocked. Furthermore, the stands "C1" and "D1" are not available for LH₂-powered aircraft with this safety zone, as it puts the terminal buildings at risk. This combined leaves the possible LH₂-powered aircraft stands with "A1", "A3", "B1", "B3", "C3" and "D3", generating a maximum capacity of six in total. As a result, the Jet-A1 aircraft have some exception for their stand usage of "A2", "B2", "C2" and "D2", which are marked with *. Namely, if an LH₂-powered aircraft is parked in a stand in a certain row, the middle stand in that row can temporarily not be used by a Jet-A1 aircraft, reducing the capacity of these aircraft. However, the more preferred stands in these rows, next to the terminal buildings, remain available to the Jet-A1 aircraft in this way.

Lastly, the implications on the stand availability for LH₂-powered aircraft with a safety zone diameter of 45 meter is comparable to the implications for a diameter of 30 meter. Nevertheless, whereas for 30 meter, in rows "A" and "B" it was allowed to park a LH₂-powered aircraft on both the first and third stand, also known as "A1" and "A3", or "B1" and "B3", for 45 meter it is only allowed to park at "A3" or "B3" in these two rows for LH₂-powered aircraft. Namely, due to the large diameter of the safety zone, large parts of the safety zone of the aircraft in "A1" and "A3" or "B1" and "B3" would overlap, which is therefore considered a too high safety risk, creating an even larger overlapping fuel zone that would interfere with a significant part of the ground operations. As a result, the LH₂-powered aircraft capacity for this safety zone is reduced to just four aircraft, namely the third stand of each row.

2.2. Turnaround Procedure

Within experiment 5, different turnaround procedures will be simulated. Given the uncertainty in safety measures during the refueling of LH₂ on the aircraft itself, there exist different variations in terms of the order and sequence of turnaround processes in parallel with refueling. As a result, the following

three turnaround procedures have been defined which will provide insights into the effects of different turnaround procedure variations on the operational efficiency. As an assumption, the amount of LH₂ to be refueled for every turnaround procedure is 1500 kg, resulting from applying Equation 3.1 and using a flight distance of 1800 km, which is average for aircraft operating from RTHA.

- **LH₂ Turnaround Procedure 1:**

The most conservative scenario assumes that no (semi-)automated or classified GSE turnaround processes are possible yet, due to the extensive testing and qualification that this new GSE requires or due to legislation prohibiting this implementation. In this case, no turnaround processes shall be executed simultaneously with refueling LH₂. The refueling is including the subsequent processes of (dis-)connecting the fuel hose, purging and chill-down. Also, since the refueling must still be operated manually, only limited flow rates are expected to be achieved as the hose diameter can not exceed a certain threshold. As a result, the processes of catering and cleaning will have to be delayed such that they are in sequence with the refueling and boarding of the new passengers, instead of parallel. The processes of (un-)loading bulk cargo and servicing the waste and water do not influence the TAT, resulting in the Gantt-chart shown in Figure 2.1.

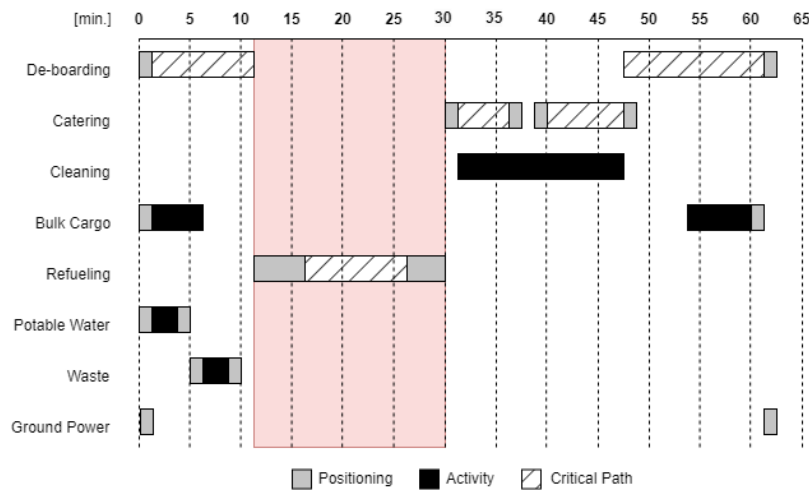


Figure 2.1: Gantt-chart representing the turnaround of a LH₂-powered single-aisle aircraft, assuming 1500 kg LH₂ to be refueled at a flow rate of 2.5 kg/s with no parallel turnaround processes allowed.

As can be seen in the Gantt-chart above, the refueling procedure can only initiate once all passengers have de-boarded. In the meantime, connecting the GPU, unloading the bulk cargo and servicing the water and waste can all be completed. Next, the refueling can take place which must be completed entirely sequentially, including connecting, purging and chill-down, hence being now part of the critical path as well. The red box represents the constraint on all other turnaround processes. Once the refueling process has been successfully completed, the personnel and crew can enter the aircraft again for catering, cleaning and preparing the aircraft for the next flight, significantly en-longing the turnaround duration. The catering consists of two separate activities since the front and aft galleys both need to be re-stocked. Furthermore, the cleaning process does not need any positioning as the cleaning crew can simply access the aircraft using the stairs. Only when the cabin is ready, the new passengers can board and the aircraft while the new bulk cargo is loaded. After the GPU is disconnected and the stairs are removed, the aircraft is ready for departure. This specific Gantt-chart is characterized by the total example amount of 1500 kg LH₂ to be refueled at an assumed rate of 2.5 kg/s. Consequently, the total turnaround time is increased to 62 minutes, being nearly a 40% increase with respect to a Jet-A1 TAT.

- **LH₂ Turnaround Procedure 2:**

In a more optimistic scenario, some specific GSE are classified to safely operate in hazardous areas such as near or around LH₂ refueling operations. In addition, the refueling itself could be a semi-automated process in which the fuel hose is guided using a mechanical arm, potentially allowing for a larger hose diameter and thus flow rate. (Dis-)connecting the fuel hose as well as purging and chill-down is considered to be significantly riskier than the actual refueling because of the chances of spills, and therefore parallel turnaround processes are not allowed during these actions but only with the actual refueling as was suggested in the FlyZero project [20]. This does provide the opportunity to already perform some (partial) turnaround processes during refueling, which is beneficial with regard to the turnaround time of procedure 1. The Gantt-chart representing this more optimistic scenario is provided in Figure 2.2.

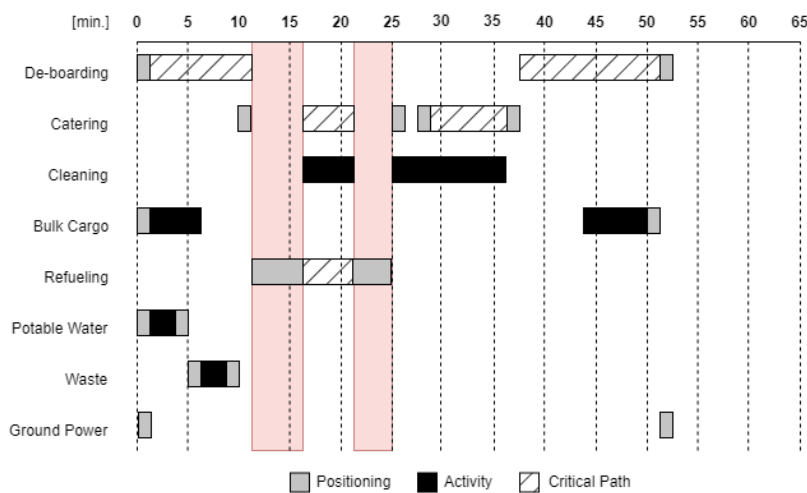


Figure 2.2: Gantt-chart representing the turnaround of a LH₂-powered single-aisle aircraft, assuming 1500 kg LH₂ to be refueled at a flow rate of 5 kg/s with limited parallel turnaround processes allowed.

From the Gantt-chart above, it can be concluded that a number of turnaround processes are partially executed together with the refueling. Nevertheless, during (dis-)connection of the fuel hose, all other turnaround processes are restricted as can be observed from the red rectangles. On one hand, the forward catering is done simultaneous with the refueling. Since this selected process is located at the front while the LH₂ refueling will be situated at the aft of the aircraft, the risk is reduced as the separation is still significant. However, the positioning of the GSE before and after the actual catering must be done before and after the (dis-)connecting of the fuel hose respectively. Since the required GSE is sufficiently classified, it is allowed to remain parked inside the hazardous area during connecting and dis-connecting of the fuel hose as well. In addition, parallel with the refueling a part of the cabin can also be cleaned already, starting from the front to minimize risk again. These two turnaround processes, executed simultaneously with refueling, demand very careful coordination, in order to ensure that no process is ongoing once the refueling is over and the fuel hose is being (dis-)connected, which would be a failure of complying with the safety regulations. Again, the refueling process is now part of the critical path. This more efficient turnaround layout, including higher possible LH₂ flow rates due to the automated fuel arm, results in a total turnaround time of 53 minutes.

- **LH₂ Turnaround Procedure 3:**

The most optimistic scenario would be no further limitations on the other turnaround processes while refueling is ongoing. This yields that all GSE are classified as safe to operate in hazardous areas, while also certain GSE such as the refueling truck itself is (partially) automated by an automated fuel arm, potentially allowing LH₂ flow rates of up to 10 and even 15 kg/s. In Figure 2.3, the Gantt-chart representing this last LH₂ turnaround procedure can be seen.

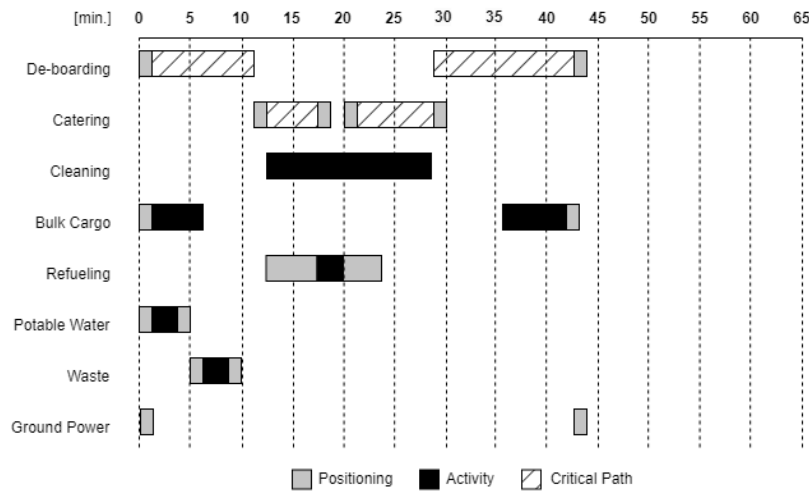


Figure 2.3: Gantt-chart representing the turnaround of a LH₂-powered single-aisle aircraft, assuming 1500 kg LH₂ to be refueled at a flow rate of 10 kg/s with parallel turnaround processes allowed.

From the figure above, it can be visualized that the LH₂ turnaround procedure is similar to the conventional turnaround procedure, which was explained in Figure 1.2, with the only main difference that the actual refueling has become significantly faster. Refueling is now no longer part of the critical path and the total turnaround time is 44 minutes, which is in range with a conventional turnaround time.

3

Model Inputs

The multi-agent system model requires a wide range of inputs before the actual simulations can be performed. This includes the environment, part of the multi-agent system model, which is introduced in section 3.1, together with a number of assumptions. Moreover, for a number of inputs, there are underlying calculations or considerations which must be elaborated upon. Hence, the mathematical procedure according to which the amount of fuel per flight is calculated is explained in section 3.2. Next up, a more detailed description of how the duration of different turnaround procedures will be modelled is defined in section 3.3. Ultimately, in section 3.4 the flight schedule, along with the number of movements, will be explained in greater detail.

3.1. Model Environment

One of the fundamental elements of the simulation model is the environment. This defines the context where the agents act in, which must be chosen based on the process that is being simulated. In this research, the environment is based on the layout of RTHA, where the entire set of the runway, taxiways and roads has been converted into a graph, consisting of nodes (blue dots) and edges (black lines). A visualization of the environment used within this research is provided in Figure 3.1.

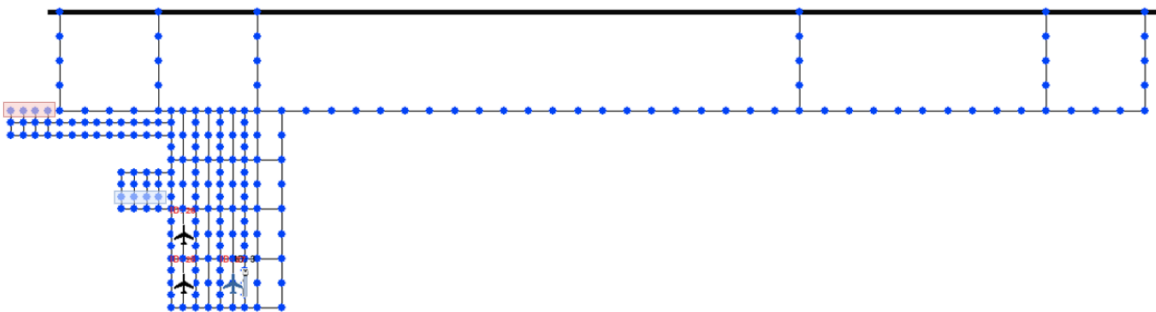


Figure 3.1: Environment of the agent-based model used for simulating the experiments.

While defining the environment, two different grids, varying in coarseness, were incorporated. Namely, a finer grid was created for the fuel trucks, in order to be able to drive at slower speeds in comparison to the aircraft, using a coarser grid. Also, the grid of the fuel trucks is partially inaccessible to the aircraft, such that the aircraft can not enter the fuel truck parking area and the fuel trailer storage facility. As a result of this, a number of assumptions had to be made in order to make the taxiing and driving of the aircraft and fuel truck agents as realistic as possible. These assumptions are as follows:

- Fine grid for the fuel trucks, consisting of nodes being 25m apart
- Coarse grid for the aircraft, consisting of nodes being 50m apart
- Constant taxi speed of fuel trucks of 15 km/h
- Constant taxi speed of aircraft of 30 km/h

- Simulation model timestep of 6 seconds

This timestep was necessary to correctly coordinate and update the movement of all vehicles simultaneously, while being as large as possible in order to minimize the computation time.

3.2. Fuel Calculation

As explained earlier, the fuel time that is used during the simulation is dependent on the amount of fuel that needs to be refueled. For this research, the amount of fuel to be refueled during the turnaround is based on a the original Breguet range equation, which is presented in Equation 3.1. This equation is uniform and can hence be applied to both Jet-A1-and LH₂-powered aircraft.

$$m_{fuel} = m_{zf} \left[\exp \left(\frac{R_d g}{\left(\frac{L}{D} \right)_{cruise} \eta_{overall} LHV_{fuel}} \right) - 1 \right] + m_{reserve} \quad (3.1)$$

In the equation above, different variables are introduced which need to be clarified. Firstly, the objective of this equation is to define the total fuel mass that needs to be refueled, referred to as m_{fuel} , expressed in kg . This mass is equal to the zero-fuel mass of the aircraft in kg , m_{zf} , multiplied by an exponential, and added to the reserve fuel that is carried along, noted as $m_{reserve}$ and also expressed in kg . It must be noted that m_{zf} refers to the weight of the aircraft and payload combined, but without fuel yet. The numerator of the exponential function consists of the distance that the aircraft will fly in meters, R_d , multiplied with the gravitational acceleration g , equal to 9.80665 m/s^2 . Ultimately, the denominator of the exponential is equal to the lift-over-drag ratio of the aircraft $\frac{L}{D}_{cruise}$ in cruise conditions, multiplied with the total efficiency of the aircraft η_{tot} and the lower heating value of the fuel, LHV_{fuel} , expressed in J/kg . This latter variable makes the equation uniform and applicable to each fuel type, with the value of LHV_{fuel} being equal to $44.1 \times 10^6 \text{ J/kg}$ for Jet-A1, and $120 \times 10^6 \text{ J/kg}$ for LH₂ [47]. The other variables are dependent on the aircraft type, and are presented in Table 3.1.

Table 3.1: Selected characteristics per aircraft type that is used within the simulation model.

	Embrear 190-E2	Boeing 737 MAX 8	Airbus 320 NEO	Airbus ZEROe
m_{zf} [kg]	46,380 [34]	65,950 [33]	64,300 [32]	67,000
V_{cruise} [km/h]	870 [34]	840 [33]	830 [32]	830
$\frac{L}{D}_{cruise}$ [-]	19.42 [21]	18.1 [38]	18.75 [48]	18
$\eta_{overall}$ [-]	0.36	0.35	0.36	0.39
SFC [g/kN/s]	14.4 [36]	15.6 [38]	14.4 [36]	15.4
Fuel Type	Jet-A1	Jet-A1	Jet-A1	LH ₂

Using the values presented in Table 3.1, the fuel used by each aircraft type for a given range can be calculated. Most of these characteristics could be learned from available information, but regarding the Airbus ZEROe, the majority of the values is based on assumptions due to the lack of data at this stage. As can be seen in the table, the m_{zf} of the ZEROe turbofan has been assumed slightly higher than the Airbus 320 NEO, built by the same manufacturer, since LH₂-powered aircraft are expected to have a longer fuselage, in order to fit the fuel tanks [6]. For simplicity, the cruise speed of the Airbus ZEROe has been assumed equal to the Airbus 320 NEO, which is also comparable with the other aircraft types. The $\frac{L}{D}$ -ratio for the ZEROe is expected to be slightly lower than the resembling Airbus 320 NEO, since the ZEROe will be exposed to more skin-friction drag, due to the longer fuselage generating a larger wetted area, as was stated by Adler et al. [1].

In addition, the overall efficiency of each aircraft $\eta_{overall}$, required for Equation 3.1, has been assumed based on the work of Penner et al. [15]. Here it is also stated that the overall efficiency of aircraft

typically ranges from 20-40%, with the aircraft considered in this research being very modern and thus relatively efficient, explaining the selected values of the three conventional aircraft.

To further elaborate on the table above, there have been several researches focusing on the potential overall efficiency of LH₂-powered aircraft. A concluding study by NATO concluded however that LH₂-powered engines will be equally efficient as a Jet-A1 variant, which is an assumption that has been made throughout the entire industry so far [39]. Nevertheless, Choi et al. also stated that likewise Jet-A1 engines, engine efficiency may increase by up to 7% every 10 years [22]. On top of that, Adler et al. found that the specific nature of LH₂ potentially allows for better cooling techniques during various stages of compression in the engine, amounting to a potential 9-12% efficiency increase in the future [1]. Given these developments and assuming that the forecasted ZEROe launch is roughly ten years away from now, an efficiency increase of 7% with respect to the Airbus 320 NEO will be considered in this research, explaining the higher $\eta_{overall}$ of 0.39. This also complies with the typical efficiency range explained above, as well as a SFC of 15.4 g/kN/s, which is 7% lower than the current SFC of the selected GE Passport TM Turbofan [42].

When computing the total fuel consumed during a flight, Equation 3.1 can be applied to calculate the most significant part of the total fuel consumed, which is the fuel consumed during cruise. Nonetheless, a significant amount of fuel is also consumed during taxiing, take-off, descent and landing, which must also be accounted for. Typically for a medium range flight, it can be taken as a rule-of-thumb that 85% of the total fuel is burned during cruise [43]. In other words, the total fuel from Equation 3.1 needs to be divided by 0.85, in order to obtain the total amount of fuel. This amount will then also be increased by 5% to account for fuel reserves that are carried along. Once the total fuel amount is known, the refueling time can be derived by dividing this amount by the applicable flow rate, which can then be communicated to the fuel truck agent executing the actual fuel task.

3.3. Turnaround Definition

With the high influence of the turnaround procedure on the KPIs, correctly defining the duration of different turnaround processes per aircraft type is of utmost importance. In section 3.2, it was already explained how the duration of one of the most important turnaround processes is defined, which is the refueling process. The remaining turnaround processes need an accurate quantification of their duration as well. On top of that, since some processes involve unpredictability, such as (de-)boarding the aircraft, probability distributions are also incorporated within the model to make it more realistic. In general, the turnaround can be distinguished by three processes, being the passenger de-boarding, passenger boarding and finally the collection of processes executed between de-boarding and boarding with refueling as the most significant process. In most cases, refueling is however not the only middle part of the critical path, and thus an additional time needs to be added to the time in between (de-)boarding, in order to account for catering and cleaning. How much this time is depends on the turnaround procedure. For conventional aircraft, this additional time is about seven minutes as was derived from internal data provided by RTHA. For LH₂-powered aircraft however, this additional time is much more variable as it depends on which restrictions imply on the turnaround procedure, as well as which LH₂ flow rate is selected. Therefore, for each individual combination of these two parameters, the correct additional time has been devised, resulting from shifting the processes in the turnaround Gantt-chart, which is presented in the following overview.

As can be observed in Table 3.2, all experiments with full restrictions on parallel turnaround processes have an additional turnaround time of 17 minutes. This is because independent of the LH₂ flow rate, full cleaning and catering can be performed only after the refueling, lasting 17 minutes in total. Next, for both the cases with some and no restrictions on parallel turnaround processes, the additional turnaround time increases as the flow rate increases as well. This might seem controversial, but the lower the flow

Table 3.2: Overview of extra turnaround time component for LH₂-powered aircraft per experiment, required for catering and cleaning.

		Restrictions on parallel turnaround		
		Yes	Some	No
Flow rate	2.5 kg/s	17 min	10 min	0 min
	5 kg/s	17 min	12.5 min	2.5 min
	10 kg/s	17 min	15 min	3 min
	15 kg/s	17 min	15 min	5 min

rate, the longer the refueling, thus ensuring that a greater (or full) part of catering and cleaning can already be performed while refueling is ongoing. As for the experiments with no restrictions, catering and cleaning can also be executed during the (dis-)connecting of the refueling equipment, less additional time is required with respect to the experiments with some restrictions. Using these additional times, the duration of the assumed turnaround procedure sequences of section 2.2 can be defined.

Another important input to the model and also a variable factor is the (de-)boarding time. Firstly, the standard de-boarding rate used in the model is 15 passengers per minute, which is used for each aircraft type, independent of the fuel type [44]. In order to simulate the uncertainty during de-boarding, a uniform distribution of Uniform[-120,300] will be used in seconds, as was based on the turnaround data at RTHA. Secondly, the mean boarding time for the A320 NEO deployed on European flights is slightly longer than de-boarding, with only 10 passengers per minute, as was researched by Hutter et al. [17]. The variation during this process was found to be more unpredictable than de-boarding, leading to a uniform distribution of Uniform[-300,600]. These boarding times are also in line with the internal experience of boarding duration at Rotterdam The Hague Airport. Ultimately, within the model an average load factor of 81.8% for each aircraft is selected, as was presented for 2023 by IATA [31].

3.4. Flight Schedule

In order to investigate the impact on several airport KPIs at Rotterdam The Hague Airport in 2050 as a result of the introduction of LH₂-powered aircraft, it is important to utilize a realistic flight schedule. As explained earlier, the exact flight schedule is dependent on which penetration rate is selected, which is in turn dependent on the simulated experiment. However, each flight schedule is based on the peak-day 17th of July 2023, which was the busiest day of that year. In this way, it can be ensured that the conclusions of this research are valid for each possible number of flights up to this maximum. Since the scope of this research focuses on 2050, the number of flights must also correspond with the forecasted number of flights in 2050. Hence, the peak-day flight schedule of 2023 can be manipulated to incorporate the forecasted differences, making the research more realistic. Therefore, the (allowed) movements at RTHA in 2050 has been forecasted.

The number of flight movements that Rotterdam The Hague Airport is allowed to facilitate per year is established in the 'Luchthavenbesluit'. This is a permit in which among others the limitations and thresholds of the airport are defined [7]. Since the airport is situated in the vicinity of large residential areas of Rotterdam, the emissions are accounted for when defining the maximum number of movements at the airport, in order to minimize the impact on the quality of livability in the area. These emissions regard CO₂, N₂ and noise amongst others. Currently, this limitation on the number of movements is constrained by the noise of the aircraft flying at RTHA. The number of movements is including all types of aviation at the airport, so commercial flights, business flights, flight school flights, general aviation and even the trauma helicopter. In the following figure, the number of flights over the past decade is

presented.

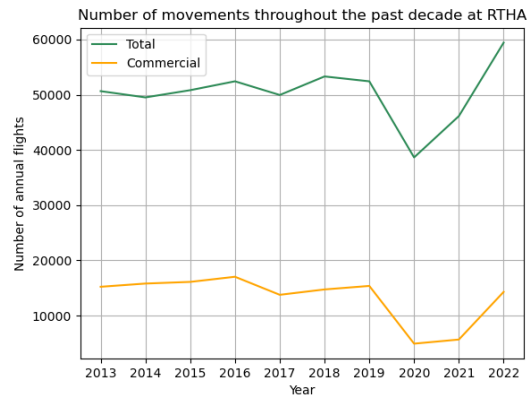


Figure 3.2: Number of total and commercial flights per year at RTHA. Information retrieved from [8].

From Figure 3.2, it is found that the number of total and commercial flights remains more or less constant, with an exception of the temporary reduction in 2020 and 2021 as a result of COVID-19. Also, the fraction of commercial flights with respect to the total number of flights remains mostly unchanged. The slight fluctuations can be explained by the fact that each aircraft type is classified within a certain noise category. Whenever more aircraft from a worse noise category fly to and from RTHA in a certain year, there can be less movements of other aircraft because a larger part of the noise 'budget' has already been used up, and this also works oppositely. In the current situation, RTHA accommodates around 16,500 commercial flights per annum, while the airport is limited at 18,000 annual movements, which was learned from the slot expert of RTHA. Thus, the airport is currently operating slightly under its capacity, as it is still recovering from COVID-19, but also due to the accommodation of some 'noisier' aircraft. However, in the coming years this recovery will be completed while also more efficient and quieter aircraft are expected to operate at the airport, such that the airport will have reached its maximum capacity. This maximum capacity comes down to an average of 49 flights per day, but in reality the busy summer days will face upwards of 60-65 flights, with peaks reaching 72 flights, while in the off-season it will be significantly below the average again [9]. One movement or flight yields either a landing or a take-off, so normally accommodating an aircraft which lands, undergoes a turnaround and takes-off after again requires two movements.

The noise limitation has been constraining the airport from further growing for over a decade now, which is why RTHA is currently working on a new permit that should allow for more movements. The main reasoning behind this is that if more efficient and hence quieter aircraft will structurally fly towards Rotterdam The Hague Airport, less noise is emitted and thus more movements can be allowed. Obtaining this new permit is a very extensive process as was learned from expert knowledge, and the new permit is only due in January 2025 [7]. Internal experts expect that the new permit will allow 4000 additional commercial movements per annum which can be used every day between 9 am and 9 pm, starting from 2030. Given the demand of new airlines willing to fly towards RTHA, it is forecasted that around 2035, all these new movements will be occupied by both existing and new airlines. An important remark is that these additional movements can only be awarded if the other budgets, those regarding CO₂ and N₂, are not exceeded as a result of these extra flights. Since this research is focusing on 2050 in which the more sustainable LH₂-powered flights will also be part of the flight schedule operating at RTHA, it is safe to assume that by 2050, all these additional movements will be in use. These 4000 movements are equivalent to an average of 11 daily flights. Again, in the summer this will be

more in the order of 15-16 extra flights, while in the off-season this will only mean 6-7 extra flights per day. When generating a realistic flight schedule for a peak-day in 2050, these additional movements for the summer must therefore be added to the already established peak movements of 72 daily flights that are currently accommodated, bringing the total to an assumed 90 movements, or 45 aircraft that both arrive and depart. As a final remark, these additional movements have been added by spreading these throughout the flight schedule of the entire peak-day. Therefore, the LH₂-powered aircraft are not only replacements of the conventional movements in the flight schedule, but also are deployed on some of the newly added flights. This yields LH₂-powered aircraft operating during peak moments throughout the day, as well as during less busy periods.

4

Model Verification and Validation

In order to ensure the robustness, reliability and consistency of the multi-agent system simulation model, verification and validation processes were executed. An adequate execution of this enhances the quality of the results, making it more useful to future researches within the aviation industry. This is especially important due to the current lack of many comparative studies. On top of the verification and validation, all model inputs, being the different experiments along with the flight schedule, were defined using expert knowledge and peer reviewed research articles. First, the verification processes will be discussed section 4.1, after which in section 4.2 the validation processes are treated.

4.1. Verification

The first part of the verification procedure consisted of executing thorough unit and system tests, in order to ensure the adequate operation of the simulation model as a whole, including different calculations and sub-simulations. The unit tests could be used to test isolated elements of the code, through performing hand-calculations or using alternative computation techniques for comparison. An example of this is the fuel mass which could be verified using another variant of the Breguet equation, involving the specific fuel consumption instead of the overall efficiency in Equation 3.1. Another example of a unit test included the blocking of aircraft stands next to which a LH₂-powered aircraft is being refueled with safety zone diameters of 30 or 45 meter, which was verified based on the measured platform occupation data. Also, extreme conditions were inputted to these tests to verify the boundary adequacy. On top of this, certain elements of the model were already verified such as the A*-algorithm. Once all isolated elements of code were verified, the integration of these sets of code could be verified which was conducted using system tests. Within these tests, several additional performance indicators were measured during (partial) simulations to evaluate if changes in the input parameters lead to the desired output of the model as a whole. This was substantiated with the visualization of the simulation model, which allowed a more informative visual verification to be performed, based on the behaviour of the agents as a function of time, represented by the timer. Ultimately, the statistical significance of the results is established, based on which graphical sensitivity analyses were executed with varying experimental inputs to verify the model performance by analyzing the associated outputs.

4.2. Validation

Once the research outcomes have been verified, ensuring that all outcomes are correctly computed, it is time to validate these outcomes. Namely, only for this research to be actually meaningful, it must be proven that the outcomes are an acceptable representation of the actual system. There are several ways to validate simulation outcomes, for example using comparable data, a comparable model or experts who consider the results [45]. The first option is not possible at this stage, given that currently there are no commercial LH₂-powered aircraft in operation yet for which data has been measured. The only data that could be validated with internal airport data using this technique were the KPIs related to the conventional aircraft at a low penetration rate, as this is still representative of the current operations. Furthermore, the results in which the LH₂ flow rate was differed could be validated using the outcome

of the model developed by Hoelzen et al., in which the impact on commercial airline operations using LH₂-powered aircraft was analyzed using varying LH₂ flow rates [13]. Also, it was observed in the work of Babuder et al. that the effects on the KPIs varied significantly between a flow rate of 5 kg/s and 10 kg/s, while the KPIs were almost identical for 10 kg/s and 20 kg/s [11]. This observation is also visible in the results of this research, in which many experiments already performed optimal for a LH₂ flow rate of 10 kg/s, hence validating these outcomes. Ultimately, the remaining outcomes could only be validated using the final option, being internal experts at RTHA.

5

Statistical Significance

In this chapter, the theory based on which the statistical significance of the results is proven is provided. Namely, in order to establish the statistical significance, different calculations and tests have been performed. First, the methodology behind calculating the coefficient of variance is explained in section 5.1. Second, the statistical tests that have been performed in order to prove certain dependencies within the simulation results are treated in section 5.2.

5.1. Coefficient of Variance

In order to obtain meaningful results from the simulations, the statistical significance of the results must be determined. This can be done using the coefficient of variance, referred to as c_v . The coefficient of variance represents how variable a certain data set is, by expressing the standard deviation in relation to the mean of the data set. This is required as the model is characterized by stochastic factors such as the stand allocation and (de-)boarding duration. The formulae, used to compute the coefficient of variance, are presented in Equation 5.1 and Equation 5.2 respectively [45].

$$c_v = \frac{\sigma}{\mu} \quad (5.1)$$

$$\sigma = \sqrt{\frac{\sum (x_i - \mu)^2}{N}} \quad (5.2)$$

In Equation 5.1, the included parameters are the standard deviation σ , divided by the mean of the data set, μ . Moreover, in Equation 5.2 the standard deviation can be computed by taking the measured KPI x_i minus the mean μ , putting this outcome to the power of two and summing this up for every solution within the data set. Next, this entire sum must be divided by the size of the data set N , and when the square root is taken from this value, the standard deviation has been obtained. Once the coefficient of variance is computed, it can be calculated and plotted after every simulation run, with c_v on the y-axis and the number of runs on the x-axis. Once the graph then converges to a stable horizontal plot, the scenario has been simulated for sufficient runs, such that the results can be considered statistically significant. For this convergence threshold, a significance level alpha of 0.1 was adhered to. This rather large alpha can be justified since the research is of an exploratory kind, involving a high uncertainty and thus a large number of experiments. In later stages and future work for which more guidance is available relating to LH₂ ground operations, for example provided by this research, a more accurate alpha can be selected. Within this research, the number of simulation runs necessary for a certain experiment scenario in order to become statistically significant ranged from 15 to 25.

5.2. Statistical Tests

Once all the experiments have been simulated and all datasets are gathered, the results can be analyzed. Nevertheless, first it needs to be proven that apparent influences of parameters on the outcomes, as well as the covariance of multiple parameters, have a proven dependence on the associated key performance indicator. In order to justify this, statistical tests have been performed on the different datasets, which establish the chance that a certain apparent relationship is not actually because of dependence, but

by chance instead. Then, based on the values in the chi-squared table, it can be determined if the null hypothesis is rejected or accepted. Which specific statistical test has been applied on which data depends on the type of data in the datasets, its distribution and the number of groups among others [45]. Ultimately, two statistical tests have been utilized to establish the statistical significance, being the Friedman test and the Wilcoxon signed rank test. For the Friedman test, the formula used to calculate χ^2 , necessary to compare in the statistical table for hypothesis testing, are provided below.

$$\chi_r^2 = \frac{12}{nk(k+1)} \sum R^2 - 3n(k+1) \quad (5.3)$$

In Equation 5.3, n is equal to the length of the dataset, with k being the number of groups in the dataset [27]. Furthermore, R is equal to the total sum of all ranks within a certain dataset. For the Wilcoxon signed rank test, the procedure is different from the calculation as explained above [50]. First, the values of two datasets need to be subtracted from each other to calculate the difference. Second, once all differences are quantified, the magnitude of the difference needs to be ranked from smallest to largest, while the cases in which there is no difference can be discarded. Third, the total of all the ranks with a positive and negative difference need to be summed respectively. Fourth and lastly, T must be set equal to the smallest of these two sums. With N being equal to the number of comparisons that have been made within the two datasets, it can be assessed if the hypothesis must be accepted or not using the statistical table. In the following overview, the proven statistical dependencies are presented for every combination of experiment parameter (row) and KPI (column).

Table 5.1: Overview of the proven statistical dependencies of each KPI versus each parameter considered within this research.

	Total OTP	TAT LH₂	TAT Jet-A1	Number of delayed Jet-A1 AC	Number of delayed LH₂ AC	Average delay of Jet-A1 AC	Average delay of LH₂ AC
Penetration rate	Yes	Yes	Yes	Yes	Yes	Yes	Yes
LH₂ flow rate	Yes	Yes	No	No	Yes	No	Yes
Number of LH₂ trucks	No	Yes	No	No	Yes	No	Yes
Turnaround procedure	No	Yes	No	No	No	Yes	No
Safety zone diameter	Yes	Yes	No	No	Yes	No	Yes

As becomes apparent in Table 5.1, the dependency of a certain KPI on the different parameters can vary significantly. Some KPIs have a proven dependency on only one of the parameters, whereas other KPIs are dependent on several or even all parameters. This will feed the decision on the type of sensitivity analysis that can be performed on the respective results. Namely, the KPIs that have a proven relationship with only one parameter, being the TAT Jet-A1 and number of delayed Jet-A1 aircraft, can be analyzed using a local sensitivity analysis, while the remaining KPIs that are dependent on multiple parameters must be analyzed using contour plots. Another remark on the table above is that only the data in which the number of LH₂ trucks is varied must be tested using the Wilcoxon signed rank test for all KPIs. This is because these datasets consist of just two groups, whereas all other datasets and thus parameter and KPI combinations constitute of more than two datasets. Hence, these other datasets can all be tested using the Friedman test.

6

Supplementary Results

In addition to the results already presented in the scientific paper, there are a number of supplementary results that have been generated within this research. This can be categorized into general results, which will be discussed in section 6.1, as well as results regarding the platform configuration, as is treated in section 6.2.

6.1. General Results

The flight schedules that have been utilized as input to the simulation model are characterized by a number of important properties, which influence the model output. In total, three different flight schedules with the three different penetration rates were generated, leading to a number of general results such as the distribution of aircraft with a certain fuel type, as well as fuel requirements. This is provided in the following overview and can assist in obtaining a better understanding of the main results that have been discussed in the scientific paper, while also providing useful insights regarding the required fuel facility.

Table 6.1: Overview of the most important characteristics of the three different flight schedules.

Penetration rates	Jet-A1 A/C	LH ₂ A/C	Amount of Jet-A1 [kg]	Amount of LH ₂ [kg]	Number of Jet-A1 trailers	Number of LH ₂ trailers
5%	52	3	164,750	4,705	5	2
25%	40	15	116,956	21,789	4	7
50%	30	25	91,741	31,163	3	9

As can be observed in Table 6.1, each of the three flight schedules consists of accommodating a total of 55 different aircraft throughout the day, including both Jet-A1 and LH₂-powered aircraft. The penetration rate alternates the total number of flights per day, instead of the number of aircraft per day, explaining why the percentage does not exactly correspond with the number of LH₂ aircraft in relation to the total of 55. Furthermore, another observation is that when comparing the 5% flight schedule with the 50% schedule, the amount of Jet-A1 required throughout the day has reduced with over 70,000 kg, while only requiring a little over 25,000 kg LH₂ instead. The downside however is that due to the high volume of LH₂, the total number of used trailers is almost doubled to a total of 12 in the case of 50%, as opposed to only seven in the case of 5%. The 25% flight schedule also leads to a significant total number of fuel trailers already, with just one less than the 50% case. This requires a re-evaluation of the fuel storage facility, which needs to be assessed in order to ensure that the facility can accommodate this larger number of trailers, as well as the trailer replacements, in and towards 2050.

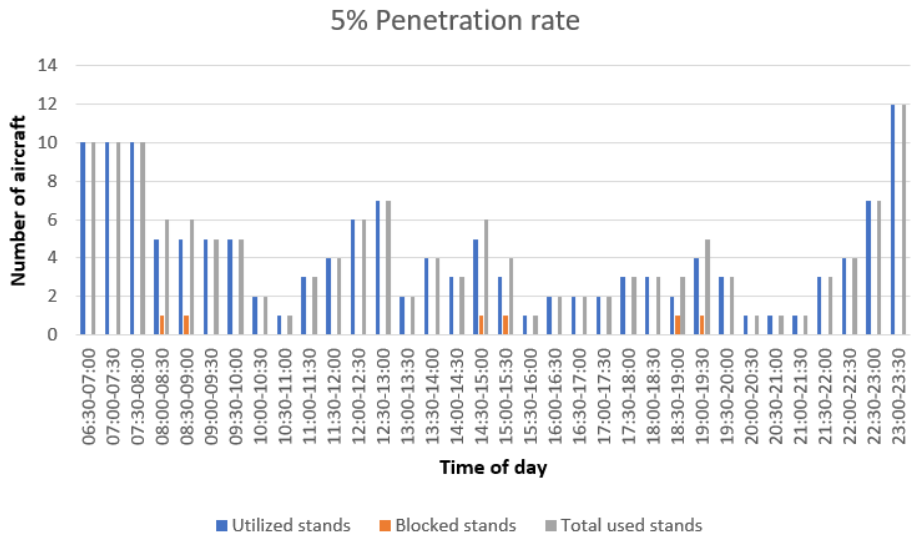
6.2. Configuration Results

As a result of the experiment parameters selected within the research, the utilization of the platform at RTHA will vary considerably with respect to today. Namely, the penetration rate determines the share of flights on which a LH₂-powered aircraft is deployed. In turn, the LH₂-powered aircraft will have to be ground handled, which potentially causes adjacent aircraft stands to be temporarily blocked due to safety, alternating the stand occupation and availability. In order to assess the impact of these blocked stands on the average stand occupation throughout the day at RTHA, an overview has been generated for the different penetration rates considered which can be visualized in Figure 6.1. For the safety zone, a diameter of 30m was selected for each of the three cases.

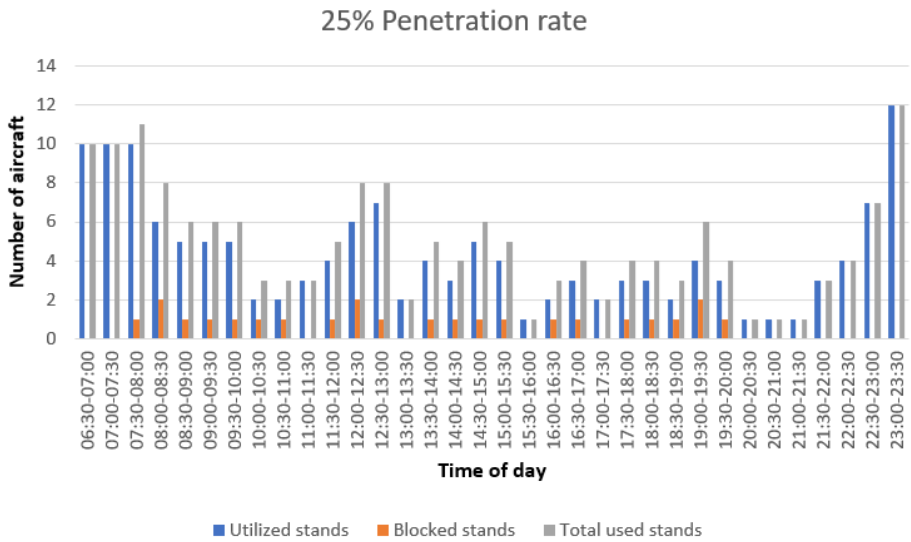
As can be visualized in the figures below, the number of aircraft being present at RTHA throughout the day really is distributed into peaks, which need to be accommodated using the 12 aircraft stands available. Namely, at night a significant number of aircraft is parked at the airport, and the majority of these aircraft departs between 07:00 and 10:00, causing a relatively low occupation at the airport from 10:00 onwards. Then, between 11:00 and 13:00, there is a peak again since most of the aircraft that left the airport in the morning have returned from their destination again. After this, this pattern is repeated a number of times again in the afternoon but at a smaller magnitude, and in the end all aircraft arrive at the airport again after 21:30, to spend the night at RTHA.

Moreover, the blue bars in the three bar charts above represent the stands actually utilized by aircraft, the orange bars represent the blocked stands because of nearby LH₂ refueling and ultimately the gray bars is the total sum of these other two bars. The first main observation is that as the penetration rate increases, the height of the orange bars increases, as straightforwardly more LH₂-powered aircraft also causes more blocked stands when these aircraft have to be refueled. Especially at peak moments throughout the day, this can cause bottlenecks. For example, the peak between 12:00 and 13:00 in Figure 6.1a accommodates only seven aircraft, whereas in Figure 6.1c the blocked stands have increased the stand occupation to 11 at the same time of day. In other words, the airport must closely monitor these effects and carefully distribute its slots, in order to make sure that these peak moments are managed. In this way, these peaks can be better distributed throughout the day, therefore minimizing the occupation of the ground handler, passenger distribution and putting a smaller demand on the infrastructure.

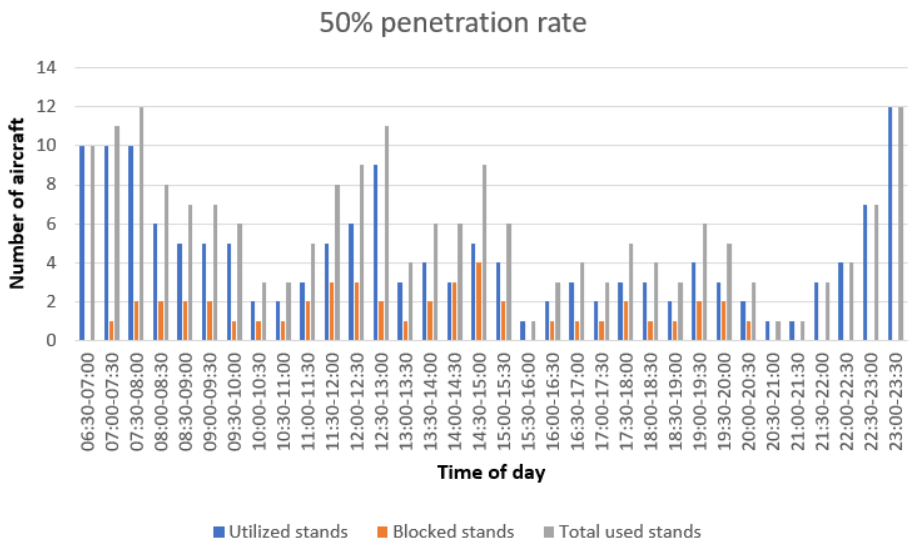
The second observation and also concern is that at a penetration rate of 25% and 50% as presented in Figure 6.1b and Figure 6.1c respectively, the maximum capacity of 12 aircraft has been reached at 23:30. As can be seen in these figures, there is no blocked stands at these times because the aircraft only arrived and do not need to operate another flight this day, explaining why they do not need refueling and thus also no stands are blocked. Nevertheless, the following morning when all flights have to depart again, first a number of conventional aircraft will need to depart before there are empty stands which is required before LH₂ can be refueled. Therefore, this is a bottleneck which requires adequate coordination in order to preferably prevent it, or otherwise ensure that this is executed as efficiently as possible. If this is not feasible, RTHA must assess its current stand layout, and seek for opportunities to improve the layout to more spacious or additional aircraft stands using areas at airside that are currently not in service.



(a) Temporal stand occupation at RTHA with a penetration rate of 5%.



(b) Temporal stand occupation at RTHA with a penetration rate of 25%



(c) Temporal stand occupation at RTHA with a penetration rate of 50%

Figure 6.1: Stand occupation at RTHA for different flight schedules.

Implications for RTHA

Given that the case-study of this research focuses on Rotterdam The Hague Airport, it is also essential to interpret the outcomes of the research from their perspective and to form implications based on these outcomes. In order to analyze these implications, for each parameter that was incorporated within this research, the findings with respect to RTHA will be discussed. These parameters are listed in decreasing magnitude of importance in the road-map provided in section 7.1. After that, a number of remarks with respect to the fuel storage facility are given in section 7.2.

7.1. Road-map

These remarks are made based on a peak-day incorporating the forecasted number of allowed movements in 2050, using the ZEROe turbofan as the LH₂-powered aircraft.

- **1. Turnaround Procedure:**

By accommodating a number of turnaround processes to be executed (semi-)autonomously, considerable improvements can be made in the field of turnaround and thus occupational efficiency. Hence, it is important for RTHA to be involved in projects considering semi-automated refueling involving an automated fuel arm, but also other innovative suggestions such as automated cleaning, baggage loading among others. The airport can also pioneer by organizing pilots to support organizations or institutions that are working on these implementations. Another suggestion is to incorporate a restricted minimum level of automation in the service provided by the current ground handler, to support those initiatives. In this way, the level of automation can gradually be build up towards 2050.

- **2. LH₂ flow rate and number of LH₂ fuel trucks:**

The LH₂ flow rate and the number of LH₂ fuel trucks are two other very important parameters to Rotterdam The Hague Airport when LH₂-powered flights are included in the operations. Namely, increasing this flow rate can result in faster turnarounds, less delays and congestion and hence more revenue to the airport, while the airlines are also more satisfied and will thus remain loyal. In addition to this, investing in another LH₂ fuel truck results in a better on-time performance, as well as less delays at the airport among others. It can be expected that if the LH₂ demand is high at RTHA, the fuel supplier itself will automatically provide higher LH₂ flow rates or more LH₂ fuel trucks if this can generate more revenue, hence automatically solving the problem.

However, to further accelerate these developments, another strategy can be consulted. Namely, after an interview with the fuel supplier at RTHA, it was found that the best alternative way to incorporate high LH₂ flow rates or more LH₂ fuel trucks would be to introduce service level agreements. This can for example be a constraint defining the maximum number of delayed aircraft because of a delayed LH₂ fuel truck per year. If this constraint is then not reached, this will result in consequences such as fines or even the termination of the contract which allows other fuel suppliers to take the opportunity. Thus, Rotterdam The Hague Airport should closely

communicate with the fuel supplier regarding when slots are allocated to LH₂-powered aircraft, such that they can scale up in-time.

It is also recommended that RTHA researches what the effect of a potential additional fuel truck will be on the platform operations. Namely, this/these additional vehicle(s) also need to be stored somewhere, requiring available space at the airside, which must be provided by RTHA. Also, these additional movements can lead to more congestion on the platform or at the fuel storage facility. The implications on the fuel storage facility will be further analyzed in section 7.2.

- **3. Penetration Rate:**

Another parameter that can greatly influence the operations at RTHA is the penetration rate of LH₂-powered aircraft. Namely, increasing the penetration rate from 5% to 25% can already introduce significant delays and occupation of the infrastructure if these other factors have not sufficiently developed yet. This problem can become even more significant if the penetration rate is increased further to 50%. Fortunately however, the airport can control the penetration rate itself to a great extent. Namely, while issuing slots, it can be determined how many of these slots will be allocated to LH₂-powered aircraft. In this way, based on the available infrastructure, refueling techniques and regulations, the penetration rate can be slowly scaled-up per year, in accordance with the level of service provided by the ground handler and fuel supplier to ensure a smooth and efficient transition while minimizing the operational impact and thus (operational) cost to the airport.

- **4. Safety zone diameter:**

The final parameter that influences the operations at RTHA when introducing LH₂-powered aircraft is the safety zone diameter. At safety zone diameters of 30 meter or larger, adjacent aircraft stands will need to be blocked from any aircraft during the refueling of LH₂, while also only a limited number of aircraft stands are available to LH₂-powered aircraft, as was explained in subsection 2.1.2. This will lead to a different utilization of the platform and aircraft stands, while also the capacity of aircraft can be seriously reduced. Due to this lower capacity, the airport must examine its flight schedule more closely to better spread the aircraft demand throughout the day, as otherwise the maximum capacity might be exceeded at certain peaks during the day. A suggestion is to re-evaluate the current platform layout and look for opportunities to extend the number of available stands, preferably modular ones which are more than 30 meter apart, at airside areas that are currently not in service. This will also be a strategic decision, as this would not only improve the operations up to 2050, but also provides opportunities for further growth after that year. An important remark for this latter benefit is that the emissions of LH₂-powered aircraft must be lower than conventional aircraft, such that the airport is permitted to operate more flights.

7.2. Fuel Storage Facility

The current fuel storage facility at Rotterdam The Hague Airport consists of six Jet-A1 trailers, parked together near 'poort 18' on the west-side of the runway. Each trailer has a capacity of 42,000 m³ as was learned from expert knowledge, which is equal to 34,440 kg, making the maximum fuel storage of Jet-A1 at RTHA 206,640 kg. Whenever one of the fuel trucks has emptied a trailer, it drives towards this storage facility, parks the empty trailer and picks up one of the full trailers. The supply-chain is completed with Shell, the fuel supplier at RTHA, delivering a full trailer to the airport and returning an empty trailer again. The number of trailer deliveries highly varies per day and is dependent on the expected air traffic, but averages around 3-5.

With the introduction of LH₂ as a fuel, the fuel storage facility is expected to see some changes. Namely, current LH₂-trailers have a capacity of 50,000 m³ [24], which translates to only around 3,500 kg, due

to the low density of LH₂ with respect to Jet-A1. With a considerably higher volume to be refueled per LH₂-powered aircraft for the same energy content, this could potentially lead to a significant increase in required fuel trailers stored and hence, the number of daily deliveries, when compared to the current situation with Jet-A1. Therefore, the airport is recommended to consider the current fuel storage facility in greater detail and look into potential opportunities to extend the facility to accommodate more trailers and be prepared for this increase in required fuel trailers, as well as deliveries.

8

Pseudocode

Below, the pseudo code of the A*-algorithm is provided, which has been used as the low-level solver for path-planning within the multi-agent system model.

Algorithm 1 A* Path Planning

Require: Set of nodes (in a graph), Starting node, Goal node

Ensure: Path for agent

```
Open_list = [Set of nodes]           ▷ This list contains all unexplored nodes
Closed_list = [Starting node]        ▷ This list contains all visited nodes
while Open_list is not empty do
    q = Closest node to starting node  ▷ The starting node yields the previous node
    Open_list.remove(q)
    Establish q's successors
    for each successor do
        if Successor == Goal node then
            End
        else if Successor != Goal node then
            f_successor = (g_q + distance between successor and q) + Distance from goal to successor
            for Node in Open_list do
                if Successor == Node and f_node smaller than f_successor then
                    Skip successor    ▷ There are shorter ways to reach this successor than this path
                end if
            end for
            for Node in Closed_list do
                if Successor == Node and f_node larger than f_successor then
                    Skip successor    ▷ This node has already been visited via a shorter path
                end if
            end for
            else if successor not in Open_list and Closed_list then
                Open_list.append(Successor)
            end if
            Closed_list.append(q)
        end for
    end while
```

As can be visualized above, a graph, representing all the nodes in the environment using coordinates, the starting node and goal node will need to be provided. In the end, the shortest path possible for that request will then be provided by the algorithm.

References

- [1] J. Adler and J. Martins. “Hydrogen-powered aircraft: Fundamental concepts, key technologies, and environmental impacts”. In: *Progress in Aerospace Sciences* 141 (Aug. 2023). DOI: 10.1016/j.paerosci.2023.100922.
- [2] Conscious Aerospace. *Technology*. Jan. 2023. URL: <https://www.consciousaerospace.com>.
- [3] Airbus. *Annual Press Conference 2024*. 2024.
- [4] Airbus. *CFM AND AIRBUS TO PIONEER HYDROGEN COMBUSTION TECHNOLOGY*. Feb. 2022. URL: <https://www.cfmaeroengines.com/press-articles/cfm-and-airbus-to-pioneer-hydrogen-combustion-technology/#:~:text=CFM%20will%20modify%20the%20combustor,turbofan%20to%20run%20on%20hydrogen..>
- [5] Airbus. *Hydrogen*. 2022. URL: <https://www.airbus.com/en/innovation/low-carbon-aviation/hydrogen#:~:text=If%20generated%20from%20renewable%20energy,by%2Dproduct%20of%20CO2%20emissions..>
- [6] Airbus. *ZEROe*. Jan. 2023. URL: <https://www.airbus.com/en/innovation/low-carbon-aviation/hydrogen/zeroe>.
- [7] Rotterdam The Hague Airport. *Luchthavenbesluit*. Jan. 2022. URL: <https://www.rotterdamthehagueairport.nl/over-rtha/organisatie/luchthavenbesluit/>.
- [8] Rotterdam The Hague Airport. *Overzicht verkeer en vervoer per kalenderjaar*. Tech. rep. Rotterdam The Hague Airport, 2022.
- [9] Rotterdam The Hague Airport. *Record in aantal passagiers juli 2022*. Aug. 2022. URL: <https://www.rotterdamthehagueairport.nl/luchthaven-en-ik/organisatie/nieuws/item/record-in-aantal-passagiers-juli-2022/#:~:text=0ok%20in%20augustus%20verwacht%20RTHA,naar%20Rotterdam%20The%20Hague%20Airport..>
- [10] Rotterdam The Hague Airport. *Vlieg naar ruim 50 Europese bestemmingen*. Jan. 2023. URL: <https://www.rotterdamthehagueairport.nl/vluchten/bestemmingen/>.
- [11] D. Babuder et al. “Impact of LH2 Aircraft Propulsion on Commercial Airline Operations”. In: (Oct. 2023).
- [12] J. Hoelzen et al. “H2-powered aviation at airports – Design and economics of LH2 refueling systems”. In: (May 2022).
- [13] J. Hoelzen et al. “H2-powered aviation at airports – Design and economics of LH2 refueling systems”. In: *Energy Conversion and Management: X* 14 (May 2022). DOI: 10.1016/j.ecmx.2022.100206.
- [14] J. Mangold et al. “Refueling of LH2 Aircraft—Assessment of Turnaround Procedures and Aircraft Design Implication”. In: (Mar. 2022).
- [15] J. Penner et al. *7.4.1.2. Propulsive and Overall Efficiency*. First. IPCC, 1999.
- [16] L. Dehée et al. “Cranfield Aerospace Composite Repair - Group Project Thesis”. PhD thesis. May 2017. DOI: 10.13140/RG.2.2.27923.89123.
- [17] L. Hutter et al. “Influencing factors on airplane boarding times”. In: (Sept. 2019).

- [18] A. Bain. “NASA space program experience in hydrogen transportation and handling”. In: (Jan. 1976).
- [19] R. Barron and G. Nellis. *Cryogenic Heat Transfer*. second. CRC Press, 2016.
- [20] Boeing. *Hydrogen Infrastructure and Operations*. Tech. rep. FLYZERO, 2022.
- [21] T. Chau and D. Zingg. “Aerodynamic Design Optimization of a Transonic Strut-Braced-Wing Regional Aircraft.” In: (Aug. 2021).
- [22] Y. Choi and J. Lee. “Estimation of Liquid Hydrogen Fuels in Aviation”. In: (Sept. 2022).
- [23] I. Coutts. *Turnaround: Here’s What Happens When An Aircraft Is On The Ground*. June 2022. URL: <https://simpleflying.com/aircraft-turnaround-process/>.
- [24] Hydrogen Europe. *Hydrogen Transport Distribution*. Tech. rep. Hydrogen Europe, 2017.
- [25] Official Journal of the European Union. *REGULATIONS*. Tech. rep. European Union, 2008.
- [26] FINAVIA. *How is an aircraft refueled? Here are the facts*. Nov. 2016. URL: <https://www.finavia.fi/en/newsroom/2016/how-aircraft-refueled-here-are-facts#:~:text=The%20aircraft's%20fuel%2Dtanks%20are%20located%20on%20each%20wing&text=Once%20parked%2C%20trucks%20park%20under%20the%20wing%20of%20the%20aircraft.&text=%E2%80%9CThe%20driver%20of%20the%20fuel,begins%20refueling%2C%E2%80%9D%20Bergman%20narrates..>
- [27] M. Friedman. “The Use of Ranks to Avoid the Assumption of Normality Implicit in the Analysis of Variance”. In: *Journal of the American Statistical Association* 32.200 (1937).
- [28] TUI Group. *Fleet renewal – TUI is receiving new modern and efficient aircraft*. 2018.
- [29] H2-Fly. *Company*. 2022. URL: <https://www.h2fly.de/company>.
- [30] Universal Hydrogen. *Product*. Jan. 2023. URL: <https://hydrogen.aero/product/>.
- [31] IATA. *Strong Air Travel Growth Continues in May as Load Factor Rises to 2019 Levels*. July 2023. URL: <https://www.iata.org/en/pressroom/2023-releases/2023-07-06-01/>.
- [32] Airlines Inform. *Airbus A320neo*. Jan. 2014. URL: <https://www.airlines-inform.com/commercial-aircraft/airbus-a320neo.html>.
- [33] Airlines Inform. *Boeing 737 MAX 8*. Jan. 2016. URL: <https://www.airlines-inform.com/commercial-aircraft/boeing-737-max-8.html>.
- [34] Airlines Inform. *Embraer E190-E2*. Jan. 2016. URL: <https://www.airlines-inform.com/commercial-aircraft/embraer-e190-e2.html>.
- [35] R. James. *How Long to Refuel an Airplane? – 15 Most Common Planes*. Jan. 2021. URL: <https://pilotteacher.com/how-long-to-refuel-an-airplane-15-most-common-planes/>.
- [36] V. Karnozov. *Aviadvigatel Mulls Higher-thrust PD-14s To Replace PS-90A*. Aug. 2019. URL: <https://www.ainonline.com/aviation-news/air-transport/2019-08-19/aviadvigatel-mulls-higher-thrust-pd-14s-replace-ps-90a>.
- [37] O. Memon. *Getting Planes Airborne: The Steps Involved In Aircraft Delivery And Entry Into Service*. Feb. 2023. URL: <https://simpleflying.com/aircraft-delivery-entry-into-service-steps-guide/>.
- [38] O. Memon. *What Factors Determine The Performance Of A Boeing 737 MAX When Cruising?* Dec. 2022. URL: <https://simpleflying.com/boeing-737-max-cruise-performance-determining-factors/>.

- [39] NATO. *LH2 as Alternative Fuel for Aeronautics – Study on Aircraft Concepts*. Tech. rep. NATO, 2007.
- [40] International Civil Aviation Organization. “Future of Aviation”. In: 2017. URL: <https://www.icao.int/Meetings/FutureOfAviation/Pages/default.aspx>.
- [41] RIVM. *Afstanden en gebieden*. Tech. rep. 1. Rijksinstituut voor Volksgezondheid en Milieu, 2023.
- [42] E. Roux. “Turbofan and turbojet engines: Database handbook”. In: (Jan. 2007).
- [43] B. Rowland. *WHICH PART OF A FLIGHT USES THE MOST FUEL?* Feb. 2022. URL: <https://www.oag.com/blog/which-part-flight-uses-most-fuel>.
- [44] M. Schmidt. “A review of aircraft turnaround operations and simulations”. In: (July 2017).
- [45] A. Sharpanskykh. *AE4422-20 Agent-based Modelling and Simulation in Air Transport*. Sept. 2021.
- [46] D. Shepardson. *Boeing 777X deliveries likely to be delayed until early 2025 -source*. Apr. 2022. URL: [https://www.reuters.com/business/aerospace-defense/boeing-preparing-new-delay-777x-air-current-2022-04-22/#:~:text=Boeing%20777X%20deliveries%20likely%20to%20be%20delayed%20until%20early%202025%20%2Dsource,-By%20David%20Shepardson&text=WASHINGTON%2C%20April%2022%20\(Reuters\),on%20the%20matter%20told%20Reuters..](https://www.reuters.com/business/aerospace-defense/boeing-preparing-new-delay-777x-air-current-2022-04-22/#:~:text=Boeing%20777X%20deliveries%20likely%20to%20be%20delayed%20until%20early%202025%20%2Dsource,-By%20David%20Shepardson&text=WASHINGTON%2C%20April%2022%20(Reuters),on%20the%20matter%20told%20Reuters..)
- [47] National Institute of Standard and Technology. *NIST Chemistry WebBook, SRD 69*. Tech. rep. 1. NIST, 2021.
- [48] J. Sun. “Drag polar estimated for common Airbus and Boeing aircraft under clean configurations at low Mach number.” In: (July 2020).
- [49] A. Wignall. *How it works: the aircraft turnaround*. Nov. 2022. URL: <https://www.aerotime.aero/articles/32767-how-it-works-the-aircraft-turnaround>.
- [50] R. Wilcoxon. “Individual Comparisons by Ranking Methods”. In: *Biometrics Bulletin* 1.6 (1945).
- [51] ZeroAvia. *ZeroAvia Makes Aviation History, Flying World’s Largest Aircraft Powered with a Hydrogen-Electric Engine*. Jan. 2023. URL: <https://www.zeroavia.com/do228-first-flight>.